UNIVERSITY OF SOUTHAMPTON

FACULTY OF LAW, ARTS AND SOCIAL SCIENCES

School of Humanities

A MATTER OF EVOLUTIONARY LIFE AND DEATH: AN ECOLOGICAL MODEL OF GROWTH AND DEVELOPMENT IN *HOMO ERECTUS*

By

CARINA A. BUCKLEY

Thesis submitted for the degree of Doctor of Philosophy

March 2005

UNIVERSITY OF SOUTHAMPTON

ABSTRACT

FACULTY OF LAW, ARTS AND SOCIAL SCIENCES

SCHOOL OF HUMANITIES

Doctor of Philosophy

A MATTER OF EVOLUTIONARY LIFE AND DEATH: AN ECOLOGICAL MODEL OF GROWTH AND DEVELOPMENT IN *HOMO ERECTUS*

by
Carina A. Buckley

This thesis investigates the evolutionary ecology of *Homo erectus*, focussing on the differential impact of the environment on the species' life history strategy. Departing from previous studies in taking an integrated approach, it examines the related factors of age-specific mortality, encephalisation, and the rate and energetic burden of growth, in order to identify the mechanism by which *H. erectus* adapted to a diverse range of climates and environments, and how thoroughly that adaptation was achieved. An exploration of the environmental tolerance of *H. erectus* is framed within a model that shows regions that comprised the core of the species, where tolerance is highest and conditions are optimum for growth and reproduction, and periphery regions which fall towards the extremes of tolerance and have repercussive effects on encephalisation, juvenile mortality and growth. Life history traits should vary accordingly, allowing the development of a model for the relationship between environmental variation and the differential evolution of *H. erectus*.

The work is organised thematically. Having provided an overview of evolutionary ecology and introduced the concept of paleo-demes as a means of organising, grouping and understanding the fossils of *H. erectus*, I address the shortcomings of the *r-K* dichotomy with a study of age-specific mortality. This work is then applied to patterns of encephalisation, and the energetic implications of increasing brain size are addressed. A comparative study of two modern human populations supports the prediction that stability of environment translates into stability of growth, and these findings are applied to *H. erectus*. I demonstrate that *H. erectus* exhibited a long-term trend of an increasing cranial capacity, but that this was not uniform across the species and had varying success, with subsequent energetic stress in the young resulting in high juvenile mortality in some areas. I conclude that the model of core and periphery relates to the latitude of the environment, and that *H. erectus* was an adaptable and flexible species with a number of strategies available to maximise survival in a range of environmental conditions.

CONTENTS

FIGURES

TABLES

ACKNOWLEDGEMENTS

I would like to thank my supervisor, Dr James Steele, for his help, encouragement and friendship over the past four years. Since he sparked my interest in human evolution during my undergraduate degree I have enjoyed our collaboration on all things Palaeolithic, as well as the occasional day on the river.

My thanks are also due to Dr Sonia Zakrzewski, my advisor, and Dr Margaret Clegg for being so generous with their time and experience, and for their cake buying. It made it all so much easier! All of my postgraduate work at the University of Southampton was made possible by the financial assistance provided by the Arts and Humanities Research Board; this too was of great benefit.

I am very grateful to John Shepherd and Bill White, at the Museum of London, and Derek Seeley and Natasha Powers, from the London Archaeological Archive and Research Centre, for granting me access to the skeletal collections in their care and providing an invaluable resource for this study.

My family have been constantly supportive and enthusiastic about my work and my seemingly endless student lifestyle. I particularly thank my parents for living by the sea, and my sister for sending emergency packs of chocolate and tea bags, always at the right time. Many friends have already shown me that completing the PhD process is indeed possible; I thank them for that, and also for teaching me not to leave submission until the last possible moment... But mostly I thank them, and all those I love, for their cheerfulness, laughter and friendship, which have carried me safely through the PhD tunnel to the light at the other end.

CHAPTER ONE

Introduction

This thesis will examine the evolutionary ecology of *Homo erectus*, focusing on the impact of the environment on the species' life history strategy. The study will incorporate variation in cranial capacity over time and space, the risk of mortality to adults and juveniles, and the costs and benefits of different rates of growth.

Evolutionary ecology is 'the application of natural selection theory to the study of adaptation and biological design in an ecological setting' (Winterhalder and Smith 1992: 5). The related factors of age-specific mortality, encephalisation, and the rate and energetic burden of growth form the mechanism by which *H. erectus* adapted to a diverse range of climates and environments; this thesis aims to assess how thoroughly that adaptation was achieved. The effect of the environment, and the stability of development, will be explored in two contrasting modern populations, through the use of fluctuating asymmetries, platybasia and overall canalisation of cranial morphology, as measured by reaction norms. The results will then be applied to the *H. erectus* sample, and the timescale of adaptation is addressed. The sample used, and the definition of *H. erectus* understood and applied here, are detailed below, in order to address the debates concerning the identification of members of the species.

Due to the wide geographical range of *H. erectus*, it is likely that the species encountered a high degree of environmental variability. The proxy measure used in this study is latitude, due to its effects on rainfall and solar radiation, with broad divisions into 'temperate' and 'tropical' zones, both of which are defined in Chapter Eight. It is expected that an exploration of the environmental tolerance of *H. erectus* will show regions that comprised the core of the species, where tolerance is highest and conditions are optimum for growth and reproduction, and periphery regions which show greater environmental variation, with repercussive effects on encephalisation, juvenile mortality and growth. Life history traits should vary

accordingly, which allows the development of a model for the relationship between environmental variation and the differential evolution of *H. erectus*. This will be explored in the following chapters using biogeography and paleo-demes as a new way of dividing up space and identifying consequent variations in life history. The proposed corollaries of the core and periphery are introduced in Table 1.1 below. The life history models of *K*-selection and bet-hedging are introduced and discussed in Chapter Three, but it is proposed here that variation in age-specific mortality and in environmental stability will select for one or the other of these strategies.

Table 1.1 Characteristics of the core and periphery in *H. erectus* evolutionary ecology

	Core	**Periphery**
Ecology	Constant, predictable	Less predictable
***H. erectus* range**	Tropical	Temperate
Encephalisation	Selected for	Not selected for; stasis
Juvenile mortality	Low	High
Life history strategy	*K*-selected traits	Bet-hedging

The relationship between the environment and life history strategy has been examined in several species to demonstrate the range of possible variation. For example, a study of the lizard species *Sceloporus undulatus* demonstrates that the same species will react very differently in contrasting environments, in this case with varying growth rates between populations (Niewiarowski 2001: 429). The Nebraska population of *S. undulatus* is marked by high juvenile mortality; only 10% of hatchlings survived to the yearling stage, but through rapid growth and abundant resources, reproductive maturity is reached at the age of nine months. The New Jersey population also experienced a low survival rate (87% mortality) but delayed reproduction until 21 months of age. In this case, it is the temperature difference rather than resource availability that causes variation in growth (Niewiarowski 2001: 429).

Since lizards are cold-blooded, and therefore dependent upon temperature for survival, they do not provide a comparable example to primate or hominin evolution. However, the relationship between life history traits and environment is recorded for a number of mammalian species. Demographic data from 15 Canadian moose (*Alces alces*) populations indicate two extreme groups incorporating differences in environment and life history traits (Ferguson 2002: 309). In this species, females are known to exhibit variation in age and size at maturity and reproductive effort with environment. Ferguson's study (2002) predicted that populations living in environments at the centre of the species' geographical range, with highly seasonal primary productivity, should have a fast life history (such as early age at maturity) to increase reproductive rate. In contrast, the populations living in the equatorial periphery, characterised by less seasonality and low forest cover, should show a later age at maturity and other traits that increase intraspecific competitive abilities (Ferguson 2002: 304).

This model examines a trade-off between increasing age at maturity with decreasing juvenile mortality and increasing density, but within an environmental context whereby productivity and seasonality are selection pressures that influence the phenotypic expression of population and life history characteristics (Ferguson 2002: 308). Indeed, although causal relationships cannot be determined, it is clear that the environment heavily determines the life history strategy of the Newfoundland moose. In those populations living in productive and low seasonal environments, resources are limited and competitive ability is maximised. With a later age at maturity and smaller offspring size and number, the geometric mean fitness is greater. More central populations vary in that they are regulated by predation, and thus have adapted to maximise reproduction by combining a reduced age at maturity with faster growth and an ability to adapt to temporal and spatial variability (Ferguson 2002: 310).

These results show environmentally-influenced variability in moose, but have also been shown in brown bears (*Ursus arctos*). Like *Alces alces*, this bear species has a

circumpolar distribution and shows considerable variability in life history traits that are likely to correspond with energy availability and environmental variability (Ferguson and McLoughlin 2000: 194). Regional differences in primary productivity and seasonality create a divide in bear populations between those living along the Pacific coast of North America in conditions of high productivity and low seasonality, and those of a highly seasonal interior that experiences lower productivity, and which is found at higher latitudes. In this latter group, seasonality explains 43% of the variation in age at maturity, and limitation of resources selects for maximisation of reproductive effort. At the other extreme of geographic range, the populations of the coastal bears are limited by intraspecific competition, so energetic resources are directed more towards somatic growth; primary productivity accounts for 91% of variation in age at maturity (Ferguson and McLoughlin 2000: 197-8).

These findings for moose and brown bear can be applied more widely, since in mammals the physical environment influences selection and life history strategy through its impact on adult mortality and density-dependent juvenile mortality. Moreover, and importantly for this thesis, environmental adaptation takes place at the population level, making intraspecific comparison the most effective way of examining trade-offs between juvenile mortality and growth rate (Ferguson 2002: 304).

This study aims to provide a better understanding of environmental adaptation in life historical terms, and the strategies *H. erectus* employed in order to persist in such varied environments. The distinctive contribution of this thesis lies in the use of an integrative approach to create a more coherent and informed ecological model of *H. erectus* life history, with the causes and consequences of each trait linking together to create a comprehensive picture. Each chapter examines an individual aspect of life history – the methodology is expanded below – and reviews the existing evidence for the relationships between the traits under investigation, applying them to *H. erectus* within an ecological context.

The ecology of *Homo erectus*

This work builds upon and is framed within a strong tradition of research into the effects of the environment on speciation and dispersal (Foley 1994; Foley 2002), the energetic cost of encephalisation in terms of reproductive decisions and dietary strategies (Foley and Lee 1991) and the life history of *H. erectus* with reference to habitat and regional differentiation (Antón 2003; Antón and Leigh 2003).

Throughout hominin evolution, the evolutionary success of a species has been marked by geographic expansion, followed by population divergence. The environmental context and the physical adaptations that allow for a more extensive or successful exploitation of available habitats contribute to this in one of two ways: either the habitat to which a species is adapted expands, or there is an adaptive change that overcomes obstacles to expansion that previously limited the population distribution (Foley 2002: 35). In *H. erectus* it appears that the latter course applied, with an increase in brain size and extension of life history phases (such as gestation and childhood) that allowed successful habitation of a range of environments across the Old World (Foley 2002: 35). This may have created a eurytopic species in *H. erectus*, providing a tolerance for a wide variation in one or more environmental factors and an improved colonising ability. My thesis will test the level and range of adaptation shown by *H. erectus* in several varying environments.

The implications of encephalisation for foraging strategies lie in the energetic requirements of a large brain, and the relatively low amounts of energy derived from plant foods, making a shift to frugivorous or carnivorous diets desirable (Foley and Lee 1991: 225). A change to a high quality, protein-dominated diet is no guarantee of encephalisation, as the extra energy might be employed elsewhere; however, the proposed link between brain growth and maternal energy budgets (Martin 1996) suggests that encephalisation will ultimately be constrained by ecological factors, and that it is likely to affect growth patterns (Foley and Lee 1991: 225). Expansion of the brain involves considerable energetic input, and maintenance of the modern human brain is three times greater than that of the chimpanzee, implying that human

mothers must increase the infant's level of nutritional intake compared to other primates (Foley and Lee 1991: 225-6). It is unlikely, though, that a change in diet or provisioning of the female would have been sufficient to compensate for the increased demands of the growing infant brain. Foley and Lee (1991) conclude that the hominin tendency towards longer birth intervals and increased infant dependence is a feature of energetic constraint on female reproduction, as a direct result of encephalisation. Significantly, they claim that modern human growth patterns are likely to have been established during the existence of *H. erectus* (Foley and Lee 1991: 228), and this is investigated further in Chapter Six.

Moving onto a broader environmental context, Susan Antón has examined variation in the morphology of *H. erectus*, and relates this, particularly with regard to the Asian examples, to ecological parameters. Indonesian and Chinese *H. erectus* do vary morphologically, and this could be a consequence of the latitudinal range of the species in this area (40° N in China to 8° S in island Southeast Asia [Antón 2002: 301]). The null hypothesis Antón seeks to reject is that the temporally intermediate Chinese fossils should also fall morphologically intermediate between early and late Indonesian specimens, and that the Indonesian populations will not group together to the exclusion of China (Antón 2002: 307).

Although the Indonesian finds seem to have inhabited both glacial and interglacial periods (comprising a continuous occupation from around 1.6Myr to 1.0Myr), Antón proposes that the Zhoukoudian hominins restricted their use of the site to temperate cycles, despite the general absence of permafrost (Antón 2002: 303, 306). It is possible that this variation in habitat contributed to cranial morphology, with the Chinese and Indonesian groups separating from each other along geographic boundaries (Antón 2002: 309, 312). This difference is apparent regardless of brain size, with the smaller-brained Indonesian fossils bearing greater similarity to the larger crania than either do to the relatively large-brained Chinese fossils (Antón 2002: 312), despite the temporal range of the Indonesian specimens. The increasing severity of glacial cycles and the duration and extent of land bridges throughout the

Pleistocene is likely to have been a contributing factor, as it provided a mechanism for isolating the two populations and allowing some differentiation. However, the presence of land bridges would also have prevented speciation by creating possibilities for gene flow between mainland and archipelago (Antón 2002: 320), thus allowing regional variation within a morphological whole.

Antón (2003) continues this line of questioning by highlighting the possibility of regional adaptations and biology in local groups. She introduces the idea that variation in morphology might also have consequences for life history patterning. However, Antón includes no further discussion of intra-specific variation in life history, since despite noting cranial divergences, she examines *H. erectus* (sensu lato) as a species rather than on a regional basis (Antón 2003). Any such investigation is hampered by the small sample sizes available, and the results derived from subsequent analysis must be treated with caution. Nevertheless, this study will address the implications and outcome of morphological variation for life history strategy on a regional (and therefore ecological) basis, particularly with regards to brain size.

Methodology and structure of the thesis

Since *H. erectus* inhabited a range of locales, it is likely that life history strategy varied accordingly, as demonstrated by the specific examples above. My thesis is structured to allow for the identification of trends that might represent selection in a variable environment, and act as markers for *K*-selection or bet-hedging (introduced in Stearns 1976), the choice of which is strongly dependent upon environmental predictability. Encephalisation is one such marker, since the costs incurred have a number of far-reaching implications for life history strategy, such as the retardation of somatic growth, the development of altriciality and the subsequent period of infant dependency, and the risk of increased juvenile mortality. Each of these factors will be examined in detail in the following chapters. Thus, directional selection for encephalisation in *H. erectus* will indicate a change in life history. Similarly, a tendency towards high juvenile survivorship suggests a stable environment of

growth. Reaction norms are introduced as a parameter of variability, as they allow the comparison of individuals within general population trends. Again, it is noted that these trends need not be uniform throughout the *erectus* cohort, as it is expected that regional and environmental variation will be expressed as life history variation.

This integrated approach provides the background for the hypotheses developed for this investigation. The focus moves from broad questions of *H. erectus* life history strategy (*Hypotheses 1* and *2*) to regional variation in specific traits (*Hypotheses 3* and *4*), and thence to two modern human populations (*Hypotheses 5* and *6*), since these will provide the sample size needed to confirm the role of the skull as a marker of environmental variation:

H. erectus life history strategy

Hypothesis 1: That *H. erectus* was a species under stress, and that this is reflected in higher juvenile mortality; encephalisation is not selected for

Hypothesis 2: That *H. erectus* was stable and well adapted, selecting for encephalisation and with lower juvenile mortality

H. erectus regional variation

Hypothesis 3: That within the *H. erectus* geographical range, there was variation in adaptation according to latitude and climate, with some regional groups demonstrating the characteristics of stability (the abundant core) but others under stress (the fragile periphery)

Hypothesis 4: That variation in *H. erectus* is due to genetic drift and isolation, and as such no regional patterns will be detected

Variation in cranial morphology

Hypothesis 5: that variation in cranial morphology is a product of environmental variation, and so will be regionally correlated with core and periphery p-demes

Hypothesis 6: that variation in cranial morphology is produced by genetic drift and isolation and is therefore unrelated to latitude or environment

The environment is defined here as everything external to an organism that affects its probabilities of surviving and reproducing (Winterhalder and Smith 1992: 8). The relationship between an organism and its environment creates a unique set of conditions that shapes the biological processes of that organism (Foley 1987: 48). The evolutionary core of these processes is natural selection, whereby organisms experience differential reproductive success from generation to generation. Natural selection does not occur in isolation, but has a number of constraints acting upon it and shaping the direction of evolutionary change. The interplay between genetics and the adaptive significance of variation allows for the selection and inheritance of the phenotype. The relationship of the phenotype to reproductive success drives natural selection, as does a competitive environment in which only those phenotypes most efficient at acquiring resources will experience differential reproductive success (Foley 1987: 51-53). This places the organism – in this case, *H. erectus* – within the physical environment, making it subject to influence and constraint. Using the principle of constitutive reductionism, whereby higher-level processes are constituted of lower-level processes which preserve their integrity no matter what the context (Winterhalder and Smith 1992: 14), it is possible to develop models in order to explain the impact of one phenomenon on another. The uniqueness of higher-level events can be understood in terms of the increased interaction and complexity of their components. In this case, the life history strategy of an organism is composed of a series of interlinking processes that impact on each other to create a novel whole. Constructing the evolutionary ecology of *H. erectus* thus requires an integrative approach, adopted by this study.

As a result, the method followed here differs from previous studies of the relationship between evolution and ecology, which have tended to focus on one aspect of behaviour or morphology and then build an adaptive model from that. For example, Kaplan and Hill (1992) make the optimisation of food-getting behaviour

their primary focus. They use this to identify links to social structure and symbolic communication (Kaplan and Hill 1992: 194-196). In a more overtly evolutionary paper, the importance of bipedality as an adaptive event, through a prime mover model, links the emergence of this trait to tool use, heat adaptation and foraging efficiency (Cachel and Harris 1998). These relationships are then used as a mechanism for adapting to diverse environmental conditions, thereby explaining morphological diversity in *H. erectus* (Cachel and Harris 1998: 117, 121). Similarly, Potts (1998) explored the importance of environmental fluctuation as an alternative prime mover, a concept I adapt to investigate the influence of the environment on the life history strategy of a species with behavioural flexibility. Previous models posited the evolution of traits including bipedality, toolmaking and encephalisation as a response to the demands of the savanna. However, this implies a constant environment, whereas climatic evidence indicates fluctuation in habitat over time (Potts 1998: 82-84). This makes the ability to be 'adaptively flexible' an important trait, through the evolution of variability selection, or the adaptive mechanisms, such as a large brain, that allow an organism to absorb and respond to environmental data (Potts 1998: 85). This notion introduces the theoretical foundation of the thesis, which examines a species' response to the environment, and the life history traits that have evolved to make that response successful. Like Cachel and Harris (1998), I will examine life history strategy in terms of the environment, and look at regional diversity in cranial morphology, but without tracing any pattern in terms of a single trait.

This study is positioned within a strong research trend focussing on the life history of *H. erectus*. This has been explored from numerous angles over the past fifteen years, but all converge on a progressive evolution of *K*-selection in the species. An increase in cranial capacity would have had a considerable impact on life history strategies, particularly with regard to female provisioning, birth spacing and the caretaking of helpless infants. A solution to this is proposed by the Grandmothering Hypothesis (O'Connell et al 1999 and reviewed in Opie 2004), which suggests that the evolution of longevity led to the survival of post-menopausal females for the

purpose of caring for their daughters' offspring. Although the ethnographic evidence is contested (see Blurton Jones et al 1992; Kaplan et al 2000), a consideration of female reproduction costs (Aiello and Key 2002) indicates a need to move to modern human birth patterns, resulting in a greater number of offspring for each adult female (but see Antón et al (2002) for the opposing argument that humans, particularly in industrial societies, are 'secondarily *r*-selected'; a condition which aided rapid hominin dispersal in the early Pleistocene). This model requires that the female and her weaned (but dependent) offspring are provisioned by males or other adults in the group, a view shared by Kaplan and co-workers (2000). The analyses carried out in this thesis on brain size increase and juvenile mortality are part of the same research continuum, since I examine the prior conditions needed for both provisioning and grandmothering to emerge.

The individual, rather than the group, is the primary unit of selection and the most relevant to evolutionary ecology since it is the individual who interacts directly with his/her environment (Foley 1987: 55). This is the premise assumed here, with each specimen of *H. erectus* examined with respect to its conformity with the group, and the implications of any divergence from the overall pattern. Foley (1987) also followed an integrative approach, using the effects of body size to assess its impact on other life history traits. Changes in body size have implications for diet, social structure and, frequently, the correlates of *K*-selection (discussed in Chapter Three). However, he examined the effects of the environment through seasonality and latitude on hominin life history strategies, linking the two together and eliminating the need for a prime mover. Body size is only briefly considered in this thesis, with emphasis instead placed on encephalisation relative to body size. However, increased brain size is not approached as a single trait through which all others are mediated; rather, the life history of *H. erectus*, and its relationship to environmental variation, is treated in a unified manner.

To this end, each of the following five chapters comprises an investigation of one of the traits contributing to the life history of *H. erectus*, framed within the context of

evolutionary ecology. Although each trait is dealt with as a separate question, it is important to establish the mechanisms of the lower-level processes within the sample before building up a model of the higher-level system; a process facilitated by my approach of examining each trait separately, but not singly. In this way it is possible to bring together the separate sets of findings from each chapter and draw a full picture of regional variation in *H. erectus* life history.

The context for this integration is established in Chapter Two. In this section I set out my working definition of *H. erectus* and justify the inclusion or exclusion of certain fossils in my sample. The analysis of *H. erectus* in this thesis is structured around Howell's (1999) principle of paleo-demes, whereby *H. erectus* is thought of as a polytypic lineage of one or a series of demes. This allows for the categorisation of regional populations of a species into taxonomically distinct subspecies, which are nevertheless linked by a common line of descent. This approach facilitates the comparison of temporally and spatially distant populations of the same species, whilst opening up the possibility of regional isolation and adaptation. Paleo-demes are thus a product of biogeographical processes, and as such are subject to localised variation in life history strategy.

The key elements of the evolutionary ecology of *H. erectus* are introduced in Chapter Three. This sets out a working definition of life history and presents a theoretical discussion of its links to the environment, in order to understand the relationship between geography and life history. I begin with a discussion of life history trade-offs, focussing in particular on reproduction and mortality. I then introduce MacArthur and Wilson's (1967) theory of *r-K* selection, which connects environmental and life history correlates to patterns of survivorship. To counter the limitations of this dichotomy, Stearns's theory (1976) of bet-hedging is presented as an additional tool of analysis through its relation to age-specific mortality. This provides a way of examining changes in life history strategy over the life span of the organism, as changes in the environment can affect the mortality profile. This then leads on to a discussion of trade-offs, focussing on the balance between rate of

growth and mortality risk, and the age at first reproduction. A brief investigation into the influence of body size on reproduction rate, gestation and growth is linked to encephalisation and the development of the condition of 'secondary altriciality' in humans, with the parallel risks of trophic/environmental stress and developmental instability. Finally, the means of measuring these through the use of reaction norms is explored, leading the physical expression of the phenotype back to environmental variation.

Having thus established a theoretical overview of the evolutionary ecology of *H. erectus*, and how the traits interlink, the next three chapters are concerned with specific aspects of life history and their expression in *H. erectus*. In Chapter Four, I continue to address the failing of the *r-K* dichotomy, in its neglect of the effects of age-specific mortality. I illustrate the importance of mortality in life history strategy using a series of data from hunter-gatherer and non-human primate populations. Using demographic data principally from Hill and Hurtado (1996) and Richard (1985), I construct survivorship curves for the Ache, a South American hunter-gatherer population, and several living primate species, which I then compare to the fossil baboon remains of the Sterkfontein valley in South Africa (data from Brain 1981). This has the advantage of monitoring the effects of taphonomic bias, in addition to evaluating risk of mortality in other primates by allowing comparisons between the age distributions of living and extinct species.

Tobias (1999) has taken this further by explicitly relating high juvenile mortality to the pressures of encephalisation in *H. erectus*, comparing the ratio of adult to juvenile specimens in four hominin species. However, in this chapter I compile a larger dataset to reverse Tobias's findings for the species in general, although a regional differentiation in survival may indicate an environmental stress that increased risk of death during the juvenile period. Finally, by including the estimated age at death of each *H. erectus* specimen, I am able to increase the resolution of the survivorship curve. Again, it is clear that the mortality profile

varies according to region, and thus by latitude, suggesting adaptive flexibility in *H. erectus*.

Chapter Five builds on the preceding chapters by modifying them within the context of encephalisation. A change in brain size over time cannot happen in isolation, but has implications for many aspects of life history. As cranial capacity increases, there is a redistribution of the body's resources, which in turn affects growth schedules and gestation length, and can be linked to survivorship. The first challenge, therefore, was to determine whether the cranial capacity of *H. erectus* did increase significantly over time, or whether it differed only by region, independent of chronology. I propose that this significant increase over time is in evidence, when all available fossils for use in the regression are collated, rather than the limited dataset previously compiled by Rightmire (1990). I conclude that the increase in brain size does not occur at a uniform rate in each region, suggesting that other evolutionary pressures are at work. This supports the idea that the life history strategy of *H. erectus* varied according to region.

In Chapter Six, my focus remains on encephalisation, with the emphasis moving to consider the energetic costs of an enlarged brain. Modern human brain function is assessed, and precocial and altricial growth patterns are related to the environmental *r-K* dichotomy. The differences between the human pattern of growth and that seen in a range of primate species are examined by using the primate dataset from Leonard and Robertson (1992), calculating the metabolic cost of the brain compared to body size in humans and a series of 18 primate species. Since body weight is necessary in order to evaluate the appropriate basal metabolic rate and the relative cost of the brain, male and female estimates of African *H. erectus* body weight are used to create two idealised specimens, which are included, together with WT 15000 (Ruff and Walker 1993), in the primate regressions. Analysis suggests that although *H. erectus* appears to have a brain slightly larger, and thus more costly, than expected for body size, the two idealised specimens and WT 15000 remain within or close to the confidence intervals on the regression slope. This indicates that *H.*

erectus had not yet attained marked encephalisation, at least in the African sample, and so would not have adopted other modern human characteristics such as secondary altriciality and a delayed period of growth. However, this chapter and the previous one conclude that Indonesia (or one of the p-demes from this region) was encephalised relative to body size, and would therefore have followed a different life history strategy compared to other regions.

The regional variation in cranial capacity in *H. erectus* may be due either to phenotypic plasticity or genetic isolation. Chapter Seven opens by hypothesising that the skull is plastic in its morphology, and is therefore subject to environmental modification. I review previous studies by Boas (1912) and Angel (1982), which seem to confirm this hypothesis by providing (contested) evidence of non-genetic, migration-influenced variation between parents and children (Boas 1912), and a flattening of the base of the skull in disadvantaged populations (Angel 1982). Fluctuating asymmetries in bilateral traits and reaction norms are then introduced as a way of measuring developmental stress in a population. However, since the evidence for *H. erectus* is too sparse to allow firm conclusions to be drawn, an alternative strategy for investigation is sought. Two modern human populations from 18^{th}-19^{th} century London are presented; one from an advantaged background and the other more deprived. Here, I test the degree of asymmetry in the orbit widths of each populations, and use cranial measurements to validate or disprove the Angel hypothesis for skull base flattening. A purported correlation between cranial length and stature (and therefore the environment) is examined, in order to assess the strength of environmental influence on cranial morphology.

I then go on to apply these findings to *H. erectus* in Chapter Eight. I argue that in certain environments, quantified by latitude, *H. erectus* experienced differential adaptation, and that this is reflected in commonalities of cranial morphology in certain populations. Interpretation of the statistics is difficult due to small sample size, and there appear to be few regional patterns in the relationships between cranial dimensions. Using analysis of variance and additional cranial measurements, I am

able to suggest that biological populations (possibly aided by geographical proximity and isolation) are more likely to share cranial characteristics, and this might be a more important factor than latitude. I test this by comparing the Zhoukoudian sample with fossils from Atapuerca, in Spain, dated to a similar period. However, it is seen that, despite coming from a biologically discrete population, the Atapuerca sample fails to display any unity in cranial relationships.

I conclude the study by constructing a model of the evolutionary ecology of *H. erectus*, through the related aspects of age-specific mortality and encephalisation, within a biogeographic framework of life history variation. Through individual studies and comparative analysis with modern human populations, I anticipate that while *H. erectus* was generally a *K*-selected species, it was better adapted to certain environments over others and would probably have adopted a flexible bet-hedging strategy as a result.

The fossils and their locations

Due to the above debates, the sample compiled for this study is necessarily conservative, in order to reflect and allow for the occasional uncertainty of species designation. This precludes many of the European mid-Pleistocene fossils, such as the Mauer mandible and the Petralona cranium, but does include, for example, earlier specimens such as the Dmanisi population (justification for these decisions, and others, is given in the following chapter). The specimen numbers for each fossil are given in the text as they are included, and are not limited to the crania. The geological ages are provided in Appendix I, along with the dating techniques used and references.

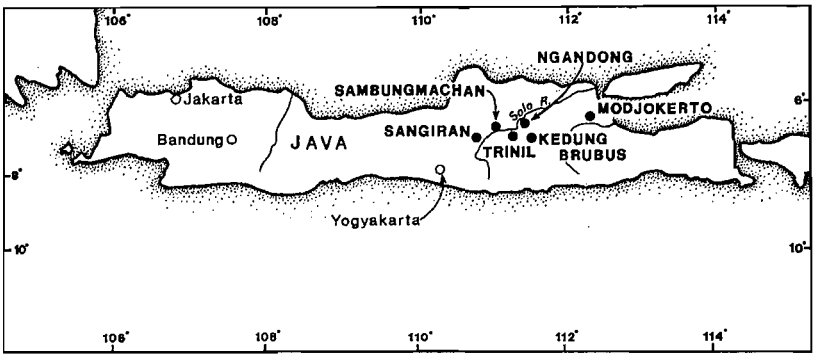

Figure 1.1 Map of *H. erectus* localities in Java (Rightmire 1990: 13)

The Javan finds include the type specimen, the Trinil calvaria, with two postcranial samples from the same location, two fossils from Sambungmachan (Sm1 and 3), the Ngandong population (nine individuals), the Modjokerto skull and the various individuals from Sangiran (conservatively estimated at 26 individuals) (Day 1986).

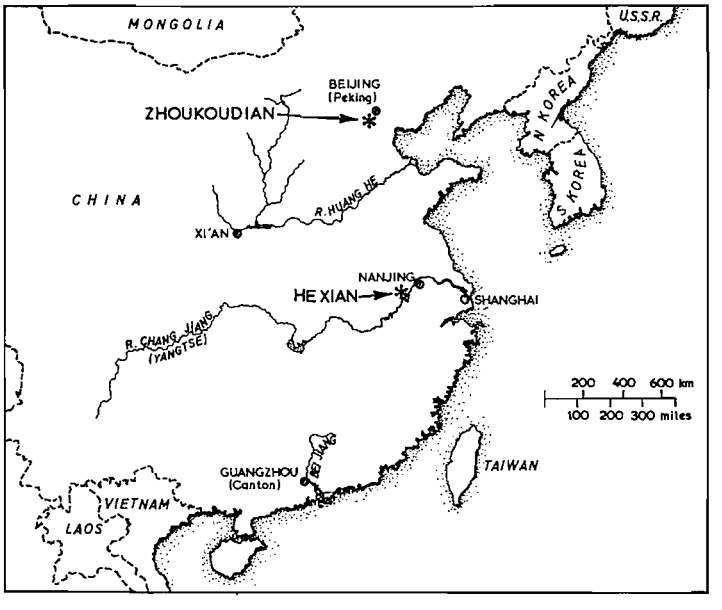

Figure 1.2 Map of *H. erectus* localities in China (Day 1986: 366)

The majority of the Chinese sample (Figure 1.2) comprises the Zhoukoudian population, represented in this study by a total of 32 individuals. The Hexian remains, the Lantian fossils (located in the vicinity of Xi'an) and the Tangshan and Guojiabao juveniles complete this group (Wu and Poirier 1995).

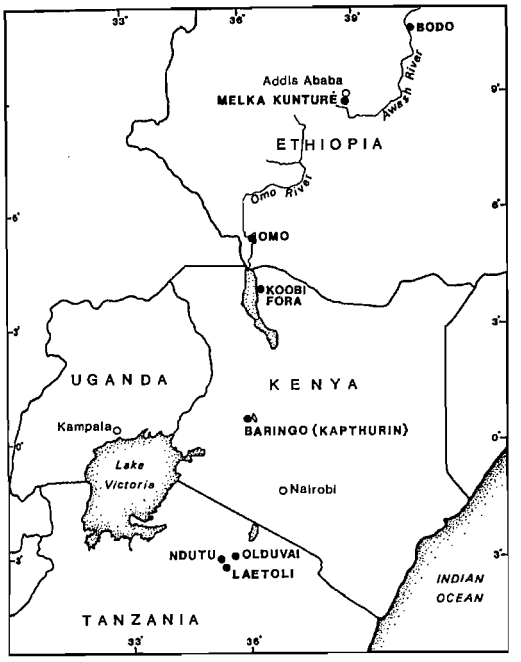

Figure 1.3 Map of *H. erectus* localities in east Africa (Rightmire 1990: 87)

Homo erectus in east Africa (Figure 1.3) is principally found at Koobi Fora (Wood 1991); later fossils from Bodo and Baringo are generally thought of as early *sapiens* forms and are therefore excluded from the following analyses (see Chapter Two). However, two earlier crania from Olduvai, OH9 and OH12, are included (Rightmire 1990). The skulls from Bouri (Middle Awash, Ethiopia) (Abbate et al 1998) and the Northern Danakil ('Daka') Depression of Eritrea (Asfaw et al 2002) are also considered, and the new find from Olorgesailie is included (Potts et al 2004).

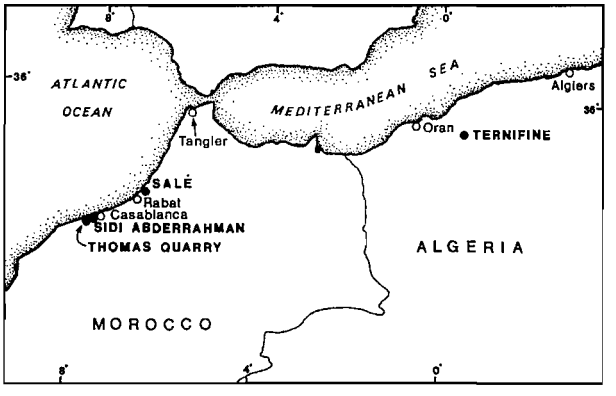

Figure 1.4 Map of *H. erectus* localities in north Africa (Rightmire 1990: 120)

In addition are the north African fossil sites of Tighenif (Ternifine), Thomas Quarry, Sidi Abderrahman and Salé. Tighenif is considered to be from the earliest Middle Pleistocene. The chronology of the remaining three sites is somewhat confused (Rightmire 1990: 121). However, the designation of all as *H. erectus* is largely accepted, if not unequivocally so (Rightmire 1990: 131-137), particularly within the demic framework introduced in Chapter Two. Three further African postcranial deposits from Swartkrans in South Africa are also included in the dataset (Rightmire 1990).

Finally, the *H. erectus* fossils from European sites are included. These sites often contain a mix of species, with less obvious designation, so only those specimens that by general consensus are regarded as *H. erectus* are considered. The Mauer mandible, and the Vértesszöllös, Steinheim, Arago and Krapina fossils are excluded as they share characteristics with *H. erectus*, *H. sapiens* and Neanderthals. Similarly, the Bilzingsleben skulls are not considered as examples of *H. erectus*, despite claims to the contrary (for a review, see Day 1986: 65; more recently, Stringer and Ullrich 1990). In the last decade, the presence of *H. erectus* in Europe has been greatly strengthened by the discovery of several ancient crania from Dmanisi, in Georgia (Gabunia et al 2000; Vekua et al 2002). The cohort for this study is completed by the addition of the crania from 'Ubeidiya (Oakley et al 1975) and Narmada (Sonakia 1985), although their use is limited to those analyses where regional variation is not under consideration.

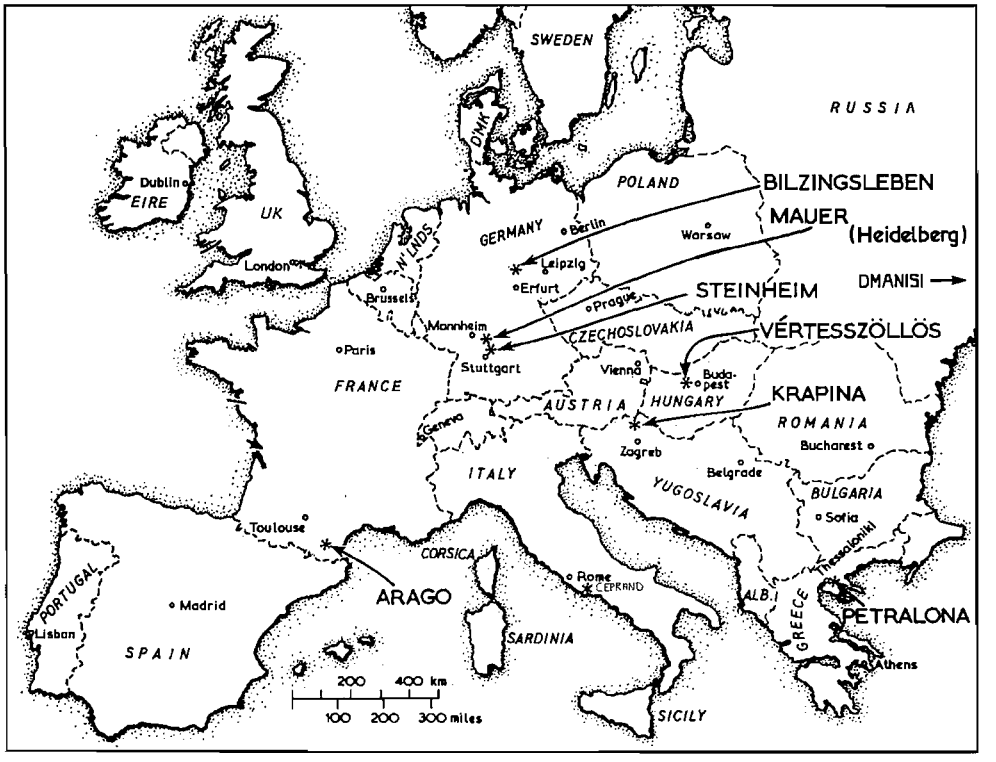

Figure 1.5 Map of *H. erectus* localities in Europe (Day 1986: 18)

I begin this study of the evolutionary ecology of *H. erectus* by constructing a biogeographical framework in which to study and assess the individual components of life history. In this thesis, I have chosen to ask a broad question of *H. erectus* life history with multiple topics, rather than focussing on a discrete issue, because in the following chapters I produce a set of mutually consistent studies that contribute to *H. erectus* life history. The interaction of these, and their balance in the context of varying environmental conditions, will be responsible for determining the life history strategy of *H. erectus*, and how the species survived and evolved.

CHAPTER TWO

The definition of *Homo erectus*

Homo erectus began its career as five separate genera, with three of them (*Pithecanthropus*, *Sinanthropus* and *Meganthropus*) confined to China and Indonesia (Java). It was only when *Telanthropus* from South Africa and *Atlanthropus* from North Africa were collapsed into the *Homo* line (Mayr 1944) that the possibility of a wider distribution of *H. erectus sensu lato* throughout the Old World was considered (Wood 1991: 32). Since then, other fossils from Europe and eastern Africa have been classified under this species name, although this has not been without debate, as discussed in detail below. When all specimens are considered, the territory inhabited by *H. erectus sensu lato* is greater than that of any previous species of hominin. In order to accomplish this, the species must have developed the ability to adapt to a range of different climates and environments to the extent that it was able to propagate and establish a long-term occupation. It is the mechanisms for this adaptation, and the consequences of environmental variation for life history that are the focus of this study.

Clade versus grade

The hypodigm of *H. erectus* has been contested and is often considered fluid in its interpretation. However, the need to define the species, and thus the fossils that it includes, is a key starting point for this study. The status of *H. erectus* as a species rests on whether it ought to be considered as an arbitrary grade within the gradually evolving *Homo* lineage, with no clear origin and founded on a wide range of cranial capacity (Andrews 1984: 168), or whether it is a stable species that can be classified morphologically, regardless of gaps in the chronological and fossil records (Rightmire 1990: 173, 180). The recognition of morphological features unique to *H. erectus* is therefore vital both when establishing the species and when justifying the inclusion of certain fossils whilst excluding others from analysis.

H. erectus was first recognised in Java, and although later discoveries from Zhoukoudian (near Beijing in China) were lost in the Second World War, these have since been added to the hypodigm, forming the comparative basis for any further additions (Wood 1991: 32). There are some traits that distinguish *H. erectus* from *H. sapiens*, but a number of these are found in earlier African *Homo*, making it all the more difficult to define *H. erectus* relative to other hominins. It is true that plesiomorphic traits – those that are shared with other species – might be present in unique combinations, but it is more desirable to identify apomorphic, or derived, characteristics that are expressed only in *H. erectus*. This is the basis of cladistic analysis (Rightmire 1990: 186-7). A cladogram is based on certain morphological character states, with the interpretation resting on the assumption that the presence of any of the characters in wider taxa than just *H. erectus* are primitive retentions from the common ancestor and thus not diagnostic of the species (Andrews 1984: 168).

Following a cladistic analysis of character traits in *H. erectus*, *H. sapiens* and *H. habilis*[1], according to Andrews (1984) there are only seven cranial features unique to *H. erectus* and therefore derived: the presence of a frontal keel; thick cranial vault bones; presence of a parietal keel; angular torus on parietal; an inion well separated from the endinion; a developed mastoid fissure; and a recess between entoglenoid and the tympanic plate. Of these, six appear only in the Asian specimens of *H. erectus*; the condition of the seventh, the separation of inion from endinion, could not be determined in the African sample. Thus, Asian *H. erectus* is characterized by a unique set of derived characteristics not found in its African counterpart, with the exception of increased cranial capacity. The characters common to both are shared primitive traits also present in other taxa and are therefore unhelpful in examining phylogenetic relationships. Andrews concludes that, although it remains unclear which population, the Asian or the African, is more closely related to *H. sapiens*,

[1] The debate over the genus of *habilis* will not be addressed in this thesis; it is acknowledged that Wood and Collard (1999) prefer to place *habilis* in genus *Australopithecus*

there are no grounds for combining the African specimens with Asian *H. erectus* (Andrews 1984: 170-174).

Wood (1984) carried out a cladistic analysis on all fossils from Asia and Africa that fell between a diagnosis of *H. habilis* or *H. sapiens*, or that could be ascribed to *H. erectus* (Wood 1984). His investigation centred on the Koobi Fora remains, particularly KNM-ER 3733 and KNM-ER 3883. While Wood acknowledges that these two crania seem to be 'erectus-like', he believes that, similar to Andrews (1984), their inclusion in the same taxon as the Asian finds would create a species without any autapomorphic features and without some of the unique features which distinguish it as a species from both *H. habilis* and *H. sapiens*. The shape of the frontal bone of these African crania, as well as the thickness of the cranial vault, depart from the Asian condition and prevent them from inclusion in the *H. erectus* taxon. The only alternative would be to widen the definition of *H. erectus*, with the consequence of removing the species' autapomorphic features (Wood 1984: 105-107).

The separation of African from Asian material is not a universally shared view, and subsequent work has attempted to establish greater cohesion in the fossil sample. An analysis of metric traits in crania from Africa, Indonesia and China suggested that there was a single species across the two continents, through the continuous variation of characters rather than determining the presence or absence of discrete entities (Bräuer 1994: 301). The ranges of variation in East Asian and African hominins fail to overlap in only two features – the frontal breadth index and the breadth of the mandibular fossa. Overall, there is unity in the morphology of the two groups, with 37 features showing a strong overlap and the values of the African specimens falling completely within the range of Asian variation. It is possible that the small sample size of 21 complete crania influenced the outcome of the analysis, and issues such as sexual dimorphism are not yet clearly understood. However, Bräuer's multivariate analyses do not indicate a clear distinction between the African and Asian hominins and support the concept of a single *H. erectus* species in

Africa and Asia, particularly as he notes that there is no direct relationship between speciation and morphological change (1994: 314-316).

One species or two?

These debates highlight the difficulty in defining the species, its component fossils of *H. erectus* and thus its spatial distribution. Complications arise with the inconsistent use of a subdivision called *H. ergaster* (Groves and Mazak 1975), often referred to as 'African *H. erectus*' (with most finds centred on the Turkana area of Kenya) or 'early *H. erectus*' due to the antiquity of the fossils (approximately 1.9-1.5 Ma) (Wood and Collard 1999: 66). Although this species is judged to be geographically and temporally distinct from *H. erectus*, there is generally a lack of consensus on the status of *H. ergaster* as a viable species. Its incorporation multiplies the diagnostic features that distinguish *H. erectus* from other species, but often confuses diagnosis within that species.

Groves and Mazak (1975) proposed the species name *H. ergaster* on the basis of the mandible ER 992. They compared the specimen with *A. africanus* and *H. habilis*, and found differences in its smaller premolars and molars; premolars that are relatively broad and in which there is often a single root; small P_4 crowns relative to P_3; a thick mandible; and a cranial capacity larger than *A. africanus* but equivalent to that of *H. habilis* (Wood 1991: 83). The problem with this approach, and the source of current confusion over the use of the name *H. ergaster*, is that they did not carry out the same comparison of the mandible with *H. erectus* – a serious oversight given the major evolutionary implications. Wood believes that the morphology of the mandible does not exclude it from a hypodigm composed of the African and Asian remains attributed to either *H. erectus* or *H.* aff. *H. erectus* (Wood 1991: 150-151). He places it in the latter category, with ER 3733, 3883, 730, 1466, 1648, 1808, 3892, 820, 1507 and 1812. In addition, he considers that ER 1821, 2592, 2595, 2598 and 731 most likely belong to the same group, but the evidence is inconclusive.

Differences between *H. erectus* and *H. ergaster* are generally founded on the identification of primitive characters in the latter species; for example, the crowns and roots of the mandibular premolars. It is also argued (Wood and Richmond 2000: 42) that *H. ergaster* can be distinguished from *H. erectus* by its lack of some of the more derived features of cranial vault and cranial base morphology such as prominent sagittal and angular tori. However, these differences are disputed by the majority of researchers, who argue either that there are no consistent or significant morphological differences between *H. ergaster* and the main body of *H. erectus* material, or that any differences that do exist are not worthy of species-level recognition (Wood and Collard 1999: 198; Wood and Richmond 2000: 43). There is an overall reluctance to use the nomenclature *H. ergaster* as anything other than a descriptive term for a subgroup of *H. erectus*; and indeed, that may be the most appropriate way of addressing the issue. If it is accepted that the species *H. erectus* incorporates those fossils sometimes referred to *H. ergaster* then the temporal span of the species ranges from 1.7 myr in Dmanisi to 50 kyr in Ngandong. While this is not an impossible proposition, there are alternative interpretations of the fossil record that may be more useful to my study, and these are explored in the following section. Furthermore, adopting a wide definition of *H. erectus*, particularly on a temporal basis, makes it difficult to justify the exclusion of mid-Pleistocene hominins that fall within this time period, such as *H. heidelbergensis*. The status of this species with regards to the analyses performed in this thesis is discussed below.

Paleo-demes and the *Homo* lineage

The fragmentary nature of the fossil record has done little to resolve disputes of hominin taxonomy and phylogeny, and has instead often served to increase confusion. In an alternative approach, a biogeographical interpretation can be used to explain speciation and extinction. In this context, *H. erectus* can be thought of as a polytypic lineage of one or a series of demes that share a common history of descent not shared by other demes, rather than a species with a single set of characteristics. Howell (1999: 203) provides three definitions of a deme: it is the unit of natural history and of evolutionary divergence, defined as a communal

interbreeding population within a species (Carter 1951: 142); a local population of a species, the community of potentially interbreeding individuals at a given locality (Mayr and Ashlock 1991: 413); and a unit distinguishable by reproductive (genetic), geographic and ecological parameters. Demes within the same line of descent constitute subspecies, which are defined as an aggregate of local populations of a species inhabiting a geographic subdivision of the range of the species and differing taxonomically from other populations of the species (Howell 1999: 193, 203). Subspecies are bounded by four categories – geographic, historical, adaptive and phenotypic – and interlinked by a fifth, genotypic. These relationships and commonalities make it possible to investigate regional variation in separate *H. erectus* demes across the Old World whilst still retaining the genotypic umbrella of species *H. erectus*. Thus, setting paleo-demes within an environmental structure creates a dynamic model for regional variation in *H. erectus*. The predictions for resultant life history variation follow below.

The use of paleo-demes (p-demes) as a fossil categorisation is, according to Howell (1999: 203-204), greatly underused and undervalued, despite the frequent need to recognise and designate a local population that is part of a taxon but does not by itself comprise a whole taxon. Thus, fossil specimens with geographic and temporal proximity can form a level intermediate between the individual specimens and a higher taxonomic category. This in itself frees this study from the constraints of morphological progression over evolutionary time, since the p-demes represent separate dynamic units of lineages, adapting and specialising in different environments. This approach also avoids the need to resolve the questions posed above regarding the status of *H. erectus* as a grade or a clade (since it is now to be considered as an evolving lineage of regional variability), the identification and status of various morphological characters, and the relationship of *H. erectus* to *H. ergaster* (since the latter may now be addressed as a p-deme within the overall *H. erectus* nomen).

The *H. erectus* p-demes

Howell (1999) identifies more than 20 p-demes within the *Homo* ancestry, exclusive of *H. habilis*, *H. rudolfensis* and *H. sapiens*. However, it cannot be assumed that these are all eligible for inclusion in a study of *H. erectus* variability; *H. heidelbergensis*, for example, requires particular attention due to its contemporaneity with *H. erectus* (as broadly defined), and its exclusion from the analyses of this thesis is justified below.

Africa

The oldest p-deme defined by Howell (1999) is that of the nomen *ergaster*, known as the Nariokotome p-deme. The holotype specimen, ER 992, is joined by the skeleton WT 15000, ER 3733, 3883, 370, 1808 and the subadult ER 820, and is probably also represented at Swartkrans. Dated to between 1.7 and 1.5 myr, these fossils are associated with a variant of the Oldowan industry and evidence for carcass-processing activity. Together, they constitute the probable source for the initial extra-African hominin dispersal into Europe (Howell 1999: 204). This is supported in part by the discovery of a new p-deme, with an equally ancient age of 1.7-1.6 myr, at Dmanisi in Georgia (with the suggestion it carry the nomen *georgicus* [Gabounia et al 2002]). This population is associated with a Mode 1 lithic industry, and is compared by Howell to the 'Ubeidiya site, which has produced over 60 artefact-bearing horizons from Olduwan and Acheulean technologies. In terms of morphology, the Dmanisi p-deme shares some characteristics with the Nariokotome p-deme, and has more autapomorphic features (Howell 1999: 214). Moreover, of the faunal remains recovered from this site, only six taxa are African in origin, indicating that the Dmanisi hominins had dispersed out of their ecological niche (Antón and Swisher 2004: 282).

Three more p-demes have been identified in Africa. The oldest of these is the Olduvai/LLK-II p-deme (nomen *leakeyi*), dated, by the assignment of the Buia (Danakil) cranium UA-31 to this deme, to around 1 myr. The fossil OH 9 is the principal specimen of this deme, and although it is not directly associated with any

tool industries, Acheulean assemblages are well known within the same archaeological horizons. These two crania are tentatively joined by OH 12, 22, 23 and 51, and the postcranial fragments OH 36 and 28. The cranial morphology suggests that this p-deme is strongly derived in comparison to the Nariokotome antecedent (Howell 1999: 205).

The second African p-deme of this period is centred in the northwest African Mahgreb. Designated by the nomen *mauritanicus*, the Tighenif p-deme has yet to be directly associated with the Acheulean industry, although it is related to the younger p-deme of Sidi Abderrahman and Thomas Quarry, where the Acheulean is known. The cranial remains of the Tighinef p-deme are poor, but do suggest some derived distinctions from, and resemblances to, the Olduvai p-deme. The Salè cranium is from this region but its extensive occipital pathology and younger geological age make it difficult to ascribe it to a particular p-deme (Howell 1999: 205-206). However, Rightmire (1990) feels that it is best placed within the *H. erectus* taxon and so it is included in the analyses of this thesis due to its geographical and temporal affinities with the north African p-demes described here.

The final p-deme from Africa is the Kabwe p-deme. This nomen (*rhodesiensis*) is represented by the cranium E-686 which, with other postcranial fragments, is related to a calvarium from Elandsfontein, South Africa, found in an Acheulean context. However, this p-deme, along with the other constitutive specimens of Ndutu, Bodo and the Baringo (Kapthurin) basin, are not included in this study. These fossils are of a younger geological age, ranging from 0.22-0.6 myr, which is moving out of the African temporal boundary for *H. erectus*. Furthermore, the p-deme includes material found in association with advanced Acheulean and earlier Middle Stone Age industries, which are not usually found within an *erectine* context (Howell 1999: 206; see also Foley and Lahr 2003: 121). This same reasoning also excludes Howell's Irhoud, Florisbad, Klasies, Singa and Dar es Soltane p-demes (1999: 207-209).

The Far East

The dispersal of hominins from Africa has often been considered to be concomitant with the transition from Olduwan to Acheulean technology (Antón and Swisher 2004: 271). However, there is substantial evidence to suggest that *H. erectus*, as broadly defined within the demic model, reached China and Indonesia much earlier, and although lithic industries in this region are less well documented, it seems that Acheulean technologies were not necessarily a prerequisite. For example, although the so-called Movius line divides the handaxe-rich West from the handaxe-impoverished East, some stone tools (usually flaked cores) have been recovered from the Sangiran formation (Antón and Swisher 2004: 283), and Yamei et al (2000) claim to have identified 'Acheulean-like' stone tools in China. The Movius line applies only to the type of technology carried into these new regions, rather than the absence of lithic industries.

The oldest hominin remains in mainland eastern Asia are from Quyuanhekou in Yunxian. Dated to 0.83-0.87 myr with a minimum age of 0.581 myr, this p-deme is morphologically similar to the Zhoukoudian p-deme; the Gongwangling crania, of comparable age, seems to be intermediate between these two groups (Howell 1999: 209). Zhoukoudian (nomen *pekinensis*) is represented by 45 individuals, 20% of which are immature. This population, ranging in age from ~580-230 kyr, was found in association with abundant lithics, relatively unrefined, on a range of raw materials. The Hexian skull is also thought to belong to this p-deme (Howell 1999: 210). A new skull from Tangshan (Nanjing) in Southeast China is purported to share similarities in cranial shape to the Zhoukoudian population, although in other respects it is wholly unlike these possible contemporaries (Wu et al 2005). Publication of this fossil came too late for inclusion in this study and so the taxonomic debate surrounding it is not entered into here.

The Dali cranium (*daliensis*) shares some, though not all, of the plesiomorphies and autapomorphies of both the Yunxian and Xhoukoudian p-demes, but nevertheless also exhibits derived cranial and facial traits that distinguish it from the antecedent

Asian p-demes (Howell 1999: 211). With a geologic age of around 200 ± 40 kyr, this skull is thus excluded from the analyses performed in this thesis, as is the cranial remains of the Jinniushan male (a distinct and derived morphotype dated to 200 kyr) and the calvarium of the Mapa/Hathnora p-deme (nomen *mapaensis*). This latter specimen is divergent from the Zhoukoudian p-deme whilst sharing traits with the Narmada cranium, found in a late Acheulean industrial complex (Howell 1999: 211). Since *H. erectus* has not been securely associated with Acheulean toolkits (in a cladistic/modal study, African *ergaster* (broadly defined) proceeded to develop a Mode 2 or Acheulean technology, whereas Asian *erectus* did not develop beyond a simple Oldowan Mode 1 industry [Foley and Lahr 2003]), the Narmada skull, though noted in the text, is also disregarded in the following study.

The islands of Indonesia have provided palaeoanthropology with, to date, the oldest examples of fossils hominins outside Africa – indeed, the type specimen of *H. erectus* is from Trinil on Java and has an age of ~1.58-0.98 myr. This p-deme (called Trinil/Sangiran) has a number of autapomorphic characters that vary consistently from those seen in the Zhoukoudian p-deme. The related Sangiran p-demes of Glagahomba and Brangkal (of the nomen *paleojavanicus* or *dubius*, and *robustus*, respectively) are thought to be much older, with (contested) dates of ~1.66-1.77 myr for Glagahomba and around 1.8 myr at Brangkal (Howell 1999: 212-213). Greater detail on this is provided in Chapter Five.

The nomen *soloensis*, represented by the Ngandong p-deme, is thought to share the same fundamental morphology of the Trinil/Sangiran p-deme whilst demonstrating its own autapomorphic traits. This population consists of numerous adult and subadult remains, and with an age of 27 ± 3 – 46 ± 4 kyr at Ngandong and 27 ± 3 – 53 ± 4 kyr at the related site of Sambungmachan, these remains provide substantial evidence for the persistence of a distinctive archaic hominin in an insular situation (Howell 1999: 213). Furthermore, the faunas associated with these eastern hominins are native to the area, and therefore represent a new niche of occupation. The Indonesian fauna, though sparse, document changing patterns of land bridges and

isolation (Antón and Swisher 2004: 282), and thus also present restrictions or opportunities for hominin movement. All the hominin populations of south east Asia display morphological affinities with their African source. However, within the region the p-demes are distinct from each other, suggesting an evolutionary history of drift and prolonged isolation. Howell (1999: 233) proposes that this justifies a species-level division between continental (*H. pekinensis*) and peninsular (*H. erectus*) populations.

As a postscript to the Asian lineage, it seems likely that the newly-discovered *H. floresiensis* (LB1) is a further p-deme of *H. erectus*, and an example of perhaps more extreme environmental adaptation in *Homo*. Dated by thermoluminescence and radiocarbon dating from before 38 kyr to at least 18 kyr (Morwood et al 2004: 1089), it is proposed that these representative individuals are descended from a central population of *H. erectus* (Morwood et al 2004: 1090), given the similar pattern of the indices of cranial shape in the two species. The isolation of *H. floresiensis* on the island of Flores, until the arrival of Mesolithic *sapiens* groups, suggests that environmental conditions placed small body size at a selective advantage, whether for reasons of resource availability, competition for space, the threat of predation or climate, which led to an endemic dwarfing of *H. erectus* (Brown et al 2004:1060-61). This new material is currently assigned to a separate species, although this does not affect its status as a p-deme of *H. erectus*. However, the vastly different body size of this deme negates its inclusion in this study of *H. erectus*, but nevertheless provides an interesting insight into the morphological flexibility of genus *Homo*.

Europe

Returning to Europe, Dmanisi is not the only example of an ancient hominin population in this region, although it is the only European p-deme that is included for study in this thesis. The Atapuerca-Gran Dolina p-deme (nomen *antecessor*) shows some resemblance, particularly in terms of molar dentition, to the antecedent African hominin structure, including the Nariokotome p-deme, although it does also

display a derived facial morphology. Overall however, this Spanish p-deme is generally less derived, and therefore unlike younger European populations. The associated lithic assemblage lacks Acheulean diagnostics but an estimated age of 800-900 kyr and a distinctive morphological pattern possibly precludes this deme from categorisation within a study of *H. erectus*. The isolated cranium from Ceprano, Italy, is assigned by Howell (1999: 214) to this p-deme, and indeed its classification as *H. erectus* has been contested (Ascenzi 2000, but see also Ascenzi 1996 and Manzi 2001); thus for the sake of consistency it too is excluded from the following analyses.

The remaining European p-demes under consideration could arguably belong to the species *H. heidelbergensis*, rather than *H. erectus*. The first, Mauer/Arago, is given the nomen *heidelbergensis* and dates to the mid-Pleistocene, although the time span of 0.45-0.6 myr is ill-defined. The overall rejection of *H. heidelbergensis*-related specimens from this study is based on the apomorphic features of certain cranial and mandibular elements in the Mauer/Arago p-deme, which appear to foreshadow the structure characteristic of subsequent Neanderthals (Howell 1999: 215) and therefore belong to a different line of descent.

Although this is not true of the remaining two principle p-demes from Europe (Petralona/Atapuerca-Sima, nomen *petralonensis* or *steinheimensis* and Skhul/Qafzeh), they too can be eliminated from an investigation into *H. erectus*. The Petralona/Atapuerca-Sima p-deme is represented by the large assemblage from Sima de los Huesos in Spain, and can also include Vèrtesszöllös, Swanscombe, Montmaurin, Steinheim and Bilzingsleben. The exclusion of this deme is based on the associated lithic artefacts, which vary from the biface-rich Middle Acheulean to flake-based, or Mode 3 industries; both unknown to *H. erectus* (Howell 1999: 216-217). More importantly, the European lineages are usually seen as distinct geographical groups on a separate evolutionary branch, and this thesis will mainly concentrate instead on the Asian/African dichotomy (Dmanisi is a principal exception, due to the close morphological similarities to the Koobi Fora material).

Similar to the Mauer/Arago p-deme, the Skhul/Qafzeh p-deme is disqualified by its morphology. However, in this case the skeletons of Skhul/Qafzeh more closely resemble *H. sapiens* than Neanderthals (Howell 1999: 216-217). Where *H. sapiens* is concerned, definition of autapomorphies depends greatly on modifications to the hypodigm (Wood 1984: 99, 104, 109). Where there is debate over the designation of a fossil to either *H. erectus* or *H. sapiens*, it has been excluded from my analysis. In summary, it appears that *H. erectus* was a widespread, polytypic species (Rightmire 1998: 220), populating diverse environments over a long period of evolutionary time and persisting for longer in some regions than in others. Rightmire (1998: 220) suggests that the characteristics of the Asian crania indicate a more specialised morphology towards robusticity, an evolutionary trend apparently not shared by the western demes that is likely to be a product of geographical distance. Nevertheless, regardless of the fate that met each p-deme, those included in this study are summarised in Table 2.1, grouped under the term *H. erectus* and compared as taxonomically distinct yet related populations. Thus, in this study, all fossils variously categorised as *H. ergaster* will be considered without discrimination, since the term merely applies to a subset of the overall species *H. erectus*.

Table 2.1 The *H. erectus* p-demes identified for this study

Region	P-deme	Principal specimens	Geologic age
Africa	*ergaster*	WT 15000, ER 992, 3733, 3883, 370, 1808, 820	1.7-1.5 Ma
	leakeyi	UA 31, OH 9, 12, 22, 23, 28, 36, 51	1.0 Ma
	mauritanicus	Tighenif 1, 2, 3, 4	~400 kyr
	Sidi Abderrahman	Sidi Abderrahman, Thomas Quarry I, II, III, ?Salè	~400 kyr
Asia	*pekinensis*	Zhoukoudian, Hexian, Longgudong	~580-230 kyr
	Yunxian	Quyuanhekou, ?Gongwangling	0.87-0.83 Ma (> 0.581 Ma)
	erectus	Trinil 2, 6-9	1.58-0.98 Ma
	paleojavanicus	Sangiran – Glaghomba: S5, 6, 8, 27, 31	1.77-1.66 Ma
	robustus	Sangiran – Brankal: S1, 4, 9, Modjokerto	1.8 Ma
	soloensis	Ngandong Sambungmachan	27-46 kyr 27-52 kyr
Europe	*georgicus*	Dmanisi: D2700, D2280, D2280	1.7-1.6 Ma

The stone tool record

As suggested by this brief description of the *H. erectus* p-demes, the movement and dispersal of hominin groups into new environments may be traced through its impact on technology. The increased distance from known sources, depletion or exhaustion of known source, lack of experience and knowledge of functional properties of local resources, and competitive exclusion create pressure for a change in raw material and the way it is used. Movement into unfamiliar ecosystems is likely to generate inventive behaviour in raw material use, as well as greater technological innovation (Fitzhugh 2001: 142, 145).

The simple stone tools of early *Homo* were suited to opportunistic scavenging strategies. Their use in new environments lay in the strategy of 'catchment scavenging', whereby the resources of a large territory can be exploited with minimal knowledge. These would have been effective on the dispersal east towards Asia, as they do not require supplies of good-quality stone for specialized chipping and handaxe production. This in turn allows time to be directed away from complex tool making (and its subsidiary needs of procurement, training and invention), a useful tactic in unfamiliar surroundings (Larick and Ciochon 1996).

The presence of stone tools in the Far East has been debated since Movius (1949, cited in Yamei et al 2000) first defined a boundary between East Asia and western Eurasia/Africa to describe a geographic separation in technology and behaviour during the Pleistocene. This implied that the Eastern populations were culturally and possibly genetically isolated, a theory borne out by the presence only of simple flaked tools, rather than the ovate large cutting tools (LCTs) such as Acheulean bifaces that characterise the African and western stone tool record of the same period (Yamei et al 2000: 1622). The Acheulean tools are considered to indicate enhanced planning ability and technical competence, traits that are therefore assumed to be missing from East Asian populations (Yamei et al 2000: 1622). However, *H. erectus* may have left Africa before the development of bifacial

technology; Larick and Ciochon (1996) base this idea on revised dates of 1.81myr at Mojokerto and 1.66myr at Sangiran, earlier than the emergence in Africa of the Acheulean/bifacial technique at about 1.5myr.

This East/West handaxe distinction is contested by evidence of stone tools from the mid-Pleistocene Bose basin in the Guangxi Zhuang Autonomous Region of China, which provide the oldest substantiation of LCT manufacture in East Asia (Yamei et al 2000: 1623). The finds consist of extensively chipped cobbles of quartz, quartzite, sandstone and chert. Three *in situ* tektites were dated by Ar/Ar analyses to give a representative age of 803 ± 3 kyr, which falls within the error values of previous calculations (tektite dating has yielded ages of 783 ± 21 kyr and 784 ± 12 kyr). More importantly, this date correlates these LCTs with the Acheulean artefacts of Africa, and is older than the earliest European example of this technology form. Thus, the Bose LCTs 'represent a target morphology rather than a graded continuum with other tool forms' (Yamei et al 2000: 1624), as shown by the number of refining flake scars. The available evidence suggests that there were similar technical, cultural and cognitive capabilities on both sides of the Movius Line (Yamei et al 2000: 1624).

P-demes as a biogeographical product

This thesis examines the relationship between morphology, life history and the environment, and as such, p-demes require a broader context in order to add to our understanding of *H. erectus*. The environment effects change on both a large and a small scale, through the emergence of new species and the development of new demes in existing species. These changes can be seen as either large scale responses to a continental level of environmental trends, or as the sum of small-scale changes occurring in particular times and places, in response to local competitive conditions (Foley 1999: 332). The biogeography of the hominin line, particularly of *H. erectus*, provides an evolutionary imperative for the demographic events of dispersal and contraction, fragmentation and isolation. Habitat theory (Vrba 1999) focuses on the dynamics that bind organisms and species to their habitats, and emphasises the

interactions between the genetic component of lineages, the physical context and the biotic context, which all determine habitat specificity (Vrba 1999: 22). Foley highlights the biotic element, and this is discussed below.

The development of p-demes, and thus the first step towards evolutionary change, results from variation in spatial distribution, which in turn can be linked to variation in climate and environment; indeed, changes in geographical distribution have been much more prevalent responses of species to climate change than have speciation and extinction (Vrba 1999: 22). Over the last 6.0 myr, global temperatures have steadily declined, with the resultant increase in aridity, particularly in the African environment after the development of the Rift Valley in the east, becoming the norm after 2.0 myr. Importantly for this study, hominin populations would have responded demographically and spatially to these events: expanding where reproduction exceeds mortality; remaining stable where they are in balance; or declining where mortality exceeds the reproductive rate. This in turn relates to ecological and spatial patterns, with an expanding population either increasing in density or dispersing into new regions. Similarly, a declining population is generally associated with reduced or more fragmented geographical ranges (Foley 1999: 338, 342):

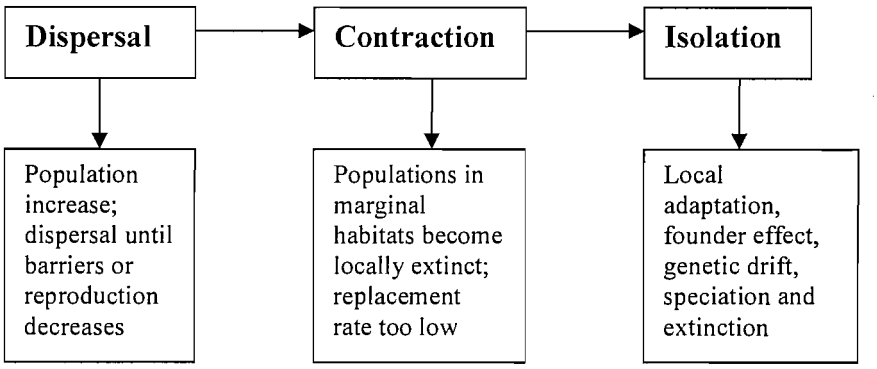

Figure 2.1 Macroevolutionary patterns and their microevolutionary processes

Using this model it is possible to see how p-demes, as regional populations, are a product of biogeographical processes. The two figures below (Figures 2.2 and 2.3)

illustrate the relationship between geographical patterns and phylogeny. Regional or isolated groups reflect geographical barriers or natural territories, with local adaptation and the chances of success depending upon the structure of resources in that area. Change over time is seen as a function of both climate patterns (through the development or failure of isolation, refugia and expansionist strategies) and of topography and vegetation, the latter also being climate dependent.

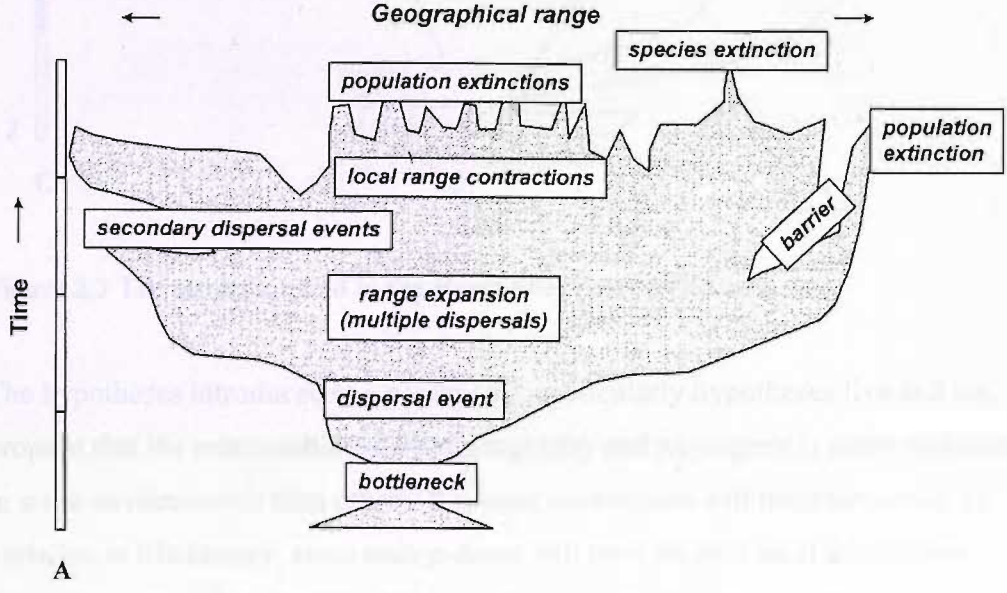

Figure 2.2 Generalised model of the evolutionary geography of a species (Foley 1999: 340)

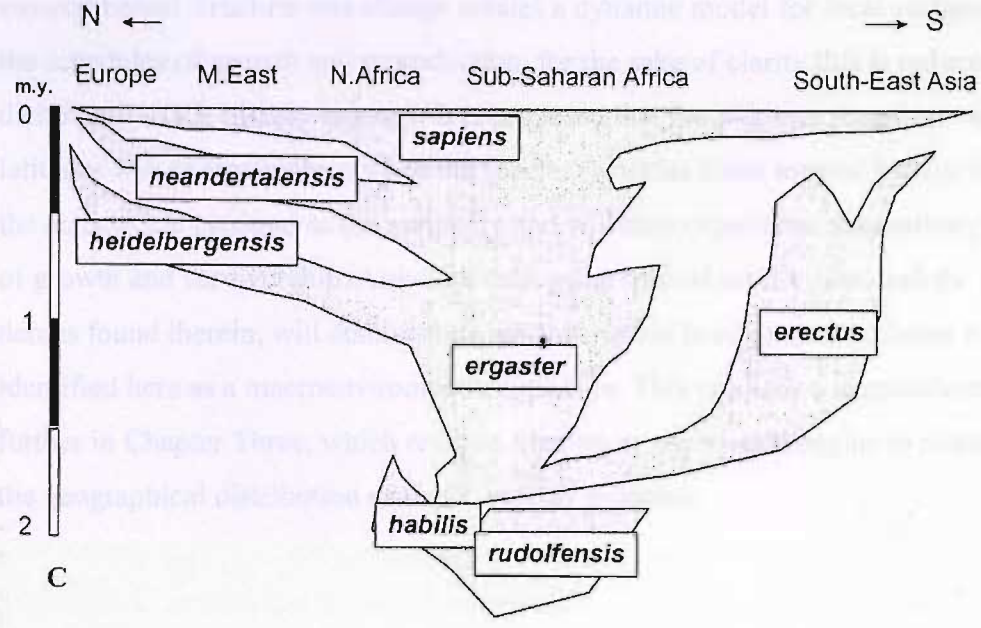

Figure 2.3 The model applied to the *Homo* line (Foley 1999: 341)

The hypotheses introduced in Chapter One, particularly hypotheses five and six, propose that the relationship between geography and phylogeny is more successful in some environments than others. Regional subdivision will therefore result in variation in life history, since each p-deme will have its own local adaptations. Climate, measured by latitude, has been shown to have a strong influence on species diversity. Species richness declines with distance from the equator, a function of energy availability, climatic stability, land surface area and temperature. Thus, close to the equator are found more species with relatively small ranges, whereas in high latitudes there are few, geographically extensive species (Foley 1999: 335). It is the indirect impact of latitude that causes this pattern, through adaptive responses to other species and intraspecific competition. The environment is experienced by a species through its effect on other species, whether as food sources, competitors or predators (Foley 1999: 333). Any variation in environment will therefore fundamentally alter a species' life history strategy.

Life history theory is examined in the following chapter, but must be considered in light of the effects of environmental variation. Placing p-demes in the context of

environmental structure and change creates a dynamic model for local variations in the schedules of growth and reproduction; for the sake of clarity this is reduced to a dichotomy in life history strategy. It is proposed that the p-demes found at tropical latitudes will comprise the core of the species, whereas those located further from the equator are grouped as the periphery and will thus experience alternative patterns of growth and survivorship. Although each geographical subdivision, and the p-demes found therein, will demonstrate microvariation in adaptation, climate is identified here as a macroenvironmental pressure. This prediction is considered further in Chapter Three, which reviews life history theory and begins to relate it to the geographical distribution of the *H. erectus* p-demes.

CHAPTER THREE

Evolutionary ecology and *Homo erectus*

Modern human life history is composed of a number of interlinking elements that combine to create a unique set of traits: a large brain for body size; helpless young; an adolescent stage of growth, and post-reproductive longevity. This chapter examines the relationship between these features within an ecological context, in order to explore their development and evolution in the *Homo* lineage, with particular reference to *H. erectus*.

The timing of these events in *H. erectus* has implications for the energetic costs of growth and reproduction to the individual at different times of life, and the subsequent survival strategies adopted, particularly important in a species with wide geographic distribution such as *H. erectus*. The spatial and temporal depth of *H. erectus* sites testifies to an ability to cope with environmental change and avoid extinction, suggesting the importance of the relationship between the environment and life history traits.

The theoretical foundation of this thesis lies in an exploration of competing models of evolutionary ecology, which are then related to the *Homo* lineage. This chapter reviews the key elements of evolutionary ecology, beginning with the evidence placing mortality and body size at the heart of life history, identifying the ways in which these factors both impact upon the timing of birth, growth and reproduction. This is followed by an examination of *r-K* theory and the link it posits between birth, death and the environment. The shortcomings of this dichotomy, with respect to age-specific mortality, are addressed by the introduction of the bet-hedging strategy. By relating age at death to life history strategy within an ecological context, it is possible to establish the relationships between encephalisation, growth and the risk of mortality in a range of environments. This theoretical overview will produce an integrated understanding of *H. erectus* life history strategy, even if all the composite traits cannot be determined from the archaeological record. Moreover, when taken in

conjunction with the biogeography of p-demes, examined Chapter Two, this will create a more coherent and informed ecological model for *H. erectus* life history, which can then be tested in the following chapters.

Energy allocation and trade-offs

Life history can be defined as:

> the allocation of an organism's energy toward growth, maintenance, reproduction, raising offspring to independence, and avoiding death...[in mammalian terms] it is a strategy of when to be born, when to be weaned, when to stop growing, when to reproduce, and when to die...[Life history theory] needs to explain how humans evolved long gestation and large neonates for body weight, few young, an extended period of offspring dependency, slow growth, delayed reproduction ...helpless young, an unusually high rate of postnatal brain growth, a brief duration of breast feeding, an adolescent growth spurt, intense maternal care...and menopause (Smith and Tompkins 1995: 257-258).

Traditionally, the study of life history relies on the trade-off between the energy allocated for reproduction and one or more of a number of traits, such as growth, storage, maintenance and future reproduction (Jordan and Snell 2002: 44). Within that initial allocation, there is a further trade-off between offspring number and offspring size (Jordan and Snell 2002: 44). In other words, when a beneficial change in one trait is linked to a detrimental change in another, a trade-off is said to have occurred (Stearns 1989: 259). Although there must be costs associated with a change in resource allocation, the ultimate aim is to maximise lifetime reproductive success by achieving the optimal life history for a given environment (Reznick et al 1986: 1338).

Three distinct forms of trade-off may arise during the life of an individual. Allocation trade-offs result from the allocation of available resources, and this is the theoretical path most commonly followed by life historians. Acquisition trade-offs focus on the maximisation of resources and the minimisation of the risk of mortality, while trade-offs that result from specialisation for a given environment are known as specialist-generalist trade-offs (Angilletta Jr et al 2003: 234).

One example of the costs incurred in the allocation trade-off between reproductive investment and survival is found in a study of the reproduction of Galapagos lava lizards, which experience large seasonal and annual variation in rainfall (Jordan and Snell 2002). It was found that the life history variables of individual females (body length, egg mass, clutch size) responded to environmental change, allowing mothers to modify their total reproductive investment. By comparing individuals within the same environment during the same time period, it was possible to identify weakened relationships and thus trade-offs (Jordan and Snell 2002: 48,49).

However, the value of trade-offs as a strand of evidence is reduced by the difficulty of observing them in the natural environment (Stearns 1989). For example, the costs of reproduction are hypothetical and not easy to show through empirical research (Reznick et al 1986: 1338). One way of identifying and evaluating them is to measure the correlations between life history variables. Rather than concentrating on the cost of the trade-off, instead one can examine the relationship between variables and the direction of influence (Reznick et al 1986: 1338). For example, the relationship between age at first reproduction and life span might be expected to show a negative correlation: if reproduction is delayed, then the life span should be extended to compensate. It is thought that negative correlations will arise predominantly in populations living in stressful environments, suggesting that reproductive cost is more likely to occur when resources are scarce (Bell 1986: 1344). This allows for a link to the core-periphery model posited in Chapter One, whereby life history strategy is altered within a species according to environmental status.

Models of life and death

The relationship between life history traits is therefore of primary importance, and this is developed at length by Charnov (1991). He found that several life history variables scale as a function of adult body size, each with an exponent near 0.25. Age at maturity, life expectancy at birth and life expectancy at maturity all produce positive relationships with body size (unless indicated otherwise, body size is taken

to specifically refer to female mass throughout the thesis), while fecundity is negative. These variables retain their correlation even when body size is held constant, and in a log-log regression, deviations from the line are also correlated with each other. For example, taxa with relatively high ages of maturity also have relatively low adult mortalities (Charnov 1991: 1134).

The association between adult instant mortality rate (M) and adult body size (W) is explained by the equation (Charnov 1991: 1135):

$$M = 0.75 \cdot A \cdot W(\alpha)^{-0.25} \qquad \textbf{(1)}$$

Here, A is a growth coefficient and $W(\alpha)$ is body size at maturity (α). Thus, adult body size is determined by mortality through the evolution of α. This scaling is expected because life expectancy is a direct function of the inverse of mortality rate (Charnov 1991: 1134-5).

Evolutionary models for α (or W_α) generally assume that the capacity to reproduce increases within a species as maturation is delayed, but with a mortality cost (i.e. the greater the delay, the greater the chances of dying before reproductive maturity is reached), since after age α resources are directed either towards reproduction (R; mass per unit time devoted to reproduction) or keeping alive, reflected by E. The optimal α (W_α) will therefore balance these two events (Charnov 2001a: 526), giving a benefit-cost ratio in E/α, the time available to reproduce, where E is the benefit (adult lifespan spent in reproduction) and α the cost (time spent preparing to reproduce) (Charnov 2002: 749).

When the adult mortality rate is given as $1/E$, this creates a second benefit-cost ratio in R/E^{-1} (Charnov 2002: 750). Species of larger body size usually also have larger R and E, allowing the fraction of body mass given to reproduction per unit of time (C) to be represented by R/(body mass). Thus, the dimensionless ratio C/E^{-1} is the fraction of a body mass given to reproduction per unit of adult death (E^{-1}), and this

benefit-cost ratio may be useful, together with E/α, in classifying life histories across various species (Charnov 2002: 750). This approach looks for invariants in the outward life history (e.g. $C \cdot E$, E/α) and thus in the trade-offs that generate the optimal set of life histories (Charnov 2002: 752).

The ultimate aim of natural selection is to maximise R_0, the net reproductive rate and a measure of Darwinian fitness. R_0 is the average number of daughters produced over a female's lifetime (Charnov 1991: 1134), and can be conceived as the product of the offspring size efficiency times an efficiency of the form total reproductive allocation divided by parental mortality (Charnov 2001b: 873). In this way, R_0 is both a measure of an individual's fitness, as well as a population parameter with a value of ≈ 1, due to density dependence holding population size approximately stable. In a stationary population of this type, R_0 can always be written as (Charnov 2001b: 873):

$$R_0 = S \cdot b \cdot E \qquad \textbf{(2)}$$

where S is the chance of survival to the age at first reproduction, b is average fecundity (number of daughters) per unit time for adults, and E is the average length of the adult lifespan. $S \cdot b$ (B, the rate of production of female babies alive at age α) should generally trade-off against E, since effort expended on offspring production should decrease the mother's own reproductive lifespan. The optimal balance between B and E is -1, an economic model that holds for all age-structured life histories when fitness can be measured as R_0 (Charnov 1997: 393).

It is possible that this model can be tested by the use of average adult body mass (W) for a species, since across many taxa the following hold approximately true (Charnov 2001b: 875):

$$R \propto W^{0.75} \text{ and } M \propto W^{-0.25}$$

Thus,

$$R/M \propto W \quad \textbf{(3)}$$

In addition, average adult lifespan (E) and age at maturity (α) also scale as quarter-power allometries with female body mass across typical mammal species (as mentioned above). When applied to primate species, the log-log lines on a regression are displaced upwards compared to typical mammals. Thus, both mammals generally and primates specifically show E and α proportional to $m^{0.25}$ but differ in the proportionality constant, which is bigger for primates (Charnov 2004: 37), giving them a later age at first reproduction than an average mammal of the same size. As body size increases, the difference between 'mammal' α and 'primate' α also increases (Ross 1998: 55). Similarly, both groups show a negative quarter-power scaling for the number of offspring produced per year (b), although in this case the primate line is displaced downwards by comparison (Charnov 2004: 307).

Charnov's work thus far serves to underline the central role of body mass in the timings of certain events in life history, such as mortality and age at first reproduction. This provides a way to examine demic variation in *H. erectus*, within the broad categories of 'tropical' and 'temperate', defined by latitude and climate as set out in Table 1.1. In addition, he consistently emphasises the role of mortality in determining both the age at first reproduction (α) and the total lifespan (E), since the prolonged period of juvenile growth in primates would necessarily result in higher rates of pre-reproductive mortality (Kennedy 2005: 125). Indeed, the low growth rate seen in primate species may be caused by a negative association between mortality rates and growth rates, in that primates may increase their chances of reaching age at first reproduction if the disadvantage of delaying maturity is outweighed by an advantage of low mortality rates when growth rates are low (although this is based on the assumption that juveniles are more susceptible to food shortages and starvation than adults) (Ross 1998: 55). Therefore, delayed reproduction seems to be expected in association with relatively low adult mortality

and a long lifespan. If this is the case, then slow growth may partly reflect a cost, rather than a benefit, of growing a large brain (Kennedy 2005: 125).

The timing of growth and reproduction, and their relationship to both adult and juvenile mortality rates, will be structured in order to maximise reproductive success (R_0) and offspring investment, within the confines of the energetic and metabolic demands of the environment. A causal chain for a female mammal is presented below in Figure 3.1 (Hill and Hurtado 1996: 39):

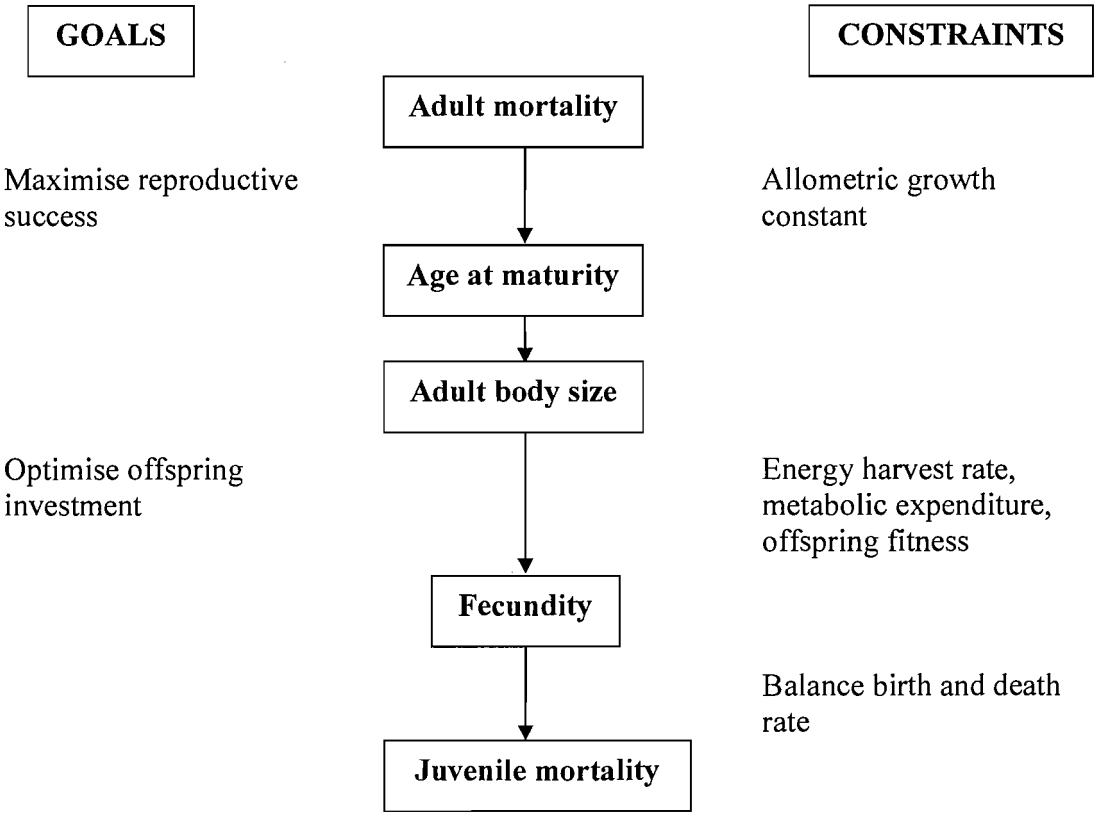

Figure 3.1 A causal chain of life history variables among female mammals (Hill and Hurtado 1996: 39)

The pace of juvenile growth thus appears to influence the timing of events throughout primate life histories, since the level of energy associated with growth matches that available for reproduction, once allocation switches from growth to reproduction. Indeed, extrinsic adult mortality rates in combination with the juvenile

growth rate may be the most important initial variables in limiting the parameters of life history traits that would maximise the fitness of an organism (Hill and Hurtado 1996: 31). Higher fecundity is related to an increase in body mass, so with each additional year devoted to growth, reproductive rate is expected to increase (although an upper limit constraint on body size will eventually bring diminishing returns to increased body size). The timing of the switch between reproductive rate and reproductive span is a fundamental trade-off in life history (Johnson 2003: 84) and is represented by the equation (Charnov 1997: 393):

$$R_0 = S(\alpha) \cdot V(\alpha) \qquad \textbf{(4)}$$

Here, $S(\alpha)$ is the number of offspring surviving until reproductive maturity. $V(\alpha)$ equals $b \cdot E(\alpha)$, the average production of offspring over the adult lifespan. In this trade-off model, S goes down with α, while V goes up. As fitness (R_0) is a product of ($S \cdot V$), the optimum is -1 (Charnov 1997: 393).

The mathematical models presented here describe general rules for life histories in mammals, and provide hypotheses about the shape of the aggregate trade-off surfaces at the equilibrium, although of necessity they ignore age-dependent allocation decisions (Charnov 1997: 394). However, having established a template for the optimal solutions governing the reproductive behaviour in an 'average' primate, it is possible to place this idealised primate in varying ecological conditions to see how it would respond. Since raw mortality data are available for very few primate populations, ecological variables are substituted into the causative relationship, as it is generally assumed that certain types of ecology are linked to certain patterns of mortality. Even so, the nature of the relationship is poorly understood (Ross 1998: 57):

ecology → mortality pattern → life history

In primate species it is usually assumed that highly variable, unpredictable environments will lead to high mortality among individuals of all age classes, but particularly among infants and juveniles. However, this supposition is neither supported nor refuted by direct mortality data from primate species. Despite this, it is in part reinforced by evidence which suggests that animals who feed on food that is easy to find and process (e.g. folivores with unseasonal food supplies) should have faster growth rates than species who have more complex feeding strategies (such as insectivores or frugivores with seasonal patchy food supplies) (Ross 1998: 56, 58). The latter scenario will favour slow-growing, energy-efficient offspring, but leave them vulnerable to competition, predation and starvation, thus raising their mortality risk. Moreover, increasing density and associate resource competition and nutritional stress generally leads to increased juvenile morality, thus raising the age of sexual maturity and lowering the birth rate. Finally, adult mortality will increase as a result (Hill and Hurtado 1996: 34).

Environmentally-led variation in mortality rates (extrinsic mortality) may have a strong influence over the costs and benefits of different trade-offs. For example, when divided into habitat groups, primates living in open, unpredictable habitats were found to have higher r_{max} values (the maximal rate of increase of a population) relative to body size than did those in more predictable habitats, resulting in higher birth rates and an earlier age at first reproduction in the unpredictable habitats (growth rate was unaffected by any measure of environmental variation). Rather than representing an adaptation to a predictable, competitive environment, this may instead demonstrate that forest species have low mortality rates for their body size, a characteristic commonly found in conjunction with a low age at first reproduction in mammals. One consequence of this for life history trade-offs is that, if juvenile mortality rates are high, individuals are unlikely to be able to trade the disadvantages of delayed reproduction for the advantages of increased fecundity at a later age, as that would risk death before reaching that age at which reproduction could commence (Ross 1998: 58-59).

Life history and environmental polarities

While the mathematical principles developed by Charnov focus on the trade-offs between life history events and their relationship to body size, Ross's ecology-mortality model above indicates that variation in the environment must be taken into account, due to its impact on growth patterns and consequent influence over the timing of reproduction and mortality. The link between life history strategy and variation in the environment, as suggested above, allows for the characterisation of species as either *r*- or *K*-selected strategists respectively, a theory first developed by MacArthur and Wilson (1967) to describe broad population trends. Different life history traits are selected according to a distinction between nonseasonal, stable and predictable environments, and seasonal fluctuating ones. The reproductive strategy of *K*-selected species is to spread out their reproductive effort over a longer lifespan, through large, single-born offspring, aided by a stable and predictable environment. Alternatively, *r*-selected species, such as some birds and fish, tend to give birth once to many small offspring, due to the uncertainties of a fluctuating environment. Primates are generally thought of as *K*-selected; by extension, *H. erectus* is also considered to be a *K*-selected species.

Environmental circumstances dictate which of the two strategies would be most advantageous, and in turn give rise to specific behavioural characteristics associated with each. The parameters of the more predictable environment are less likely to exceed the tolerance limits of the species occupying them (e.g. temperature, rainfall, diet breadth or competition), and so there is a higher chance that animals will survive from one breeding season to the next (*K*). This is not the case in unpredictable, fluctuating environments, increasing the uncertainty of long-term survival (*r*) (Richard 1985: 281). However, just as an environment is never completely stable and predictable, so organisms are never completely *r*- or *K*-selected, but instead are located along a continuum (Pianka 1970: 592). The position of *H. erectus* on the *r*-*K* continuum has implications for its life history strategy and its means of survival in varying habitats, and is investigated below.

Population density is regulated according to the demands and predictability of the environment. *K* signifies the carrying capacity of the environment (MacArthur and Wilson 1967: 78), which will limit the maximum size of the population and is defined as:

$$K = (\lambda / \mu)^{k}$$

(where λ = the per capita birth rate and μ = the per capita death rate)

The power factor *k* again represents carrying capacity, and indicates that the relationship between the schedule of births and deaths is dependent upon and modified by it.

Alternatively, $K = r(\lambda + \mu)$

Here, *r* is the intrinsic rate of increase of a population (the rate at which an age structured population increases with constant birth and death schedules [Stearns 1992: 222*g*]). The sum of the slopes of the birth and death rates ($\lambda + \mu$) is equal to z, or *r*/*K* (MacArthur and Wilson 1967: 78). This factor, *z*, is the density-dependent constant that is analogous to the density-independent constant r_{max} (Pianka 1994: 187), mentioned above and described in more detail below.

With the alternative pattern of *r*-selection, *r* can simply be defined as $\lambda - \mu$, although this does not indicate how *r* is related over time to the schedule of births and deaths in a real population. A good colonizer would be expected to maximize the ratio λ / μ, as the aim would be to achieve a large *r* through a low mortality rate, rather than by a high birth rate (MacArthur & Wilson 1967: 83, 88).

Figure 3.2 illustrates the relationship between *r*, *K* and population density. For these two hypothetical populations, K_1 and K_2 are the carrying capacities of the *r* and the *K* strategist respectively (taken from Pianka 1972: 583):

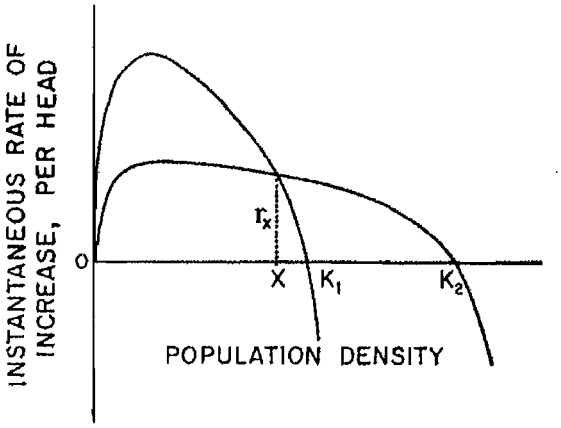

Figure 3.2 The instantaneous rates of increase for two hypothetical populations and the relationship between life history strategy and population density (Pianka 1972: 583)

At density X, the rates of increase of both populations (or species) are identical. To the right of X the *K* strategy is competitively superior; to the left the *r* strategist takes precedence. Density-independent rarefaction reduces the rate of increase by the same amount at all densities. If this rarefaction proceeds at a rate greater than r_x then selection will favour the *r* strategist. If the removal rate is less than r_x then the *K* strategy will be favoured (Pianka 1972: 583). Once the maximum population size (*K*) has been attained, populations will tend to reduce their intrinsic rate of increase, or *r*. At the same time, *K* will tend to increase as a result of finer adaptation to the local environment. From that point, relative amounts of *r*-selection and *K*-selection will depend on fluctuations in the local environment (MacArthur & Wilson 1967: 178).

Locating the *r*-*K* continuum within an ecological context makes possible the identification of different traits in *H. erectus*. Table 3.1 (from Pianka 1970: 593) provides a series of correlates that would be expected to apply to overtly *r*- and *K*-selected species. In terms of survivorship, Pianka (1994: 149) made the following distinctions:

Table 3.1 Suggested correlates of r- and K-selection (Pianka 1970: 593)

	r-selection	*K*-selection
Climate	Variable and/or unpredictable; uncertain	Fairly constant and/or predictable; more certain
Mortality	Often catastrophic, non-directed, density independent	More directed, density dependent
Survivorship	High juvenile mortality (Often Type III)	More constant mortality (Usually Type I and II)
Population size	Variable in time, non-equilibrium; usually well below carrying capacity; unsaturated communities; ecological vacuums, annual recolonisation	Fairly constant in time, equilibrium; at or near carrying capacity; saturated communities; no recolonisation necessary
Intra- and interspecific competition	Variable, often lax	Usually keen
Selection favours:	• Rapid development • High maximal rate of increase • Early reproduction • Small body size • Single reproduction • Many small offspring	• Slower development • Greater competitive ability • Delayed reproduction • Larger body size • Repeated reproduction • Fewer, larger progeny
Length of life	Short, usually less than 1 year	• Longer, usually more than 1 year
Leads to:	Productivity	Efficiency

Pianka drew the distinction between types of survivorship from a 1947 paper by Deevey, written at a time when life history was only just emerging as a sub-discipline of ecology. The three survivorship curves identified are represented in Figure 3.3 (Deevey 1947: 285):

Type I – little mortality until some age, then fairly steep thereafter

Type II – constant risk of death/numbers of deaths per unit time

Type III – steep juvenile mortality and relatively high survivorship thereafter

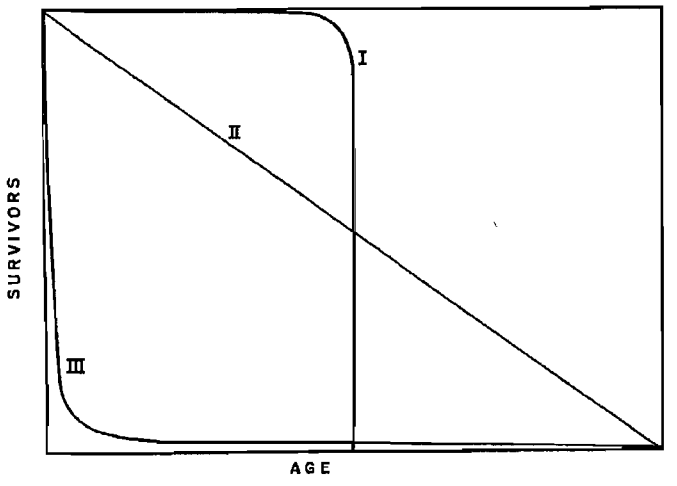

Figure 3.3 Schematic representation of theoretical types of survivorship curve (Deevey 1947: 285)

Type I is the negative skew triangular; Type II is the diagonal (the logarithm of number of survivors against age); and Type III is the positive skew triangular. Under this system, *r*-selection has been associated with Type III survivorship, in that high juvenile mortality would be expected. The clearest explanation for this is that an organism must reproduce as soon into its own life span as possible, because of a greater risk of death due to an unpredictable environment. The population can thus be imagined as very young, with an overall short life span, and a high juvenile to adult ratio. This makes it statistically more likely that juvenile mortality will be higher. In opposition, *K*-selection is linked to the Type I and II patterns of mortality, since juvenile survival is low and adult mortality is fairly predictable, leading to a constant yet non-catastrophic risk of death.

Body size and life history

When MacArthur and Wilson (1967) first developed their theory it was explicitly microevolutionary. However, it was adopted and scaled up for use on mammals, by comparing them with insects. Since body weight influences most life history traits (as set out above; see also Stearns 1992: 105; Savage et al 2004: 430), this assumption proved to be problematic. In data where the effects of weight were not removed, the population parameters indicated by *r*- and *K*-selection were strong,

accounting for 68% of co-variation in 10 life history traits. When weight was factored in, the strength of the pattern was reduced by 26% (Stearns 1992: 105).

Age at maturity (i.e. the age at first reproduction) is strongly correlated with adult body size in 65 mammalian species (given as Equation 1 above). Table 3.2 demonstrates the effect of body weight on calculations of age and fecundity, and makes clear that any model for life history must take adult body size, and thus lifespan, into account:

Table 3.2 Correlations between life expectancy (LE), age at maturity (α) and fecundity (Fec) (from Stearns 1992: 127)

	Birds			**Mammals**		
	LE	**α**	**Fec**	**LE**	**α**	**Fec**
LE	*1*	0.78	-0.81	*1*	0.70	-0.55
α	0.85	*1*	-0.74	0.79	*1*	-0.56
Fec	-0.87	-0.83	*1*	-0.77	-0.80	*1*

Below the diagonal: before effects of adult weight are removed. Above the diagonal: after effects of weight are removed.

Similarly, body size affects the replacement rate of a population (the average number of female offspring left during the life of each female: R_0). Under optimal conditions, when R_0 is as large as possible, the maximal rate of natural increase (r_{max}) is achieved (MacArthur and Wilson 1967: 87-88). This measure varies among animals by several orders of magnitude, with small, short-lived organisms having a relatively higher r_{max} value than larger and longer-lived organisms such as humans (Pianka 1994: 158).

Reproduction is also influenced by body size through the increased period of growth required for maturation. Figure 3.4 (adapted from Foley 1987: 146) links these factors together:

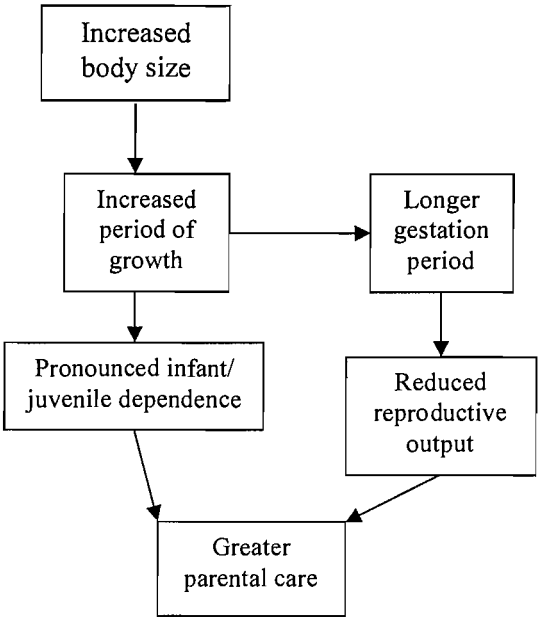

Figure 3.4 Suggested links between increased body size and selected life history traits (based on Foley 1987: 146)

An increase in body size requires a longer period for growth, which can have two effects: the infant is vulnerable and dependent on its parents for longer, and also requires a longer gestation period. This has an impact on the parents, particularly the mother, since a longer pregnancy, as well as the metabolic demands of a helpless infant, means that birth-spacing must also increase, thereby reducing reproductive output. The greater vulnerability of the slow-growing infant demands a higher degree of parental care, whereas the latter condition of increased birth-spacing promotes parental care almost as a by-product.

Neonatal mammals generally follow one of two possible patterns in the development of their offspring, and Figure 3.4 links these patterns to body size. Altricial young are immature and helpless, lacking hair, hearing, vision and locomotor capacity, while their precocial counterparts are far more developed, with these features at a relatively advanced stage. Altricial mammals are also born in large litters after a short gestation period, and have a smaller brain for body size. The opposite condition in precocial offspring is explained by the greater proportion of growth that takes place in the womb, compared to that of the altricial species. Although modern

humans have a large brain and are born singly (or as twins), they are not classified as precocial as they lack the relative locomotor skills seen in other primates (Taylor Parker 2000: 296). Instead, humans are described as secondarily altricial, a condition made necessary by the high degree of encephalisation that the species has undergone. If gestation were to continue until somatic maturity were equivalent to that seen in the great apes, the brain would have become too large to fit through the female pelvic inlet. As a result, the brain at birth is only a quarter of full adult size, and somatic growth is arrested during the first two years of life to allow diversion of resources into the growing brain. These increasing metabolic demands mean that the pattern of human life history must thus diverge from the standard primate model (Kennedy 2005: 133). The role of brain size in *H. erectus* life history is examined in more detail in Chapter Five, and forms an integral part of the ecological model constructed below.

Problems and gaps in the *r-K* polarity

Although *r-K* selection seems to be an adequate means of identifying population trends and subsequent life history traits, and allows for a way of showing where a species is in a life history continuum, it is an unsuitable and incomplete tool for analysis. The primary problem is that the theory is structured at the level of population regulation, rather than examining the demographic mechanisms involved. Population processes are reduced to statistical description and there is no discussion of the selection pressures on individual organisms (Stearns 1992: 206). The central role of mortality rate in setting the pace of life history events is denied, and it does not measure fitness in terms of offspring quality or number. For example, experiments on fruit flies (Taylor and Condra 1980) found that although the *r*-selected strains exhibited rapid development, the *K*-selected group experienced higher survivorship, a likely result of increased parental investment. However, there was very little correlation between the *r-K* model and body size, and between the model and elements of reproduction, such as fecundity and timing of reproduction (Taylor and Condra 1980: 1191-2). Therefore, according to this theory there is no indication that life history strategy corresponds to ecological circumstances.

Furthermore, this approach excludes hypotheses based on age-specific models of selection. Ecological differences may exist among individuals of different ages, or different developmental stages, within the same population. The division of environment type into 'variable' and 'stable' might then not hold true for every member of the population (Barclay and Gregory 1981: 944-5). Thus, the age structure of a population is important when examining its life history strategy, since it can be used to determine the direction and extent of energy allocation. When the age structure is factored in, two conclusions are generally seen: if a variable environment predominantly affects the mortality of adults more than the young, then *r*- and *K*-selection are predicted in variable and stable environments respectively; however, if the effect on juvenile mortality is greater, then the results are approximately opposite (Barclay and Gregory 1981: 945). This methodology, analysing the fluctuations in adult and juvenile mortality, has been named 'bet-hedging' (Stearns 1976), and is described in detail below.

The use of *K* as a function of life history traits carries serious problems, since it cannot be expressed in terms of reproductive fitness or as a population parameter. If a trade-off does exist between *r* and *K* then it is likely to be due to physiology and social behaviour, and as such vary from species to species and not be mediated by demographic or density-dependent means in a predictable manner (Stearns 1977: 155). This form of trade-off cannot be characterised in the same way as those models presented by Charnov and discussed above. Thus, it is apparent that the use of the terms *r*- or *K*-selected, even if only as labels for sets of reproductive traits, implies a type of causation that has yet to be established (Stearns 1992: 207).

The bet-hedging strategy

The population predictions of *r*-*K* selection rely on the categories 'density dependent' and 'density independent', but these contain age-specific selection pressures that are capable of reversing the interpretation of a group's life history strategy (Stearns 1992: 206). For example, density-dependent mortality applied equally to all age classes selects for increased reproduction early in life, which the

model identifies as being *r*-selected in density *in*dependent regimes. The age-specific effects of the mortality must be analysed, in addition to the mode of population regulation that generates the mortality (Stearns 1992: 207). It is not surprising that the dichotomy fails for 50% of the species for which there is data (Stearns 1977: 168), and so it will not be relied upon here.

A more useful method of constructing life histories than that proposed by the *r-K* polarity, in contrast to previous studies, is the alternative approach of the bet-hedging strategy. With its focus on age-specific patterns of mortality, identified by Charnov as a vital factor in understanding patterns of life histories, it takes precedence in this thesis, as this returns the influence of mortality on reproduction and growth to the centre of life history theory. The bet-hedging model suggests that fluctuating environments will favour individuals with a long lifespan and who have a few offspring at a time throughout adulthood. In this way, they maximize the chance of leaving descendants by spreading out their reproductive effort, instead of producing all their offspring at once, when there is a chance that all the offspring born in a particular year will die. Thus, the main predictive direction is towards populations in which mortality rates are greatest or most uncertain among juveniles (Richard 1985: 282).

When there is variation in the optimal number of offspring from generation to generation, fitness is measured by the geometric means of reproductive success taken over generations, rather than by the arithmetic mean fitness. The geometric mean of n numbers is the nth root of their product. If the numbers vary, then the geometric mean is always less than the arithmetic mean, and generally becomes smaller as the numbers averaged become more variable. Thus, reducing the variance of the fitness of a genotype over generations will increase its geometric mean fitness, even if the reduction of variance also involves a reduction of the arithmetic mean (Philippi and Seger 1989: 41).

If mean reproductive success evolves independently of the variance, then the fittest genotype has the lowest variance for a given mean. Therefore, this hypothesis is unconstrained by the costs of reproduction in terms of adult mortality. In real terms, a bad year will affect a larger clutch size much more than a smaller clutch. It pays to reduce reproductive effort in order to live longer and reproduce more times, sample a greater number of reproductive conditions, and thereby increase the number of offspring born in good conditions. This is the bet-hedging strategy (Stearns 1992: 167-169). Figure 3.5 demonstrates the hypothesis in action through a series of observations of great tit reproduction:

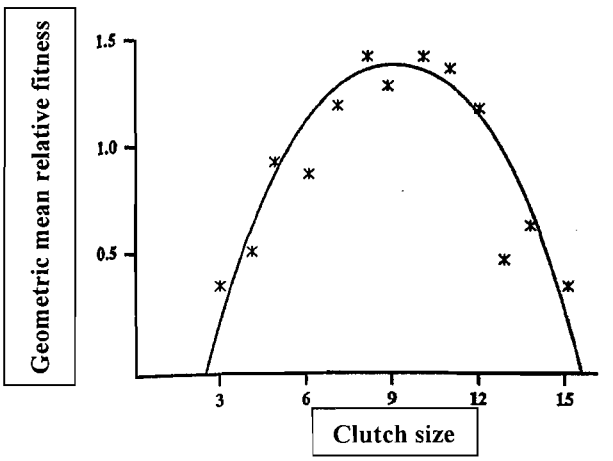

Figure 3.5 Geometric mean fitness as a function of clutch size for great tits (Stearns 1992: 169)

The environment varies in time and space with respect to probabilities of offspring survival. In a more variable environment, parents must achieve a given probability that a certain mean number of offspring will survive at least until the age of first reproduction by producing more clutches. In relation to the bet-hedging strategy explained above, the parent faces a trade-off between the mean and the variance in the mean number of offspring produced. If lowering the mean will reduce the variance, then higher geometric mean fitness will result through a lower mean per generation fitness. However, this will only be the case if the reduction in the mean brings about enough of a reduction in the variance (Stearns 1992: 193).

If a genotype AA has a phenotypic value of *a*, then as *a* grows larger the population is more responsive to selection, since gene effects are magnified. When successive environments are strongly correlated (in hypothetical, modelling terms to mean a more stable environment), then there is an optimal value of *a* approximate to the environmental variance. When the correlation between successive environments is less strong, then the greater the genetic flexibility and the lower the overall fitness. It follows that in a poorly correlated sequence of environments it is much better not to try to track the changes that occur, but to have a constant phenotype at the average optimum. Conversely, when environments are more strongly correlated one after the other, it is more beneficial to have a degree of genetic variance and track the environment (Lewontin 1965: 89-90). This principle, used in conjunction with geometric mean fitness, supports the view that bet-hedging emerged as a feature of unstable or poorly correlated environments. But how do we go from this stance to asserting that a bet-hedging strategy necessarily involves an increase in juvenile mortality, or risk of mortality?

Iteroparity is the act of reproducing repeatedly over the course of the life span, and although it is an ineffective method of increasing the intrinsic rate of increase *r*, it is widespread, suggesting a competitive advantage. It might, along with long life and late maturity, have been the product of either an environment in which density-independent factors (such as the weather) cause wide variation in the survival of pre-reproductives, or of an environment that is biologically inhospitable to pre-reproductives because of intense competition with the reproductives (Murphy 1968: 391-2).

According to *r-K* theory, populations that are near the carrying capacity of the environment tend to result in stable juvenile and adult mortality. However, iteroparity is favoured in situations of high adult survival and a variable environment, in which either offspring number or juvenile survival varies rather than adult survival (Ranta et al 2000: 299), since there is uncertainty in the survival of juveniles to reproductive maturity. The complementary system of semelparity

(reproducing only once) arises in situations of high or variable adult mortality, leading to early reproduction, high fecundity, and few or single reproductions (Murphy 1968: 392).

The physical expression of the bet-hedging model is very similar in appearance to that of *K*-selected species, but for an entirely different reason, as explained in the following summary of the population corollaries of the three theories. Table 3.3 below is based heavily on Alison Richard's work (1985: 283), but she had originally transposed the probability of dying for juveniles and adults in *K*- and *r*-structured environments, contrary to that shown below. The predictive direction of mortality in *K*- and *r*-selected species is maintained below according to that first postulated by MacArthur and Wilson (1967) and subsequently found in Pianka's approach (1970). To this is added the proposed population corollaries for the bet-hedging model:

Table 3.3 The population corollaries of three environmental survival models (based on Richard 1985: 283)

Environment	Probability of dying	Individual life history traits	Adaptive explanation	Population corollaries
Stable	Constant/ stable mortality	Slow maturation, long life span, few young, high level of parental care (*K*-selected)	Competition	Stable size; regulation density-dependent; slow dispersal
Unstable	High among juveniles	Rapid maturation, short life span, many young, low level of parental care (r-selected)	Taking maximum advantage of favourable conditions that are unlikely to persist	Unstable size; re density-independent; efficient dispersal mechanisms
Unstable	High among juveniles; or less variation in adult survival	Few young at a time, reproductive effort spread over many seasons (many traits characteristic of *K*-selected species)	Bet-hedging	Density dependent; less stable size than for K-selection

It might be supposed that increased competition, thought to characterise *K*-selection, would make juveniles more vulnerable during times of food scarcity and, thus,

increase their risk of mortality, a hypothesis at odds with the constant Type I or Type II mortality patterns seen in *K*-selected species. However, it must be remembered that bet-hedging is not only beneficial in situations of greater variation in juvenile survivorship, but also in conditions of less variation in adult survivorship (Sibly et al 1991).

I propose that the bet-hedging strategy would result in a survivorship curve resembling Type II in Deevey's classification. As stated above, a long-lived species in a fluctuating environment will be adapted for iteroparity, in order to offset any adverse density-independent factors that might lower the survival rate of immature individuals. An unpredictable environment, according to MacArthur and Wilson (1967) and Pianka (1970), is a corollary of *r*-selection, which is understood diagrammatically as having a Type III survivorship curve due to the uncertainty of juvenile survival. A bet-hedging approach would offset the risk of juvenile survival by spreading out reproductive effort and effectively lift the steep drop of the Type III curve, creating a curve closer to Type II.

It has been demonstrated that *r-K* theory is inadequate without recourse to age-specific analyses of demography, and this is examined in detail in the following chapter with particular reference to the final aspect of bet-hedging – the level, or risk, of juvenile mortality. If juvenile mortality is high, then the rate of growth during the juvenile period would also be high in order to lower α and thereby increase the reproductive span. This has repercussions for adult lifespan through the benefit-cost ratio of E/α, with fitness (R_0) as a product. However, it is impossible to tell on the basis of survivorship alone if *H. erectus* was a bet-hedger; instead the stability of the environment of *H. erectus* is important for determining this, as an unstable environment will promote a bet-hedging strategy. This question is further examined in Chapters Seven and Eight, where cranial morphology is explored in relation to environment in modern humans and in *H. erectus*.

Habitats do not map directly onto life history strategies (Stearns 1992: 207-208) but can affect the mortality regime. The environment remains a framework within which to consider questions of fecundity and mortality schedules. The environmental correlates given above in Tables 3.1 and 3.3 indicate that a stable environment is associated with a pattern of constant mortality (although growth rate and body size may be a greater influence), while a bet-hedging strategy is most advantageous in an unpredictable environment, in order to reduce the variance in the mean number of offspring. The environment can allow for a differentiation between '*K*-selection' and bet-hedging, and the development of a model of age-specific mortality. In both cases there are few, large offspring, but the mechanism is not the same:

For '*K*-selected' *H. erectus*:

Stable environment + few young = low juvenile mortality

For 'bet-hedging' *H. erectus*:

Unstable environment + high juvenile mortality = few young

Thus, climate and environment are important predictors in determining the nature of *H. erectus* life history, and it is possible that there is a divergence between the geographical regions of this particular species on the basis of environmental variation, as suggested by the model above. Although it is outside the bounds of this particular study to investigate the specific nature of the Pleistocene environments experienced by *H. erectus* beyond that suggested in Chapter Two, it is the adaptive response of the species to the environment that is of significance here, since the energetic demands of growth and encephalisation must be balanced by changes in life history strategy. Variation in the environment requires differential allocation of energy, necessitating a series of trade-offs, which have implications for the growth, reproductive investment and survival of *H. erectus*.

Life history strategy and the stability of growth

Although the encephalisation of *H. erectus* is investigated in depth in Chapter Five, it is first necessary to place brain size within an ecological context, rather than

studying it in isolation, in order to understand the repercussions of this, and other, evolutionary trends. The majority of brain growth occurs in the postnatal period before weaning, and so the energetic costs are borne exclusively by the mother. Consequently, she must have a secure nutritional base, especially given that female reproductive success is a function of access to resources (Foley 1995: 29). This clearly relates to the bet-hedging argument outlined above. However, despite the potential distribution of reproduction effort over a range of environmental conditions, occasionally nutritional returns are low and developmental instability results in the offspring.

Trophic stress or dietary insufficiencies can be identified through asymmetries in bilateral features of the skeleton (West-Eberhard 2003: 511), based on the assumption that lower precision in development reflects these disruptive effects (Kellner and Alford 2003: 931). Moreover, growth rate and fluctuating asymmetries, the measure of instability, have been shown to be negatively correlated (Møller and Manning 2003: 19), and evidence from a range of taxa indicates that increasing population density results in decreased developmental stability (Møller and Manning 2003: 144). Therefore, instability occurs at the extremes of tolerance of the population, when competition for food, space and other resources is heightened. Under these conditions, somatic growth may be compromised, leading to skeletal asymmetries or reduced growth rate. This allows for a conceptual link between the reaction norm of a trait (defined below) and the life history strategy adopted by a species, since the breadth of the former has repercussions for the latter.

A reaction norm is the set of phenotypes (the physical expression of the genotype) produced by a single genotype (the genetic content of an organism) across a range of environmental conditions (West-Eberhard 2003: 26). This mapping of the genotype onto the phenotype is a function of the environment such that if a single genotype were to be cloned and tested across a range of environments, the reaction norms would transform environmental variation into phenotypic variation (Stearns 1992: 41). Parents and their offspring are unlikely to encounter an identical environment at

the same stages of development, so genotypes that are able to produce stable phenotypes under a range of frequently encountered environmental conditions are more likely to multiply at a faster rate than those with greater susceptibility to environmental change (Møller and Swaddle 1997: 58). This suggests that a broad reaction norm would be correlated with *r*-selection, since this is associated with a wide range of environmental conditions, and a physiological inflexibility would not be conducive to long-term survival. Conversely, in the stable conditions related to *K*-selection, a broad reaction norm would not be necessary for survival. Bet-hedging is a more complex matter, as it shares many of the characteristics of *K*-selection but within a variable environment. It is this ecological factor, though, which is important for determining the breadth of the reaction norm, and so, like *r*-selection, bet-hedging might produce traits with broad reaction norms, to aid survival.

The relationship between the breadth of the reaction norm and the developmental stability of a population, as measured through fluctuating asymmetries, can allow the empirical application of reaction norms to any study of growth and tolerance. A change in the shape of the reaction norm, or a reduction in distribution of environments, can reduce trait variation (Arnold and Peterson 2002). Any fluctuation in environment will, therefore, cause a change in the shape of the reaction norm, which will impact on the trait by increasing variation and reducing stability. A broad reaction norm implies that a wider range of environments is tolerated without giving rise to a larger number of phenotypes and thus creating instability, as Figure 3.6 helps to explain (adapted from Arnold and Peterson 2002: 308):

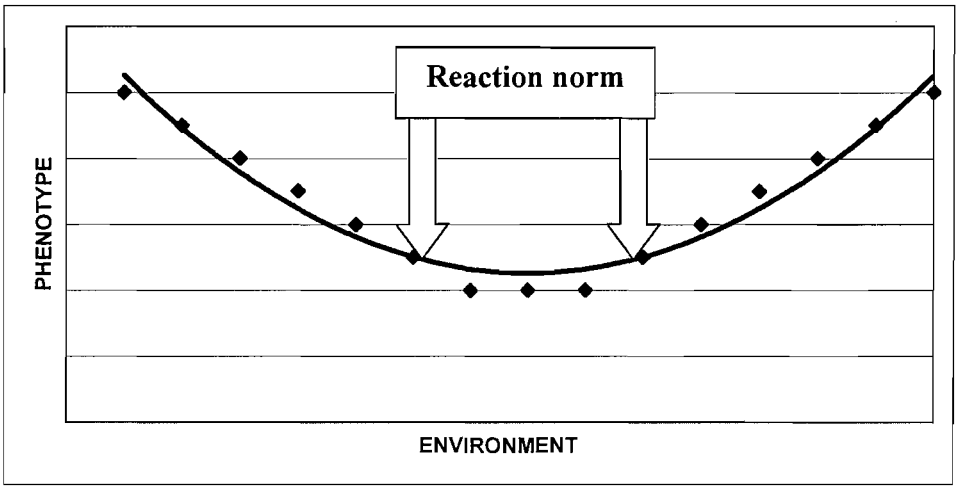

Figure 3.6 Model for an optimal reaction norm: environmental variability translated into phenotypic variability for a particular genotype

If an organism is predominantly *K*-selected (typically density dependent), the reaction norm will be quite narrow, since the ability to tolerate environmental variation will be relatively low. In contrast, if the organism is *r*-selected, then the reaction norm will be broad. The same will apply to bet-hedging species, as *H. erectus* is proposed to be. This creates greater stability, as the organism can tolerate a wider range of environmental fluctuation before it begins to have an adverse effect on growth, development and survival. Furthermore, if variation in the habitats of *H. erectus* does not correlate with the life history traits under study in this thesis, it might be confirmation of a broad reaction norm for these traits, and therefore greater stability in the species.

Modelling *H. erectus* life history strategy

Together with the ideas of biogeography and p-demes presented in the previous chapter, this review of life history provides a firm theoretical context for an investigation of the strategies followed by *H. erectus* in different environments. The model developed below for *H. erectus* life history follows a dichotomy between the core (tropical, stable and predictable environments) and the periphery (temperate, variable and unpredictable environments). The testing of this model relies heavily on the available archaeological evidence and must be based on what is already known about *H. erectus*.

It has been demonstrated above that body size is a key variable in determining the scheduling of growth, reproduction and mortality. However, in the absence of extensive information on body size, brain size is used as an alternative indication of overall size (the relationship between the two, and the position of *H. erectus* compared to modern humans and other extant primates, is explored in Chapter Six). The centrality of body size to life history theory, as conceived by Charnov and discussed above, allows for a link to age-specific mortality, a second and vital factor in the construction of evolutionary ecology, as shown by the bet-hedging strategy. Although *r-K* theory and the degree of encephalisation provide a model for reproductive strategy and have implications for growth schedules, age-specific mortality examines the risk of death at different ages, as well as the timing of other life history events, such as the age at first reproduction and the rate of growth, and is more specifically related to environmental variation.

It is possible to make predictions for *H. erectus* based on the relationships between life history variables given above. In order to understand the evolutionary ecology of *H. erectus*, the timings of life history events must be placed within a biogeographical framework, rather than being considered in isolation. Mortality is a key indicator for strategy, and is expected to vary absolutely between the core and periphery, and is taken to be a response to variation in brain size. An increase in brain size will have the effect of increasing body size and thus the age at first reproduction and the total adult life span (with low adult mortality), to compensate for a longer period of juvenile growth. However, this is expected to be offset by a decrease in the number of offspring produced per year. Thus, cranial capacity becomes a predictor variable for this ecological model.

The equations of Charnov above have provided dimensions beyond the relatively simple distinction between *r* and *K* for characterising life history, but his work does not allow for a broad distribution of variation. Plasticity is not accounted for in his models, but is an important feature both of the physiological and the life historical response. Although there is predicted to be an over-arching dichotomy in life history

strategy between the core and the periphery, the smaller demic subgroups will have, within that broader context, their own traits and patterns. This is to be identified through the stability of growth and fluctuating asymmetries (considered in greater detail in Chapter Seven). It is predicted that the p-demes located within the core will show a reduced frequency of asymmetry and instability, suggesting a more favourable set of environmental conditions. These specimens are also predicted to exhibit a larger cranial capacity, due to the potential for slower growth without increased risk of mortality in a predictable environment. The obverse will be true for the periphery, which is therefore expected to demonstrate a higher degree of instability in growth, seen through fluctuating asymmetries, and a smaller overall cranial capacity, as a consequence of a higher risk of juvenile mortality and thus the requirement for a faster growth period and a lower age at first reproduction.

The model therefore predicts recognisable patterns in brain size and juvenile mortality in each of the *H. erectus* p-demes under examination, with a broad division between the core and periphery, proposed here as a function of latitude and thus climate. These key features are expanded upon in the following chapters. The study of the encephalisation of *H. erectus*, in an ecological (demic) context, provides a way to identify the similarities and differences in the life history strategy of each deme of that species in relation to latitude. The testing of the model begins in Chapter Four, which analyses patterns of survivorship in a number of primate species, including the *H. erectus* p-demes, investigating and comparing the mortality rates of infants, juveniles and adults in order to begin to construct a model of hominin life history.

CHAPTER FOUR

Age-specific mortality

Age-specific mortality is a key feature of the bet-hedging hypothesis, and as discussed in Chapter Three, the mortality profile of a population is vital in determining the scheduling of birth and growth rates. The previous chapter stated that one major limitation of the *r-K* dichotomy (MacArthur and Wilson 1967) was that it does not consider age-specific mortality, despite its importance in relation to changes in reproductive decisions and, thus, the demographic mechanisms of life history strategy. This chapter will rectify this omission by examining the age-specific mortality of a series of modern human hunter-gatherer populations and primate species, as well as that of *Homo erectus, Australopithecus africanus* and *Australopithecus boisei*[1], before interpreting the findings within a life historical context. By doing so, it will be possible to establish whether other primate species have a survivorship pattern indicative of *K*-selection. If so, this would suggest that it is an ancestral condition and, therefore, an early feature of the genus *Homo*. It will be easier to see how and if *H. erectus* diverges as a result of environmental variation if it is first known how the mortality profile of the species is expected to look. In order to accomplish this, the demography of a hunter-gatherer population is reviewed first, and the survival rates compared to other global populations. This is followed by a review of primate mortality data, used to give access to our evolutionary past and the life history strategy of *H. erectus*. As such, the chapter closes with an original analysis of *H. erectus* mortality, pooling all known fossils of the species in order to assess survivorship.

The hunter-gatherer mortality profile

Like any primate, *H. sapiens* is subject to the life history trade-offs that govern growth, fertility and mortality. With these similarities comes variation, since, as

[1] As with *H. habilis* in Chapter One, the debate surrounding the genus of *boisei* is not addressed in this thesis due to the restrictions of space; *Australopithecus* is used, although the alternative preference of *Paranthropus* is acknowledged.

noted in Chapter Three, environmental factors can and do affect the probability of dying or giving birth through time (Hill and Hurtado 1996: 6). Of particular interest to this study are those populations maintaining a foraging way of life, since their life history strategies are not buffered by technology or industry, and so are more directly affected by the natural environment. This provides a way to begin to understand the evolution of the life history characteristics of *H. sapiens*, as all significant morphological evolution of our species took place in a band-level foraging context (Hill and Hurtado 1996: 10).

The Ache, a small native population of eastern Paraguay, have been extensively researched by Hill and Hurtado (1996), who investigated the demographic parameters of the Northern Ache between 1890 and 1993. Until 1970, the last year before peaceful contact, most of the Ache lived in the forest, before subsequently moving onto reservations (although a degree of flexibility is maintained, with individuals moving freely between the two areas). Hill and Hurtado stress that their results should not be taken as representative of all hunter-gatherer/forager populations, and so the demographic data they obtained is presented here as an indication of one possible human life history strategy.

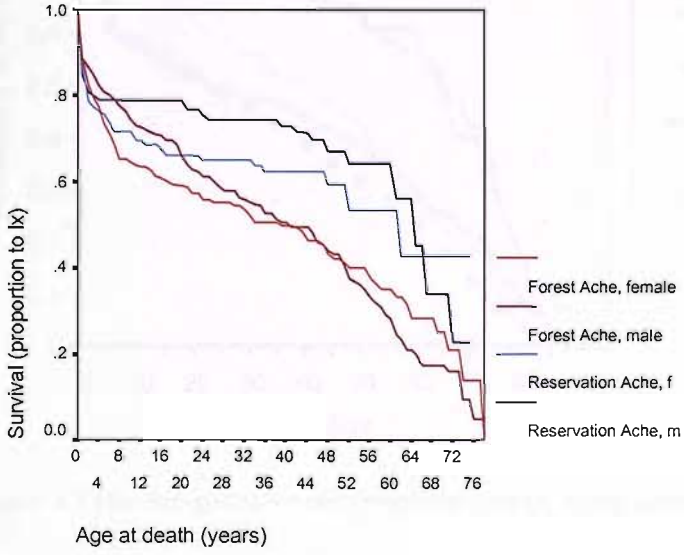

Figure 4.1 Probability of surviving to successive age classes for forest-dwelling and reservation-dwelling Ache, by sex (data from Hill and Hurtado 1996)

Figure 4.1 compares the age- and sex-specific mortality profiles of forest-dwelling and reservation-dwelling (1978-1993) Ache. There is a clear dichotomy between the two environments, with a higher chance of survival for those Ache living on the reservation (likely to be a direct function of access to healthcare, education and economic assistance [Hill and Hurtado 1996: 192]). Moreover, for much of the lifespan, males have a higher chance of surviving from year to year than females in both environments, until reaching around 45 years of age in the forest, and approximately 65 years of age on the reservation, whereupon male survival falls below the female line. A high rate of infant mortality is common to each category, due in part to the practice of infanticide under certain conditions.

When the age- and sex-specific mortality profiles of the Ache are compared with other technologically primitive populations, is it clear that they are characterised by similar mortality rates over the lifespan (Figure 4.2).

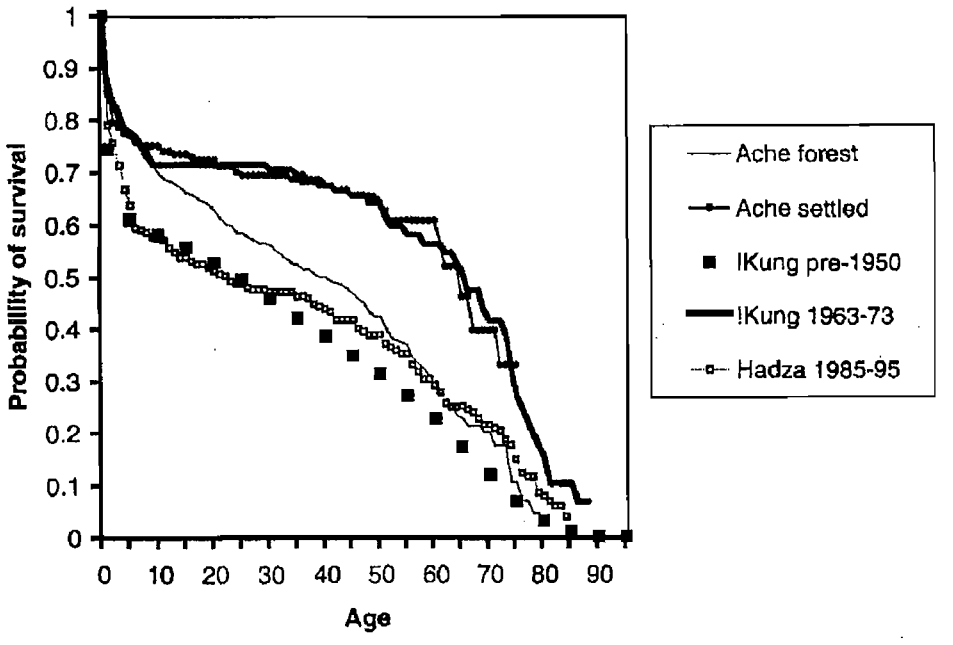

Figure 4.2 Hunter-gatherer survivorship curves, sexes combined (Pennington 2001: 191)

A sample of bush-living !Kung (pre-1950) shows significantly higher infant mortality among this group compared to the Ache ($p = 0.008$), but a comparable pattern of mortality throughout childhood and the middle adult years (Hill and Hurtado 1996: 187). Likewise, the Hadza of Tanzania also experience high levels of infant mortality, with only about 50% of newborns surviving until the age of 15. In contrast, the settled !Kung and Ache populations have a better than 50% chance of surviving to 60 years of age (Pennington 2001: 190).

Pennington (2001: 192-3) provides a wider picture of hunter-gatherer survivorship by comparing the proportion surviving to the ages of 15 and 50 in a global sample of hunter-gatherer populations. Her data is displayed graphically below in Figure 4.3, and indicates a disparity in survival rates across populations.

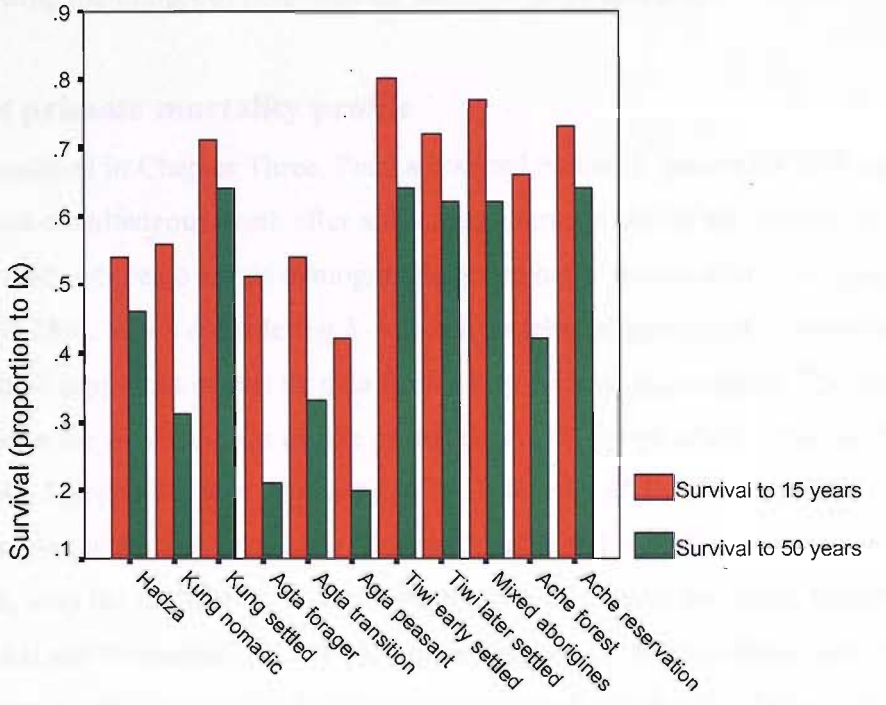

Figure 4.3 Global survival rates in hunter-gatherers (data from Pennington 2001)

Sedentary groups generally show the best life expectancy for children, with the highest proportion surviving to the age of 15 years found in the Australian

populations, particularly the Tiwi. Similarly, the settled !Kung and Ache experience relatively good prospects of survival, and this is reflected in the adult mortality rate too for these peoples. The Agta of the Philippines fare generally badly, and are the only group not to undergo an improvement in life expectancy following economic change. The poor survival rates of the Hadza may be due to a diet of poor quality, albeit abundant, food (Pennington 2001: 194-5).

These figures indicate that there is no standard mortality profile for hunter-gatherers and that *H. sapiens* demonstrates a wide range of survival rates. This is likely to be influenced, amongst other factors, by the environment and climate, and suggests that the p-demes of *H. erectus* will also show such variation. To aid the transition from modern hunter-gatherers to the deep evolutionary past, the mortality profiles of several primate species are examined below. This has the additional advantage of allowing the impact of body size on mortality to be assessed.

The primate mortality profile

As outlined in Chapter Three, Pianka asserted that each generation will experience almost simultaneous death after a life span characteristic of the species, or a constant mortality where no single demographic group has a greater chance of dying (Deevey 1947: 286). When considering *K*-selected patterns of age-specific mortality, this claim is supported in part by data from living primate populations. This section reviews the survival rates of five primate species (*Pongo abelii* [from Wich et al 2004], *Macaca mulatta, Macaca fuscata*, *Pan troglodytes* [Richard 1985] and *Propithecus diadema edwardsi* [Pochron et al 2004] – all female data) over their life span, with the probability of surviving to each successive age class. Following Acsádi and Nemeskéri (1970), the proportion (*dx*) of the population who died at a particular age is gained by dividing the number of individuals (*Dx*) who died between age x and $x + 1$ by the total number of individuals who died during the entire period of deaths, thus:

$$dx = \frac{Dx}{\sum Dx}$$

From this value, the number of survivors (lx) is calculated by subtracting dx of the previous year, following $l_1 = l_0 - d_0$; $l_2 = l_1 - d_1$ and so on. Survivorship of 100% is assumed at the outset (no peri- or post-natal births), and the number of deaths in each age class (dx) is deducted incrementally to form a pattern of mortality risk, or the probability of survival, over the life span of a hypothetical individual. Using this method, the mortality profiles for the females of the five species listed above are compared in Figure 4.4:

Figure 4.4 Probability of surviving to successive age classes for females from five primate species (data from Pochron et al 2004; Richard 1985; and Wich et al 2004)

According to the schematic representation of survivorship curves in Figure 3.3, the apes, the chimpanzee (*P. troglodytes*) and the orangutan (*P. abelii*) in Figure 4.4 display a Type I pattern, with a sharp drop at the end of the natural life span. The remaining three species seem to share a similar trend, with a high risk of mortality during infancy (although this is also apparent in *P. troglodytes*).

This difference between apes and monkeys could be a consequence of body size and its effect on maturation time, as discussed in the previous chapter, and so variation in mortality may not be significant even if individuals from each species may

ostensibly be the same age (Richard 1985: 168). However, this conclusion requires confirmation, as some of the age groups have been conflated, which creates comparative difficulties; the stepwise progression in Figure 4.4 is a product of this, with a single value for survival given for several successive age classes. To overcome this, I have condensed the data in order to produce a smooth curve. As well as eliminating superfluous data points, this technique has the added benefit of allowing for direct comparison of the shape of the survivorship profile between species, regardless of absolute life span (thus the *x*-axis, time, does not have a numbered scale). The three monkey species are compared in this way in Figure 4.5.

Data were also available to compare male and female chimpanzees and orangutans, and the resulting survivorship curves for these two species are plotted below in Figures 4.6 and 4.7. In Deevey's original exposition, he considered a logarithmic scale to be more instructive, 'in that a straight line implies equal *rates* of mortality with respect to age' (Deevey 1947: 285; original emphasis). Following this method, the graphs shown in Figures 4.5-4.7 have a logarithmic scale[2].

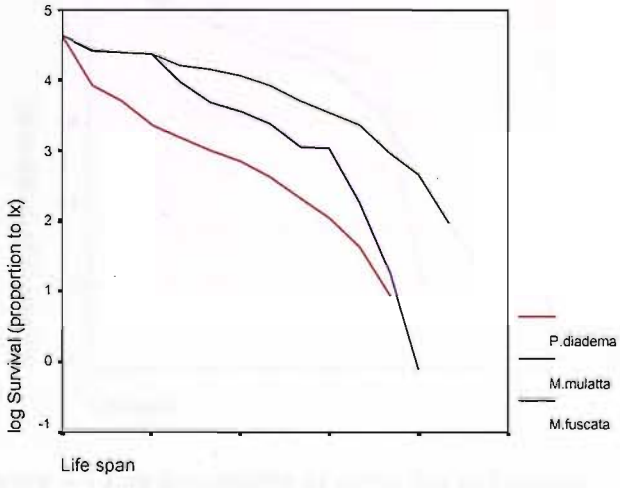

Figure 4.5 Log probability of surviving to successive age classes (condensed) for female P. diadema, M. mulatta and M. fuscata (data from Pochron et al 2004 and Richard 1985)

[2] Natural logs are used throughout the thesis.

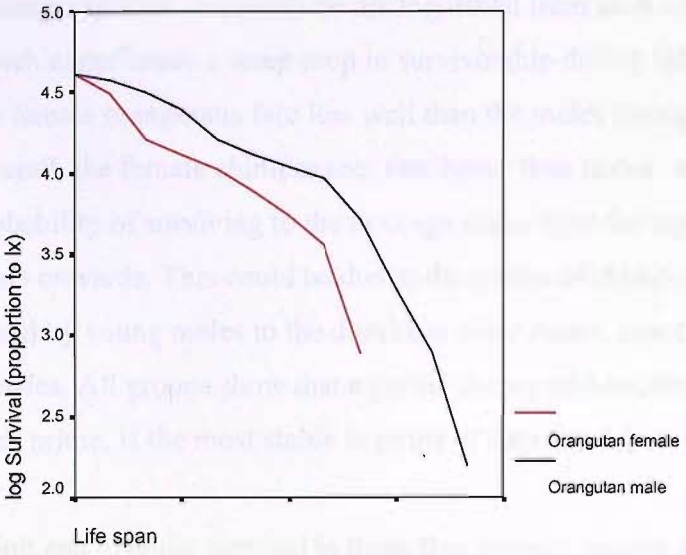

Figure 4.6 Log probability of surviving to successive age classes (condensed) for male and female P. abelii (data from Wich et al 2004)

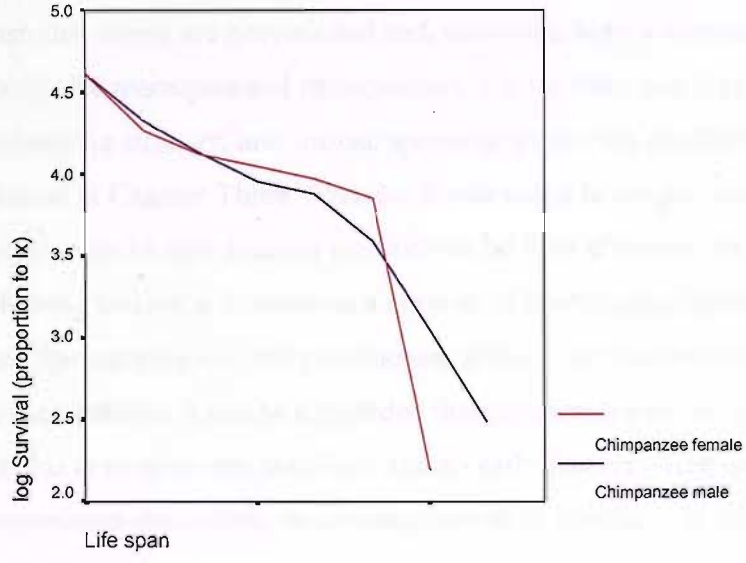

Figure 4.7 Log probability of surviving to successive age classes (condensed) for male and female P. troglodytes (data from Richard 1985)

Logging the data has smoothed out the curves and produced a more recognisably linear relationship with a resemblance to the Type II line in Deevey's chart, while having little effect on the general shape of the distribution. The profiles of the two

macaque species can easily be distinguished from each other and from the sifaka, which experiences a steep drop in survivorship during infancy. In the ape examples, the female orangutans fare less well than the males throughout the entire lifespan. Overall, the female chimpanzees fare better than males, who experience a lower probability of surviving to the next age class, from the age of approximately 20 years onwards. This could be due to the nature of chimpanzee society, and the threat posed by young males to the dominant older males, especially over access to females. All groups show that a period during mid-adulthood, when adults are in their prime, is the most stable in terms of survivorship.

Adult and juvenile survival in these five primate species appears to be constant, with risk spread evenly across life span, in accordance with Deevey's survivorship typology (Figure 3.3). Stability in adult survivorship is a condition of the bet-hedging model, since each individual can consequently risk delaying reproduction until a more favourable year if necessary. However, since three of the populations illustrated above are provisioned and, therefore, have a constant and reliable food supply (the macaques and chimpanzee), it is unlikely that they would need to adopt a bet-hedging strategy, and instead appear to follow the predictions of *K*-selection as outlined in Chapter Three. Even so, it was noted in the previous chapter that *r-K* theory relies on age-specific mortality to be fully effective. In view of that, the following section will examine a number of baboon populations. Importantly, these were free-ranging and not provisioned. If their survivorship curves resemble those produced above, it can be concluded that primates are bet-hedgers, suggesting either that this is an ancestral condition and an early feature of the genus *Homo*, or that it is environment-dependent, as investigation of *H. erectus* will show. This is explored further below.

The baboon evidence

The comparative demographic structure for the baboon populations is drawn from Dunbar (1980), who followed a population of Ethiopian gelada baboons (*Theropithecus gelada*) over two field seasons in 1971-72 and 1974-75 in order to

determine their demographic processes. It was noted in Chapter Three that life tables formed from the age structure of a population are only valid when population growth is stationary (Caughley 1966). Dunbar's baboon population, though not stationary, was increasing at a steady rate, and so the age specific mortality rate could be established (Dunbar 1980: 498). The survivorship curve was calculated in the same way and is displayed below in Figure 4.8.

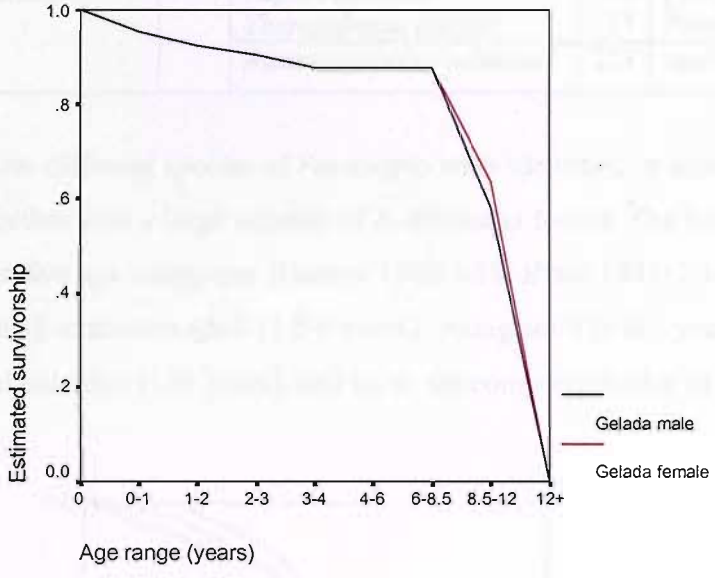

Figure 4.8: The age-specific mortality rates of a free-ranging population of gelada baboons (data from Dunbar 1980)

As a representation of a relatively successful and healthy population, these figures provide a good study of age-specific mortality, indicating a very high level of juvenile survival with approximately 87.7% of infants reaching at least four years of age. This is not universal in baboons, with some populations in poor habitats experiencing only 40% survival to 18 months of age (Dunbar 1980: 499). This would suggest a necessity for the bet-hedging strategy, which is usually associated with low juvenile survival in iteroparous organisms, especially in marginal environments. In agreement with this conclusion, the shape of the distribution is unlike that seen in the provisioned populations above, yet similar to the following graphs based on archaeological data. Taphonomic bias is a secondary concern, since

it might affect the survivorship profile of the fossil record. As such, it is relevant to the study of *Homo erectus*. To counter this problem, the Dunbar population is assessed with reference to the primate remains from the Sterkfontein valley in South Africa. Table 4.1 details the populations included:

Table 4.1 Baboon and hominin species included in the taphonomic analysis

Modern comparison	***n***	**Swartkrans Member 1**	***n***	**Sterkfontein Member 4**	***n***
Theropithecus gelada	N/a	*Parapapio jonesi*	8	*Parapapio jonesi*	27
		Papio robinsoni	40	*Parapapio broomi*	91
		Theropithecus danieli	17	*Parapapio whitei*	10
		Australopithecus robustus	113	*Australopithecus africanus*	47

Three different species of *Parapapio* were identified in Member 4 of Sterkfontein, together with a large number of *A. africanus* fossils. The baboons were classified into five age categories (Dunbar 1980: 488; Brain 1981: 204-5): juvenile (0-3.5 years), immature adult (3.5-6 years), young adult (6-8.5 years), adult (8.5-12 years) and old adult (12+ years), and these are compared below in Figure 4.9:

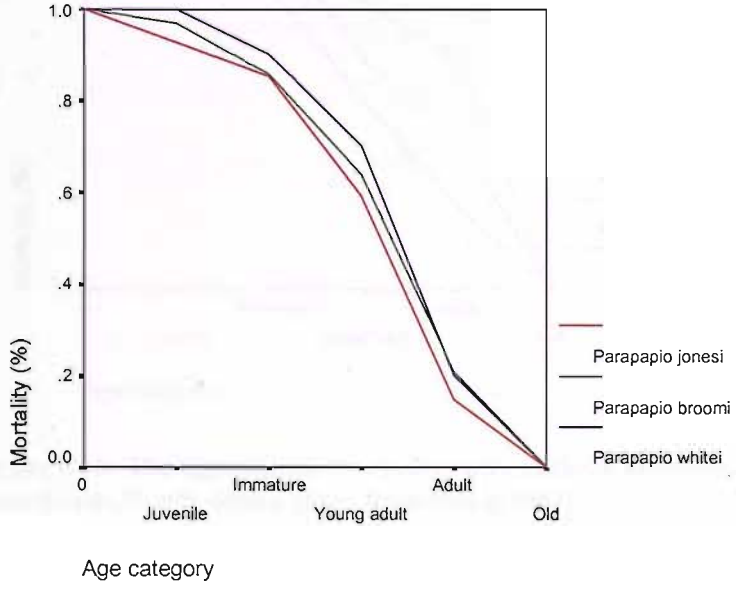

Figure 4.9: The age-specific mortality rates of three baboon species from Sterkfontein, South Africa (data from Brain 1981)

Despite the conspicuous deviation from the data displayed in Figure 4.8, this graph shows unity in the mortality profiles of these species. Furthermore, all have a survivorship rate of higher than 40% to 18 months of age, although this seems very likely to be due to taphonomic bias in the formation of the profile. However, bias can be at least partially accounted for by the hypothesis that predation choice is based on body mass (Brain and Watson 1992: 363), investigated further below.

The profiles displayed in Figure 4.9 share some similarities with the equivalent finds from Swartkrans, detailed below in Figure 4.10. This cave also produced three primate species, in addition to a number of *A. robustus* remains, but unlike those depicted in Figure 4.9 they did not share the same genus, which might have been partly responsible for the pattern of mortality.

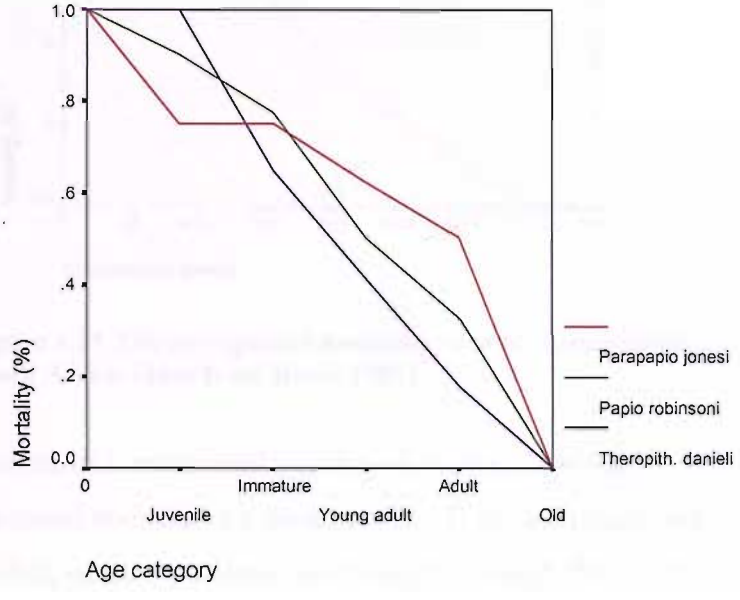

Figure 4.10: The age-specific mortality rates of three primate species from Swartkrans, South Africa (data from Brain 1981)

Variation in genus apparently coincides with variation in mortality rates, but juvenile mortality seems to have a closer link to body size. Figure 4.10 demonstrates that *Theropithecus danieli*, the largest of the three, experienced a higher rate of mortality over every period in the life cycle from the juvenile stage onwards. In

terms of predation, the most vulnerable phase of the life cycle appears to be the immature adult to young adult boundary for all three species.

One species of *Australopithecus* was also identified at each location, allowing a comparison of hominin and baboon life history strategies within the same cave site context. Swartkrans yielded a large population of *A. robustus*, numbering 113 individuals (Brain 1981: 229-232). These were assigned to age classes by Brain (1981) and a survivorship curve was generated, as for the baboon samples:

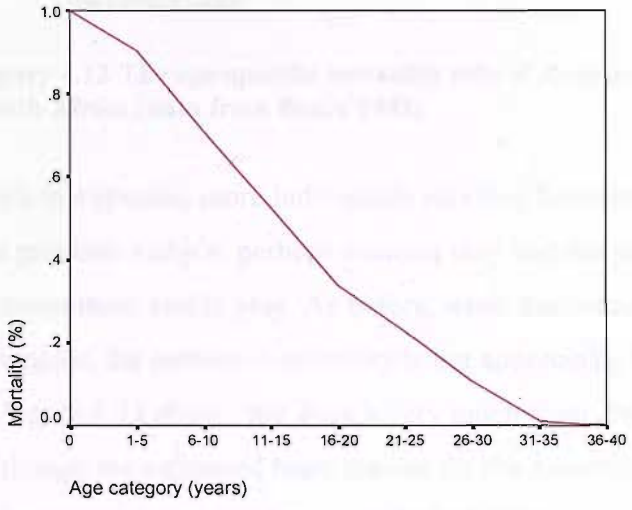

Figure 4.11 The age-specific mortality rate of *Australopithecus robustus*, Swartkrans, South Africa (data from Brain 1981)

This curve is most similar to that of *T. danieli*, which may be due to the overlap in estimated body size for these species: *T. danieli* ranges from 60-100lb, or 27.2-45.4kg, while *A. robustus* was thought to weigh 80-150lb, or 36.3-68kg (Brain 1981: 268). *A. africanus* was discovered at Sterkfontein, and comprised a slightly smaller population of a minimum 47 individuals. These animals have been estimated to be of a lower body mass, at around 26-28kg (Kappelman 1996: 256), so it might be expected that the pattern of mortality would change accordingly.

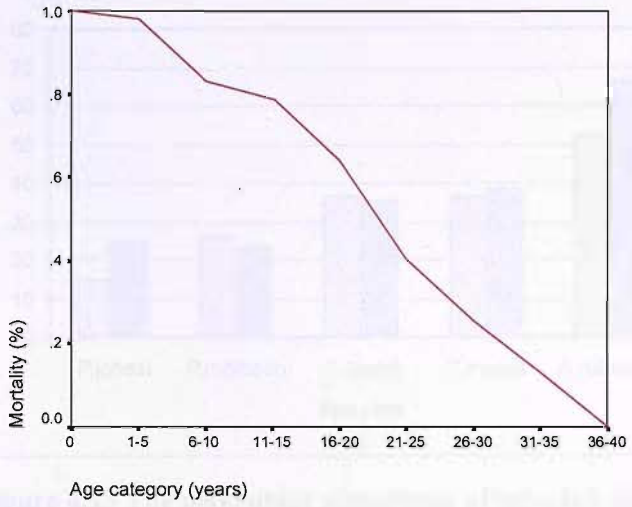

Figure 4.12 The age-specific mortality rate of *Australopithecus africanus*, Sterkfontein, South Africa (data from Brain 1981)

With this species, more individuals survived between the ages of 11-15 years than in the previous sample, perhaps because they had not yet achieved a desirable weight to make them viable prey. As before, when the hominin is compared to the baboon examples, the pattern of mortality is not appreciably different from those portrayed in Figure 4.11 above; nor does it vary much from *Papio robinsoni* in Figure 4.10. Although the estimated body masses for the Swartkrans trio are not available, *P. robinsoni* is thought to have weighed 35-80lb, or 15.9-36.3kg (Brain 1981: 268), thereby overlapping with *A. africanus*.

Similarly, the body weight of *H. erectus* is a significant factor in the reconstruction of the life history of this species, as well as in the assessment of mortality risk, as Brain has demonstrated with respect to South African baboons. He noticed a correlation between estimated live weight and the percentage of subadults found within each species' assemblage in Swartkrans Member 1. Figure 4.13 demonstrates that the relationship to body weight holds across *Parapapio jonesi*, *Papio robinsoni*, *Theropithecus danieli*, *Dinopithecus ingens* (a papionin species) and *A. robustus*, even when the boundaries for adulthood are lowered from 21 to 16, reducing the subadult remains from 66.7% to 48.3%. The body weights used below are the mean of the estimated range (Brain 1981: 268):

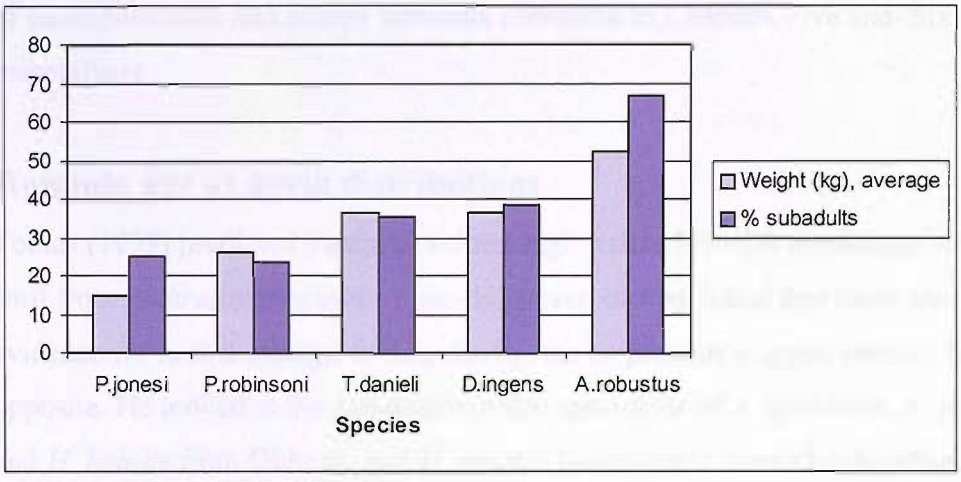

Figure 4.13 The percentage abundance of subadult individuals among primates of different adult live weights, Swartkrans Member 1 (data from Brain 1981)

Primates comprise over 50% of the Swartkrans Member 1 macrovertebrate assemblage, although they form only a small part of contemporary leopard diet. If Brain were correct to believe that the cave was used as a baboon sleeping-site, there would have been ample opportunity for leopard predation (Brain 1981: 271). Figure 4.13 suggests that the principal taphonomic bias was a certain body weight, thus making only a certain proportion of the prey most appealing to their predators.

However, the risk of predation was not the only one a hominin population would have had to overcome (Tobias 1999). Variation in climate and subsequent changes in temperature, precipitation and food supply would have made juvenile survivorship unstable, with greatest mortality during periods of environmental stress, as outlined by the bet-hedging hypothesis favoured in this study. The pressures from increasing brain size and higher nutritional demands, particularly from *Australopithecus* to *H. erectus*, might also have influenced differential longevity (Tobias 1999: 66-68). Having presented and discussed existing datasets for primate and modern hunter-gatherer demography, I collate below a new dataset of all know *H. erectus* specimens, in order to address the question of survival in this extinct species. To provide a point of reference within the literature, Tobias's findings of hominin age-specific mortality are evaluated below, with the questions

of encephalisation and energy demands addressed in Chapters Five and Six respectively.

Hominin age at death distributions

Tobias (1999) predicted a transition from high-risk to low-risk conditions with the shift from *Australopithecus* to *Homo*. However, he concluded that there was no evidence for such a change; in fact, the figures he presents suggest entirely the opposite. He looked at the age-determinable specimens of *A. africanus*, *A. robustus* and *H. habilis* from Olduvai, and *H. erectus [pekinensis]* from Zhoukoudian, dividing them into the broad age ranges of anatomically immature (aged approximately 20 years and younger) and anatomically mature (aged over 20 years). The results are tabulated below:

Table 4.2 Percentage distributions of age at death of age-determinable hominin species[3]

Species	Anatomically Immature (%)	Anatomically Mature (%)	Geologic Age
A. africanus (n = 63)	35	65	~3.5-2.5 Ma
A. robustus (n = 119)	60.5	39.5	1.8-1.5 Ma
H. habilis (n = 22)	73	27	2.3-1.6 Ma
H. erectus pekinensis (n = 22)	73	27	0.5 Ma

It is immediately clear that there is a trend of decreasing survivorship of anatomically mature individuals, from the small-brained *A. africanus* to the much bigger-brained *H. erectus*. In Tobias's own words,

> these figures negate any preconceived notion that the evolution of the Plio-Pleistocene hominids might have been accompanied by an improvement in the demographic pattern from high risk [high frequency

[3] There is some question over the date of the Indonesian fossils (detailed in the text), but the Chinese dates are generally accepted.

> of juvenile deaths and low mean life expectancy] to low risk [lower incidence of juvenile deaths and a higher mean life expectancy]. On the contrary, the available evidence suggests that the evolution of the hominids from the later Pliocene to the earlier and Middle Pleistocene was apparently accompanied by a diminution in the chances of survival to adulthood (Tobias 1999: 56, 58).

Taphonomic, environmental and bio-evolutionary biases acting on the fossil remains mean that the distribution of the sample cannot be assumed to represent the distribution of the whole population (Tobias 1999: 59-60). Most noticeably, there are no infants under the age of 2 years, nor are there any 'elderly' (40 years old or more) individuals. The former is most likely an artefact of taphonomy, due to the more delicate nature of the smaller bones, and the latter probably reflects a demographic reality (Tobias 1999: 59-60). This leaves Tobias free to conclude that the appearance in his sample of a surprisingly large number of anatomically immature individuals in later species is 'a conservative reflection of a general trend in the living populations from which those fossils were drawn' (Tobias 1999: 61).

Since these results affect our understanding of hominin life history by framing the *K*-selected correlates of primates within a context of high juvenile mortality, they are reassessed below, taking into account the limitations of Tobias's original study. Tobias restricted his investigation of *H. erectus* to those fossils from Zhoukoudian, basing his findings on this relatively small group (the sample size is just over a third that of *A. robustus* and only a little over a fifth of the australopithecine sample). He did not detail the individual specimens included in the study, but it is possible that the 16 juvenile representatives he identifies (73% of the sample) have been derived from dental remains, since it is not clear otherwise how his figures could have come from purely skeletal material. Teeth will not be counted in my own analysis, due to the uncertainty of the minimum number of individuals present. As such, and using only skeletal material, 15 juveniles from Zhoukoudian are identified below.

A reassessment of the Zhoukoudian collection for this thesis, based solely on skeletal (and not dental) material, showed a minimum of 35 individuals in total, including mandibular and postcranial remains as well as cranial fragments. Of these, 15 were considered to be juvenile or, following Tobias, as anatomically immature, amounting to only 43% of the sample – far less than the 73% cited above. This figure finds support from Antón (1999: 224), who considers that a population composed of equal numbers of adults and juveniles must be taphonomically unlikely. However, the survivorship of *H. erectus* cannot be determined on the basis of this single population, so all known *H. erectus* remains were counted and catalogued according to their status as anatomically mature or immature, and divided further as cranial or postcranial (including mandibular) finds. This treatment of the specimens is limited by inaccurate knowledge of the minimum number of individuals present and the age at death of each one, as well as the spatial and temporal range, but it nevertheless provides a helpful overview of mortality in *H. erectus* as a starting point. The results of this research are displayed below in Table 4.3:

Table 4.3 Catalogue of all H. erectus finds according to their assessed age at death

	Subadults	Ref.	Adults	Ref.
Cranial (including fragments)	Mojokerto	Antón 1997	Ngandong 1, 3, 5, 6, 9, 11, 12	Antón 1999
	KNM-WT 15000	Smith 1993	OH 9, 12	Wood 1991
	Zhoukoudian III, VIII	Antón 1999	KNM-ER 3733, 3883	Antón 1999
	Ngandong 2, 8	Antón 1999	Sangiran 2, 3, 4, 10, 12, 17	Antón 1999
	D2700	Vekua 2002	Sangiran 13, 14, 15, 18, 19, 20	Jacob 1975
	D2282	Vekua 2002	Sangiran 26, 27, 31, 37	Wolpoff 1986
	Tangshan	Wolpoff 1996	Trinil 2	Antón 1999
	Zhoukoudian IV, VII, IX	Wu 1995	Zhoukoudian II, X, XI, XII	Antón 1999
	Zhoukoudian GII, JI	Oakley 1975	Zhoukoudian I, V, VI, HIII	Wu 1995
			D2280	Vekua 2002
			SM 1, 3	Delson 2001
			BOU-VP-2/66	Asfaw 2002
			UA 31	Abbate 1998
			KNM-OL 45500	Potts 2004
			PA 1051-6	Wu 1995
			PA 830	Wu 1995
			Salè	Day 1986
			KNM-ER 730, 1466, 1648, 3892	Wood 1991
			Thomas III	Rightmire 1990
			Narmada	Sonakia 1985
			'Ubeidiya	Oakley 1975
	SUBTOTAL	**14**	**SUBTOTAL**	**53**
Postcranial[4]	Guojiabao	Wu 1995	PA 102, 831	Wu 1995
	Sangiran 38	Wolpoff 1986	Dmanisi 1	Gabunia 2000
	Zhoukoudian BI, BIII, BIV, BV, CI, FI	Wu 1995	Tighenif 1, 2, 3	Day 1986
			OH 22, 23, 28, 36, 51	Day 1986
	KNM-ER 820, 1507	Wood 1991	Sangiran 1, 5, 6, 8, 9, 22, 33, 34, 39	Wolpoff 1986
			Trinil 3	Day 1986
			Trinil 6	Oakley 1975
			Zhoukoudian AII, KI, MI, MII, CIII	Wu 1995
			Zhoukoudian GI, HI, HIV, JII, JIII, MIV	Oakley 1975
			KNM-ER 992, 1808, 1812	Wood 1991
			KNM-ER 1506	Rightmire 1990
			SK 15	Rightmire 1990
			SK 45, 85	Oakley 1967
			Sidi Abderrahman	Rightmire 1990
			Thomas I	Rightmire 1990
	TOTAL	**24**	**TOTAL**	**95**

[4] Includes mandibular remains

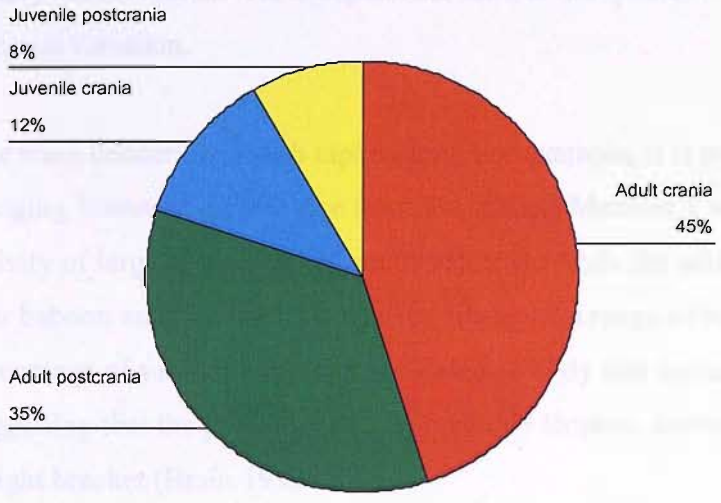

Figure 4.14 Age at death distributions for all known specimens of H. erectus, according to category of find and level of maturity

Table 4.3 shows far more adult than immature *H. erectus* fossils, and on the same basis as Tobias it can be suggested that this is a true representation of the living population. The disparity in age at death is highlighted further in Figure 4.14. The total adult share is 80%, leaving the juvenile section with 20% – almost a complete reversal of Tobias's calculations. This is a dramatic result, which carries implications for the interpretation of the life history of *H. erectus* contrary to that previously assumed by Tobias. As such, it is vital that the figures are as robust as possible in order to withstand analysis and portray an accurate reflection of *erectine* life history. However, it is also essential to interpret them within the context of the hunter-gatherer and primate data reviewed above, and this is discussed further below.

A major problem with this approach is that these fossils could not have been members of the same population, as some of the Zhoukoudian specimens conceivably could. The time period of these specimens stretches from 1.75 Myr (D2700) to 0.037 Myr (Ngandong), rather than centring on the 0.5 Myr of the Chinese sample (this information is not included in the table for the sake of clarity,

but is given in full in Appendix I). However, as a first step in establishing the life history of *H. erectus*, it is acceptable to look at the species overall, before examining regional variation.

One main concern lies with taphonomy. For example, it is proposed that the Hanging Remnant assemblage from Swartkrans Member 1 was formed by the activity of large carnivores (Brain 1993: 258). While the adult representatives of the four baboon and two hominin species displayed a range of body sizes, the percentage of sub-adult remains increased as body size increased (Figure 4.13), suggesting that the predator species, probably leopard, hunted within a specific weight bracket (Brain 1993: 258).

Thus, predator preferences may account for the relative lack of small/young hominin individuals in the *H. erectus* dataset of Table 4.3. The climate and environment can also affect assemblage constitution, such that groups may be differentially adapted for exploiting resources in two very similar environments (Tobias 1999: 59), with consequent higher mortality at the vulnerable ages of infancy, the juvenile period (when sub-adults must start to compete more directly with adults) and old age. Finally, the importance to the mortality rate of injuries due to accidents and violence, among children in particular, as well as 'diseases resulting from the factors of the natural environment or their changes' should not be underestimated (Acsádi and Nemeskéri 1970: 181).

Given these survival risks, the apparent lack of juvenile remains is perhaps surprising. The absence of very young infants and very old individuals has been discussed, with 'the fragility of infantile remains [militating] against their accumulation and preservation' (Tobias 1999: 60), and elderly individuals simply not existing as a demographic reality (Tobias 1999: 60). Looking at the distribution of the age at death (Figure 4.15) is a useful way of seeing whether this was the case.

Figure 4.15 Age at death frequency for all known specimens of *H. erectus*

This diagram indicates that the majority of deaths occurred during adulthood (quantified as age 21), with few reaching old age and yet with little mortality during infancy and adolescence. This may well be due to taphonomy and seems to justify Tobias's reasoning for their absence in the archaeological record.

However, it must also be considered that the risk of death for juveniles was simply not as high as Tobias supposed, and that *H. erectus* was well adapted to its environment. There is no need to assume otherwise. To investigate this possibility, the *H. erectus* sample was regionally subdivided into the four general groups of Africa, Europe, Indonesia and China. These subdivisions will show if this low risk of death is species wide or varies spatially.

In Africa, based on Table 4.3, only 9% of all finds can be attributed to juveniles, with the remaining 91% indisputably adult, translating as 28 adult individuals and three juveniles. This discrepancy might be attributable to taphonomic processes, as smaller, more delicate juvenile bones are less likely to survive the hot and arid environment, and as with the australopithecines, predation could still be a factor in juvenile mortality. Even so, this seems unlikely to account fully for such a disparity since Indonesia produces comparable results, with an adult to juvenile ratio of 92:8

reflecting a reality of 37 adults and three juveniles. The environment of Indonesia is wholly unlike that of Africa and yet the general mortality profile is almost exactly the same, which diminishes the taphonomic concerns.

Similarly, adult remains account for 71% of all European *H. erectus* finds, although the far smaller sample size numbers five adult individuals compared to just two juveniles, reducing the reliability of this result. The only area where the percentage of juveniles and adults approaches parity is China, with 62% adults and 38% juveniles, or in real terms 23 and 14 individuals respectively. The total number of individuals found compares well with those of Indonesia (37 vs. 40) and yet there is a marked variation in the number of juvenile remains. It is possible that the explanation lies in the difference in the latitude of these territories and the consequent variation in environment. China covers several parallels of latitude and is centred around 31°12' N, with the principal site of Zhoukoudian located at 39° 40' N. In contrast, Indonesia ranges from approximately 10° 10' S to 3° 35' N; the latter is comparable to the latitude of Kenya (Nairobi stands at 1°16' S), scene of many of the African finds. However, like China, Tbilisi (the capital of Georgia) is found at 41° 43' N, 44° 48' E (www.bcca.org/misc/qiblih/latlong_oc.html[5]). Unfortunately there are too few remains from Dmanisi to be sure of the pattern of survivorship, but of the three individuals recovered, two are subadults. Latitude and environmental variation may be the principal factor forcing adaptation and the adoption of new life history strategies, and this is explored in greater detail in Chapter Eight.

In all four regions, the distributions of the ages at death show that the modal value of the life span – the peak on the graph – occurs consistently at 21, i.e. during adulthood but before 'old age'. It is highly likely that, similar to many modern populations, the number of deaths is greatest during the first year of life, dropping sharply thereafter (Acsádi and Nemeskéri 1970: 39). Unfortunately, this data is not preserved, although the effects of a hypothetical high infant mortality rate on the

[5] Accessed 12.11.03; further detail is provided in Chapter Six.

distribution of deaths and on the model of life history was examined in Chapter Three, where it was suggested that high infant mortality was a feature of an unstable environment in a bet-hedging species.

A comparison between the number of adult and sub-adult individuals was also carried out for all *A. africanus* finds, the species which, according to Tobias (1999), had a similar age at death distribution to that depicted above for the reassessed *H. erectus* dataset. The *A. boisei* specimens, primarily from Koobi Fora, are used as an independent sample and to increase the evolutionary context.

The data for *A. africanus* (compiled from Oakley and Campbell 1967) are summarised below in Table 4.4 and displayed graphically in Figure 4.16:

Table 4.4 Summary of A. africanus finds according to assessed age at death[6]

Site	Adult crania	Juvenile crania	Adult postcrania	Juvenile postcrania
Makapansgat	8	2	14*	4
Sterkfontein	27*	2	13	3
Swartkrans	4	1	0	0
Taung	0	1	0	0
TOTAL	**39**	**6**	**27**	**7**

[6] All data are taken from Oakley and Campbell (1967) with the exception of *, incorporating Reed et al (1993); Lockwood and Tobias (1999); Partridge et al (2003) and Toussaint et al (2003)

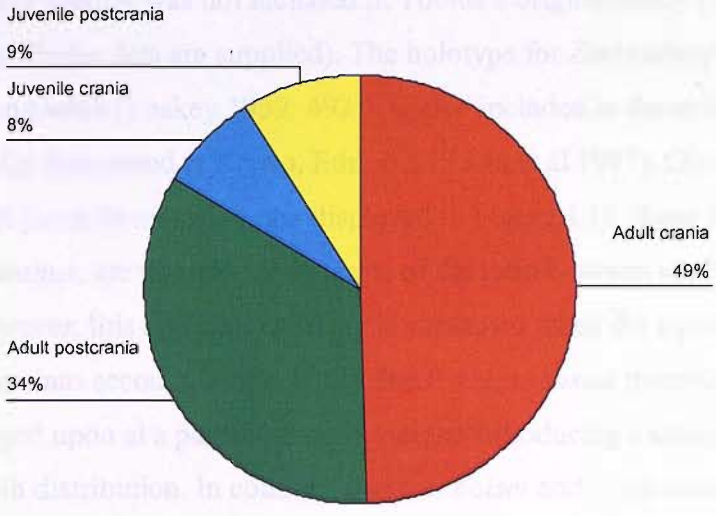

Figure 4.16 Age at death distributions for specimens of A. africanus, according to category of find and level of maturity

With a total adult share in *A. africanus* of 83%, compared to the 80% calculated above for *H. erectus*, these results resemble those of the later species in their distribution of anatomically mature and immature specimens. There are 11 more juvenile *H. erectus* finds than australopithecine examples, but that equates to a difference of only 3%. Again, these figures differ from those produced by Tobias (1999) in Table 4.2. His specimens came from Sterkfontein and Makapansgat, whereas Table 4.4 adds fossils from Swartkrans and Taung, thereby explaining the difference between the two studies.

Since *A. africanus* precedes the known advent of *H. erectus* by one to two million years, it is possible that conditions of risk and survival had not changed notably in that time with the rise of a new species. However, these data are not strong enough to support such a statement on its own, as it was not possible to assess the minimum number of individuals with enough confidence. As such, it is conceivable that, in reality, there are fewer adults than suggested by Table 4.4 above, although any alteration incurred is unlikely to have a significant impact on the shape of the distribution.

The fossils of *A. boisei* from Koobi Fora (Wood 1991) were chosen for comparison, as this species was not included in Tobias's original study (note that only cranial and mandibular data are supplied). The holotype for *Zinjanthropus boisei,* OH 5 (a young adult [Leakey 1959: 492]), is also included in the analysis, along with three skulls discovered at Konso, Ethiopia (Suwa et al 1997). Given the approximately 50% juvenile mortality rate displayed in Figure 4.13, these data, and those of *A. africanus*, are unexpected in terms of the ratio between adults and juveniles. However, this apparent anomaly is explained when the taphonomy of Sterkfontein is taken into account, as it is likely that the *A. robustus* juveniles were selectively preyed upon at a particular body weight, introducing a strong bias into the age at death distribution. In contrast, these *A. boisei* and *A. africanus* specimens are from the open area of Koobi Fora, where there is no evidence that they form part of a predator kill site. As such, other taphonomic problems (such as weathering) notwithstanding, they are taken to be a more reliable marker of juvenile survivorship.

Table 4.5 Summary of A. boisei finds according to assessed age at death

Adult crania	Adult mandibles	Juvenile crania	Juvenile mandibles
10	22	1	3

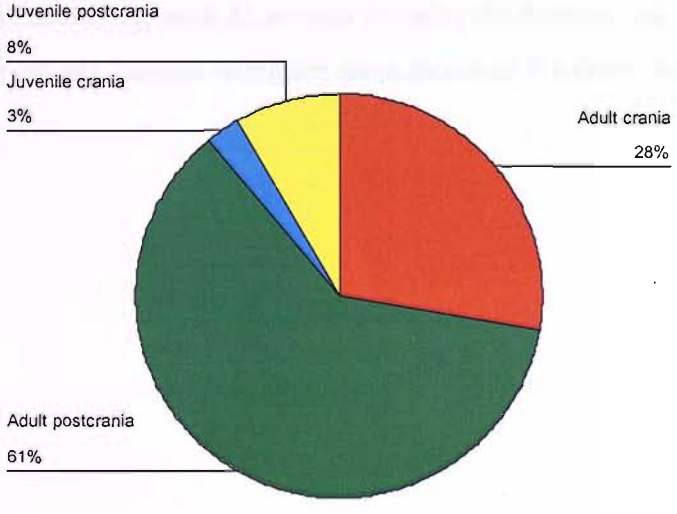

Figure 4.17 Age at death distributions for specimens of A. boisei, according to category of find and level of maturity

Here the difference in the distribution of anatomically mature and immature specimens is much more obvious, due to the presence of a single juvenile cranium. Even so, the percentage share of juvenile (mandibular) postcrania for this species is comparable to that of Figures 4.14 and 4.16. All three of these juvenile mandibles were estimated to be around 2.5-3.5 years old at the time of death (citations in Wood 1991), which could suggest that the risk of death was highest during this stage of life. However, such a small sample size makes it unwise to place much confidence in these findings.

With regards to the adult sample, the 67% provided by the postcranial remains might not be a true reflection of the number of individuals, with many of these finds associated with one of the relatively few cranial remains. If this were the case then the disparity between the numbers of individuals in each of the two age groups would be much less. Unfortunately, there is no way to prove or disprove the minimum number with any certainty, and so the analysis must stand as it is.

Below, Figure 4.18 presents a summation of the total adult and total juvenile sample proportions for each species, in order to allow a direct comparison of the shape of these distributions. They are presented in rank order of increasing incidence of pre-adult mortality, with *H. erectus* showing the highest risk of survival in immature individuals, despite being the most recent of the three species.

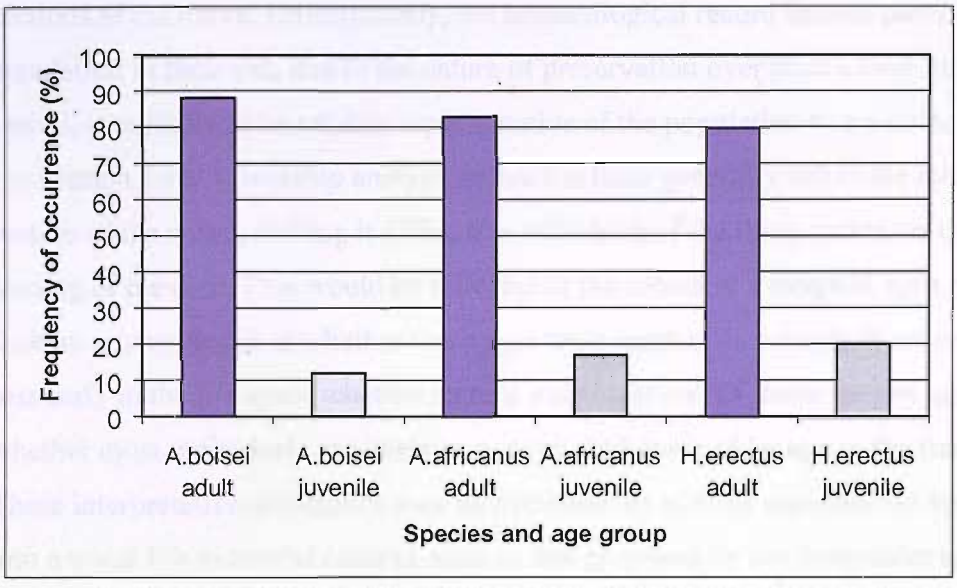

Figure 4.18 The distribution of finds for all three hominin species according to species and age group

However, there is very little relative difference between the adult and juvenile distribution of finds for the three hominin species, whether by geography, taxonomy or geological age. Tobias's 1999 findings cannot be relied upon as an accurate representation of changes in life history pattern over the course of human evolution. Throughout a long evolutionary process, and reflected by these three species, the risk of death for the immature members of each species does not appear to have been great enough to push their mortality rates above those of anatomically mature individuals. This implies a constant risk of death, expressed by the Type II curve in Figure 3.3, or alternatively, a steep drop in survivorship once a certain adult age is reached, such as that illustrated by the Type I curve. This latter interpretation is difficult to sustain without more precise details on age at death, but it is clear that none of these species experience high juvenile mortality compared with adult mortality. It might be concluded that at this early stage in human evolution, as indeed has been shown above in chimpanzees and macaques, the patterning of life history was marked by a *K*-selected strategy, or more of a bet-hedging approach.

There are some problems with the concept of the survivorship curve, however. When following a single population in a longitudinal study, it is possible to see all

sections of the curve. Unfortunately, the archaeological record freezes part of a population in time and, due to the nature of preservation over such a long time period, is unlikely to be reliably representative of the population as a whole. The implication for survivorship analysis is that the finds generally fall in the middle section of the curve, making it difficult to tell which of the three options is the best reading of the data. This would be reflected in the record as a range of ages, but without any evidence of whether these ages were reached as a result of catastrophic loss early in the life span; whether there is a constant risk of death for any age; or whether most individuals are likely to survive until some older age in the future. These interpretative difficulties may be overcome by placing age-specific mortality into a wider life historical context, such as that proposed by the integrative approach followed in this thesis. In order to begin this, the suggested mortality profiles for *H. erectus* and the comparative species *A. africanus* are calculated and examined below, using the method described for Richard's (1985) data. While this is not a true survivorship curve, the distribution of the ages at death will nevertheless locate a 'peak' in the most common age at death.

The dataset for the approximate age at death was kept as close as possible to the one displayed in Table 4.3, in order to create a link between each separate investigation and so make the results more meaningful with respect to each other. Due to the nature of the evidence available, it was not possible to produce survivorship curves directly comparable to those for macaques and chimpanzees above, as a population of *H. erectus* cannot be followed over time and its mortality observed in the same way. Instead, the entire body of *H. erectus* specimens was taken to be a single population, disregarding the geologic time scale and geographical distribution at this stage. At present, the principal concern is with the pattern of mortality for this species, so it is more instructive to group every known member of the species together.

Approximate ages at death for 103 *H. erectus* specimens were obtained from the literature, from sites in Africa, China, Indonesia and Europe. The only discrepancy

between this dataset and that of Table 4.3 is that there were no age estimates for a number of the Sangiran fossils, and it was felt more prudent to disregard them completely rather than risk skewing the distribution unnecessarily. The juvenile specimens provided a greater opportunity for assigning an age at death, due to tooth eruption, suture fusion and overall robustness of the bones. Where a range of ages was given for a specimen, particularly for the juveniles, the average was taken. The adults were more problematic, as the literature generally records their age at death as either 'adult' or 'elderly'. To reflect this in the survivorship calculations, and to quantify these two categories, all those deemed to be adults were grouped together in a 21+ age group, similar to Tobias in Table 4.2 above and continued in Table 4.3. The elderly specimens were separated into a group denoted as 30+ years old at the time of death.

These latter two age groups are not intended to replicate exactly the age at death of these individuals. Rather, the purpose is to show the number who reached maturity, and then the proportion who lived for a noticeably longer time. As such, the choice of 30+ as an age category is arbitrary. The other ages into which the specimens were classified were 3 years, 5, 6, 7, 8, 11, 14, 16 (based on estimates in the literature) and then the adult stages. These terms are compromised slightly by an inexact knowledge of the rate and manner of growth of *H. erectus* (estimates tend to rely on comparisons with modern human growth data; inaccuracy could be as high as ±3 years), but enquiry is restricted here to the pattern of mortality rather than an assessment of growth. For that reason, the focus is less on the precise age at death than the life history stage into which each individual falls (following the definitions in Bogin 1999).

Table 4.6 allots each fossil to an age class and life stage, with a conservative selection of the minimum number of individuals. The majority of finds belong to the mature adult category, with a relatively large number reaching 'elderly' status. The references for individual specimens are as those given in Table 4.3, and the percentage distributions are displayed graphically in Figures 4.19 and 4.20.

Table 4.6 Summary of estimated age at death for all available H. erectus specimens

Age class	Life stage	Specimen	Total
3 5	Childhood	Zhoukoudian JI Mojokerto; Zhoukoudian BIV; KNM-ER 820, 1507	1 4
6 7 8	Juvenile	Zhoukoudian IX Zhoukoudian VII, Ngandong 2 Zhoukoudian BI, BIII, CI, FI	1 2 4
11 14	Adolescence	Zhoukoudian BV KNM-WT 15000; D2700	1 2
16	Young adult	Zhoukoudian III, IV, GII; Ngandong 8; Tangshan; Guojiabao; D2282	7
21+	Adult	Ngandong 5, 6, 9, 12; OH 9, 12, 22, 23, 28, 36, 51; Dmanisi 1, D2280; SK 15, 85; Trinil 2, 3, 6; SM 1, 3; Narmada; BOU-VP-2/66; UA 31; Sangiran 1, 2, 3, 4, 5, 6, 9, 10, 17, 22; PA 830; Salè; 'Ubeidiya; Thomas I, III; Sidi Abderrahman; KNM-ER 730, 992, 1466, 1506, 1648, 1808, 1812, 3733, 3883, 3892; Zhoukoudian I, II, VI, X, XI, XII, AII, CI, GI, JII, JIII, KI, MI, MII, MIV; Tighenif 1, 2, 3; Bilzingsleben 1, 2	70
30+	Elderly	Ngandong 1, 3, 11; Sangiran 12; Zhoukoudian V, HI, HIII; SK 45; PA 102, 831, 1051-6	11

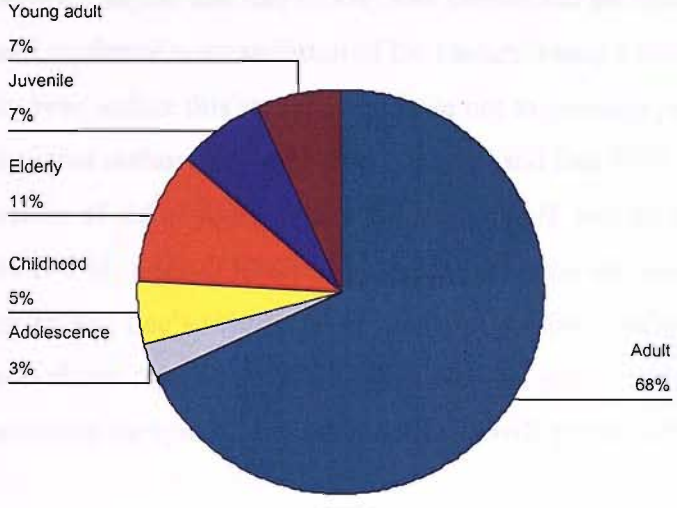

Figure 4.19 Percentage distribution of life stages for H. erectus

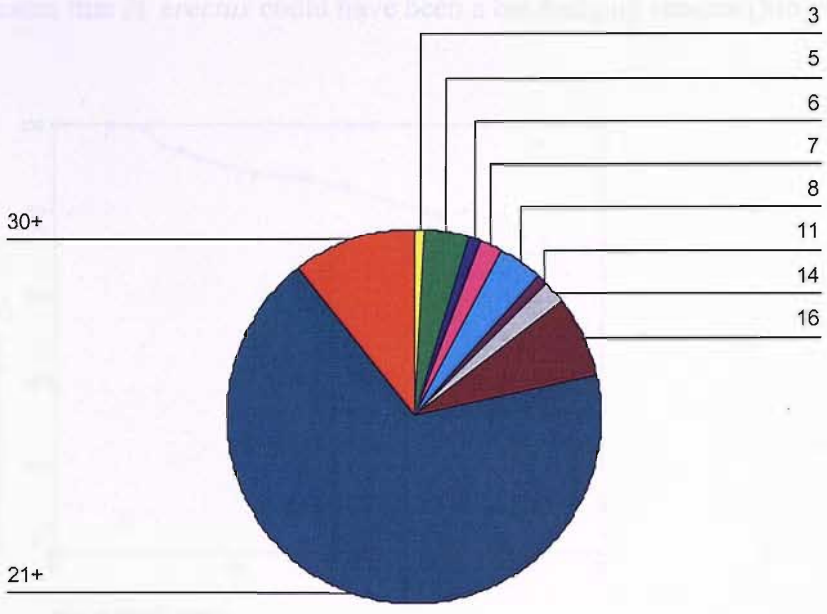

Figure 4.20 Percentage distribution of age at death for H. erectus

Notably, Caspari and Lee (2004) also carried out an investigation into age at death, based on dental wear seriation of the molars, using a wide range of fossil hominins. However, unlike this study, they chose not to consider juveniles because of the associated taphonomic problems (Caspari and Lee 2004: 10895). They calculated the ratio of old to young adults (OY ratio) in *H. erectus* to be 0.25. Here, the OY ratio is 0.16, a result likely to be dependent upon the specimens used in this sample. Caspari and Lee's results indicate an evolutionary tendency for increasing adult survival into the Upper Palaeolithic (Caspari and Lee 2004: 10896), although due to limitations the question of adult life span will not be further discussed.

Based on the percentages derived from Figure 4.20, Acsádi and Nemeskéri's (1970) methodology was used to create a survivorship curve for a single hypothetical *H. erectus*. This curve is displayed in Figure 4.21 and shows that *H. erectus* seemed to follow the same survivorship model as that experienced by modern primates (cf. Figures 4.4 and 4.8). The data are unlogged, but there is a recognisable Type I diagonal, with a decline in old age. Although there does not appear to be a greater

risk of death for immature individuals, the reduced variation in adult mortality indicates that *H. erectus* could have been a bet-hedging species (Sibly et al 1991).

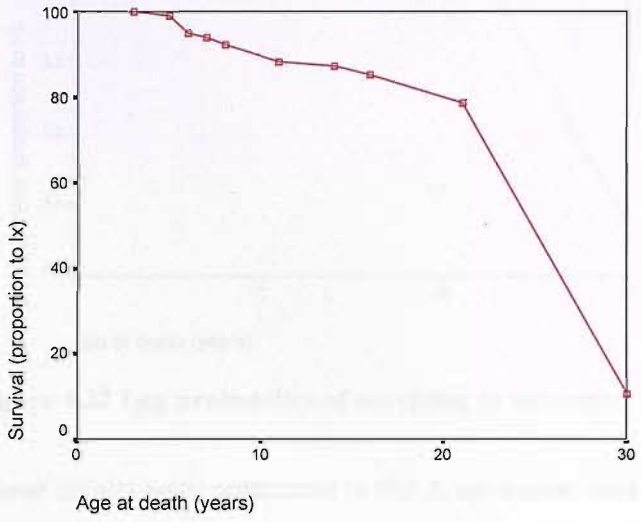

Figure 4.21 Probability of surviving to successive age classes for H. erectus

The survival data were then logged to see if the shape of the curve changed. There is always a concern that logarithmic transformation might 'encourage' the data by creating trends that bear no relation to reality. However, refining the distribution and assessing the robustness of the apparent diagonal trend observed on the left half of the graph could help to overcome this problem. Figure 4.22 shows the results of the transformation, which underline the view that *H. erectus* followed a Type I diffusion of survivorship, rather than the Type II suggested by the primate data. These results imply, on the evidence available, that the majority of *H. erectus* individuals survived until at least reproductive maturity, although it seems that few adults made it into what we would term old age.

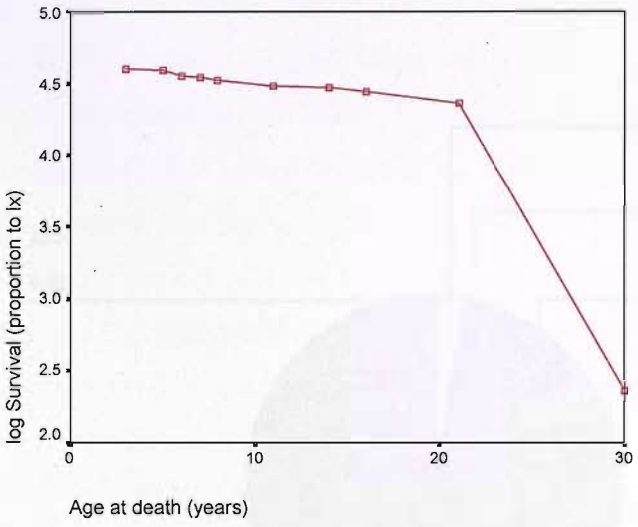

Figure 4.22 Log probability of surviving to successive age classes for H. erectus

These results were compared to the *A. africanus* data introduced above, in order to look at patterns of age-specific mortality in other hominin species and identify early hominin traits. *A. boisei* was excluded from this particular analysis, as the three non-adult specimens, all of whom were around 3 years old at death, reduced its usefulness to this particular study. Table 4.7 shows that this species is represented by fewer age classes, due to a smaller sample size (an estimated 75 individuals) with no young adults:

Table 4.7 Summary of estimated age at death for available A. africanus specimens

Age class	Life stage	Specimen	Total
3	Childhood	MLD 3, 35	2
6	Juvenile	Taung	1
10 14	Adolescence	MLD 11; Sts 2, 18, 24, 52, 70; SE 255; TM 1516 MLD 2, 25	8 2
21+	Adult	MLD 6, 9, 10, 12, 14, 15, 17, 18, 19, 20, 22, 27, 28, 29, 31, 32, 36, 37, 39; TM 1511, 1512, 1513, 1522, 1526; MLC 1; Sts 5, 8, 10, 12, 14, 17, 19, 20, 25, 26, 27, 32, 34, 35, 36, 38, 41, 52, 57, 61, 62, 65, 66, 67, 68, 69, 71; SK 48, 49, 79, 83	56
30+	Elderly	MLD 40; Sts 7, 13, 63; TM 1514, 1515	6

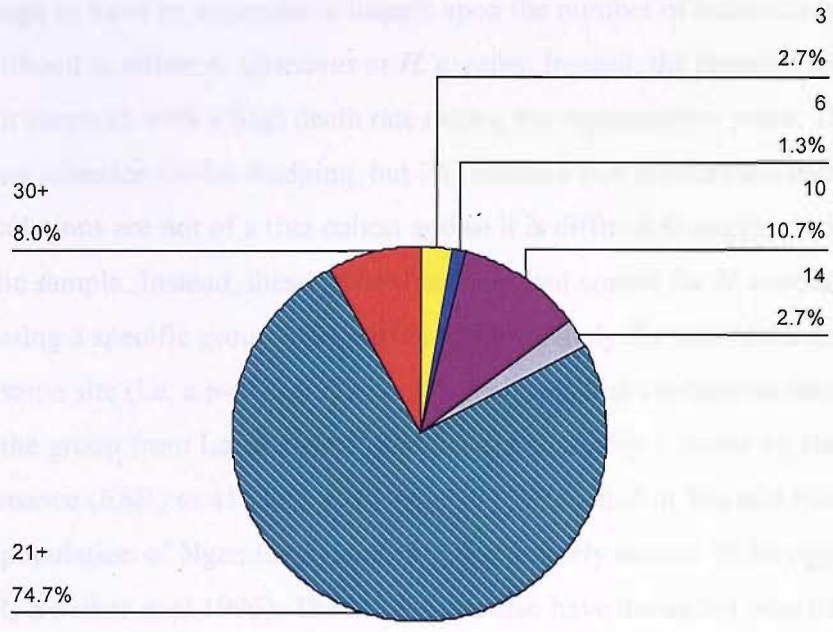

Figure 4.23 Percentage distribution of age at death for A. africanus specimens

Again, a mortality profile was generated for these values (Figure 4.24). The data have been logged and show a striking similarity to the pattern of age at death in *H. erectus*:

Figure 4.24 Log probability of surviving to successive age classes for A. africanus

The implication of these initial findings is that juvenile mortality was not great enough to have an appreciable impact upon the number of individuals surviving to adulthood in either *A. africanus* or *H. erectus*. Instead, the pressure appears to be on adult survival, with a high death rate during the reproductive years. This would create selection for bet-hedging, but it is stressed that the datasets used in these calculations are not of a true cohort and so it is difficult to apply a single hypothesis to the sample. Instead, these generalised survival curves for *H. erectus* can be tested by using a specific group from within approximately the same time period, and from the same site (i.e. a p-deme). The only specimens that conform to these requirements are the group from Layer 8-9 of Zhoukoudian Locality 1, dated by electron spin resonance (ESR) to 418 ka by Huang et al (1991; cited in Wu and Poirier 1995), and the population of Ngandong, centred approximately around 40 ka (again through ESR; Swisher et al 1996). These two sites also have the added benefit of a relatively large number of individuals for a single *erectus* site, of seven and nine respectively.

Zhoukoudian comprises four individuals and three young juveniles, estimated to be three years or less, six years and seven years old. Their presence in the group reduces the adult share of the population to just over 57%, far less than the 80% recorded for the generalised artificial population. However, the Ngandong data does not follow the Chinese pattern. Only two of the nine individuals have been identified as juvenile, aged nine and 16 years and, thus, older than the Zhoukoudian juveniles. The division between adults and juveniles at this site is 77.8% and 22.2% respectively, providing support for the earlier result of Figure 4.17. Although it appears that the Ngandong population had a reasonable chance of surviving until the age of first reproduction, this does not seem to be the case for the Zhoukoudian hominins. A key difference between Indonesia and China is the latitude, and this may be a factor in survival, due to the corresponding differences in rainfall, annual temperature and vegetation. Since the Indonesian latitude is more similar than China to that of Africa, China might have presented too great a divergence from the evolutionary environment, making it more difficult to raise offspring to adulthood.

While these figures may be true for the fossil remains of *H. erectus*, they cannot necessarily be translated into the life history strategy of the species. The results of this chapter, and the model of infant mortality outlined in Chapter Three, suggest that *H. erectus* displayed *K*-selected population characteristics, but in terms of age-specific mortality was a bet-hedging species, according to the environment. However, the level of juvenile mortality in *H. erectus* is far lower than that seen in modern hunter-gatherer populations (where, on average, each newborn has a 50% chance of surviving until the age of 15) and indeed, all other primate species examined here have demonstrated a relatively steep drop in survivorship during infancy. There is no reason to suppose that this did not also apply to *H. erectus*, as well as the australopithecine examples given here. In this sense, Tobias (1999) was right to ascribe such high mortality to the juvenile members of this species, the queries raised regarding his sampling notwithstanding. Nevertheless, by using rank order position of mortality rate it seems that *H. erectus* generally experienced higher levels of survival through infancy and the juvenile stage than did the earlier hominin species included in this study; and the hunter-gatherer data above show that the demise of half of all juveniles before reaching the age of 15 need not be a barrier to a long life. Therefore, in relative terms, allowing for a 50% infant mortality rate, *H. erectus* experienced stable levels of mortality during the juvenile period and into reproductive maturity, and the energetic implications of this are discussed in Chapter Six.

CHAPTER FIVE

Encephalisation

Any change in brain size has life history implications for a species, due to the consequent changes in energetic cost and redistribution of energy resources throughout the body. Since this has ramifications for diet choice and survivorship, the pattern of brain size in *Homo erectus* is explored in this chapter. Evolutionary stasis in morphology and cranial capacity may have been the optimum solution for a bet-hedging species, rather than a gradual increase over time, if the environment was unpredictable or unstable enough to result in high levels of juvenile mortality. Chapter Four demonstrates a differential survival of juveniles in each of the four regions examined, possibly as a result of environmental uncertainty but localised adaptation must also be considered. If encephalisation occurred in the species on a regional basis, as the model developed in this thesis proposes, then this must be placed within an ecological and energetic context in order to understand the impact on life history. The concept of encephalisation in *H. erectus* has been the subject of extensive debate, the evidence for which will be reviewed below, followed by a re-examination of the available fossil evidence in order to determine the presence and nature of any increase in the cranial capacity of this species.

Brain size – stasis or change?

Rightmire, one of two principle contributors to the stasis debate, believes that the increase in brain size seen in *H. erectus* is not a statistically significant trend, and that it is merely intra-specific variation rather than an evolutionary trait (Rightmire 1981). In contrast, Milford Wolpoff argues that 'there are significant evolutionary changes within a conservatively defined sample of *H. erectus*' (Wolpoff 1984: 402). Much of the argument rests on which specimens should be included and which omitted from any study, as *H. erectus* as a clade has suffered from unresolved spatial and temporal relationships (Asfaw et al 2002: 318).

Rightmire maintains that there is 'little directional change' over the course of the species (Rightmire 1981: 241), seeing in the record a series of fluctuations rather than any progressive modification. He analysed cranial capacity, breadth of the cranial base, width of the first mandibular molar and the robusticity of the mandible, identifying these four traits as those that 'should provide preliminary indications of change or stasis in key regions of the skull dentition' (Rightmire 1981: 242). The crania in his investigation comprised all the Asian examples (i.e. those from Ngandong, Zhoukoudian, Gongwangling, Trinil, Sambungmacan and Sangiran, dating from 1.2 Ma to 0.2 Ma [Rightmire 1981: 242]), the Olduvai, Turkana and Salè crania from Africa (dated from 1.5 Ma to 0.2 Ma [Rightmire 1981: 242]), but also the Petralona specimen, often viewed as being archaic *H. sapiens*, at 0.2 Myr (e.g. Conroy 1997: 349). Similarly, the mandible sample also included possible post-*erectus* material, such as the Mauer specimen. Rightmire justified the inclusion of all these specimens on the grounds of increased sample size and thus greater accuracy of the statistical results.

For Rightmire's dataset, the least squares linear regression of time against cranial capacity (volume in ml) gave the relationship:

Cranial capacity = 1100.3 – 175.58*time

In individuals of more recent date, volume increases at a rate of approximately 175ml per 1.0 Myr. However, as the 95% confidence limits are -175.58 ± 252.92 there is no evidence that the regression is significant. Rightmire repeated the analysis a second time without the OH 13 cranium, sometimes considered to be *H. habilis*, and without the Petralona fossil, which, as mentioned above, shares a number of morphological features with *H. sapiens*. On this occasion the regression line was less steep and once again, the regression coefficient was not distinguishable from zero (Rightmire 1981: 244). He concluded that there was little systematic change over time in either cranial capacity or in the other three traits examined.

However, Rightmire did not control for sexual dimorphism, nor did he establish the age at death of the individual specimens. Due to the relationship between brain size

and body size, these are important omissions, as a slight trend in increasing brain volume might merely be a corollary of increasing body size. Unfortunately, there are no complete or semi-complete *H. erectus* skeletons that would allow for such a comparison: there is a single fragmentary adolescent female tibia from Guojiabao, 250 miles south of Yuanmou in China, which is an isolated find of doubtful provenance (Wu and Poirier 1995: 16); and male and female femora from Zhoukoudian (catalogued as C III, J II, J III, M I, M III and IV [Wu & Poirier 1995: 36]). On this evidence, *H. erectus* appears to have been a static species until the close of the Middle Pleistocene, when there was an increase in the rate of change during the transition phase into *H. sapiens* (Rightmire 1981: 245).

Levinton contested this verdict a year later (1982), pointing out that small sample size and poor quality specimens, and the ensuing high sample variance, would combine to give a misleading representation of stasis. He described this as a 'classic statistical trap [of] attempting to prove statistical homogeneity' (Levinton 1982: 307). Using the results of biauricular breadth as an example, Levinton noted that with 95% confidence limits, the regression slope lies between –28.33 and +25.99. An investigator cannot, therefore, discern a slope differing by 53.62, a situation that is not the same as a trend of zero slope. Levinton's alternative hypothesis proposed that the slope for Rightmire's dataset was near zero with narrow confidence limits, although he believed that the data would reject this. In his reply, Rightmire contended that even if this were the case, the result would still be considered insignificant, showing no evidence of directional change (Rightmire 1982: 307-8). Improved results are dependent on an increased sample size, a move that is clearly not (for the time being) possible.

Rightmire's procedure was also criticised by Wolpoff (1984), who believed that the fossil sample had been divided into too few temporal components to give a significant result in regression analysis. Accordingly, Wolpoff divided a group of 65 fossils into six broad age-based classes, creating only five degrees of freedom regardless of sample size (Wolpoff 1984: 390). He also noted that the inclusion of

(what he described as) late australopithecine (OH 13) and archaic *H. sapiens* (Petralona, Arago II and XIII, Montmaurin and Mauer) should have produced some kind of significant trend between these extremes, when in fact no such trend was found by Rightmire, suggesting no evolutionary change. This statement is somewhat diminished by the inclusion of only one cranial representative of each of these outermost species (OH 13 and Petralona) and so their effect would surely have been diluted (although one outlier will not necessarily seriously skew a regression). Instead, Wolpoff focussed on 'a conservatively and narrowly defined *H. erectus* sample', i.e. those specimens which fulfil the originally described features of the taxon. He then divided his sample into three temporal subsets to attempt to gain finer temporal resolution, and looked for evidence of stasis between these subsets, arguing that this procedure is weighted in favour of stasis (1984: 390-1).

Wolpoff's first sample comprised the finds of the Lower Pleistocene: fossils from east Turkana, Olduvai Beds II and III, the Lower Pleistocene Beds at Laetoli, Omo Member J and above, the Modjokerto and Sangiran remains, and teeth from Jianshi and the Badong District in China. This group contains 36 specimens, although it is noted that for the majority of the Asian finds, only the breadth of the first molar could be measured. His second group was of the earlier Middle Pleistocene sites: Olduvai Bed IV and the Masek Beds, Chad, Ternifine, St Thomas Quarry, Gomboré II, Baringo Kapthurian Formation, Swartkrans Member II, Trinil, Sangiran Kabuh Formation, the Lantian remains and Longgudong, producing 25 individuals. Finally, the sample from the later Middle Pleistocene included those specimens from Zhoukoudian, Hexian, isolated teeth from south China and the Sambungmacan finds, totalling 31 individuals. However, unlike Rightmire, he excluded the Ngandong, Petralona, Vértesszöllös, Bilzingsleben and Arago specimens. The status of some of these fossils as *H. erectus* is disputed and could cause some inaccuracy in the results.

Wolpoff took the mean for each subset and tested the divergence with the Student's *t*-test. He found that 'with only a few exceptions, the differences between the early

and late *H. erectus* samples are marked and significant' (1984: 397). In a footnote he observed that if ER 1805 were removed from the early group, then the difference in cranial capacity between the early and middle groups would cease to be significant. ER 1805 is clearly an important fossil in this argument and the effect of its inclusion must properly be assessed, since its cranial capacity of only 582cc, despite being assessed as an adult male (Holloway 1978, cited in Wood 1991: 83, 84), is likely to have influenced the analysis. It is true that the Dmanisi skull D2700 has a cranial capacity of 600cc, but this individual is classified as a juvenile. Its adult cranial capacity can be assumed to be close to the 775cc of the adult D2280. Wood concluded that the affinities of ER 1805 'apparently lie with early *Homo* in general, and with *H. habilis* (as presently defined) in particular' (1991: 85). Results based on either the inclusion or exclusion of ER 1805 cannot be considered as reliable indicators of the presence or absence of stasis.

The addition of juvenile material such as the Modjokerto fossil further complicates the analysis, despite Wolpoff's argument that this juvenile had only 8% additional brain growth, 'if one assumes an adult growth curve were followed' (1984: 398n). This growth curve is, of course, that of a modern human adult, and so is not a reliable method by which to assess one of the earliest examples of *H. erectus* in Indonesia.

Wolpoff concluded from his data that 'there are significant evolutionary changes within a conservatively defined sample of *H. erectus*' (1984: 402). Not all of the measurements he compared exhibited these changes, but he believed enough did so to show a trend in the lineage (Wolpoff 1984: 402). By using the unit of darwins[1], he showed that the rate of change of cranial capacity (0.09 darwins) is more rapid than the average fossil vertebrate rate. The rate of reduction for M_1 breadth falls below the fossil vertebrate mean, but remains significant in *H. erectus* (Wolpoff 1984: 402).

[1] The darwin, a measure of evolutionary speed, is defined as a change by a factor *e* (the base of the natural logarithms) per million years, or about 0.1 per cent of the value of a character in 1000 years (Stearns 1992: 115).

The case against stasis in this study rests on the assumption that the observed changes are bi-directional: the expansion of the cranial vault, and the reduction of the masticatory apparatus. Moreover, Wolpoff reasoned that his study met or exceeded the criteria of sample size and geographic range that had previously been considered to disprove gradualism and confirm stasis (1984: 403; cf. Rightmire 1981). His evidence consistently concludes that stasis for *H. erectus* can be rejected. Rightmire questioned these findings, claiming that Wolpoff's method of allocating the fossils into three temporal subsets was not done in a biologically reasonable manner (Rightmire 1986: 324). Perhaps more importantly, there may be discrepancies and inaccuracies with dating techniques that rendered this method unreliable, with a number of Asian fossils perhaps being considerably older than first thought (see below).

Wolpoff hinted at a problem with the inclusion of the Koobi Fora fossil ER 1805 (1984). Although described by Day and co-workers (Day et al 1976) and later by Wood (1991), it was never ascribed to a taxon, and its morphology makes it a highly unlikely candidate for *H. erectus*. The foramen magnum is placed more anteriorly relative to the bitympanic axis than is characteristic of *Homo* species, and its general basicranial proportions resemble those of robust australopithecines (Rightmire 1986: 324).

Rightmire also raised the issue of the Modjokerto juvenile (1986), the estimated cranial capacity of which remained uncorrected for age. It has been suggested that a Modjokerto adult may have attained a cranial capacity of 1,000cc (LeGros Clark 1978). In addition, according to Rightmire the Sambungmacan cranium is partially filled with hard matrix, making assessment of cranial capacity of either of these two specimens difficult, and unfair to use in a study such as this. When Rightmire repeated the calculations without all three of these problematic skulls, the middle group showed a decrease in cranial capacity compared to the Lower Pleistocene fossils, but a two-tailed *t*-test did not measure this change as significant (Rightmire 1986: 324).

The difference between the early and later Middle Pleistocene groups is significant, with a *p*-value of less than 0.01, probably due to the decrease in the middle group's average. However, the mean difference between the Lower and late Middle Pleistocene groups is 150cc, with a *t*-value of –2.234 and a probability greater than 0.05. These figures confirm for Rightmire that there was no 'dramatic' expansion of cranial capacity in *H. erectus*. Later individuals do have a tendency to a greater vault size but, when an increase in capacity of around 135cc per 1.0 Myr is regressed against geological age, this is not statistically significant (Rightmire 1986: 325). Rightmire did not publish a *p*-value in support of this statement.

In his rebuttal, Wolpoff (1986) agreed to repeat the calculations without either the Modjokerto child or ER 1805, and yet still show that stasis could be refuted without analysing cranial capacity. He substituted the dimensions bregma to inion length (cranial length), auriculare to bregma height (cranial vault height) and biparietal breadth, and the height of the mandibular corpus between M_1 and M_2. To the sample group, he added the Narmada cranium from India and WT 15000 from Nariokotome. As this latter fossil is only a juvenile, he used modern European growth curves to estimate adult cranial capacity. It may have been more useful to apply African growth data instead, because the contrast between temperate Europe and equatorial Africa is such that the pattern of growth, and final build and stature, is highly dissimilar between the two populations. In addition, hominin growth rates may have varied still further; modern growth curves can only provide an indication. The discrepancies in the age at death of the WT 15000 skeleton, estimated from stature, dental age and epiphyseal closure, are found in many modern human children, and it is not assumed that delay in one will coincide with delay in another (Eveleth and Tanner 1976: 175). However, Wolpoff acknowledged that European estimates are too large if growth in *H. erectus* was either faster or lasted for a shorter period (Wolpoff 1986: 327).

In any case, Wolpoff continued to claim that the results indicated significant changes in cranial vault and masticatory size. For the three vault dimensions, he found a

'very significant increase between the early and late subsamples' (Wolpoff 1986: 327), with $p < 0.01$, and the middle subsample intermediate in magnitude for each of the three measurements. Wolpoff also confirmed that the height of the mandibular corpus decreased significantly over time from the early to the late sample, $p = 0.01$ (Wolpoff 1986: 327). On balance, and in light of the limitations of the fossil sample, the evidence is firmly in favour of a gradual increase in cranial size over time in *H. erectus*.

Trends in *Homo erectus* brain size: Rightmire

Finally, in 1990 Rightmire compared the four Turkana and Olduvai hominin crania (average capacity of 905ml), with the five Sangiran crania (average cranial capacity 925ml) and found that the 20ml increase was insignificant. He then paired the African subset (classed by Rightmire as *H. ergaster* and detailed below in Table 5.1) with the Zhoukoudian population (average capacity of 1029ml), but the greater difference in size remained insignificant ($t = -1.618$, $p > 0.1$). When the Ngandong crania were included in a linear regression, the outcome suggested that brain size increased at a rate of approximately 180ml/Myr. However, there have been doubts about the age of these specimens, so until this is satisfactorily resolved, any kind of age-based regression remains unreliable. Ultimately, least-squares regressions have not conclusively shown that there was continuous expansion of the brain vault during the time of *H. erectus* (Rightmire 1990: 195-6, 202).

Table 5.1 Data used in Rightmire's analyses

Species	Location	Specimen number	Endocranial capacity	Date (approx.)
H. ergaster:	Koobi Fora	KNM-ER 3733	848cc	1.6-1.8 Ma
	Nariokotome	KNM-WT 15000	880cc	1.6-1.8 Ma
	Olduvai	OH 12	727cc	1.25 Ma
		OH 9	1067cc	0.73-0.62 Ma
H. erectus	Zhoukoudian	[average from 7]	1,043 ± 113cc	0.5-0.25 Ma
	Sangiran, Java	[average from 5]	934 ± 101cc	0.8-0.3 Ma
	Ngandong	[average from 5]	1255cc	0.8-0.3 Ma (?)

(Data from Rightmire 1990: 195 and Wolpoff 1996)

Table 5.1 reveals a difference between the (so-called) African *ergaster* and Asian *erectus*, in terms of both cranial capacity and the geologic age of the fossils. Before these data can be analysed, it is necessary that they fit the assumptions of any parametric tests. Figure 5.1 indicates that the maximum number of observations within this analysis (18) do not fall within a normal curve, a fundamental assumption of a *t*-test. This is probably due to the very small sample size under investigation.

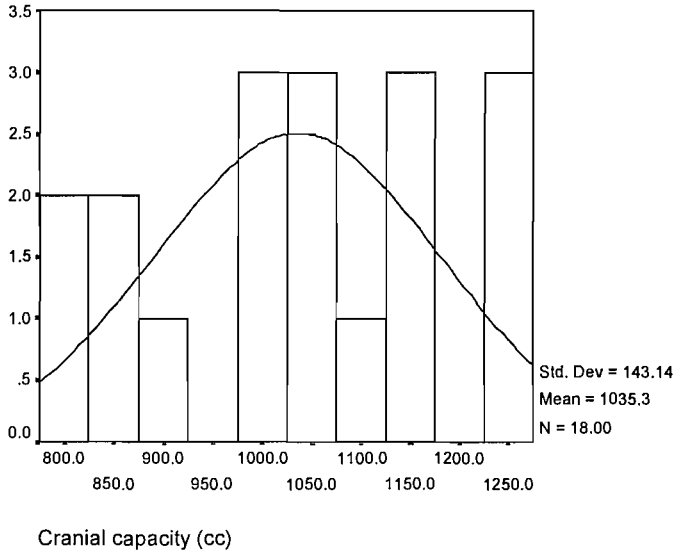

Figure 5.1 Distribution of cranial capacity for African and Asian hominins included in this analysis

The problem is compounded when the dataset is broken down into its constituent regions, reflected most clearly in Figures 5.2 and 5.3 below. Figure 5.2 shows an apparent negative trend of decreasing cranial capacity over time in the *ergaster* subset (the mean of which was taken where a range was provided). However, due to the extremely small sample size the *r*-squared value (R^2 or the co-efficient of determination) is only 0.148, which means that less than 15% of the variation in the figure is accounted for by the regression. Furthermore, this relationship is not significant, with a *p*-value of 0.615 (following statistical convention, the level of significance is set throughout at $p< 0.05$, unless stated otherwise).

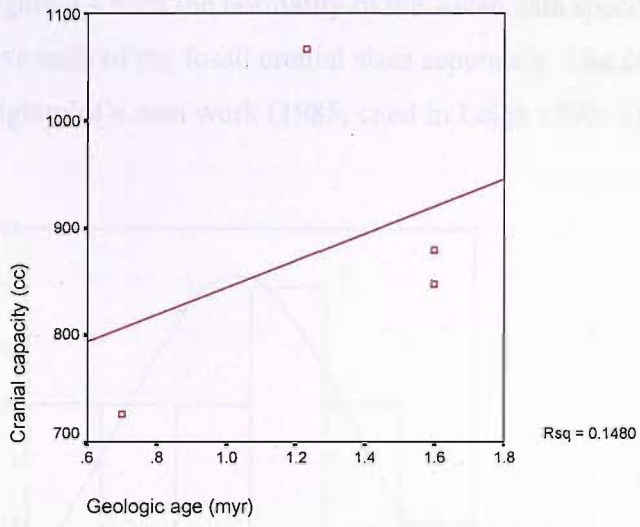

Figure 5.2 Cranial capacity against geologic age for a selection of African hominins

Figure 5.3 represents the Asian *H. erectus* subset compiled by Rightmire in Table 5.1. Due to his use of an average value for each locality, the R^2 value is a mere 0.0332; only 3% of the variation in this figure can be accounted for by the relationship between the two variables. A negative line is again produced, although no implication can be drawn from this; as before, this is not a significant trend (p = 0.883). This cannot be used as evidence either for or against stasis.

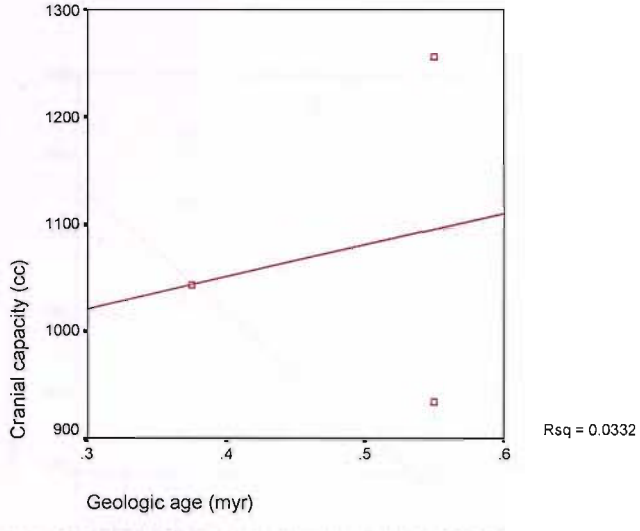

Figure 5.3 Cranial capacity against geologic age for the mean values of selected Asian hominin fossil sites

Figure 5.4 tests the normality of the Asian data specified above, but expanded to give each of the fossil cranial sizes separately. The data for this were taken from Rightmire's own work (1985, cited in Leigh 1992: 3).

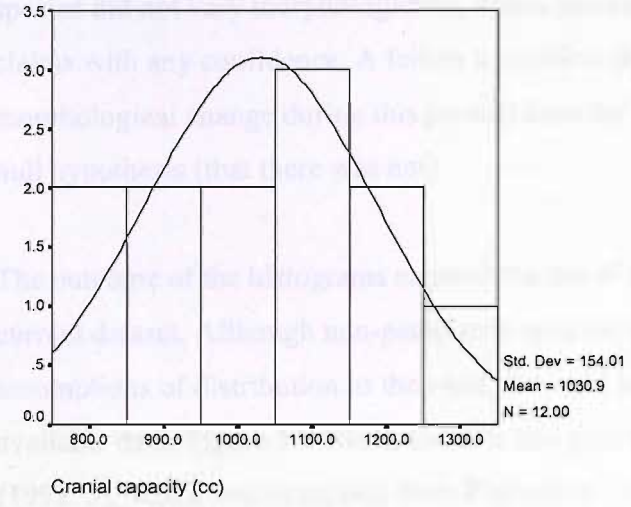

Figure 5.4 Distribution of cranial capacity for the individual Indonesian crania used in Rightmire's analysis

Although the right half of the graph follows the bell-shaped curve of normal distribution, the left half does not and so parametric tests cannot be accepted. This bias towards crania of smaller capacity is illustrated in the regression in Figure 5.5.

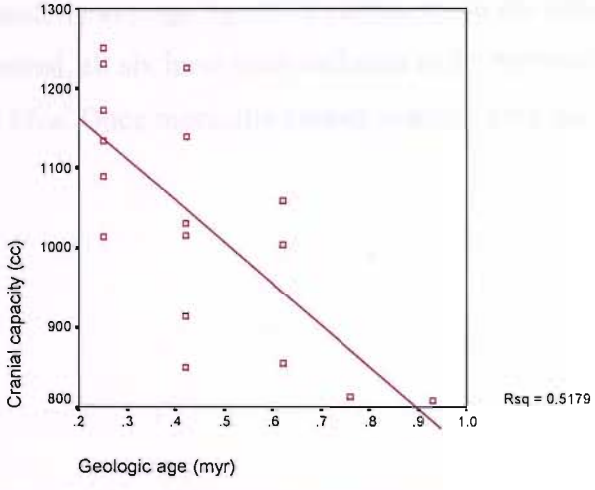

Figure 5.5 Cranial capacity against geologic age for a selection of Asian hominins considered individually

There is a marked increase in the R^2 value to 0.5179, or 52%, a moderately strong result suggesting a closer relationship between the two variables for the Asian samples. Due to the histogram result in Figure 5.4, significance cannot be tested. These results are not conclusive enough to undermine Rightmire's certainty that the species did not vary morphologically, although equally, there is little to support his claims with any confidence. A failure to confirm the hypothesis (that there was morphological change during this period) does not equate with a confirmation of the null hypothesis (that there was not).

The outcome of the histograms negated the use of *t*-tests to determine stasis in the current dataset. Although non-parametric tests do not operate with the same assumptions of distribution as the *t*-test, it would be more useful to increase the available data. Figure 5.7 works towards this goal by using data taken from Leigh (1992: 3), which was compiled from Rightmire's 1985 analysis of the known *H. erectus* sample. The specimens included reflect the content of the table above with a few variations: of the African *ergaster* subset, the Nariokotome skeleton is not represented, but ER 3883 and the Salè specimen are; of the Asian *erectus* group, Trinil, Gongwangling and Hexian have been added to the analysis. As such this is a more complete study, with the regression based on 26 fossil specimens. It was not possible to distinguish which five Ngandong skulls of the possible six Rightmire based his average figure of 1255cc on, as the calculation could not be replicated. Instead, all six have been included in the regression, with a mean cranial capacity of 1147cc. Once more, the dataset is tested for a normal distribution (Figure 5.6).

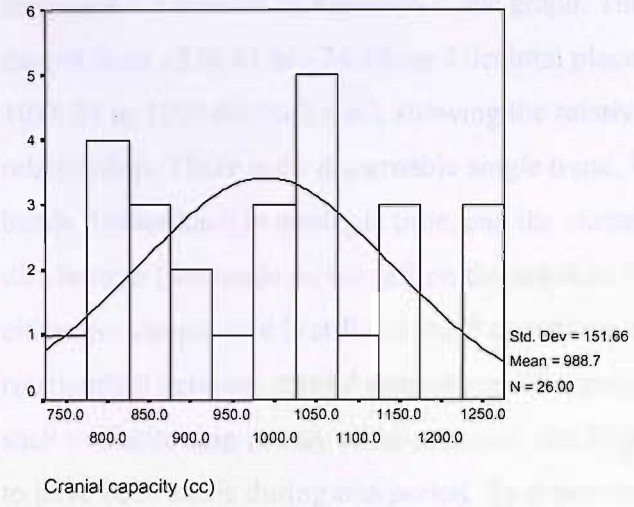

Figure 5.6 Distribution of cranial capacity in Rightmire's expanded dataset

The two model values violate the conditions required for parametric testing; although the distribution of cranial capacity is regressed against geologic time in Figure 5.7 below, it is not possible to test the significance of the trend.

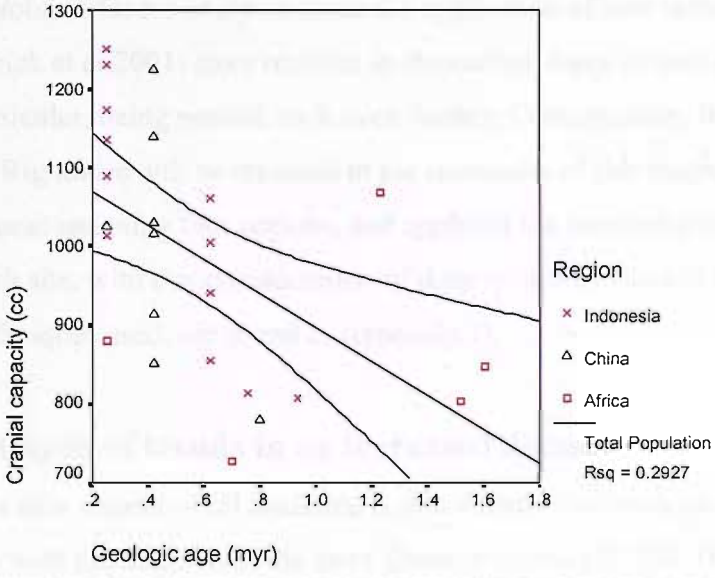

Figure 5.7 Cranial capacity against geologic age for an increased sample of African and Asian hominins

The equation for the line is 1112.79 + -213.61*geologic age. The R^2 value of 0.29 still only suggests a moderately weak relationship, since the added data have

increased the amount of variation in the graph. The variance of the regression slope ranges from –356.81 to –74.40 (to 2 decimal places) and the intercept extends from 1015.95 to 1209.63 (to 2 d.p.), showing the relative lack of cohesion in the relationship. There is no discernable single trend, illustrated by the wide confidence bands further back in geologic time, and the clustering of points on the left of the distribution (the mode on the left on the graph in Figure 5.6). This suggests that either the sample size is still too small to achieve a true representation of the relationship between cranial capacity and the geologic age of the specimens; or that such a relationship is only tenuous at best and Rightmire is correct in believing there to have been stasis during this period. To determine which of these options is the case, further analyses will be carried out on all available *H. erectus* crania.

This action is necessary because Rightmire's analyses are not reliable enough to draw strong conclusions on the evolution of *H. erectus*. His sample size is restricted in both time and space, although it is acknowledged that since his work was published numerous fossils have been discovered and dated. The latter aspect is also a problem for his analysis, since the application of new techniques (see for example Larick et al 2001) have resulted in the earliest dates of occupation, in Indonesia in particular, being pushed back even further. Consequently, the analyses carried out by Rightmire will be repeated in the remainder of this chapter, using an increased dataset spanning four regions, and applying the most recently published dates for each site, with due consideration of their reliability (details of this, and the dating techniques used, are found in Appendix I).

Analysis of trends in an increased dataset

The new dataset of all available crania mirrors the previous analysis of Rightmire but with the addition of the three Dmanisi crania (D2700, D2280, D2282); the Bouri fossil from Middle Awash, Ethiopia (BOU-VP-2/66); the Eritrean specimen from Danakil (UA 31); the new Olorgesailie partial cranium (KNM-OL45500); and the two Sambungmacan crania (SM1, SM3). The Modjokerto cranium is at present ignored, as it is a young juvenile and would introduce a bias into the regression;

consequently the juvenile Ngandong crania are also not considered here. The Ceprano cranium is excluded on demic grounds, as explained in Chapter Two. The new expanded dataset must first be tested for a normal distribution.

Table 5.2 Descriptive statistics for the increased dataset

	Cranial capacity (cc)	Geologic age (Myr)
N	35	35
Minimum	600	0.37
Maximum	1251	1.750
Mean	949.23	0.750
Standard deviation	164.65	0.556
Skewness	-0.061	0.128

The skewness statistic is less than 1, which signifies a distribution that does not differ significantly from a normal, symmetric distribution.

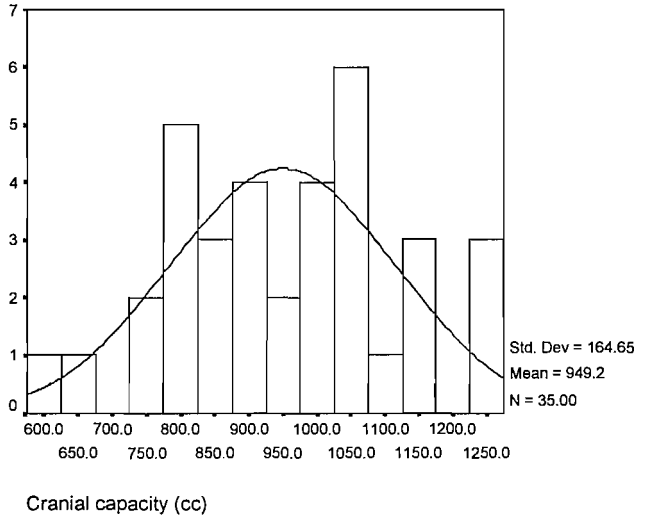

Figure 5.8 Distribution of the cranial capacities of all available H. erectus crania

The graph shows two clear peaks in the distribution of the data, at 800cc (mostly small-brained African demes) and at 1050cc, probably as a result of the relatively larger capacities of the Ngandong and Zhoukoudian skulls. To test whether this exceeds the bounds of normality, a one-sample Kolmogorov-Smirnov test was

carried out on the distribution of cranial capacities. The result was not significant (p = 0.909), to indicate that the data follow a normal distribution, in agreement with the skewness statistic in Table 5.2. This permits the use of parametric testing on the sample of cranial capacities presented here.

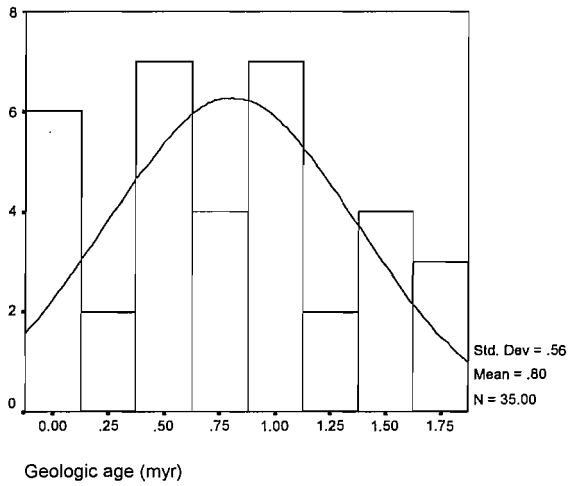

Figure 5.9 Distribution of the geological ages of all available H. erectus crania

Although time cannot be considered as a selection pressure, Figure 5.9 shows how the fossils in this study are temporally distributed. A pattern emerges of a greater number of geologically young, large-brained hominins than older, smaller-brained specimens, which fits the theory of increasing brain size over time, although this pattern may be regionally specific. Moreover, the bias towards the more recent finds seems likely to be a product of taphonomic processes. The youngest fossils from Ngandong, represented by the peak on the far left, are outside one standard deviation, and their influence on the analyses is investigated carefully below. The distribution of geologic ages in the dataset was checked for normality using a one-sample Kolmogorov-Smirnov test. Again, the result was not significant (p = 0.614) and so the distribution is normal and suitable for parametric testing.

Temporal distribution and cranial capacity

These data were then linearly regressed and the R^2 value calculated in order to assess whether this increased dataset follows Rightmire's findings of morphological stasis over time; whether it shows an indisputable increase in cranial capacity over time; or

whether patterns in brain size are particular to individual regions, as the model predicts.

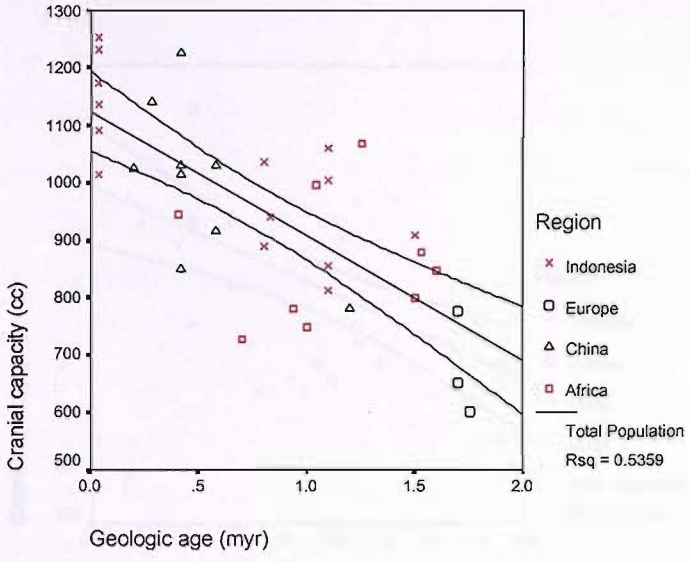

Figure 5.10 Cranial capacity against geologic age for an increased number of H. erectus fossils

Table 5.3 Model for the linear regression of cranial capacity against geologic age

	Unstandardised Coefficients		Sig.	95% Confidence Intervals for B	
	B	Std. Error		Lower	Upper
(Constant)	1123.743	34.201	.000	1054.161	1193.325
Geologic age	-216.896	35.138	.000	-288.385	-145.407

With an R^2 value of almost 0.54, this is a stronger relationship than that shown in Rightmire's smaller dataset, although the slope varies little from Figure 5.7 with an equation of 1123.74 + -216.89*geologic age (Table 5.3). The confidence intervals also show a tighter fit, implying that in 95% of cases the regression line will fall into this narrower boundary (Shennan 1997: 173). This dataset produces a significant result ($p < 0.001$), and superficially shows morphological change over time in terms of the cranial capacity of *H. erectus*. Moreover, this relationship is strong even without logarithmic transformation.

To monitor the influence of the larger Ngandong crania on the regression, Figure 5.11 displays all the data of the previous regression, but excluding the Ngandong values.

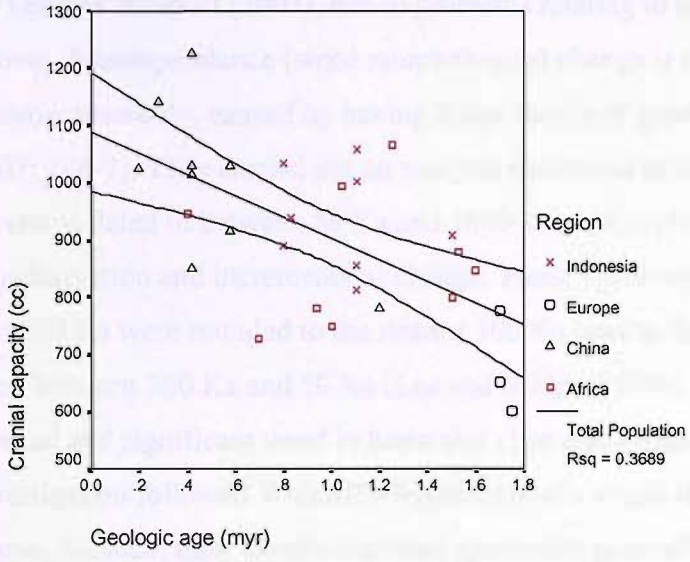

Figure 5.11 Cranial capacity against geologic age for the larger H. erectus dataset, but excluding the Ngandong specimens

Table 5.4 Model for the linear regression of cranial capacity against geologic age, excluding Ngandong

	Unstandardised Coefficients		Sig.	95% Confidence Intervals for B	
	B	Std. Error		Lower	Upper
(Constant)	1088.684	50.479	.000	985.109	1192.259
Geologic age	-187.561	47.214	.000	-284.437	-90.684

Whereas it can be seen that the R^2 value has been reduced to 0.37, the fairly narrow bands of the confidence intervals demonstrate that this is a moderately strong relationship, with only a little more variation than that produced in Figure 5.10 (reflected in the equation 1088.68 + -187.56*geologic age; see Table 5.4, which indicates that most variation is the product of geologic age). The exclusion of the larger Ngandong crania, whose status as *H. erectus* could be debated but is accepted here on the basis of being an *erectine* p-deme, continues to produce a highly

significant regression with $p < 0.001$. Therefore, the crania will be included in all further analyses, because their exclusion is statistically unjustified.

The use of regressions in describing trends in cranial capacity over time is rejected by Lee and Wolpoff (2003), due to problems relating to sample size (addressed above), interdependence (since morphological change is examined) and heteroscedasticity, caused by having fewer fossils of greater age (Lee and Wolpoff 2003: 186-7). They carried out an analysis structured to address these issues, using 94 crania dated to between 50 Ka and 1800 Ka, and applying logarithmic transformation and increments of change. Those specimens dated to within 1800 Ka and 300 Ka were rounded to the nearest 100 Ka, and to the nearest 50 Ka for those aged between 300 Ka and 50 Ka (Lee and Wolpoff 2003: 188). While they did find a gradual and significant trend in brain size (Lee and Wolpoff 2002: 100), their investigation followed Wolpoff's hypothesis of a single lineage of Pleistocene *Homo*. As such, their sample included specimens generally assigned to *H. neanderthalensis* or *H. heidelbergensis* (such as La Ferrassie, the Qafzeh specimens and the Swanscombe skull), and so their findings are not directly applicable to this current study (Lee and Wolpoff 2003: 190, 194). Instead, their work indicates a general change in brain size over evolutionary time, rather than the species-specific investigation of this thesis.

In order to explore the possibility that changes in cranial capacity are a consequence of evolutionary time, unrelated to a particular species or locality, the dataset (Figure 5.10) is expanded to include eight fossils of *H. heidelbergensis* in the regression (Dali, Petralona, Bodo, LH 18, Kabwe, Omo 2, Arago 21 and Ndutu). Howell (1999) does not place these specimens within the same p-deme (see Chapter Two). However, their inclusion, as later specimens (increasingly referred to as a distinct Middle Pleistocene species, and defined morphologically rather than geographically [Rightmire 1998]), allows a regression of geologic age in the manner of Lee and Wolpoff (2003), rather than being restricted to a single species, and this is informative of any trend over time. In Figure 5.12, 56% of variation in the figure is

accounted for by the regression, almost double that of the smaller Rightmire dataset, and the confidence intervals are narrow, with $p < 0.001$ (Table 5.5). This may suggest that a larger sample size is the main factor in producing a stronger relationship and that, since the trend still holds for *H. erectus* alone, it is concluded that cranial capacity does increase markedly over time for this species.

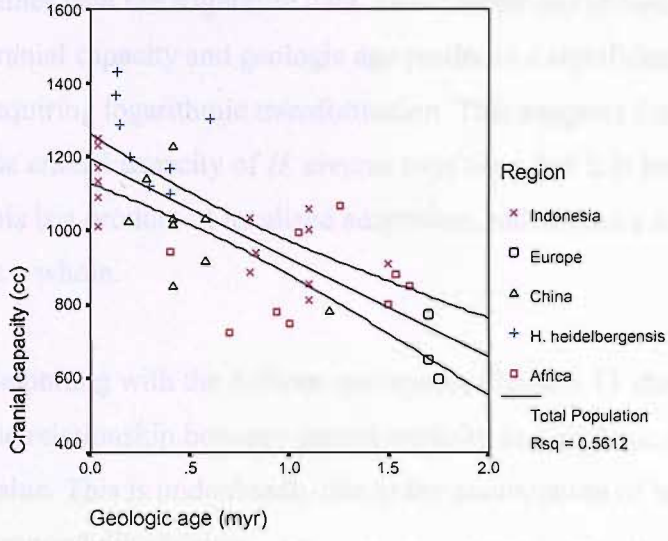

Figure 5.12 Cranial capacity against geologic age for the increased number of H. erectus fossils, and including H. heidelbergensis

Table 5.6 Model for the linear regression of cranial capacity against geologic age, including H. heidelbergensis

	Unstandardised Coefficients		Sig.	95% Confidence Intervals for B	
	B	Std. Error		Lower	Upper
(Constant)	1194.453	32.942	.000	1127.926	1260.98
Geologic age	-268.184	37.034	.000	-342.975	-193.393

Since the original Rightmire cranial dataset and the increased one used here share information (most of the Asian cranial capacities were taken from Rightmire's 1990 review), they are not significantly different ($p = 0.47$). Similarly, the geologic ages used in each dataset were not significantly different $p = 0.066$. However, in recent years a large amount of work has been carried out to determine with greater certainty the geologic age of the Asian fossil beds. These dates are often very

different to earlier estimates; for example, Ngandong is now thought to be only a fraction of the age first estimated (see Appendix I for full details of dating), and this will have a major impact on interpretations of the evolution of *H. erectus*.

Spatial distribution and cranial capacity

All of the following analyses use only the more complete and up-to-date dataset, rather than the Rightmire data. This chapter has shown that the correlation between cranial capacity and geologic age produces a significant relationship, without requiring logarithmic transformation. This suggests that there is a general increase in the cranial capacity of *H. erectus* over time, but it is important to investigate how far this is a product of localised adaptation, rather than a trend applicable to the species as a whole.

Beginning with the African specimens, Figure 5.13 shows no discernable pattern to the relationship between cranial capacity and geologic age, as reflected in the R^2 value. This is undoubtedly due to the combination of small sample size and wide temporal distribution.

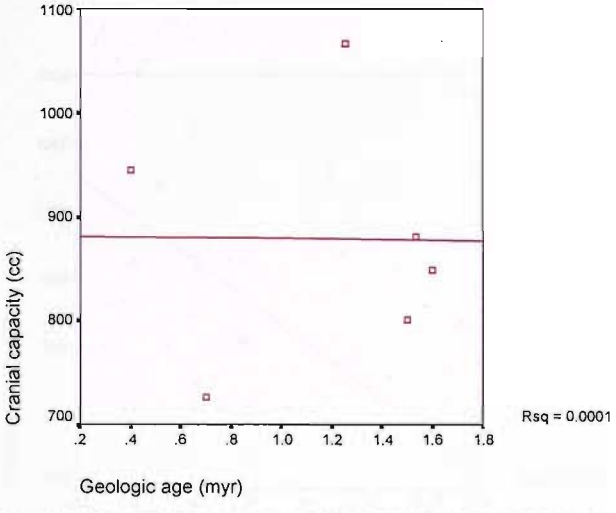

Figure 5.13 Cranial capacity against geologic age for all African H. erectus

The Chinese and Indonesian subsets (Figures 5.14 and 5.15) show more of a trend, although in each case the regression line is influenced by one or a cluster of outlying

points. This is particularly true for China, where Gongwangling is a clear outlier. However, the Indonesia group has an R^2 value (0.595) higher than that for the population as a whole (excluding Indonesia, $R^2 = 0.413$, so Indonesia does not wholly influence the overall trend). However, both of these groups have a larger sample size than Africa, and this is likely to have a bearing on the strength of the relationship.

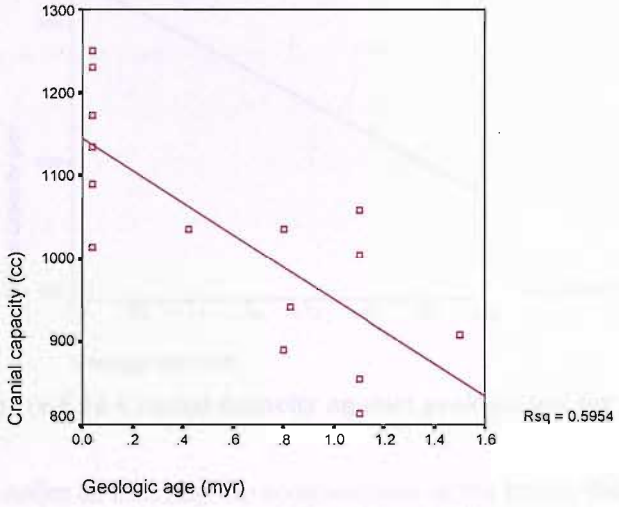

Figure 5.14 Cranial capacity against geologic age for all Indonesian H. erectus

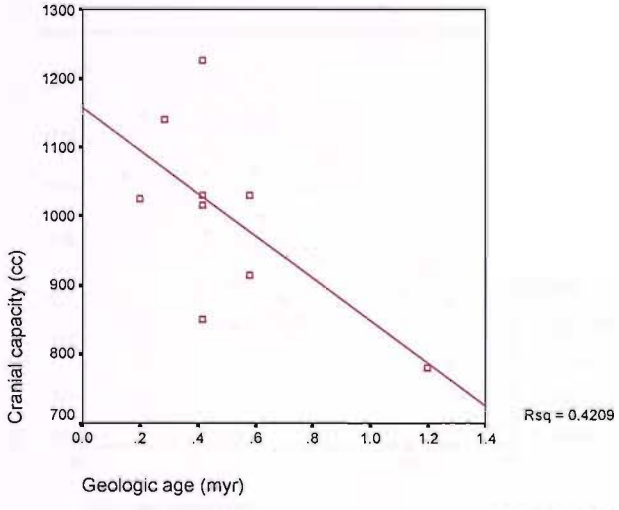

Figure 5.15 Cranial capacity against geologic age for all Chinese H. erectus

In the European subset, sample size is even more problematic, comprising only three fossils from the Dmanisi (*georgicus*) p-deme. Since they are all so close in age, there is little to be gained from the regression, other than to note that cranial capacity is generally small in this sample.

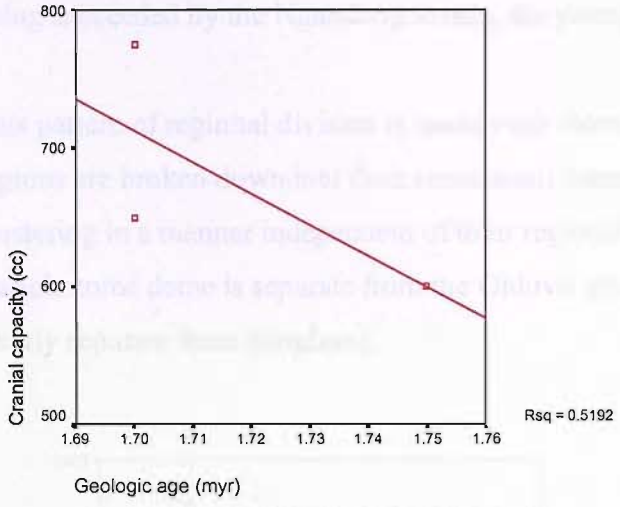

Figure 5.16 Cranial capacity against geologic age for all European H. erectus

In order to identify the composition of the trend, the subsets were plotted together with the regions demarcated on the graph as before. The result, in Figure 5.17, shows clear overlap between distinct regional groups.

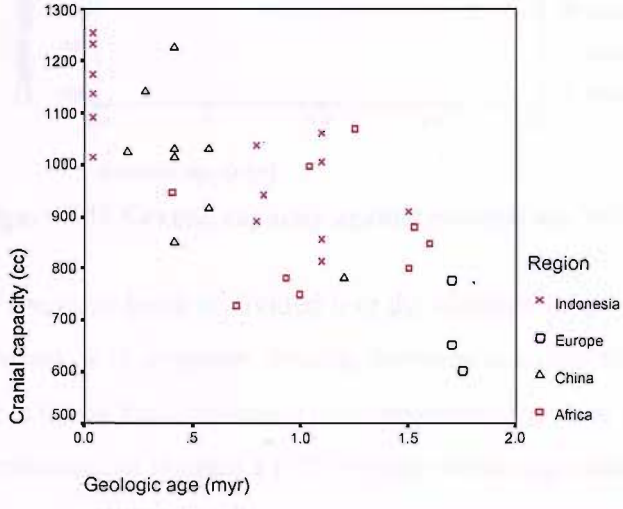

Figure 5.17 Cranial capacity against geologic age for the whole dataset, with fossils identified according to region

In this dataset, Europe, and not Africa, provides the oldest examples of *H. erectus*, although the two are not greatly separated in age (this is not to suggest that *H. erectus* arose in Europe; merely that the oldest specimens discovered so far are from there). Indonesia overlaps considerably with the African sample, giving rise to questions of evolution and dispersal. Finally, Chinese *H. erectus* emerges before being succeeded by the Ngandong fossils, the youngest of this species.

This pattern of regional division is made even more apparent when the four principal regions are broken down into their constituent demes. Figure 5.18 shows the fossils clustering in a manner independent of their regional designation (for example, the Nariokotome deme is separate from the Olduvai group; likewise, Ngandong is clearly separate from Sangiran).

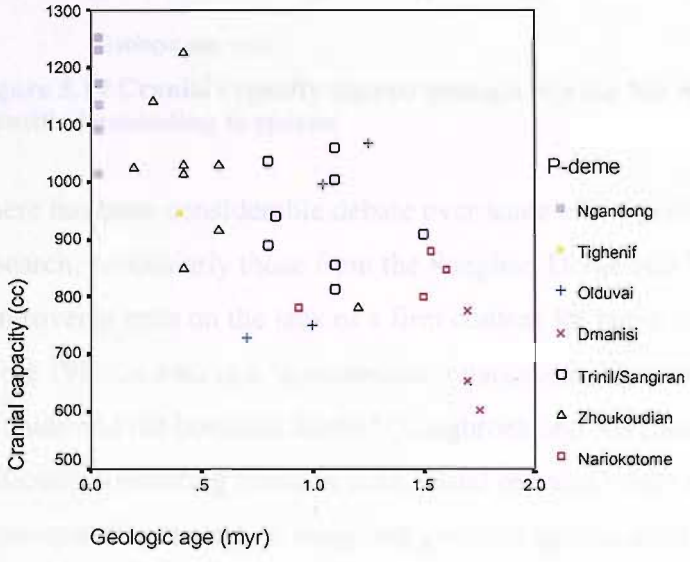

Figure 5.18 Cranial capacity against geologic age with demic subdivision

When each fossil is divided into the alternative species designations of either *H. erectus* or *H. ergaster*, overlap between two distinct groups can once again be seen. This thesis has chosen not to discriminate between *H. erectus* and *H. ergaster*, in preference of Howell's (1999) paleo-deme argument in order to avoid taxonomic debate (see Chapter Two). However, with that in mind, when these two labels are applied as in Figure 5.19, the apparent gap in the Indonesian sample is adequately

filled by the Chinese fossils, creating a continuous span of existence of *H. erectus* in the Far East. Similarly, the African and European subsets complement each other and overlap with the 'classic' *erectine* group:

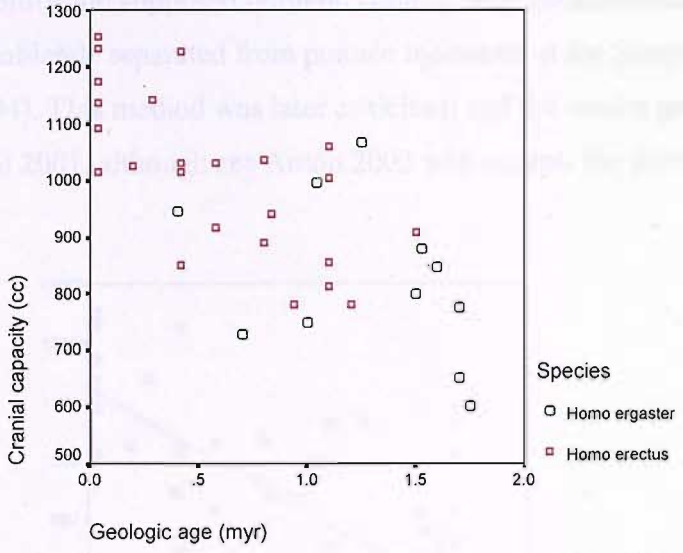

Figure 5.19 Cranial capacity against geologic age for the whole dataset, with fossils identified according to species

There has been considerable debate over some of the geologic dates used in this research, particularly those from the Sangiran Dome and Ngandong. Much of this controversy rests on the lack of a firm context for many of the fossils, first excavated in the 1930s, creating a 'questionable relationship between the dated volcanic samples and the hominid fossils' (Langbroek and Roebroeks 2000: 595), and similar difficulty correlating hominin with faunal remains (Grün and Thorne 1997: 1575). Consequently, the task of assigning geologic ages to each fossil is difficult. Those applied in this dataset were chosen on the strength of the reliability of the techniques used to establish them (see Appendix I for details).

The problems this uncertainty causes are demonstrated below. Figure 5.20 shows the original regression first presented above in Figure 5.10, with an R^2 value of 0.51. Superimposed is a second regression, based on the conflicting dates for the two Indonesian sites. The alternative Ngandong date of approximately 50,000BP

(Bartstra et al 1988) is derived from $^{230}Th/^{234}U$ dating of animal bones found in the locality of the hominin fossils, based on the stratigraphic information of the excavations carried out in the early 1930s (Bartstra et al 1988: 327). The dates for Sangiran are far more controversial. Again, the dating method relies on stratigraphic stability and supposed hominin context, as it measures the $^{40}Ar/^{39}Ar$ ratio in hornblende separated from pumice recovered at the Sangiran site (Swisher et al 1994). This method was later criticised, and the results generally discounted (Larick et al 2001, although see Antón 2002 who accepts the dates).

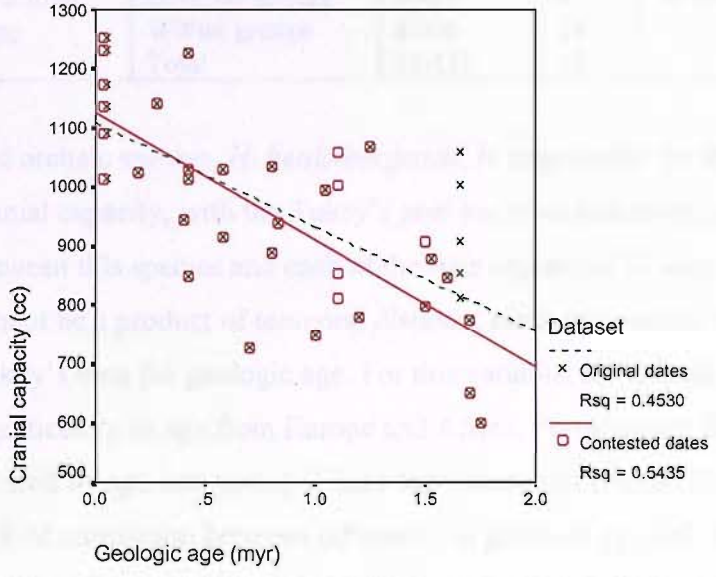

Figure 5.20 Cranial capacity against geologic age for the original dataset and including the contested Indonesian dates

This graph shows that the more conservative dates, originally chosen, produce a stronger regression, and it also demonstrates that uncertainty over dating can cause substantially different results. To reiterate, this thesis accepts that Europe and Africa, as illustrated in Figure 5.17, were home to the oldest known examples of *H. erectus*, and the dispersal to Asia followed later.

The possible morphological and chronological relationship between each region is explored below. The comparisons are made using ANOVA, since the multiple *t*-tests that would be required carry the risk of Type I and Type II errors. The ANOVA was

run between geographical regions, to assess the affiliation between the cranial capacities and the geologic ages of each region. The findings from both are displayed in Table 5.7, which also includes the *H. heidelbergensis* cohort.

.

Table 5.7 One-way ANOVA results for cranial capacity and geologic age in the four regions of *H. erectus* and *H. heidelbergensis*

		Sum of squares	df	F	Sig.
Cranial capacity	Between groups Within groups Total	973507.3 620331.3 1503839	4 38 42	14.909	.000
Geologic age	Between groups Within groups Total	6.411 6.026 12.437	4 38 42	10.106	.000

The archaic species, *H. heidelbergensis*, is responsible for the significant result in cranial capacity, with the Tukey's post hoc tests indicating significant differences between this species and each of the four regions of *H. erectus*. However, this cannot be a product of temporal distance, since this pattern is not repeated in the Tukey's tests for geologic age. For this variable, the archaic group differed significantly in age from Europe and Africa. Furthermore, the *erectus* groups were divided by age into young (China and Indonesia) and old (Europe and Africa). The lack of correlation between difference in geologic age and difference in cranial capacity suggests that it is not only evolutionary time that is responsible for trends in brain size.

To represent these findings, mean cranial capacity and mean geologic age were plotted by region, and the fossils classified for graphical purposes as either *H. erectus* or *H. ergaster*, denoting the eastern and western distributions respectively. The use of boxplots, with confidence intervals, allows a simple determination of whether the differences observed are significant or not: if the error bars do not overlap, then the result is statistically significant.

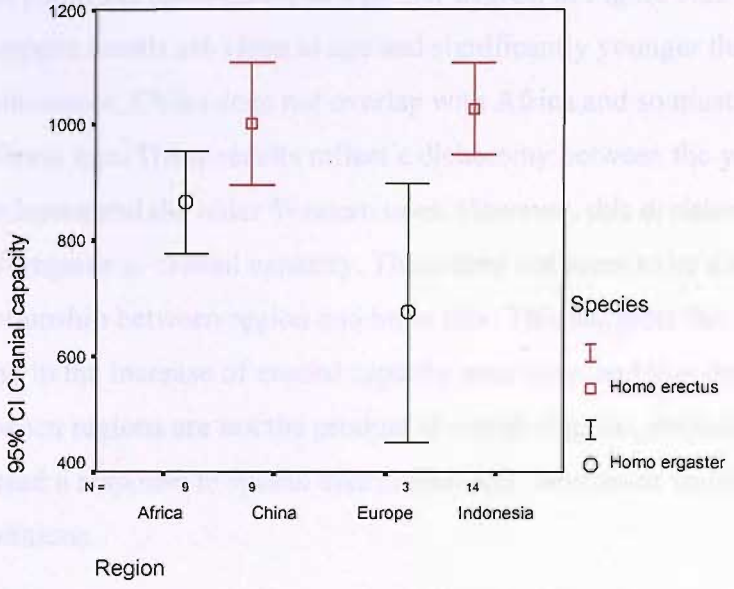

Figure 5.21 Boxplot with confidence intervals of the mean cranial capacity of H. erectus/ergaster by region

Figure 5.21 shows a significant difference in cranial capacity between the European cohort and the Indonesian sample, the only case in which the error bars do not overlap.

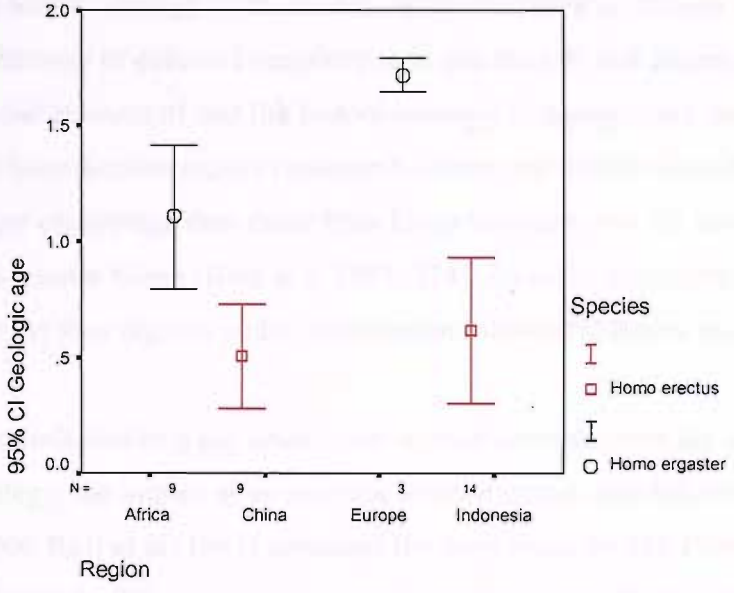

Figure 5.22 Boxplot with confidence intervals of the mean geologic age of H. erectus/ ergaster by region

This pattern is reproduced, to a greater degree, in Figure 5.22 to show that the European fossils are close in age and significantly younger than any of the others. Furthermore, China does not overlap with Africa and so must be of significantly different age. These results reflect a dichotomy between the younger Asian specimens and the older Western ones. However, this division is not as apparent with regards to cranial capacity. There does not seem to be a straightforward relationship between region and brain size. This suggests that there is no definitive trend in the increase of cranial capacity over time, and that the differences apparent between regions are not the product of morphological, evolutionary change, but instead a response to spatial distribution and subsequent variation in environmental conditions.

Discussion

The analyses performed in this chapter arose from the debate surrounding the question of stasis in *H. erectus* cranial capacity, but go beyond a straightforward agreement or rejection of Rightmire's argument. Although the data presented here do suggest a significant increase in cranial capacity over time, it is not sufficient to look at the species as a whole. The model developed in this thesis proposes that the life history strategy of *H. erectus* varies according to latitude within the broad dichotomy of core and periphery, and that the rate and degree of encephalisation is a crucial element of that life history strategy. Ecogeographic patterning in body mass has been demonstrated in modern humans; populations from higher latitudes are larger on average than those from lower latitudes, and the same is true for Pleistocene *Homo* (Ruff et al 1997: 174). As such, the results presented here indicate that the four regions under examination followed different evolutionary trajectories.

The evolution of a big brain is not in itself a requirement for alteration in life history strategy; the impact of an increase in brain size is only felt when body size remains stable. Ruff et al (1997) estimated the body mass for 163 Pleistocene *Homo* individuals. Taking variation caused by sex and geography into account, they found that relative brain size within the genus remained static from 1,800 to at least 600kyr

(Ruff et al 1997: 175). This period covers the African and European fossils included in this thesis, and thus implies that any increase in brain size seen in these regions was accompanied by a proportional increase in body size. In turn, this suggests that life history strategy would not have been adjusted to keep pace with changes in cranial capacity, since energetic cost (as far as can be judged) remained constant. With reference to the model constructed by this thesis, stasis in cranial capacity (i.e. encephalisation is not selected for) is a feature of the periphery. Under these conditions, thought to be characterised by a temperate and unpredictable environment, bet-hedging will be the key feature of the life history strategy followed. Although Africa cannot be classified as 'temperate', clearly this was an environment, like Dmanisi, unsuitable for the attendant risks of encephalisation, namely energy-demanding infants and a prolonged period of growth. These factors classify the African and European regions as being the periphery of the species.

This does not seem to be the case for the more recent Indonesian and Chinese representatives of the species. However, although Ruff et al (1997) included specimens from across the Old World (with the exception of Australia), only 18% of them were of Asian origin (just 3% from east Asia). On this evidence, it is difficult to come to a firm understanding of the relationship between brain and body size in the East. Following the general trend uncovered by Ruff et al (1997), it does seem that over the course of the early to early Middle Pleistocene, body size underwent a gradual increase while, at the same time, brain size increased, explaining part of the analyses performed in this chapter. Yet, by the early Late Pleistocene (150-100 kyr), the encephalisation quotient had reached values to within 10% of modern humans (Ruff et al 1997: 174), and this may also be true for the Asian fossils included in my study. If this were indeed the case, the Asian *H. erectus* p-demes would have experienced selection for encephalisation (the energetic consequences of this are examined in Chapter Six). The model predicts that this would have been associated with a predictable environment of low juvenile mortality and a *K*-selected life history strategy.

While this thesis is interested in constructing an environmental model for life history variation, there are alternative explanations for encephalisation that should be taken into account in order to test the proposals of my hypotheses. The Expensive Tissue Hypothesis (Aiello and Wheeler 1995), developed in response to the energetic cost of encephalisation, is discussed in detail in Chapter Six and suggests that a change to a higher quality diet, such as meat, allowed a reduction in the size of the gut. In return, this 'paid' for a rise in cranial capacity greater than that predicted for body size. This separates the hominin from the environment by reducing this extrinsic factor to the acquisition of meat, whereas I argue that diet breadth is a function of latitude. The Expensive Tissue Hypothesis is compatible with the model developed here, but only as part of a larger biogeographic whole.

A second hypothesis that attempts to explain the drive to encephalisation in *Homo* has its focus outside the body and instead concentrates on group size and the complexities of social interaction. Dunbar 's model (1996) looks at the effect of social behaviour on the development of the hominin brain, specifically the neocortex. Social complexity is represented by group size on the grounds that this would entail 'an exponential increase in the strategic possibilities within polyadic interactions and relationships' (Barton and Dunbar 1997: 246), mediated in primate societies through social grooming. Aiello and Dunbar (1993) see a linear relationship between group size and time spent grooming each day in the servicing of relationships (Aiello and Dunbar 1993: 185), having established that mean group size is a function of relative neocortex volume in primates (Dunbar 1992: 287).

Although Dunbar's (1993) focus was on the evolution of speech as a 'cheap' form of social grooming, thereby allowing the maintenance of larger groups, the link between brain size and group size is intriguing. However, the model has problems both with its technique and even its concept (see the Commentaries following Dunbar 1993 for a ranging critique). Here, neocortex size is the constraint that group size follows, so there is no inherent explanation for the evolution of a big brain (Dunbar 1992: 287; Barton and Dunbar 1997: 249); rather, the selection pressure is

on the need for an increase in group size. While this is a novel approach to an old question, it does not share the focus of this thesis and is not considered further.

It is clear that there are a number of factors identified thus far that may, together or singly, have contributed to the evolution of a hominin brain increasing in size relative to the body. These create a context for the understanding of certain elements of life history, such as encephalisation, but are not in themselves the focus of this thesis. Instead, I concentrate here mainly on the consequences of an increase in cranial capacity, rather than the causes. These are traced in the fossil record through their impact on juvenile mortality and the potential implications of producing encephalised infants. As such, the following chapter reviews the energetic cost of the modern human brain and compares it to extant primate species, in order to set up the exploration of the metabolic burden of the *erectine* brain. The consequences for life history strategy are then examined, with reference to the latitude-influenced model introduced through the first three chapters of this thesis. It is important to consider the possibility that the same species may have had the behavioural flexibility to express variation in its life history strategy according to differences in the regional environment, and this includes maintaining or increasing brain and body size.

CHAPTER SIX

Energetics

As a species, *Homo erectus* experienced an increase in brain size throughout its existence. The previous chapter, in support of the p-deme hypothesis proposed in Chapter Two, indicated that this increase was not uniform, but varied according to geographical location, with the strongest trend in the Indonesian p-deme. However, any increase in brain size has implications for the distribution of the body's resources, and for the rate of development of the young. This in turn will impact upon life history strategy, and in the model developed in this thesis, is expected to vary between regions.

Humans are notable for the impact that a large brain has had on birth schedules, juvenile helplessness and the development of a childhood period of growth, compared to other primates. Particular attention is paid here to the altricial/precocial dichotomy, and the conditions that give rise to each. When examining juvenile mortality, the energetic argument looks at the benefits of delayed growth versus those for early reproduction. This chapter will begin by evaluating the changing energy budgets of infants and juveniles, the metabolic cost of encephalisation, in terms of both individual growth rates (cranial and postcranial) and the burden of the pre-weaned infant on the mother in modern humans. Having reviewed modern human and primate metabolism, the chapter continues by estimating relative body and brain size in *H. erectus* in order to investigate whether the species had to raise metabolically costly offspring. These data are available only for the African p-deme, but provide a starting point for the model. By measuring the costs of encephalisation and its impact in our own species, the effect of an increase in brain size can then be gauged in *H. erectus*, particularly with regard to the species' strategies for negotiating the environments in which it lived.

Encephalisation

The human brain is three times as large as would be expected for a primate of our body size (Passingham 1982: 78). Much of this enlargement has taken place in the cerebellum and neocortex areas of the brain, the latter of which increases in proportion to total brain size in primates as brain size increases (Passingham 1982: 83, 85). In placental mammals, the well-being of mother and offspring during parturition directly depends on an adequate dimensional relationship between the cranium of the foetus at birth and the pelvic girth of the mother. This relationship is governed by the size of the foetus at term relative to the size of the mother, and by the degree of encephalisation at birth. Neonatal and maternal weights are thus allometrically related with an exponent of 0.69, although humans deviate markedly from the regression line with an average birth weight of 3.3kg, rather than the lower predicted 2.2kg (Leutenegger 1982: 87). However, in terms of brain size, modern human neonates are not more encephalised at birth relative to their body size than would be expected through comparison with other primates. When the neonatal brain and body weight of 18 primate species were regressed against each other, the human values did not diverge from the line (Leutenegger 1982: 88). This was established using Western data as a proxy for modern standards, but it may be assumed that it is equally applicable to other populations.

Despite this, humans produce neonates with cranial dimensions considerably larger than would be predicted, relative to maternal pelvic size, due to an overall larger neonatal size. Even so, the infant brain is only a quarter of full adult size at birth, the delay of the remaining three-quarters to the postnatal period thus acting to overcome obstetrical limitations (Leutenegger 1982: 92). One significant consequence is that humans are born 'secondarily altricial', a concept discussed in detail below.

Modern human brain function

The normal adult brain consumes oxygen at the rate of about 3.5ml/100g/min, or 49ml/min for the whole brain (based on an average brain size of 1400g) in the basal, or resting, state. An adult man weighing 70kg consumes approximately 250ml

oxygen/min in the basal state. Consequently, the brain's oxygen requirement in a human adult can account for about 20% of that of the whole body for a relative weight of only 2% (Nehlig 1996: 178). Uptake is even higher in children in the first decade of life, when the brain consumes up to 50%, or 60ml/min, of the total oxygen supply to the body (Sokoloff 1972: 315), as a higher percentage of body weight is accounted for by brain weight.

The proportion of body weight accounted for by brain weight varies between birth and adulthood, and this contributes to the observed greater requirement for oxygen in the infant brain compared to the adult brain. Figure 6.1 illustrates this trend (data from Korenchevsky 1961), showing that the infant brain accounts for six times as much body weight as it does in the adult (12.2% decreasing to 2.2%) (Elia 2001):

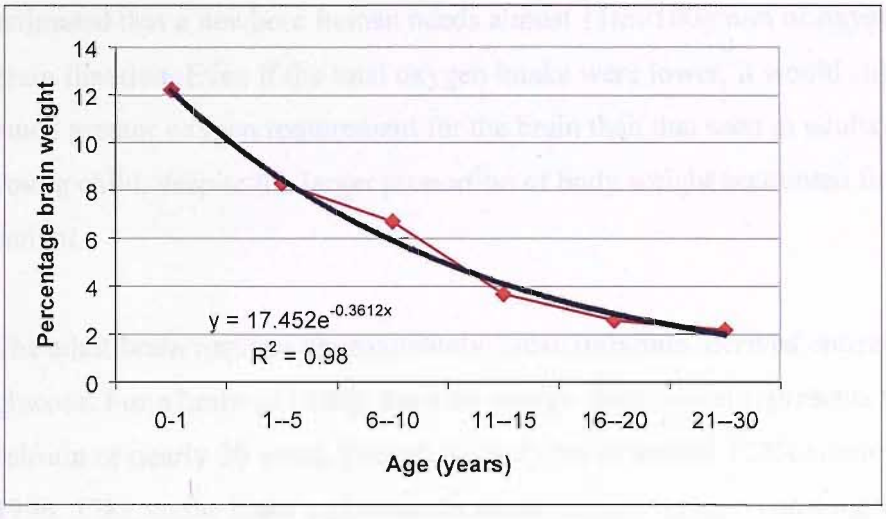

Figure 6.1 Percentage of body weight accounted for by brain weight, over the modern human lifespan (data from Korenchevsky 1961)

An exponential curve was fitted to the data, as it was considered a more representative description of the trend produced by the data than a linear regression, since the rate of decrease of brain weight as a percentage of body weight is not a constant relationship over time. Figure 6.1 indicates that a newborn baby's brain uses up to 50% of the body's oxygen supply, but accounts for 12.2% of the total weight. From this it can be determined that a newborn baby with an average body

weight of 3kg has a brain weight of approximately 366g at birth, a figure that corresponds well with the literature (cf. Zuckerman 1928: 33-34).

Sokoloff provides figures for total oxygen intake and the oxygen demands of the brain for a six-year-old child (1972: 314). As stated above, 60ml/min of oxygen, or 50% of total intake, is necessary for brain function during the first decade of life. This volume is distributed as 5.2ml/100g/min, equating to a brain weight of around 1150g. If it is assumed that for the first year of life total oxygen intake is lower (around 80ml/min for the whole body) due to much smaller body size (approximately 6kg at three months old compared to around 20kg at six years old), the rate of oxygen uptake in the immature brain can be established using the previously calculated neonatal brain weight. With 50% of total oxygen, or 40ml/min, directed towards brain maintenance and a brain size of 366g at birth, it is estimated that a newborn human needs almost 11ml/100g/min of oxygen to support brain function. Even if the total oxygen intake were lower, it would still result in a much greater oxygen requirement for the brain than that seen in adults or even in a young child, despite the larger proportion of body weight accounted for by brain weight.

The adult brain requires approximately 17cal/100g/min, derived entirely from glucose. For a brain of 1400g, the total energy requirement represents about 240 cal/min or nearly 20 watts. The whole body needs around 1275cal/min (Nehlig 1996: 178), so the brain's glucose demands are, like oxygen consumption, around a fifth of the body's total intake. The energy produced by the breakdown of macronutrients (carbohydrate, fat and protein) is transferred to the body's cells by ATP, or adenosine triphosphate, which also facilitates the transfer of energy to cell functions. The chemical reaction (Krebs cycle), which removes the terminal phosphate group from ATP, is accompanied by the release of 7cal/mol (Vander et al 2001: 67). This large amount of energy illustrates that the brain is a costly organ to sustain, as the expenditure of the brain is directed towards the turnover of 7μmol, or 4×10^{21} molecules of ATP, per minute in the entire brain (Sokoloff 1972: 305).

Moreover, since the oxygen in the brain is utilized almost exclusively for the oxidation of glucose, it follows that the infant brain uses more glucose for its size than the adult brain, in the same way as oxygen. However, the infant brain is modified to reduce its dependence on glucose. Ketone bodies (derived from the breakdown of fatty acids [Vander et al 2001: 598]) are usually only present in the adult human bloodstream in quantities greater than negligible during extreme metabolic conditions such as starvation, untreated diabetes, uraemia and hepatic insufficiency. While the brain cannot function without glucose, it can make use of this additional source when necessary. This difference is vital in calculating the cost of the newborn's brain. Whereas ketone utilisation is a survival mechanism in adults, in newborn humans it is a physiological mechanism, whereby as much as 30 to 70 per cent of the total energy metabolism of the brain is accounted for by ketone bodies (Nehlig 1996: 179-180). Although immature brains are expensive in terms of their oxygen demands, their utilisation of available glucose is not, therefore, as great as expected. On the same basis as the adult calculation, a 366g brain requires around 62 calories per minute, or just over 4 watts. The use of ketone bodies as metabolites reduces this glucose need to between 19 and 43 calories per minute, implying that the infant brain is less costly to maintain than adult metabolism would suggest.

Altricial and precocial growth patterns

Brain weight reaches its adult value of around 1400g by 10-12 years of age. Its rate of growth is fastest during the first five years of life, so that by the age of three the brain is already 90% of its ultimate size (Paus et al 2001: 258). In non-human primates, adult brain size is around twice that of neonates. However, because of the much larger size of the adult human brain, a neonate brain of half that size, i.e. about 700g, could not fit through the birth canal. To correct for this, yet still allow time for full brain growth, human infants are born 'early', or 'secondarily altricial' (explained further below), and the foetal rate of brain growth continues into the first year of post-natal life. Figures 6.2 and 6.3 compare the human condition with the rate of brain development in macaque monkeys (Martin 1995: 20-21):

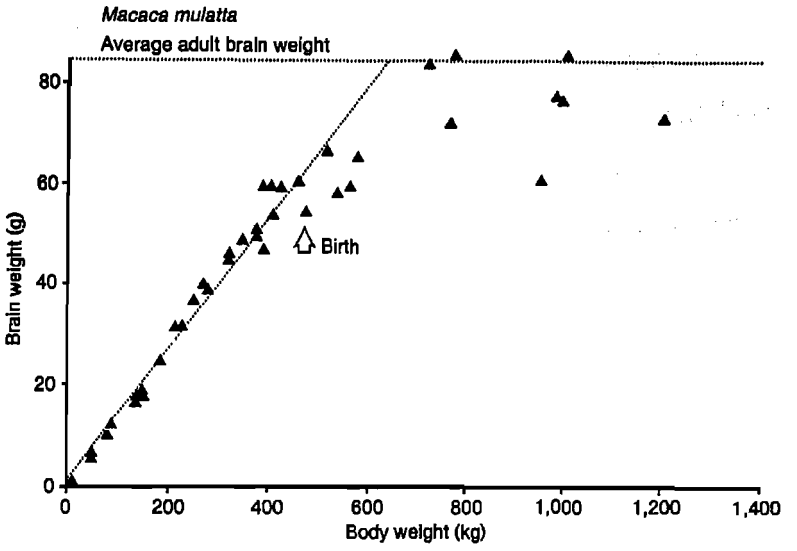

Figure 6.2 Brain weight against body weight during foetal and postnatal development for *Macaca mulatta* (Martin 1995: 20-21)

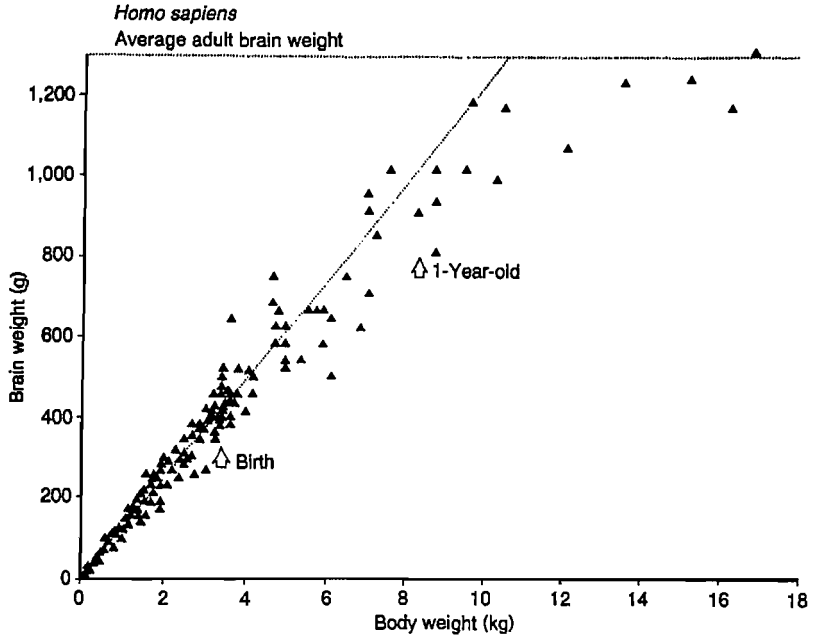

Figure 6.3 Brain weight against body weight during foetal and postnatal development for *Homo sapiens* (Martin 1995: 20-21)

The deceleration of brain growth in chimpanzees occurs somewhat later than in macaques, but appreciably earlier than in humans – one estimate suggests that this change in rate occurs when the infant chimpanzee is around 3kg, or six months old

(Dienske 1986: 148). In Figure 6.3, the hypothetical human neonate's brain size of 725g (following the primate model) is achieved approximately just before the point at which the rate of brain growth relative to body growth begins to tail off.

The dichotomy between precocial and altricial offspring provides a useful context for human life history, linking it to the *r-K* continuum. It is not uncommon for entire mammalian orders or suborders to be characterised by one or other type of offspring. Precocial neonates are born well developed into a small litter after a relatively long gestation period, suiting a strategy of slow reproduction. In contrast, large litters of poorly developed animals born after relatively short gestation periods are classed as altricial, and these species are better adapted to a high reproductive turnover. The level of parental energetic investment in altricial offspring is relatively low, reducing the loss to the mother if the litter is abandoned or dies soon after birth. Maternal investment in precocial offspring is much heavier, and over a longer period of time, making the loss of an infant more costly. Despite this, in precocial species a smaller proportion of the mother's daily intake is devoted to foetal development than in altricial species. This has the effect of buffering the foetus more efficiently from conditions of nutritional stress caused by any environmental fluctuation that the mother might be exposed to. The precocial model generally seen in primates must be a part of our evolutionary history (Martin 1995: 22), although this has been modified in humans to produce a secondarily altricial form, whereby a single, costly, yet helpless infant is born.

The connection between precociality and *K*-selection lies in the size of the offspring at birth and the energetic investment required for growth. Since most development occurs *in utero*, it is not energetically viable to give birth to many offspring at a time. In modern humans, a higher degree of encephalisation prioritises brain growth in the first two years of life. Thus, somatic growth is relatively retarded in order to allow the majority of available resources to be diverted to the brain. For at least part of this time the infant is fed exclusively by its mother, increasing her own energetic burden and making it difficult to care for more than one pre-weaned offspring at a

time, in terms of resource output. Once full adult brain size has been achieved, the scheduling of the energy budget changes to favour the body, observable as the adolescent growth spurt in modern humans. The human condition varies from the ape pattern, therefore, through relative brain size. The position of each primate species, including *H. erectus*, along this scale has implications for the timings of events in the life cycle, as Table 6.1 demonstrates (from Wolpoff 1996: 108).

Table 6.1 A comparison of primate life periods

	Foetal phase (days)	Weaning Age (days)	Infant phase (years)	Juvenile Phase (years)	Adult phase (years)	Birth interval (years)[1]	Adult brain expansion[2]
Lemur	135	135	0.8	1.8	24	1.4	2.9
Baboon	175	420	1.6	4.4	23	1.7	2.3
Chimpanzee	228	1460	3.0	7.0	34	5.6	2.8
Human[3]	267	720	6.0	12.0	50+	3.0	3.3

1 Interval between births for which the offspring whose birth begins the interval does not die within it
2 Ratio of adult to neonatal brain weight
3 The human values for weaning age, juvenile phase, total life span and birth interval are all variable

Figure 6.4 plots these values as percentages in order to aid interspecies comparisons. From lemur to human, the relative amount of time spent as an adult has decreased, to 'pay' for a greater proportion of time spent as an infant or a juvenile.

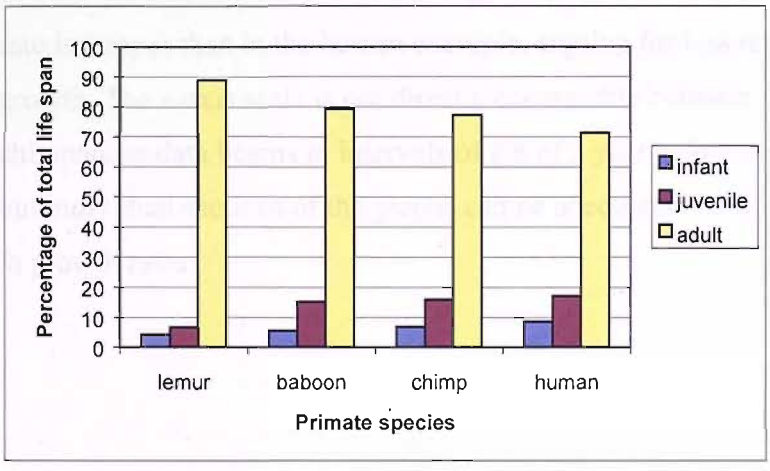

Figure 6.4 Relative proportion of life periods in four primate species (data from Wolpoff 1996)

The infancy period is dedicated to brain growth, and thus varies according to adult brain size relative to body size. The rates of bodily growth for humans and chimpanzees from birth to adolescence were compared. Figure 6.5 (Expert Group 1990) suggests that somatic growth in modern humans is slow during infancy (but note that the first four data points relate to the first year of life), with the rate of weight increase climbing more steeply at the onset of puberty, around 11 years of age.

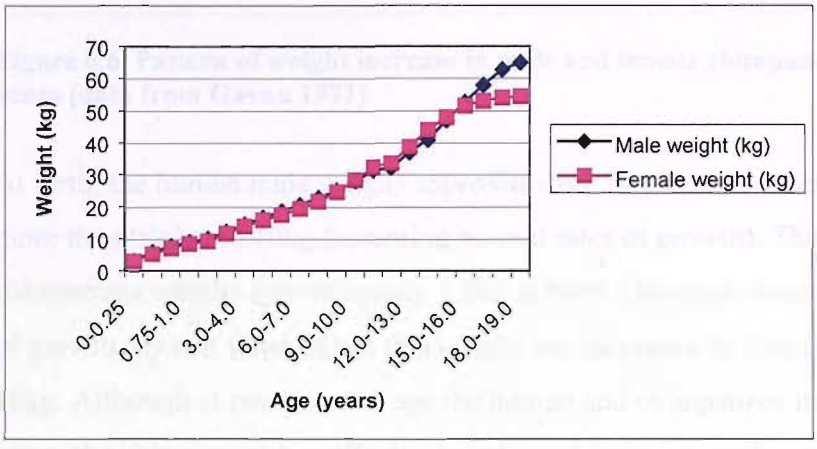

Figure 6.5 Pattern of weight increase in male and female children from birth to 18 years (data from the Expert Group for the Indian Council for Medical Research 1990)

In contrast, the chimpanzee data in Figure 6.6 (Gavan 1971) indicate that growth rate is steeper than in the human example, arguing for less retardation of somatic growth. The *x*-axis scale is not directly comparable between the two graphs, as the chimpanzee data begins in intervals of 0.8 of a year before increasing to a full year, but individual sections of the graphs can be adequately compared to show variation in growth rates.

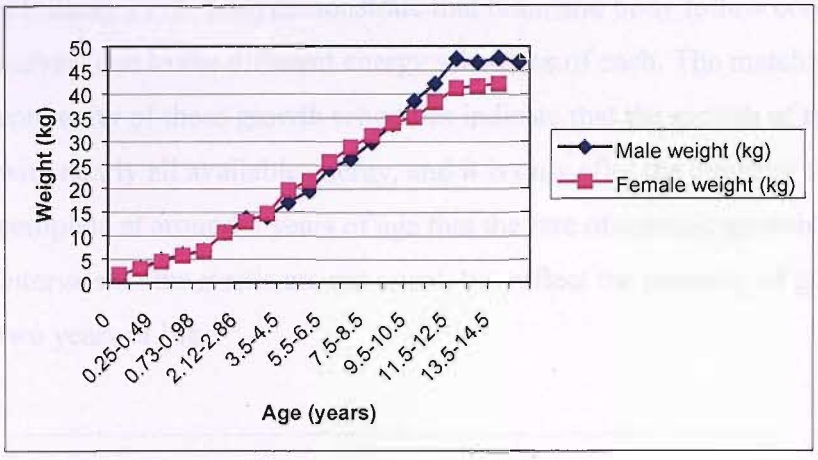

Figure 6.6 Pattern of weight increase in male and female chimpanzees from birth to 15 years (data from Gavan 1971)

At birth, the human male weighs approximately 3kg; by two years of age this has more than tripled to 10kg (assuming normal rates of growth). The smaller male chimpanzee weighs approximately 1.8kg at birth. However, assuming normal rates of growth, by two years of age this weight has increased by five times to just over 10kg. Although at two years of age the human and chimpanzee infant weigh the same, the chimpanzee has effectively achieved twice as much growth.

For each species, age was plotted against the cubed root of weight, a process similar to logarithmic transformation, to create linear data and better contrast the relationships between these two variables. In male chimpanzees the resulting equation for the line is:

$$Y = 0.0747\,x + 1.1114 \qquad R^2 = 0.9599 \qquad (1)$$

The same procedure in the human sample produced the equation:

$$Y = 0.1118\,x + 1.5962 \qquad R^2 = 0.9923 \qquad (2)$$

The increase in weight in human infants was separated out into body weight and brain growth, and the patterns for each were compared. Figures 6.7 and 6.8

(Holliday 1978: 124) demonstrate that brain and body follow contrasting growth curves, due to the different energy schedules of each. The matching concavity and convexity of these growth schedules indicate that the growth of the brain proceeds with nearly all available energy, and it is only after the majority of brain growth is complete at around 5 years of age that the rate of somatic growth rises steeply. The intervals on the *x*-axis are not equal, but reflect the intensity of growth over the first two years of life.

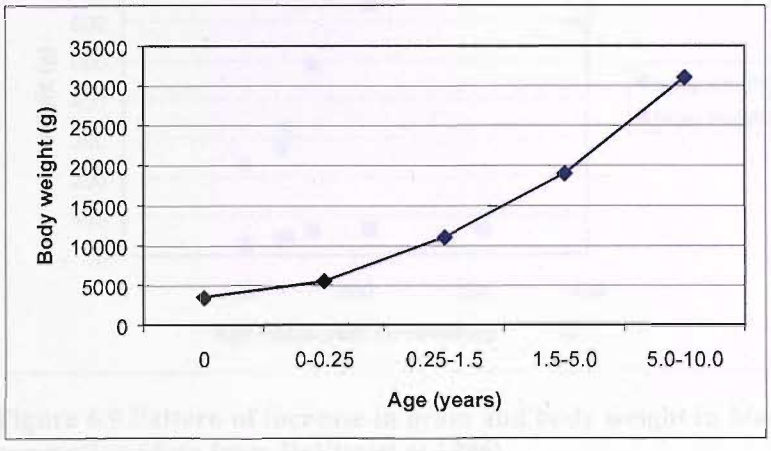

Figure 6.7 Pattern of increase in body weight in humans from birth to ten years (data from Holliday 1978)

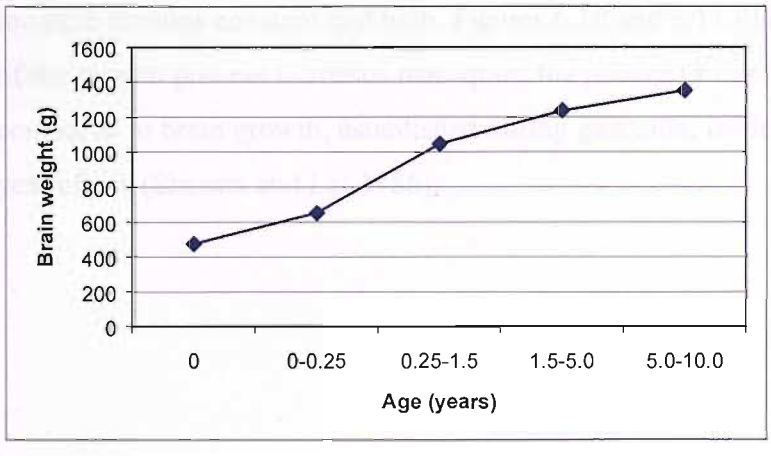

Figure 6.8 Pattern of increase in brain weight in humans from birth to ten years (data from Holliday 1978)

Similar data are available for macaques. While the time scale is not comparable to that of the human or chimpanzee data above, it nevertheless represents differences between the growth patterns of these species. Figure 6.9 focuses on the weight of the brain and body at varying ages post-conception, and shows the much faster rate of somatic growth compared to that of the brain (data from DeVito et al 1986):

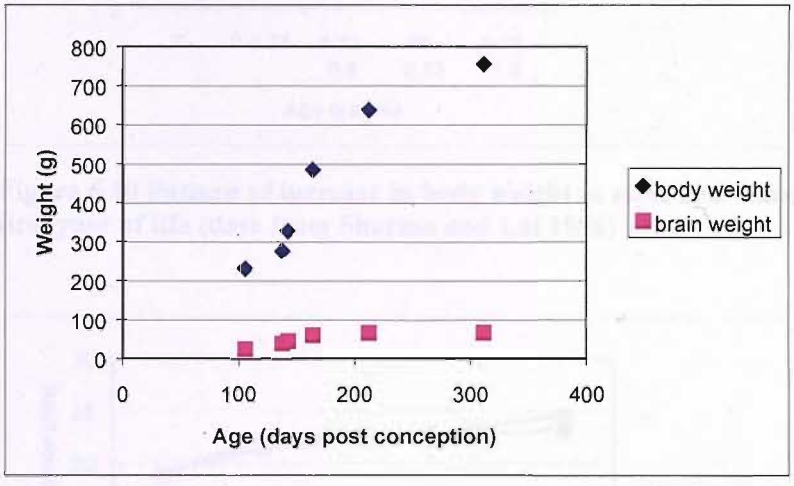

Figure 6.9 Pattern of increase in brain and body weight in *Macaca nemestrina* post conception (data from DeVito et al 1986)

The percentage increases for brain and body weight confirm that, initially, brain weight gains rapidly but the pace is short lived, while the rate of body weight increase remains constant and high. Figures 6.10 and 6.11 illustrate the continuation of the growth process in rhesus macaques; the pattern of rapid somatic growth compared to brain growth, established during gestation, is identifiable over the first year of life (Sharma and Lal 1986):

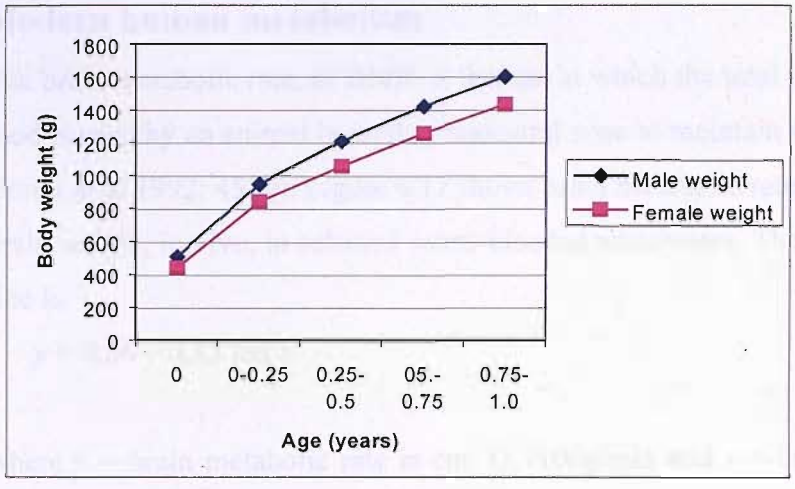

Figure 6.10 Pattern of increase in body weight in male and female *M. mulatta* over the first year of life (data from Sharma and Lal 1986)

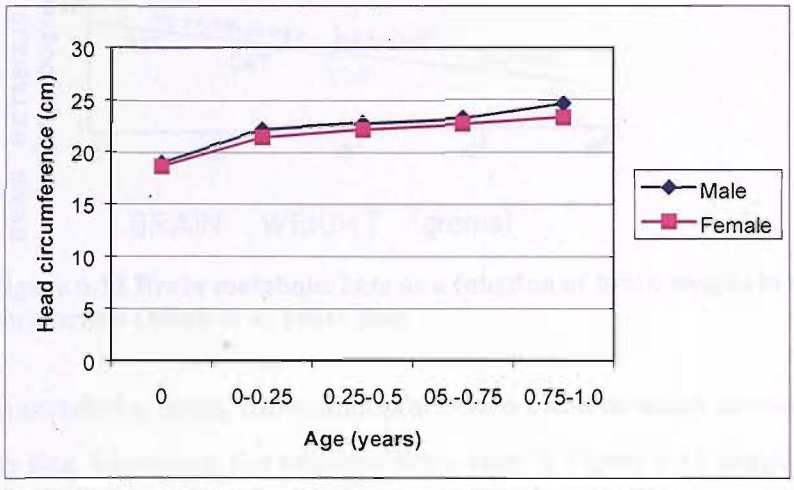

Figure 6.11 Pattern of increase in head circumference in male and female *M. mulatta* over the first year of life (data from Sharma and Lal 1986)

The brain and body have been shown here to follow different patterns of growth in humans and other primates. This implies that the costs of growth, measured by the metabolic rates of brain and body relative to weight, and the distribution of resources around the body, will also differ between brain and body. Consequently, life history strategy will vary between these species, and *H. erectus*.

Modern human metabolism

The basal metabolic rate, or BMR, is the rate at which the total energy obtained from food is used by an animal in its thermoneutral zone to maintain body processes (Jones et al 1992: 459*g*). Figure 6.12 shows brain metabolic rate as a function of brain weight, in vivo, in selected warm-blooded vertebrates. The equation for the line is:

$$y = 0.86 - 0.13 \log x \qquad \textbf{(3)}$$

where y = brain metabolic rate in cm^3 O_2 /100g/min and x = brain weight in grams (Mink et al 1981: 204).

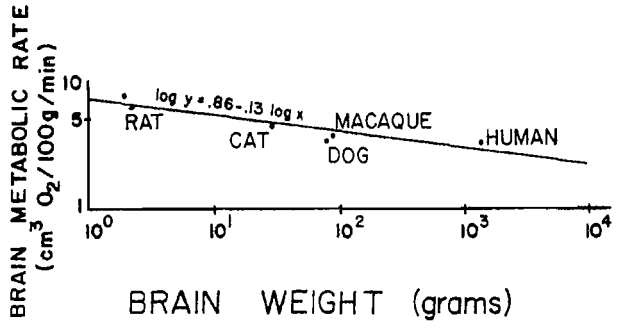

Figure 6.12 Brain metabolic rate as a function of brain weight in warm-blooded vertebrates (Mink et al 1981: 204)

In metabolic terms, the human brain costs about as much as would be expected for its size. Moreover, the negative slope seen in Figure 6.12 suggests that as the brain increases in size, it becomes relatively cheaper, or more efficient to run.

The brain metabolic data from Mink et al (1981) were used to develop an equation (which varies slightly from that produced in Figure 6.12) to describe the relationship between brain metabolism and brain size, using brain weight as a proxy measure. From this, the values for brain metabolic rate in a number of primates were derived (Leonard and Robertson 1992: 186):

$$\text{Log (brain MR)} = -0.301 + 0.874 \log (\text{brain weight}) \qquad r^2 = 0.99 \qquad \textbf{(4)}$$

The derived exponent of 0.87 was then used to relate brain metabolism to body metabolism for 18 anthropoid species (full details of the species included in the study and all values obtained can be found in Appendix II). The log-log regression that best fit the data is:

$$\text{Log (brain MR)} = -0.89 + 0.930 \log (\text{RMR}) \qquad r^2 = 0.87 \qquad \textbf{(5)}$$

When humans were excluded from the calculation, the regression became:

$$\text{Log (brain MR)} = -0.63 + 0.819 \log (\text{RMR}) \qquad r^2 = 0.95 \qquad \textbf{(6)}$$

Using this latter, more generalised equation, humans would be predicted to have a brain metabolism of about 89kcal/day (372kJ/day). Instead, according to Leonard and Robertson (1992: 186), the adult human brain uses 315kcal/day (1318kJ/day), 3.5 times more than other anthropoids. This figure compares well to the one given previously above from Nehlig (1996) of 240cal/min, which equates to a total of 345.6kcal/day.

Our evolutionary divergence is clearer when looking at the relationship between brain size and body size. Figure 6.13 (Martin 1996: 151) shows that modern humans have a larger brain than expected for body size. The human sample is highlighted as a filled circle, and sits well above the line (for which the equation is log E = 0.77 * log W + 1.66, where E = adult brain weight and W = adult body weight), although there is no grade shift in evidence as the next species closest to us in terms of relative brain size is the dolphin, rather than other primates (Martin 1996: 153).

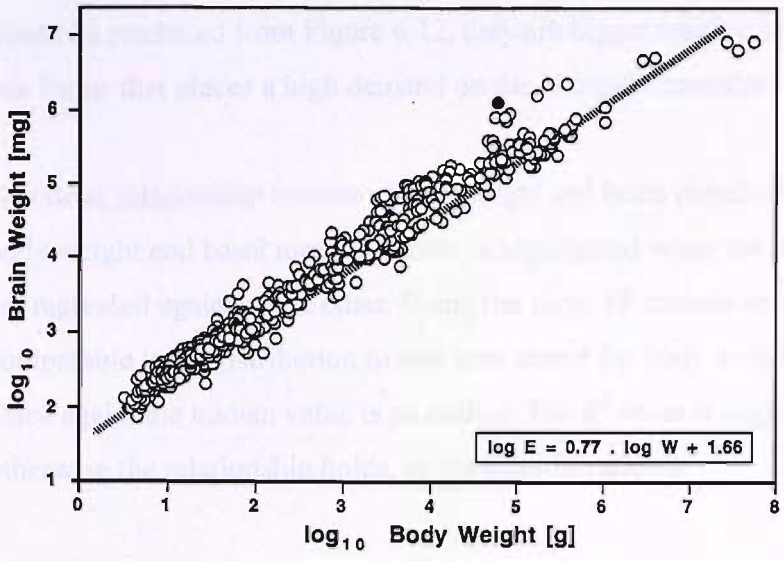

Figure 6.13 Scaling of adult brain weight (E) against adult body weight (W) in a large sample of placental mammal species (Martin 1996: 151)

When primates in the Leonard and Robertson dataset are evaluated on their own, the human outlier (Figure 6.14) is the only species that appears to have a brain weight far bigger than its body weight would otherwise predict:

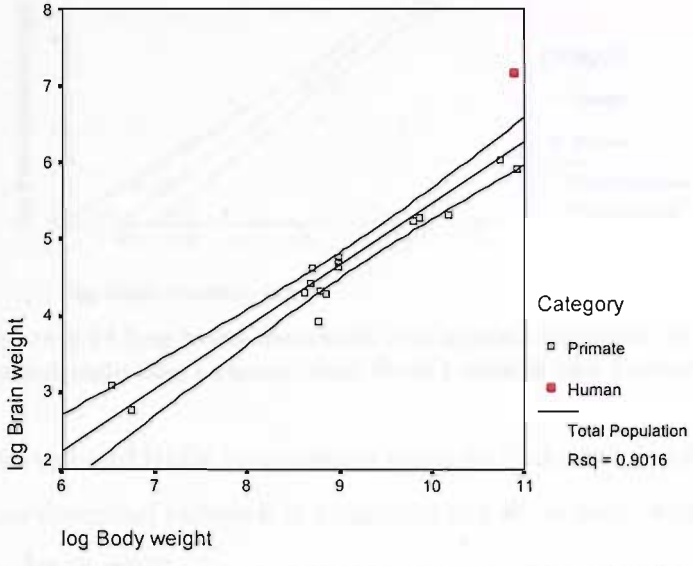

Figure 6.14 Log brain weight against log body weight for 18 primate species including humans (data from Leonard and Robertson 1992)

$$\text{Log brain weight} = 0.807 * \text{log body weight} - 2.606 \qquad (7)$$

Thus, while modern human brains are apparently not much more expensive than would be predicted from Figure 6.12, they are bigger relative to body size, and it is this factor that places a high demand on the energetic resources of the human body.

The close relationship between brain weight and brain metabolic rate, and between body weight and basal metabolic rate, is highlighted when the metabolic variables are regressed against each other. Using the same 18 primate species, Figure 6.15 is comparable in its distribution to that seen above for body weight and brain weight. Once again, the human value is an outlier. The R^2 value is slightly reduced, but otherwise the relationship holds, as the equation shows:

Log brain metabolic rate = 0.93 * log basal metabolic rate – 2.05 **(8)**

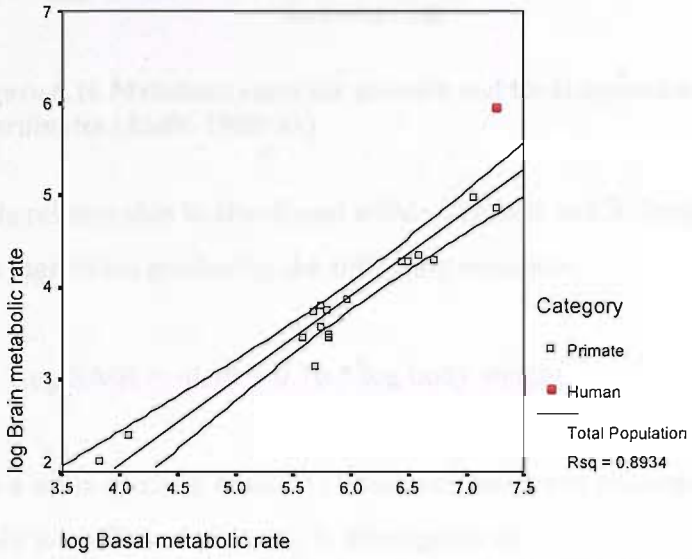

Figure 6.15 Log brain metabolic rate against log basal metabolic rate for 18 primate species including humans (data from Leonard and Robertson 1992)

The value of BMR is dependent upon the body weight of the species, as Kleiber's Law describes (where k is a constant and W_B is body weight [Aiello 1992: 41]):

$$BMR = kW_B^{0.75}$$

The exponent 0.75 (reflected empirically in Martin's data in Figure 6.13) shows that, although larger mammals require more energy, smaller mammals have higher basal metabolic rates per unit body weight. This relationship generates a straight line after

log transformation across a wide range of animals, with the average adult human having a metabolic rate as expected for weight (Figure 6.16) (Aiello 1992: 41):

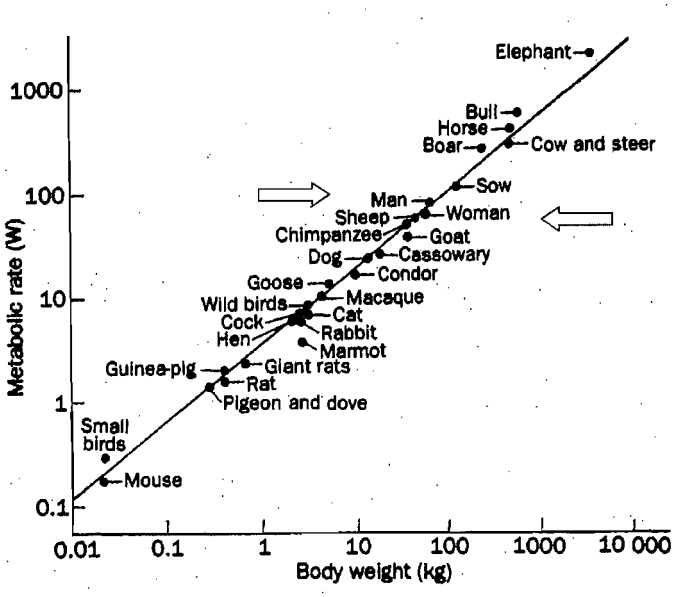

Figure 6.16 Metabolic rates for animals and birds against body weight on logarithmic coordinates (Aiello 1992: 41)

This relationship is also found within Leonard and Robertson's primate dataset, with the regression producing the following equation:

$$\text{Log RMR} = -0.99 + 0.76 * \text{log body weight} \qquad \textbf{(9)}$$

On a mass-specific basis, the basal metabolism of mammals is inversely related to body size. The relationship is often given as

$$\dot{V}O_2/M_b = 0.676\ M_b^{-0.25}$$

where $\dot{V}O_2/M_b$ is the mass-specific rate of basal metabolism in litres O_2/hr/kg and M_b is body weight in kilograms (Hochachka et al 1988: 1128).

However, this relationship does not apply when brain weight is regressed against the total metabolic rate of the body, illustrated in Figure 6.17 by the Leonard and

Robertson dataset. Brain weight was held as dependent, as its size is constrained by the energy available.

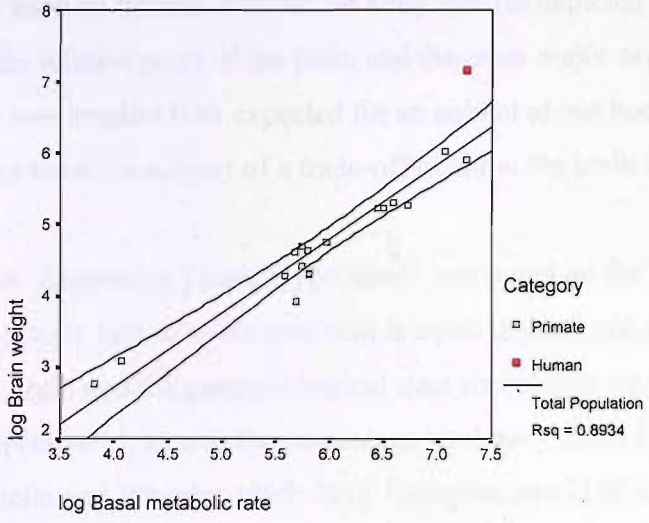

Figure 6.17 Log adult brain weight against log resting metabolic rate for 18 primate species including humans (data from Leonard and Robertson 1992)

Again, the human value indicates a brain bigger than would be expected for a primate with our basal metabolic rate. Despite this, the R^2 value shows a strong correlation between all 18 species. The goodness of fit is further improved when the human values are removed from the analysis (Figure 6.18), with the high R^2 value representing almost a 1:1 relationship.

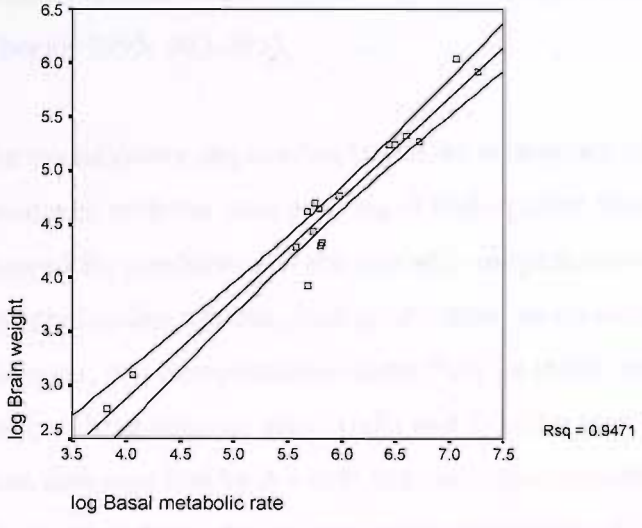

Figure 6.18 Log adult brain weight against log resting metabolic rate for 17 primate species excluding humans (data from Leonard and Robertson 1992)

Aiello and Wheeler (1995) attempted to explain how this extra cost of an enlarged brain could reasonably be 'paid for' by the body, particularly as modern humans do not have an increased BMR for body size (as depicted in Figure 6.16). They looked at the relative sizes of the brain and the other major organs, and concluded that the gut was smaller than expected for an animal of our body size, and must therefore have been the subject of a trade-off to allow the brain to increase proportionately.

This 'Expensive Tissue Hypothesis' was based on the finding that the total metabolic rate in watts (one watt is equal to one joule of work done per second) of the brain and the gastro-intestinal tract was almost equal (14.6 and 13.4 respectively), as was the percentage total body BMR (16.1 and 14.8 respectively) (Aiello and Wheeler 1995: 201). Using the model of a 'standard' 65kg male, they calculated the expected organ masses, and found that the mass of the splanchnic organs (the liver and the gastro-intestinal tract) was 900g less than expected. Conversely, the brain was estimated to be around 850g more than would otherwise be expected. While Aiello and Wheeler make clear that this is a size relationship and not a metabolic relationship, they go on to hypothesise that the approximate saving of 9.5 W from having a smaller gut directly 'pays' for a larger brain in the sense that the hominin BMR would not have been elevated above that expected for a typical primate, if these size changes were contemporary evolutionary events (Aiello and Wheeler 1995: 203-205).

The evolutionary implication is that the emergence of the genus *Homo* was associated with the incorporation of high-quality food into the diet, which then allowed for a reduction in the size and energetic cost of the gut, and so funding encephalisation without placing additional strain on the overall energy budget. However, this interpretation cannot fully be relied upon, due to some ambiguity over the use of the original data. Aiello and Wheeler took their values for metabolic rate from data supplied by Aschoff and colleagues (Aschoff et al 1971: 44). However, in this original study, the oxygen uptake measurement for the gastro-intestinal tract did not differentiate between the gut, the spleen or the liver; they were grouped as one.

This is not reflected in the Aiello and Wheeler study, and so for now the issue must remain unresolved.

The Maternal Energy Hypothesis

There are some species whose BMR values deviate from the metabolism-body size line predicted by Kleiber (Figure 6.16). For example, the New World monkey *Cebuella pygmaea* has a BMR 20% lower than that expected by Kleiber's Law. In contrast, all other anthropoid species, including humans, remain true to the scaling law, with deviations from the line of less than 10%. It can be assumed that *H. erectus* was also true to this pattern. However, maintenance of the human brain requires a proportion of BMR 3.5 times greater than other primate brains, exhibiting a positive deviation of 255% (Leonard & Robertson 1992: 186). An explanation of this might be found in the Maternal Energy Hypothesis.

Martin (1996) notes that as the empirical scaling exponents for basal metabolism and for brain size to body size are both close to 0.75 (0.73 and 0.77 respectively, according to his data), the relationship between brain size and BMR must be isometric (i.e. close to 1). He posits a possible link between brain size and metabolic turnover (Martin 1996: 150). As it has already been demonstrated that humans have neither a metabolic rate greater than expected for either brain weight or for body weight, they must be linked in another way.

Martin found that the residuals for brain size exhibited a fivefold range of variation on either side of the regression line compared to the residuals for BMR, which showed a threefold range of variation. He concluded that a 'significant' amount of variation in adult brain size could not be explained by variation in BMR. Since any connection between brain size and BMR must, therefore, be indirect, Martin hypothesised that this is mediated through the mother during pregnancy (Martin 1996: 154; the problems associated with this strategy are examined fully in Bateson et al 2004). During pregnancy and lactation, the mother is the sole provider of energy to her offspring, and it is mainly during the first of these two stages that the

majority of brain growth is completed (as illustrated in Figure 6.3). This implies that all mammals have the largest brain that is possible, given the metabolic resources available to the mother during pregnancy and lactation, rather than a linking of adult brain size to some behavioural function.

Using data from 53 placental mammal species, Martin carried out a series of partial correlations between body weight, brain weight, BMR and gestation period, with the results shown below in Figure 6.19 (Martin 1996: 154):

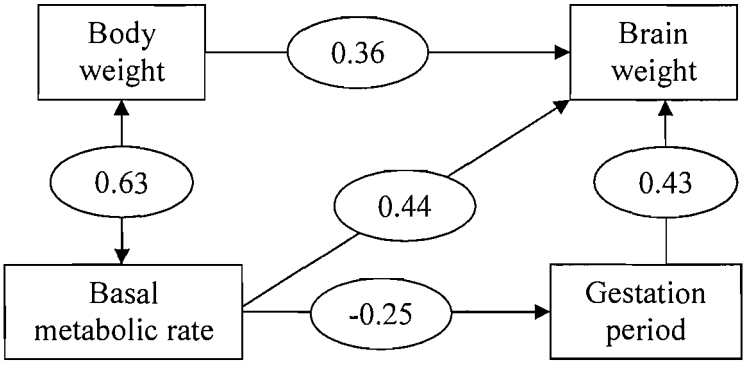

Figure 6.19 Partial correlations between body weight, brain weight, basal metabolic rate and gestation period, with possible directions of effects (Martin 1996: 154)

Both the length of the gestation period and BMR have a greater effect on brain weight than does body weight, supporting the idea that ultimate brain size is determined principally by the mother's BMR, mediated in part by the gestation period. A negative partial correlation between gestation period and BMR also strengthens this argument, as a low maternal BMR is likely to constrain the rate of foetal growth (1996: 154-155).

The maternal energy hypothesis can, therefore, incorporate the scheduling of foetal growth, in that only those animals whose brain growth is dependent on maternal resources would exhibit a high correlation between maternal BMR, brain weight and gestation period. Conversely, in animals where brain growth tails off after birth and thus is not dependent on the energy derived from lactation, the correlation would be lower. These principles can be applied to *H. erectus* to judge whether its brain size

required a high rate of growth after birth, elevated energy resources from the mother and a long gestation period. As cranial capacity increases throughout the existence of this species, it can be hypothesised that the scheduling and energetic demands of different life history phases would also have changed.

In the case of human infants, the relationship between basal metabolic rate and brain weight does not strictly apply (Figure 6.20). During the first year postpartum, the slope produced by the regression is much higher, with the ratio in favour of a greater relative brain size compared to body size. Consequently, the metabolic rate in infancy is higher in order to compensate (Mink et al 1981: 205). For nine months, the foetus has been a part of the mother and so adopts the metabolic rate consistent with her larger body size. Within the first 36 hours after birth, the infant's metabolic rate increases to attain the value predicted by Kleiber in proportion to its own smaller body size (Aiello 1992: 44). This is not a linear relationship, and so there is no equation available for comparison with the adult values, but Figure 6.20 illustrates the pattern of infant BMR (Aiello 1992: 45). Throughout pregnancy, and for as long as the infant is exclusively breastfed, these elevated costs are funded solely by the mother (Garza and Rasmussen 2001: 437), who must also continue to 'pay' for her own somatic needs.

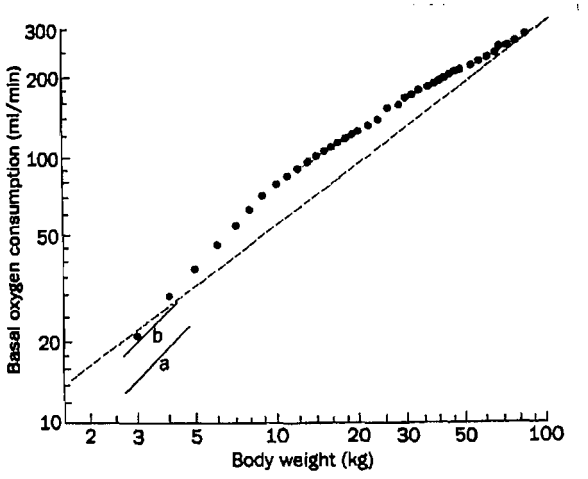

Figure 6.20 The relationship between basal metabolic rate and body weight from birth to adulthood in humans (Aiello 1992: 45)

In Figure 6.20, line *a* indicates that a baby's BMR is much lower than would be expected for its body weight. Within 18 to 30 hours of birth, the BMR has increased to the level predicted by Kleiber's Law (line *b*). The dotted curve shows that during the first year of life BMR increases more rapidly in relation to body weight than would be predicted, with the rate of increase then slowing after the first year (Aiello 1992: 45).

This situation gives rise to two central considerations: the size of an individual's brain is constrained by the amount of energy available to sustain it; and the amount of energy available is constrained by the metabolic resources of the mother, since most brain growth occurs in the foetal stage and during the postnatal period before weaning. The high level of encephalisation seen in humans must therefore be compatible with maternal energetics (Foley and Lee 1991: 223), or it could never have arisen. This is not a scenario mutually exclusive of the Expensive Tissue Hypothesis, and the two hypotheses underline the importance of diet and metabolism to human brain evolution.

The metabolic cost of pregnancy and lactation

During human pregnancy, total energy expenditure (TEE) and its components basal metabolic rate (BMR), sleeping metabolic rate (SMR) and minimal SMR (MSMR) were found to be 15-26% higher than in the postpartum period, adjusted for fat-free mass, fat mass and net energy balance. The mean ratios of TEE to BMR under experimental conditions were between 1.29 and 1.36, showing the minimum energy requirement for maintenance during pregnancy, i.e. between 1.3 and 1.4 times BMR (Butte et al 1999: 305-306). The amount and composition of the weight gained during pregnancy are major determinants of the energy available to the mother and her nutritional needs: the storage of adipose tissue is assumed to anticipate the needs of foetal growth in the last quarter of gestation, as well as the increased energy demands of lactation (Garza and Rasmussen 2001: 439). In late pregnancy, the foetus uses 8ml O_2/kg/min, or 234kJ/kg/day. For a 3kg foetus, this is equivalent to

703kJ/day, which amounts to approximately half the increment in the mother's TEE of 1264kJ/day (Butte et al 1999: 306).

Metabolic efficiency may increase during pregnancy when maternal nutritional status is poor, for example as seen in The Gambia (Table 6.2, from Garza and Rasmussen 2001: 440). Here, the demands of the mother's own somatic needs keep the proportional contribution of BMR to the energetic cost of pregnancy much lower than for other populations.

Table 6.2 Energy cost of pregnancy (MJ) in human populations

Component	Scotland	Netherlands	Gambia	Thailand	Philippines
Foetus	34.0	34.4	29.9	29.9	28.9
Placenta	3.05	3.10	2.34	2.51	2.51
Expanded maternal tissues	12.1	12.3	10.4	10.4	10.1
Maternal fat*	106	92.0	27.6	64.4	59.8
Basal metabolic rate	126	144	7.9	100†	79
TOTAL	**281**	**286**	**78**	**208**	**181**

*estimated from 10 weeks
†estimated from 13 weeks

Lactation is the most energy-demanding phase of the human reproductive cycle (Butte et al 1997: 299). The additional energy needs for exclusively lactating women (i.e. their infant is not gaining energy or liquid from an alternative source) are estimated to be around 670kcal/day. Allowing for gradual weight loss, the net increment needed is about 500kcal/day (Dewey 1997: 19), an additional burden of 25% (Butte et al 1997: 299). The increase in energy required during lactation is met partially through energy mobilization from tissues, but primarily from an increase in dietary energy intake, since 'energy-sparing mechanisms affecting BMR and physical activity were not evident' (Butte et al 2001: 56). Thus, women exclusively breastfeeding need about 2000kJ/day to support milk production, in addition to the minimum energy requirement of 1.4 times BMR noted above (Butte et al 1999: 306).

During the first three years of life, the infant is estimated to require approximately 400kJ/kg/day, with around 35% of this derived from fat (Golden 2001: 456). During the first year of life, half of this expenditure is directed solely towards the growth of the infant brain. Moreover, the weight of the infant at weaning might be a vital factor in its survival. It has been shown in several species that slow-growing infants of low birth weight have reduced survivorship (see citations in Lee et al 1991: 100). Weaning age is, therefore, responsive to ecological variation (Lee et al 1991: 100). This channelling of energy into the developing brain would have had major repercussions for the evolving hominin, not least the adoption of strategies providing high nutritional returns (Foley 1992: 160).

The energetic cost of *Homo erectus*

The relationship between body size and brain size is key to understanding the energetic demands of primates. However, unlike other primates, modern humans have a brain far bigger than expected for body size, and as a result, its relative metabolic demands necessitate alterations in the timings of birth and juvenile growth. Therefore, in order to insert *H. erectus* into the broad primate pattern, its body size must be known. Moreover, it has been established in Chapter Five that brain size in *H. erectus* has changed over time and, more importantly for the hypotheses of this thesis, at different rates within different p-demes (environments). Any increase relative to a more stable body size has implications for changing energy budgets and growth schedules in the species, and the model developed in this thesis proposes that this encephalisation would not be uniform across the species but rather localised to certain p-demes on the basis of latitude (for climate). This chapter turns now to an investigation into *H. erectus* brain size relative to body size within the East African p-deme, compared to other, living, primate species.

There are no reliable estimates of adult stature in *H. erectus* – the Nariokotome skeleton WT 15000 is a juvenile, and two long bones recovered from China cannot provide an accurate representation of a wider population. Once body weight has

been established for this species, the BMR of *H. erectus* can be determined by using brain size and Equation 4 in order to calculate the metabolic rate of the brain.

The cranial capacities of all the *H. erectus* fossils (see Figure 5.8) were converted into brain weights (taking into account the estimated volume of meninges, blood vessels, etc.) by using the formula:

Brain weight (g) = cranial capacity (cm^3) / 1.05

The results were then entered into Equation 4 and logarithmically transformed to find the metabolic rate for the size of the brain.

Log brain MR = -0.301 + 0.874 * log brain weight **(4)**

However, these data cannot be used without having an estimation of the body size of *H. erectus*, because otherwise the species will appear to have a higher basal metabolic rate than expected, and it is known from the regressions set out above for modern humans that this is not the case. The calculations for BMR must be derived with reference to body weight, rather than relying on estimations gained wholly from brain size.

McHenry provides estimations of both male and female *H. erectus* body size, although there is a high degree of potential error (McHenry 1994: 78). Nevertheless, his work remains a useful guide to relative mass, since all hominin postcranial specimens were compared to equivalent elements in humans and apes, derived in turn from individuals of known body weight at death (McHenry 1994: 79). The male estimate of 63kg is based on KNM-ER 736, 1808 and WT 15000, while the female weight of 52kg is calculated from the two femora of OH 28 and OH 34, and KNM-ER 737 (McHenry 1994: 78). There are no associated crania, introducing problems of correlation and inference, although these figures can be used for general extrapolation in conjunction with African cranial capacity. The most complete specimen of *H. erectus* is KNM-WT 15000, the juvenile from Nariokotome on Lake Turkana. Again, the application of juvenile values to an adult sample is inadvisable

but, based on stature and bi-iliac breadth, his adult weight is estimated to be 68kg (Ruff and Walker 1993: 259), which is not conspicuously higher than that estimated for the isolated postcrania above. Similarly, the adult estimate of brain weight is calculated to be 909g (Begun and Walker 1993: 347). These two values are plotted together into the primate dataset, shown in Figure 6.21. The point for the Nariokotome skeleton is joined by the cranial capacity for ER 3883, a male fossil correlated with McHenry's body weight estimate of 63kg ('Male erectus') and that of female ER 3733, regressed against the estimate of the female's 52.3kg body weight ('Female erectus').

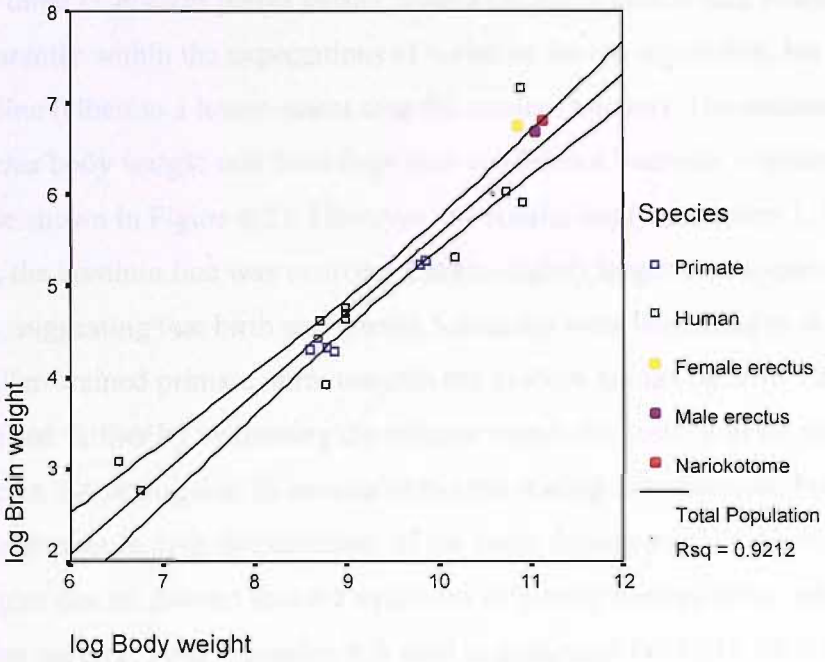

Figure 6.21 Log brain weight against log body weight for 21 primate species including *H. sapiens* and three estimates for *H. erectus* (based on data from Leonard and Robertson 1992)

$$\text{log brain weight} = -3.15 + 0.87 * \text{log body weight} \quad \textbf{(10)}$$

The regression produces a convincing R^2 result and tight confidence bands. The 95% confidence interval values, given in Table 6.3, show a high degree of certainty,

although the hominin estimates can only be considered as a prediction of the (African) *H. erectus* condition, rather than a definitive appraisal.

Table 6.3 95% confidence intervals for the regression between log brain weight and log body weight

Model	Unstandardised coefficients		95% confidence interval for B		Sig.
	B	Std. Error	Lower	Upper	
(constant)	-3.148	0.556	-4.312	-1.985	0.000
log body weight	0.872	0.058	0.749	0.994	0.000

The three *H. erectus* points cluster around the upper confidence boundary, apparently within the expectations of variation for the regression, but a little above the line (albeit to a lesser extent than the modern human). The estimates for *H. erectus* body weight will have their own confidence intervals, overlapping with those shown in Figure 6.21. However, the results imply that, even 1.5 million years ago, the hominin line was evolving a brain slightly larger than expected for body size, suggesting that birth and growth schedules were beginning to depart from the smaller-brained primate norm towards the modern human pattern. This can be clarified further by examining the relative metabolic costs of brain and body in *H. erectus*. Assuming that *H. erectus* obeys the scaling laws between brain weight and brain metabolic rate, the estimates of the male, female and Nariokotome body weights can be entered into the equations originally derived from calculations on extant species. Thus, Equation 9 is used to determine the BMR of *H. erectus*.

$$\text{Log BMR} = -0.99 + 0.76 * \text{log body weight} \quad \textbf{(9)}$$

The logged values derived from this for the composite *erectus* estimates (Nariokotome, male erectus and female erectus) are 7.4688, 7.408 and 7.2636 respectively. However, using a regression equation to generate new values will not give an independent relationship when those two variables are then regressed against each other. For that reason, there is little worth in regressing log BMR against log

body weight. So far, the problem of circularity has been avoided by the use of raw data (brain weight, body weight) to calculate logged values for metabolic rate. This method has allowed the calculation of the metabolic rate for the body and the brain, as seen in Equations 4 and 9, and the two are regressed together below in Figure 6.22:

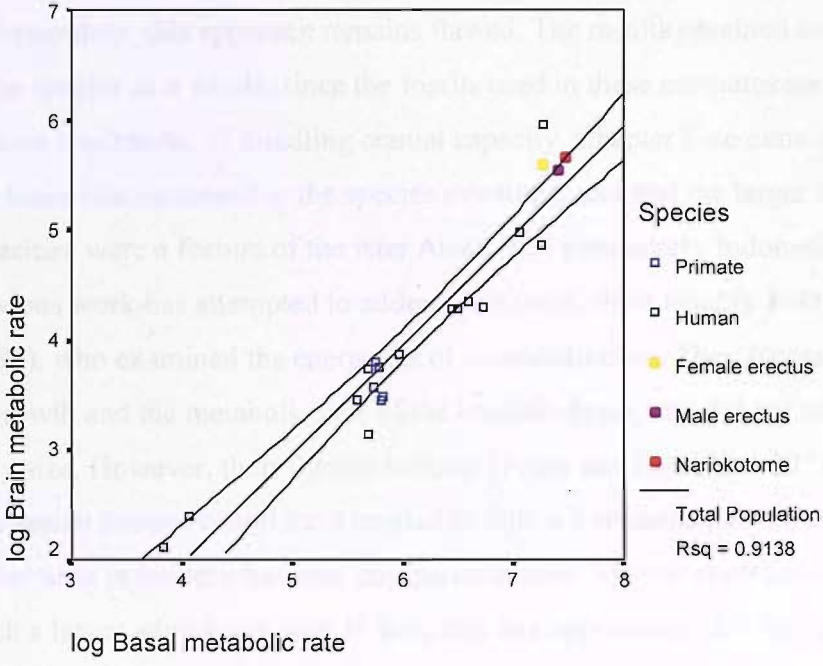

Figure 6.22 Log brain metabolic rate against log basal metabolic rate for 21 primate species including *H. sapiens* and three estimates for *H. erectus* (based on data from Leonard and Robertson 1992)

$$\text{log brain metabolic rate} = -1.99 + 0.99 * \text{log basal metabolic rate} \qquad \textbf{(11)}$$

Echoing the results of Figure 6.21, the metabolic rate of the human brain is greater than expected for BMR. Most of the primate sample falls within or close to the narrow confidence bands (Table 6.4), creating another high R^2 value. This pattern applies equally to the three examples of *H. erectus*, which fall between the primates and the human point, although no further from the confidence interval than several of the living species.

Table 6.4 95% confidence intervals for the regression between log brain metabolic rate and log BMR

Model	Unstandardised coefficients		95% confidence interval for B		Sig.
	B	Std. error	Lower	Upper	
(constant)	-1.991	0.436	-2.904	-1.077	0.000
log BMR	0.991	0.070	0.845	1.137	0.000

Unfortunately, this approach remains flawed. The results obtained are not indicative of the species as a whole, since the fossils used in these estimates are all early African specimens, of middling cranial capacity. Chapter Five convincingly showed that brain size increased in the species over time, and that the larger cranial capacities were a feature of the later Asian (and particularly Indonesian) material. Previous work has attempted to address this issue, most notably Foley and Lee (1991), who examined the energetics of encephalisation. They focussed on the rate of growth and the metabolic cost of the hominin brain, and did not attempt to tie it to body size. However, their figures indicate (Foley and Lee 1991: 227) that the Indonesian sample would have needed to follow a retarded pattern of growth similar to that seen in modern humans, compared to their African predecessors, in order to reach a larger adult brain size. In turn, this has implications for the metabolic scheduling of brain and body growth. As such, it is likely that these late examples of *H. erectus* in the East should be placed midway between early African *H. erectus* and modern humans in Figures 6.21 and 6.22.

Following a modern human pattern of growth has a number of consequences, one of which is the period of growth needed in order to reach adult brain size. Due to rapid childhood growth, the brain reaches 90% of adult size by the age of three years (Paus et al 2001). According to modern human scheduling, an infant member of Indonesian *H. erectus* would have to reach a brain size of 990cc by the age of five years (allowing for some divergence from the modern condition) in order to achieve an adult size of 1100cc (compared to a 90% size of 1260cc for an adult size of 1400cc in modern humans). Holding pelvic inlet and a neonatal brain size of 350cc

constant, this 90% rule might then have increased the maternal energy budget of Indonesian *H. erectus*, leading to the development of secondary altriciality and the need for additional caretakers (e.g. see Alvarez 2000; Hawkes 2003).

Discussion

Compared to other anthropoid primates, modern humans have a brain bigger than expected for body size, although its metabolic cost does not deviate from that expected. However, as a consequence of its increased size, the human brain consumes a greater proportion of the body's total energy budget, which, nevertheless, also remains within anticipated levels. This pattern has implications for the rate of infant growth, both pre- and post-natal, since somatic growth is retarded (relative to other primates) in order to allow the majority of the body's resources to be directed to the brain. Thus, the condition of secondary altriciality, whereby gestation length is constrained by brain size, is a direct consequence of human encephalisation. Most brain growth takes place in the period before weaning, thereby adding to the energetic burden of the lactating female, particularly as body weight at weaning appears to be a factor in long-term survival.

Three estimates for the brain and body weight of *H. erectus* were integrated into the primate database of Leonard and Robertson (1992). These are not definitive figures, and the conclusions are inferential. Two estimates for body weight, averaged from a number of African fossils, were paired with the most appropriate brain sizes in order to reduce stochastic error as far as possible, whereas the body weight of the juvenile skeleton WT 15000 is associated with its cranial capacity. The results from the regressions showed that, while the modern human condition of enlarged brain and raised brain metabolic rate is not fully mirrored in *H. erectus*, this species was located above the regression line, midway to the human point. Even so, the three markers for *H. erectus* remained within or close to the bounds of the confidence intervals, and did not stray further from the line than other primate species. This suggests that the hominin had yet to develop the brain size relative to body size that

distinguishes humans in the primate family; nor did the species experience the elevated brain metabolic rate found in humans.

However, this conclusion can only be applied to the African sample tested here. The previous chapter noted that brain size was not constant over time or across regions, with the larger capacities evident in the Asian line, most notably the younger specimens from Indonesia (Ngandong) and a number of the later Chinese fossils. Though hampered by the lack of a body size for these groups, it is possible that young Indonesian *H. erectus* was closer to the modern human condition than the African individuals included here, due to their much larger cranial capacities, and a potential rise in their encephalisation quotient (Ruff et al 1997). Thus, it is possible that in these locations, encephalisation had made it necessary to adopt the strategy of giving birth to few, helpless, slow growing young, so brain growth could be adequately supported metabolically. Since the African hominins do not exhibit the same degree of encephalisation as eastern members of *H. erectus*, they are unlikely to have developed secondary altriciality, or other traits of modern human life history strategy.

Despite having a slightly raised brain size for body size, the African *H. erectus* infant is not likely to have been a drain on maternal resources in the same way that modern infants are, since their brains do not consume the same proportion of the body's energy. A move to secondary altriciality would not have been a feature of the African *H. erectus* lifecycle, since in this region, *H. erectus* effectively appears to have had a well-budgeted brain. In contrast, given the adult cranial capacity of the Indonesian population and following the modern human growth pattern, it is likely that maternal energy budgets would have been affected by an intense period of infant brain growth and subsequent lactation demands, potentially as great as the additional 500kcal, or 25%, seen in modern human females. The African p-demes, in contrast, would not have needed to wean this intensively, or for as long, as the smaller brains followed a different pattern of growth and development.

Thus, since the schedules of reproduction and growth are expected to vary in *H. erectus* infants between the two disparate regions examined here, it can be surmised that the same will also be true for maternal energetics. The Maternal Energy Hypothesis links pre-natal growth to the metabolic resources of the mother, measured by her BMR. This implies that *H. erectus* would have had the largest brain possible given the mother's energetic constraints. In the African example given above in Figure 6.21, the female of the species shows a brain size slightly increased for body size, and corresponding increase in brain metabolic rate for BMR (Figure 6.22), although relatively far below the level of the modern human outlier. This suggests that although the *H. erectus* female would not have needed to increase her minimum energy requirement for maintenance during pregnancy to 1.3 times BMR, as modern human females do, she would nevertheless have carried an increased metabolic burden. It is hypothesised that this value would have been higher in the Indonesian p-demes, due to the larger cranial capacities of that region. Likewise, the cost of weaning would have been higher in Indonesian *H. erectus*, potentially giving rise to provisioning of the female.

The question of regional variability, and the effect of the environment on growth, is explored in further detail in the following two chapters. It has been shown that the rate and outcome of evolution was not uniform in *H. erectus*, and instead varied according to region. Costing the *erectine* brain has concentrated, by necessity, only on African data, but the conclusions drawn cannot be applied generally without knowing more about the impact of latitude and climate on growth. This thesis examines the life history of *H. erectus* within an ecological context, so it is appropriate that that context is now further explored.

CHAPTER SEVEN

Developmental instability and reaction norms

Phenotypic plasticity affects both the actions of natural selection on phenotypes and the genetic response to selection (Stearns 1992: 60), and is defined as the 'ability of the individual to be adaptively modified by response to the environment during growth' (Roberts 1995: 2). A heterogeneous environment creates the potential for the production of one several possible phenotypes from a single genotype, under different environmental conditions (Stearns 1992: 60). The interactions between genes and the environment 'manifest different degrees of plasticity for different variables' (Lasker 1995: 112), but for plasticity to evolve there must be reliable environmental cues. In addition, no single phenotype can experience superior fitness in all environments, and the costs of plasticity must be kept relatively low (Relyea 2002: 272).

The hypotheses set out in Chapter One propose that the evolutionary ecology of *H. erectus* varied on a regional basis through modification to different environments of growth. Chapter Five tracked changes in the cranial capacity of this species both over time and in relation to the diverse Pleistocene environments in which the species lived. Since the patterns of change in cranial capacity are not identical for each of these regions, this might be an example of phenotypic plasticity and show a general flexibility in the species to adapt to varying environments. However, even within a demic framework, the temporal span of *H. erectus* is great enough to mask any environmental effects. The evidence for *H. erectus* is not sufficient alone to answer the questions raised in the opening chapter of this thesis. To counter this shortfall whilst retaining the core problem of the extent of environmental influence, the alternative strategy of this chapter is to look instead at two modern human populations, temporally and spatially related.

The dichotomy outlined in Chapter One sets physical (environment-driven) plasticity, and thus behavioural flexibility, against poorly-adapted developmental

instability. This is in order to establish whether the multi-branching lineage of *H. erectus* adapted equally to the diverse environments in which it has been found, or whether it had a core region of optimum adaptation compared to a periphery of suboptimal environmental conditions that required a different strategy. In the periphery, nutritional or energetic stress, for example, will reduce energetic efficiency, disrupting the stability of developmental pathways as energy is diverted away from development. Unpredictability of a resource is also a form of nutritional stress (Møller and Swaddle 1997: 135-138). The model constructed in this thesis states that life history strategy will vary according to latitude (with space divided as the core and periphery of the species), and that encephalisation is a feature of that strategy. Chapter Five showed that a move towards a larger brain relative to body size will correspond to *K*-selection, entailing low juvenile mortality and generally stable conditions of growth; possible characteristics of the Asian p-demes. However, stasis in cranial capacity is found in conjunction with bet-hedging, a method of bringing stability of selection to an unpredictable environment (Sasaki and de Jong 1999: 1329) where risk of death may be higher. Developmental instability is predicted to occur under these conditions.

Although encephalisation thus acts as an indicator for life history strategy and the level of adaptation to an environment, it is a long-term evolutionary trend and, therefore, not suitable for investigation in two contemporaneous modern human populations. Any alternative must be analogous, since the aim of this chapter is to use modern human skeletal material to identify responses to the environment that then may be seen in *H. erectus*. As such, this chapter will examine differences in stature and cranial morphology between one economically and nutritionally advantaged population, and one deprived population, in order to assess the human body's susceptibility to environmental fluctuation. A poor quality diet can impede the genetic potential for somatic growth (Golden 2001: 456). Children require certain nutrients (for example zinc, selenium, potassium and magnesium, and the essential amino acids) for rapid linear growth and brain development (Golden and Golden 2001: 515-6), and a relative deficiency in any one of these potentially limits

growth (Golden 2001: 456). Thus, the relative statures of the two populations will provide an initial marker for nutritional stress. This will then be linked to cranial morphology, as the majority of *H. erectus* finds comprise the skull, to investigate whether the cranium is also vulnerable to modification according to environmental conditions.

Evidence for the stature of *H. erectus* is sparse, particularly in association with cranial capacity. The notable exception of the Nariokotome WT 15000 skeleton displays the disjunction of age indicators that is common in modern humans (Eveleth and Tanner 1976: 145-6). Different systems develop according to different growth rates, so while the Nariokotome fossil's dental age was estimated to be 10.5-11.3 years, epiphyseal fusion suggested an older 13-13.5 years, while stature inferred an age of between 12-15 years old at death (Smith 1993). These maturity indicators have also been shown to vary within recent populations (Lampl and Johnston 1996; Clegg and Aiello 1999). While the fossil evidence suggests a pattern within the normal range of variation found in modern humans (Clegg and Aiello 1999: 81), as a single point it is unhelpful to this study because it does not show the pattern of growth of the population from which WT 15000 came.

This chapter compares cranial capacity, cranial shape and stature variation according to nutritional status, and introduces fluctuating asymmetries to provide a measure of stress. The degree of growth in the left and the right sides of the body is not necessarily equal, and this may be caused by genetic factors, environmental factors or a combination of the two. Craniofacial asymmetry is observed throughout the population (although it is often masked by soft tissues) and is not influenced by sex or age; nor is it related to the appearance of dentition in children (Rossi et al 2001: 381-384), although asymmetries in the dentition itself have been noted in laboratory animals after exposure to stress during development (Albert and Greene 1999: 342). Bilateral asymmetries in the postcranial skeleton are known to result from occupational or mechanical stressors (for example, see Steele and Mays 1995), but are also a documented indicator of environmental stress (Albert and Greene 1999).

In this way, a morphological comparison of two modern human populations can be used to provide a context for patterns identified in *H. erectus*. Through the following investigation into the extent of developmental instability and fluctuating asymmetry (defined and outlined below) in two contrasting human populations, the chapter aims to establish a link between the environment of growth and the development of the skeleton.

Developmental plasticity and fluctuating asymmetry

This section will explore two contrasting views of environment-driven phenotypic shifts, differentiated by the extent and time scale of the alteration. The phenotype of an organism is the physical expression of its genotype, 'the sum of [its] observable and measurable properties' (Pritchard 1995: 19), produced by the interaction between the genome and the environment. 'Plasticity' is used to describe intra-individual variation, whereby an organism has the ability to react to the environment through a change in form, state, movement or rate of activity (West-Eberhard 2003: 34-35). This reaction can take the form of either the plastic response to environmental change, or the plastic adaptation to environmental stress. The latter will demonstrate irreversible changes to the adult phenotype, with a consequent impact on survival and reproduction (Schell 1995: 228). The dichotomy between the response to variation (plasticity) and the response to stress (fluctuating asymmetries, examined below) is crucial to understanding the nature of environmental impact. Plasticity is a long-term adaptation with an underlying genetic structure that allows for a controlled reaction to oscillations in environmental conditions. Fluctuating asymmetries arise in an individual's lifetime and are a marker of stress and instability during the period of growth.

Life history is a set of rules that governs age-specific allocations of time and energy over the life span of an individual. The rate of growth signals the proportional allocation of net assimilated energy (NAE) to growth, maintenance, storage and reproduction. Differences in growth between populations could be an indication either of differences in NAE under identical proportional allocations, differences in

proportional allocation, or a combination of both. Only the latter two options involve genuine plasticity (Niewiarowski 2001: 422).

The action of the plastic response can be demonstrated by the theoretical plotting of the adaptive surface of a population, i.e. mean fitness against mean phenotype. Figure 7.1 indicates how plasticity may contribute to a 'peak shift' in the adaptive surface whereby a population increases its fitness (Price et al 2003: 1434).

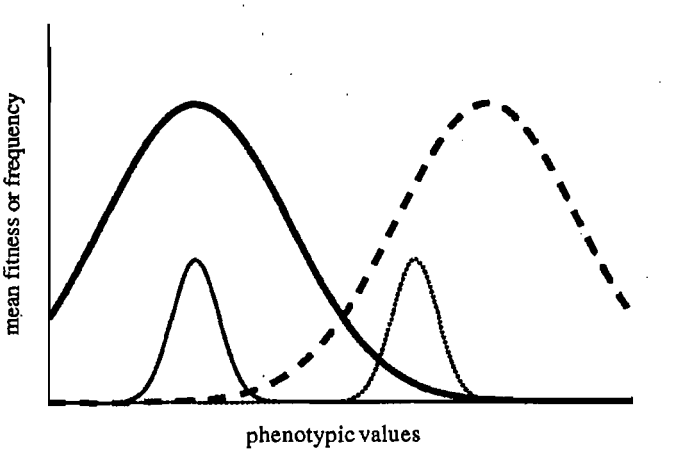

Figure 7.1 The contribution of plasticity to a peak shift in a changing environment (Price et al 2003: 1434)

The bold line represents the mean fitness of the population, while the dashed line indicates the mean fitness in a new environment. The thin solid line shows the population distribution in the original environment, compared to the thin dotted line on the right, which represents the population distribution in a new environment after such a reaction. Without the plastic response, population extinction appears inevitable (Price et al 2003: 1434). Plasticity may thus be required for population persistence, which, in this example, can also lead to a new peak on the adaptive surface and subsequent genetic change.

Boas and the environmental impact on growth

In 1912 Franz Boas published the first major study into the effect of the environment on the pattern of growth. He had disagreed with the prevailing idea at the beginning

of the 20th century that cephalic index (a ratio of head length to width) was a stable measurement resistant to environmental influences. Having observed in European studies that populations showed morphological differences by 'geographical localities' rather than by nationalities, he selected a uniform American environment (cities) to determine whether it had a favourable or an unfavourable effect upon the descendants of immigrants (Boas 1912a: 1-2). He 'compared the features of individuals of a certain type born abroad [to those] born in America within ten years after the arrival of the mother, and [those] born ten years or more after the arrival of the mother' (Boas 1912a: 5, 7). Concentrating on head form (expressed by the cephalic index: width taken as a percentage of the length), he found that in the American descendants of Central European types (Bohemians, Slovaks and Hungarians, Poles), both the length and width of the head decrease. In Hebrews, the length of the cranium increased whilst width decreased, while the Sicilians and Neapolitans indicated an opposite trend (Boas 1912a: 55-56). Boas believed that the American environment had an immediate impact on cranial form, increasing as the time elapsed between the immigration of the parents and the birth of the child also increased (Boas 1912a: 61); the foreign-born and American-born children of the same parents differed in cranial shape, with the latter group varying from their siblings and parents (Boas 1912a: 70).

Despite the absence of significant differences in cephalic index for some national groups (specifically Poles, Scots and Hungarians), due perhaps to small sample sizes, later studies seem to have confirmed these findings (e.g. Gravlee et al 2003). Using analyses of variance and covariance, and parent-offspring correlations and regression coefficients, a linear relationship was demonstrated between time span and cephalic index when studying the time elapsed between mother's immigration and baby's birth (Gravlee et al 2003: 134). This corresponded to Boas's conclusion that the 'intensity' of American environmental influence increases according to this factor (Boas 1912b: 530, 554), although it accounted for less than two per cent of the variation in cephalic index (Gravlee et al 2003: 134). More persuasively, modern analysis confirms that children born in the US environment are indeed less similar to

their parents in terms of head form than foreign-born siblings are to theirs, as Boas hypothesised ($R^2 = 0.412$ and 0.648 respectively). Cephalic index therefore shows sensitivity to environmental influences (Gravlee et al 2003: 134).

However, this reanalysis has been criticised, most prominently by Sparks and Jantz (2002, 2003), who identified a small number of potential areas for error, such as inter-observer bias and the lack of a theoretical perspective, all of which were subsequently addressed by Gravlee and colleagues (2003). Nevertheless, Sparks and Jantz's own re-examination of the data failed to find any evidence that might support Boas's original conclusions, and contend that most of the variation is genetic variation (Sparks and Jantz 2002: 14637). Specifically, Sparks and Jantz (2002) found that most of the significant differences in cranial shape are found in the Hebrew sample, and that 73% of the tests relate to cranial index, indicating a general reduction in cranial index in American-born children between seven and 14 years of age. They believe that the predominant influence is age, rather than the duration of American residence, suggesting that, overall and contrary to Boas (1912a), the cranial index is stable in response to changing environments (Sparks and Jantz 2002: 14637). This modern statistical re-evaluation concludes that that there is a high heritability in the family data and variation among the ethnic groups under study, in the American environment. Thus, Boas's claims for the overriding influence of the environment on cranial shape are not supported (Sparks and Jantz 2002: 14637).

Boas made no claims in his original report for the strength of plasticity over genetics (Boas 1912b: 557-8, 562); he merely noted a possible environmental effect on those born in the US and those born outside, and the intrafamilial correlations conducted by Gravlee et al (2003) seem to support this. In opposition, Sparks and Jantz (2002) found that, rather than allowing immigration any influence over cranial morphology in a single generation, 'cranial dimensions are capable of revealing "genetic" patterns in human populations over time and space' (Sparks and Jantz 2002: 14638). Likewise, this thesis accepts that genetics and environment must interact. There is a known correlation between stature and head length (though not head breadth),

whereby head length increases as stature does. In turn, stature tends to increase (within genetic bounds) with improved nutritional conditions, thereby linking cranial shape to the environment, albeit in a less direct way than Boas (1912a) hypothesised. In the examination of cranial morphology in *H. erectus* in Chapter Eight, the competing hypotheses for regional variation are thus used to set genetic isolation against environmentally-driven changes to life history strategy.

Support for environmental impact on growth is found throughout nature. A similar type of response has been shown experimentally in wild barley (*Hordeum spontaneum*), which exhibited a decrease in all growth-related characteristics with decreasing nutrient level, to a significant degree (for a series of 210 growth characteristics and morphological traits, 45 had a p-value of less than 0.001, and a further 46 were significant to either $p = 0.01$ or $p = 0.05$) (Elberse et al 2003: 374-5). While the relative growth rate did not differ among populations, all morphological traits such as leaf area ratio and leaf mass fraction differed in plasticity between populations (Elberse et al 2003: 376). This indicates that when examining plasticity in *H. erectus*, it is not enough to focus on the gross capacity of the skull; plasticity may be found in other characteristics.

It has been suggested (Jordan and Snell 2002: 51) that plasticity itself is the reproductive trait 'subject to the most intense natural selection'. Indeed, it is more favourable for the long-term survival of the female and her offspring if in unpredictable environments she is able to reproduce under a range of conditions and make use of the most resources, in order to raise the maximum number of offspring to maturity (Jordan and Snell 2002: 51). The idea of trade-offs in life history has been discussed in Chapter Three, but here plasticity is considered the primary contributing factor that enables such trade-offs to take place.

Fluctuating asymmetry

Environmental variability may exceed the tolerance levels of a species and provoke short-term, non-genetic changes to the skeleton. Fluctuating asymmetry (FA) refers

to random variation in bilateral traits and acts as a measure of developmental instability (as opposed to developmental plasticity), as development is repeated twice, once on each side of the body (Hasson and Rossler 2002: 73). Departures from FA include directional asymmetry (deviations from symmetry with a mean different from zero) and antisymmetry (deviations from symmetry with a bimodal distribution) (Black-Samuelsson and Andersson 2003: 1107). Developmental instability can be representative of the health of a population, since it is based on the assumption that environmentally or genetically induced deviations from the ideal phenotype are a sign of the precision of development, with lower precision (and therefore greater asymmetry) resulting from the disruptive effects of environmental stressors, poor genetic quality, or both (Kellner and Alford 2003: 931).

This has been demonstrated through comparison of the Hadza, a foraging society of northern Tanzania, with American college students (Gray and Marlowe 2002). Ten bilateral traits, including ear width and wrist width, were measured and controlled for body size, and the FA of each trait was added together to give each individual a combined FA value. It was found that Hadza FA is considerably higher than FA among the American students. Possible reasons for this are that the Hadza are exposed to more physical stress, receive no regular medical care, lead an energetically demanding life with a subsistence diet and sleep on the ground all year round (Gray and Marlowe 2002: 499). However, this interpretation overlooks the demographic profile of American college students, who tend to be middle class with a high standard of living, and cannot therefore be thought of as typical Americans. Their selection in Gray and Marlowe's study might then have placed the Hadza results within a misleading context.

Differential growth rates can be a confounding factor in the scrutiny of FA. Slower growing children aged 0-20 years in Dominica exhibited a lower FA value than faster growers of comparable age. For the same reason, FA among Jamaican children was shown to be lower than FA, for the same traits, in British children of similar age. These results could be attributable to growth rate or basal metabolic

rate, both of which decrease along a similar trajectory, and with a similar velocity, at this stage of life (Gray and Marlowe 2002: 499-500). The continuous process of growth may thus influence interpretation. For example, one study into the FA of epiphyseal fusion found significant differences between the left and right sides of the body, although this could have been an observation of distinct growth phases (Albert and Greene 1999: 346). In this study, investigation of developmental plasticity and FA in the adults and juveniles of two contrasting populations is restricted to the measurement of orbit height and width and various cranial dimensions, and so growth rates are unlikely to confound analysis, though they will be taken into consideration.

The interpretation of these results has implications for understanding the time scales involved and the means of adaptation employed. For example, if FA is seen in various traits in adults or juveniles, but not in both, it may signal that the environment was only stressful during the developmental period of that particular group. The response will then be plastic. However, if there is a difference in morphology at the population level, then the response is more likely to be genetic and the result of an adaptation to a change in environmental conditions.

Cranial plasticity

Plasticity impacts upon the skeleton. The remodelling of bone during growth occurs both on the outer surface of the bone and in the internal cancellous material (Roberts 1995: 10). It is a continuous process throughout life and not only in situations of environmental stress, providing the mechanism through which the skeleton is modified. A prolonged deficiency in dietary energy causes growth-faltering during childhood and, if sustained, will lead to a smaller overall body size in adulthood (Ulijaszek 1995: 92). The correlation between stature and cranial length (Holloway 2002) removes the focus of variation in cranial shape from the Boas model of environmentally influenced 'types', to a more ecological standpoint whereby the level of nutrition (and environmental fitness) is indirectly evident in the cephalic index. Stature, assessed through femur and humerus length, is used in the study carried out later in this chapter as a control for any cranial changes observed.

Boas's dominant conclusion that the skull is susceptible to environmental change set a precedent for looking at cranial morphology in terms of developmental instability or environmental stress. Angel (1982) proposed that the cranial base is sensitive to nutritional status, as it must support the weight of the brain and head during growth, in the same way that the pelvic inlet, also affected by malnutrition, must support the weight of the body (Angel and Olney 1981). Failure of the skull to maintain its shape in this way, regardless of cause, results in a flattening of the base of the skull, termed platybasia. If this condition were to occur throughout a group, rather than varying individually through genetic influence, it is more likely to have an environmental, nutritional basis.

In Angel's study, the skull heights of a skeletal population composed of healthy, mostly middle class Americans (countrywide, generally non-urban in origin) were compared with those of less nourished, socio-economically deprived individuals. This latter group comprised part of the Terry Collection, a large skeletal sample of low income Americans. Angel measured porion-basion height and multiplied it by 100, then divided the result by biauricular breadth to control for gross skull size. The difference calculated in skull height between the two populations was significant, with an 11% increase in skull base height in the advantaged group (gross cranial size increase was much lower at 1%, as was stature increase at 3%) (Angel 1982: 302). While the correlation between skull base height and pelvic inlet depth can, in individuals, be influenced by genetics, hormones and social practices, Angel showed that the relationship holds on a population level and must therefore be subject to a broader environmental influence (Angel 1982: 304).

Although these results are convincing, Angel did not control for circumference, and so failed to control for general size. However, the evidence of variation in height and cephalic index suggests that his conclusion may well be correct. The study detailed below will compare the findings of Angel with two modern human populations, with the dual aims of determining both the robusticity of Angel's work and the effect of

controlling for circumference. The same populations will also be used to examine the potential for variation in cranial shape according to nutritional status, by comparing patterns in cephalic index.

Reaction norms

Optimal phenotypic plasticity is specified by the optimal reaction norm (Sasaki and de Jong 1999: 1329). When a single phenotype varies as a continuous function of an environmental variable, its reaction norm is the full set of phenotypic responses to that variable. This can be visualised as a curve plotted for phenotype value versus the value of the environmental variable (West-Eberhard 2003: 26-27). If the reaction norm is linear (Figure 7.2), then the range and variance of a phenotypic distribution will be altered. If instead the reaction norm is conceived as curved (Figure 7.3), then it will transform the shape of the distribution from symmetrical to skewed (Stearns 1992: 41, 223*g*).

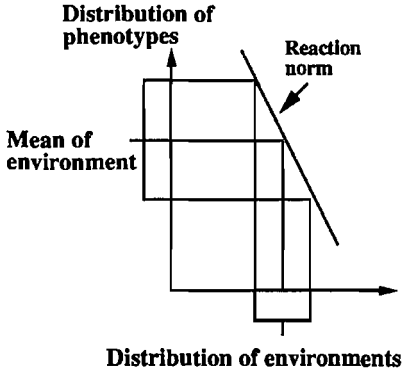

Figure 7.2 A linear reaction norm: broadens the distribution of phenotypes (Stearns 1992: 41)

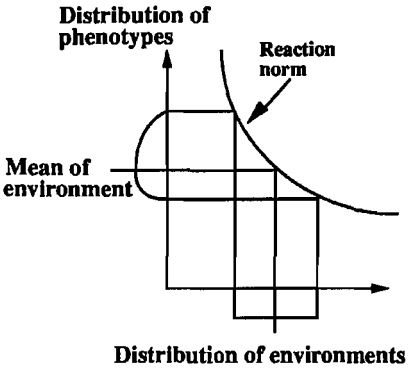

Figure 7.3 A curved reaction norm: turns a symmetrical distribution of environments into a skewed distribution of phenotypes (Stearns 1992: 41)

The inherent plasticity of the phenotype can be understood as the product of a heterogeneous environment, and the interaction between phenotype and environment determines the resultant fitness of the organism, as Figure 7.4 (Daan and Tinbergen 1997: 314) demonstrates:

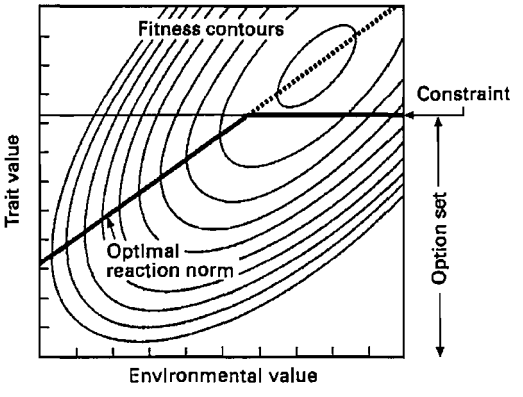

Figure 7.4 The interaction of some concepts of life history theory (Daan and Tinbergen 1997: 314)

Where there is environmental variation, different trait values produce different fitness contours. The dashed line is the optimal reaction norm, connecting the optima from a range of environments. The array of trait values possible in the species (and thus the array of potential fitness contours) is collected into the option set, the boundary of which acts as a constraint for the optimal trait value. The solid line represents the constrained optimal reaction norm (Daan and Tinbergen 1997:

314). This is not a straightforward process of adopting the optimum phenotype, as the habitat in which an individual is subject to selection might be randomly changed from the environment in which the individual first developed. This would necessarily lead to a population consisting of multiple genotypes with different reaction norms (Sasaki and de Jong 1999: 1330).

Phenotypic variance, or V_p, is expressed as:

$$V_p = V_g + V_e + 2\mathrm{Cov}_{ge}$$

This divides phenotypic variance into the three factors of genetic variance, environmental variance and genotype-environment covariance. The gradient of environmental variation determines the fitness of a phenotype, in that fitness is usually highest at an intermediate value and lowest at either extreme. The phenotypic plasticity of an organism is, therefore, the breadth of environmental tolerance. For example, if fitness remains high across a range of environmental conditions, centred on the intermediate optimum, then the breadth of tolerance is large. The reverse is also true (Stearns 1992: 60, 64).

The reaction norm of a genotype is determined by phenotype and environment frequency, and the interaction between the two. The genotype is mediated by the environment through the reaction norm, and gives rise to phenotypic variation. At the extreme reaches of environmental variation, encountered rarely, the frequency of phenotypes will decrease since fitness will also decrease. The mean of a range of environments will theoretically co-occur with the mean phenotype, acting together to produce mean fitness. As long as selection is frequency independent, the reaction norm will tend to evolve in a direction that maximises average fitness in a population, making the phenotype a continuous function of the environment (Arnold and Peterson 2002: 307). Outside the bounds of the reaction norm, where environmental and phenotypic variability increase, fitness will decrease respectively. Knowing how organisms may react to change in habitat clarifies the impact of different environmental conditions on *H. erectus*, and the question of whether life

history strategy varied according to environment, or whether the species as a whole had a broad tolerance to environmental variation.

This idea can also be applied to childhood nutritional status, since if the environment (food intake) is beyond the margins of the reaction norm, then instability of the phenotype will result. The consequences of this might take the form of fluctuating asymmetries, as well as known penalties such as growth-faltering and disease. Malnutrition results from an imbalance between the body's needs and nutrient intake, and can be defined as 'the failure to achieve normal growth' during development (Golden and Golden 2001: 515). Young children are particularly vulnerable, but it affects all age groups across the entire life span (WHO 2000: 10). Normal growth is characterised by a continuous balanced accretion of tissues in a predictable way. Disturbances in this trend, caused by factors like illness and severe decrease in available food, create two conditions: stunting (failure to achieve height but normally proportioned); and wasting (normal height attained but thin and wasted). Malnutrition can refer to excess as well as deficiency, thus including over-eating and obesity, so it would be possible to determine upper and lower limits of an average reaction norm for nutrition. However, the focus here is deprivation, specifically its impact on growth in childhood and adolescence, and so only the lower threshold will be examined.

Growth retardation can occur at different stages of life. For example, intrauterine growth retardation for full-term babies is diagnosed by a birth weight of less than 2500g at 37 or more weeks gestation (WHO 2000: 11). In the postnatal period and throughout childhood, growth retardation can be assessed using a number of indices: height-for-age (performance of linear growth, i.e. stunting); weight-for-height (body proportion, i.e. wasting); and weight-for-age (a synthesis of the two) (de Onis et al 1993: 703). Any deficit calculated by these methods is expressed in terms of multiples of the standard deviation of the American National Centre for Health Statistics 1997 Standard (NCHS) to create a Z-score, calculated as: $(x - \bar{x}) / s$, where

$\bar{x}$ is the mean value of the reference population, s is the value of the standard deviation for the reference population, and x is the observed value.

The problems associated with the use of the NCHS Standard have been increasingly recognised since its adoption by WHO in the 1970s, and it is in the process of being replaced by a new international standard[1]. However, the advantage of using the Z-score method is that this statistic is age-independent and relates stunting and wasting in the same units. The normal range for a Z-score in children is ±2, although those in the lower range of this bracket are classed as mildly wasted or stunted. When examining the weight-for-height and weight-for-age measures, one Z-score unit is equivalent to almost 10% of the median, dropping to 5% of the median for the height-for-age Z-score, and is detailed in Table 7.1 (Golden and Golden 2001).

Table 7.1 Child malnutrition as Z-scores of the NCHS population of children

	Normal	Mild	Moderate	Severe
Weight-for-height (wasting)	90-120% (+2 to –1 Z)	80-89% (-1 to –2 Z)	70-79% (-2 to –3 Z)	<70% (<-3 Z)
Height-for-age (stunting)	98-110% (+2 to –1 Z)	90-94% (-1 to –2 Z)	85-89% (-2 to –3 Z)	<85% (<-3 Z)

This provides a standard boundary for the reaction norm, calculating the point at which wasting and stunting will occur, i.e. when weight is reduced by 10% relative to height from the median of the age group, as a result of malnutrition, and when height is reduced by 5% within an age group relative to the median. Further reduction of weight and height is dependent on the duration and severity of malnutrition. The use of Z-scores is not limited to nutrition, and is calculated for certain traits in the two modern populations introduced below in order to establish whether any instability is still within the bounds of tolerance for that population.

[1] For discussion and references, see www.who.int/nutgrowthdb/intro_text.htm (9.11.04)

Plasticity and the effect of the environment: A case study of two London populations

The statistical analyses of survivorship and encephalisation in Chapters Four and Five showed the difficulties of working with and establishing patterns in a small sample, especially when that sample is composed of individuals that are spatially and temporally distant. Too few examples of *H. erectus* exist to allow any potential plastic response to environmental variation or stress to be studied, even if the nature of those stresses or environments were known. Modern human populations provide greater scope for such an investigation, in terms of sample size, range of age at death and greater environmental control. This study is not intended to make a direct comparison between modern humans and *H. erectus*, since the species, environment and lifestyle differences are insurmountable. The analogy is too broad for a direct comparison, but nevertheless this modern human study remains useful for an investigation into the relationship between the cranium and the environment.

Method

Most finds of *H. erectus* comprise the crania, with only one or two opportunities to estimate stature. As a result, this study concentrates more on the relationship between cranial dimensions and the environment, using the expected patterns of stature as a control, in order to look for population level similarities. This is not an attempt to replicate Boas's work, but rather to establish whether nutritional status (environmental fitness) can separate two populations through an impact on cranial development and morphology. Although formulae exist for the estimation of stature from long bone length (e.g. Trotter 1970), raw femur and humerus length will be relied on here for a more accurate representation of height variation. Fluctuating asymmetry is also explored, concentrating on the orbits and molars. A number of measurements have been taken in order to satisfy this requirement (Table 7.2).

Table 7.2 Osteometric measurements undertaken

Measurement	Definition	Technique
a.Maximum cranial length	Glabella – inion	Spreading callipers
b.Cranial width	Maximum bi-temporal width	Spreading callipers
c.Cranial height	Basion – bregma	Spreading callipers
d.Chordal width	Auriculare – bregma	Spreading callipers
e.Circumference	Glabella - squamal sutures - inion	Measuring tape
f.Stature	Maximum long bone lengths	Osteometric board
g.Orbit width	Dacryon – ectoconchion	Digital callipers
h.Orbit height	Perpendicular to breadth	Digital callipers
i.Mandibular M_1 width	Across the midsection	Digital callipers

The five cranial measurements (a-e) will determine the precise nature of any changes in cranial morphology, in conjunction with a number of indices defined below. Maximum length and bi-temporal breadth can be used to monitor population-level changes in the shape of the skull through the horizontal plane, and can also be related to changes in head circumference. The remaining two (c,d) will accomplish the same in the vertical plane. Furthermore, auriculare to bregma, measured as a chord rather than along the same plane as vault height, is useful in assessing the degree of flattening of the skull as prescribed by Angel (1982), in ratio terms.

The nature and extent of fluctuating asymmetry will be explored using the height and width of the orbits and the width of the mandibular first molar (M_1). The orbits were selected since they are free from mechanical or weight-bearing influence, unlike long bones. Any asymmetry seen is thus solely a product of developmental instability. Each orbit was measured three times to minimise intra-observer error, and was only measured when both orbits were intact. The width of the first molar was chosen as a variable because tooth formation is fairly robust to environmental influence and nutritional variation (Smith 1991: 143), and would hence provide a control for the orbital measurements. The width of M_1 was taken with digital callipers across the midsection. Generally, the teeth were in good condition and wear

was minimal. On occasions where this was not the case, measurement remained accurate since the callipers were positioned down the height of the tooth, rather than just at the tip. When the mandibular M_1 was missing, the first molar on the maxilla was measured instead; in the absence of these teeth the mandibular second molar was measured in its place. This was sufficient to ensure a control measurement. Gross size differences are accounted for in later analyses.

Studies of variation in *H. erectus* tend to focus on cranial capacity and its relative value across specimens. Accordingly, cranial capacity was calculated for the modern human populations studied here, using the Lee-Pearson formula (cited in Manjunath 2002). This allows the calculation of volume from the linear dimensions length (glabella-inion), breadth (bi-temporal) and height (basion-bregma) using formulae based on sex:

For males: volume = 0.000337(L-11) x (B-11) x (H-11) + 406.6
For females: volume = 0.0004(L-11) x (B-11) x (H-11) + 206.01

While this might not be the most ideal method as, similar to stature, this is an inferred measure, the results obtained are comparable to those derived from different methods (e.g. Elton et al 2001). In addition to these measurements, indices are used to assess the relationship between dimensions (Buretić-Tomljanović et al 2004):

Cranial index: cranial length / cranial height
Cephalic index: (cranial width x 100) / cranial length

Several methods are used to determine age at death (Table 7.3), to place cranial and somatic growth within a demographic context, and to supply information on survivorship.

Table 7.3 Methods of age determination undertaken

Age category	Method	Reference
Adult	Pubic symphysis morphology	Buikstra and Ubelaker 1994
Adult	Auricular surface morphology	Buikstra and Ubelaker 1994
Adult	Cranial suture closure	Buikstra and Ubelaker 1994
Juvenile	Tooth emergence	Buikstra and Ubelaker 1994
Juvenile	Epiphyseal fusion	Buikstra and Ubelaker 1994

The level of precision achieved by these techniques is not great, as adults in particular can only be assigned to broad age bands. Occupation, health and environmental conditions can all combine to create a misleading portrayal of age at death, and are further complicated by subjectivity and level of experience on the part of the observer. Variability is also increased by the individual's own rate of maturation (Molleson and Cox 1993). To prepare the derived ages for statistical analysis, the mean value of the age range was taken. Where ranges did not overlap between procedures, the mean of the upper and lower limit was used instead. While this increases the degree of inaccuracy, in the majority of cases age as given in the text can be assumed to be within ± 3 years for the juveniles, and ± 5-10 years in adults, as every skeleton is aged according to the same standards and is directly comparable with each member of the population.

The second component of demography required to complete the analysis is sex determination (Table 7.4), but this is only applicable to the adult sample. The juveniles have been classified as 'unknown' and are treated throughout as a single group, as it is extremely difficult to sex juveniles, due to the immaturity of the skeleton and generally gracile build (Buikstra and Ubelaker 1994: 16). A number of methods of estimation are used here:

Table 7.4 Methods of sex determination undertaken

Element	Method	Reference
Innominate	Ventral arc	Buikstra and Ubelaker 1994
Innominate	Sub-pubic concavity	Buikstra and Ubelaker 1994
Innominate	Greater sciatic notch	Buikstra and Ubelaker 1994
Cranium	Nuchal crest	Buikstra and Ubelaker 1994
Cranium	Mastoid process	Buikstra and Ubelaker 1994

Each feature was scored as being male, female or ambiguous, and then totalled for each individual to ascribe the likely sex. Not every element tabulated above was available for every skeleton, but it was always possible to determine likely sex.

Statistical analysis

A number of statistical tests were applied to the data collected: Pearson's statistic for bivariate correlation, Student's 2-tailed *t*-test for independent samples, linear regression with 95% confidence intervals, and principal components analysis. All analysis was carried out using SPSS for Windows, Release 11.5.0. The *p*-value for significance is set at the conventional 0.05 unless stated otherwise.

Sample

The two populations used in this study are curated at the Museum of London and originate from 18th-19th century London, giving some control over the time period and geographical setting, and thus providing a more viable comparison between the two. Selection was guided both by availability of large skeletal groups and the possibility of an environmental dichotomy between them. All data collected are presented in Appendix III. The difficulties in accounting for bias in the study of past populations have been covered elsewhere (Waldron 1994) and are compensated for as far as possible in this investigation, although 'there is little that is random about the place in which one is buried' (Waldron 1994: 12).

The first population comprised the inhabitants of the tenement buildings in Redcross Way in Southwark (referred to throughout as 'Redcross'), buried in Southwark poor

persons' graveyard, St. Saviour's Burying Ground. The excavations of this site yielded a total of 166 burials, the majority of which are dated to the 19th century (Brickley 1999). This study uses a random selection of 78 individuals to give an approximate cross section of the population. The Redcross population is considered here as 'disadvantaged' since there is likely to have been malnourishment, and crowded and stressful living conditions for the people involved.

The second population was from Old Church Street, Chelsea ('Chelsea'), excavated under difficult conditions in 2000 (Cowie 2000). Known to be a more affluent population relative to that from Southwark (from the presence of lead-lined coffins, and burial on consecrated ground, contrary to Redcross), of the 288 individuals found, 70 were assessed for inclusion in this study. Again, selection was random. To provide an historical framework for each of these populations, and to ensure that the samples obtained are representative of the population of London as a whole, the demographic data from London's Bills of Mortality are introduced as a control. These indicate a juvenile mortality of 45-57.7% (Molleson and Cox 1993: 208-209). Using the ageing criteria set out above, Figures 7.5 and 7.6 provide a basis for comparative analysis:

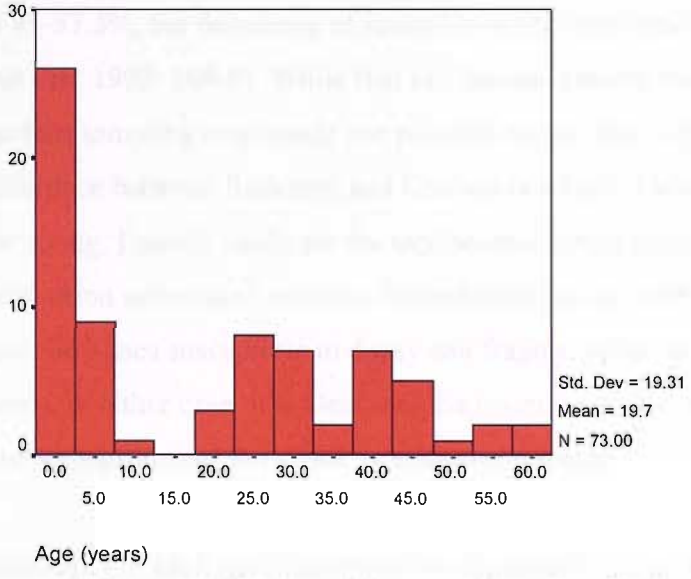

Figure 7.5 Age distribution of the population from Redcross Way

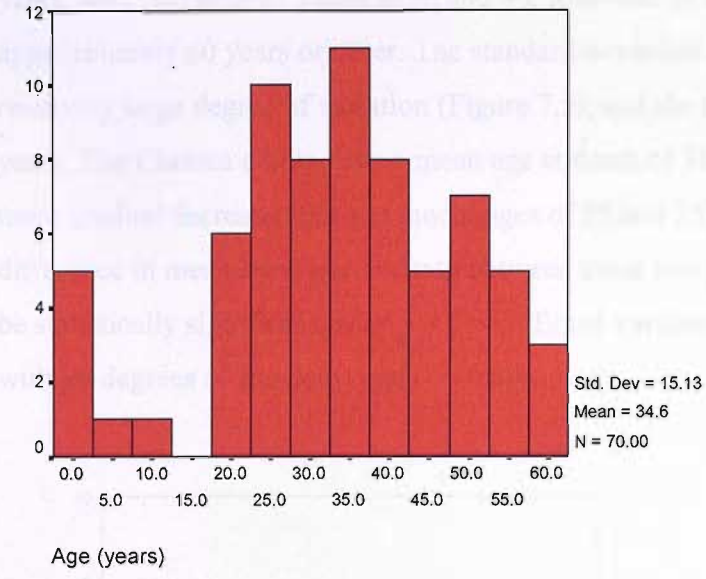

Figure 7.6 Age distribution of the population from Old Church Street, Chelsea

The first conclusion drawn is that more juveniles died in the 'poor' Redcross sample than did in the 'rich' Chelsea sample. Of the total Redcross population, just under half (48.6%) were classed as juveniles, in marked contrast to the 10% juvenile occurrence in the Chelsea collection. However, this is not to say that the infant mortality rate in the Chelsea area was so low. It has been reported for the Spitalfields assemblage that despite an underlying juvenile mortality rate in London of 45-57.5%, the frequency of juveniles in the crypt reached only 18.9% (Molleson and Cox 1993: 208-9). While that of Chelsea remains lower, regardless of the random sampling employed, one possible reason that might account for such a difference between Redcross and Chelsea is a class distinction in burial practices of the young. Equally likely are the taphonomic issues connected to a complex excavation undertaken within a limited time period, with the smaller, more delicate juvenile bones susceptible to decay and fragmentation at a greater rate than adult bones. In either case, it is clear that the juvenile section of the Chelsea population, and perhaps also of Redcross, is under-represented.

Although the adult ages incorporate a degree of inaccuracy, their age at death distribution is still interesting. In Redcross, the modal age at death for adults is 25

years, with two smaller peaks at 30 and 40, followed by a fairly steep drop to approximately 60 years or older. The standard deviation is 11.07, indicating a relatively large degree of variation (Figure 7.5), and the mean age at death is 36.9 years. The Chelsea adults have a mean age at death of 38.1 years and demonstrate a more gradual decrease after the modal ages of 25 and 35 (Figure 7.6). However, the difference in mean adult age at death between these two populations is not found to be statistically significant, with $p = 0.658$. Equal variances were assumed ($F = 0.036$ with 99 degrees of freedom) and $t = -0.444$.

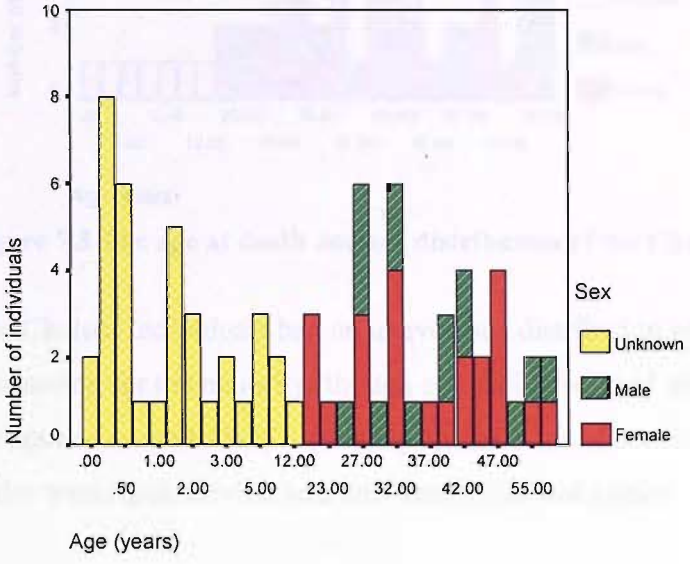

Figure 7.7 The age at death and sex distribution of the Redcross population

The Redcross adult population displayed a sex ratio of 60.5% women and 39.5% men (Figure 7.7). This is somewhat different to the near 1:1 ratio seen in the Spitalfields sample (Molleson and Cox 1993: 208-209), and may either be a product of the sampling process or have a basis in reality. There is a preponderance of female deaths in the Redcross sample in the mid- to late-forties, possibly due to complications of late childbirth, while male mortality remained fairly constant, with the exception of this female-dominated period.

By comparison, the Chelsea group was much closer to equilibrium with a 50.8:49.2 divide in favour of men (Figure 7.8).

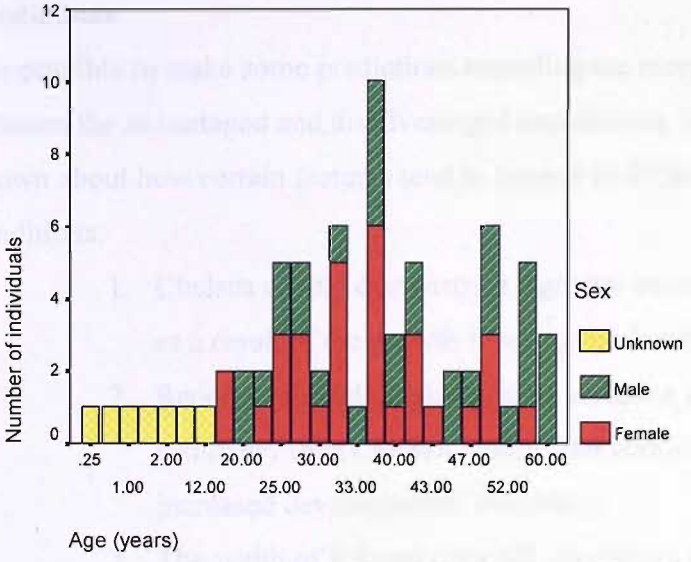

Figure 7.8 The age at death and sex distribution of the Chelsea population

The Chelsea individuals had an uneven sex distribution of age at death, with females accounting for the majority (though not exclusively) of deaths taking place between the ages of around 25-35 – possibly an indicator of death in childbirth – with more males tending to survive into their late fifties and sixties.

All measurements used throughout this study were screened for a normal distribution prior to their use in the analysis, since this is required for the validity of *t*-tests and correlations. Using histograms (collated in Appendix IV) it was seen that the majority of factors, including long bone length and cranial capacity, did not deviate too much from a normal distribution in both populations but this assumption was investigated further. The distributions of cranial length, cranial breadth, circumference, orbit width, molar width, humerus length and femur length were tested for normality using an assessment of skewness and a one-sample Kolmogorov-Smirnov test, as in Chapter Five. These were applied to each population as a whole, and then restricted to the adults of each population; in all

cases, the resulting statistics indicated that the measurements collected for this study follow a normal distribution, a principal requirement for parametric testing.

Predictions

It is possible to make some predictions regarding the morphological divergence between the advantaged and disadvantaged populations, based on what is already known about how certain features tend to behave in different environmental conditions:

1. Chelsea should demonstrate a greater overall stature than Redcross, as a result of the growth faltering mechanism.
2. Redcross should display greater variation in bilateral orbital symmetry than Chelsea, with wider confidence intervals from the increased developmental instability.
3. The width of left and right M1 should not differ significantly either within or between groups.
4. Redcross should have a flatter cranial base and be grouped above a regression line for height against width. Chelsea, with a greater skull base height, should be found below the line.
5. Chelsea should have a larger head, apparent both in a larger overall circumference and cranial capacity, and in a regression of length against breadth, where this population will group further up the line than Redcross.

The presence of fluctuating or directional asymmetries will identify growth in a stressful environment. Morphological variation of the skull in the absence of asymmetries is more likely to have arisen as a result of plasticity, i.e. an alternative form of morphology in different environmental circumstances that may or may not be adaptive (West-Eberhard 2003: 33).

Results

Stature

The first prediction anticipated an indication of growth faltering in Redcross. The distribution of height within and between the two populations was thus compared, using the best formulae from Trotter (1970). The result was not significant (p = 0.085), although Chelsea emerged with taller adults (mean height of 163cm) against the 161cm of the Redcross group. In this calculation, equal variances were assumed (F = 0.86 at 89 d.f. and t = -1.741). The range of statures in each population is more instructive: Redcross varies by 33.18cm (140.9-174.07cm) with a standard deviation of 7.42cm from 36 individuals, while Chelsea shows greater constancy with a range of 30.25cm (150.69-180.94cm) and a standard deviation from 55 individuals of 7.44cm. This supports the biological principle, explained above, that prolonged malnourishment in a poorer environment will give rise to shorter individuals due to the growth-faltering effect, and this is almost certainly what is seen here, albeit to a modest degree. However, stature is an inferred variable, and calculated from an inconsistent set of data for each individual, so raw femur and humerus lengths are substituted instead. Unfortunately there is an inequality in the number of adult bones available for each population, primarily affecting the femur.

The humerus did not differ significantly in length between all adults, between males or between females, with no more than a millimetre separating the groups. The number of individuals with long bones intact varied between populations, but not enough to skew the calculation (Figures 7.9 and 7.10). However, for the femur, equal variances were not assumed in any permutation, due to markedly different sample sizes. For example, although for all adults p = 0.012, there were 45 individuals from Chelsea compared to only 22 from Redcross. Despite this, the Chelsea femora were consistently longer than those from Redcross (mean length 437mm compared to 397mm), caused by a number of considerably shorter femora in the Redcross population. The latter group also exhibited greater variance in limb length than the more tightly clustered Chelsea individuals.

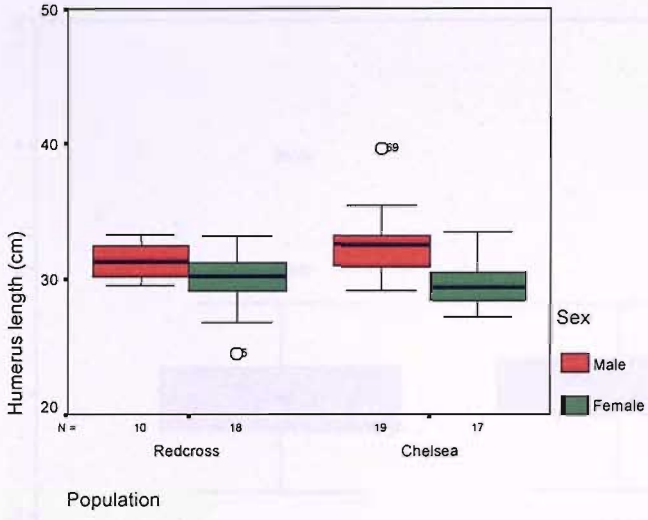

Figure 7.9 Humerus lengths in the Redcross and Chelsea adult populations, by sex

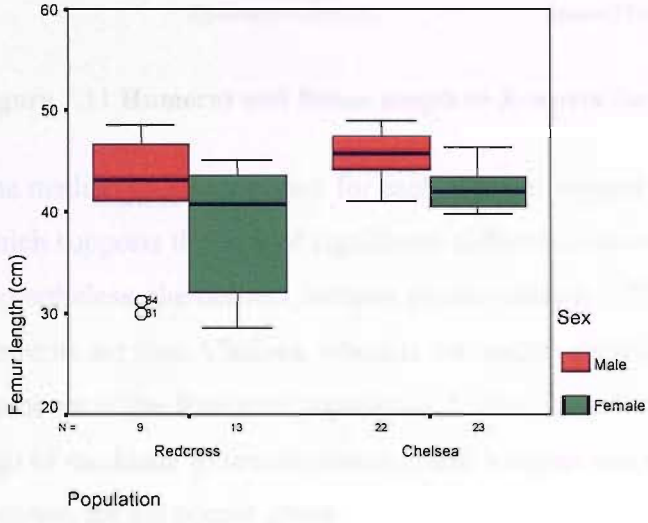

Figure 7.10 Femur lengths in the Redcross and Chelsea adult populations, by sex

The discrepancy in stature between these two populations may indeed be caused by environmental influences, but this cannot be conclusively shown. The calculation of Z-scores, with which to assess the reaction norm, will highlight any individuals who fall more than 5% outside the median height (Table 7.1). For this, all adults are combined for comparison (Figure 7.11).

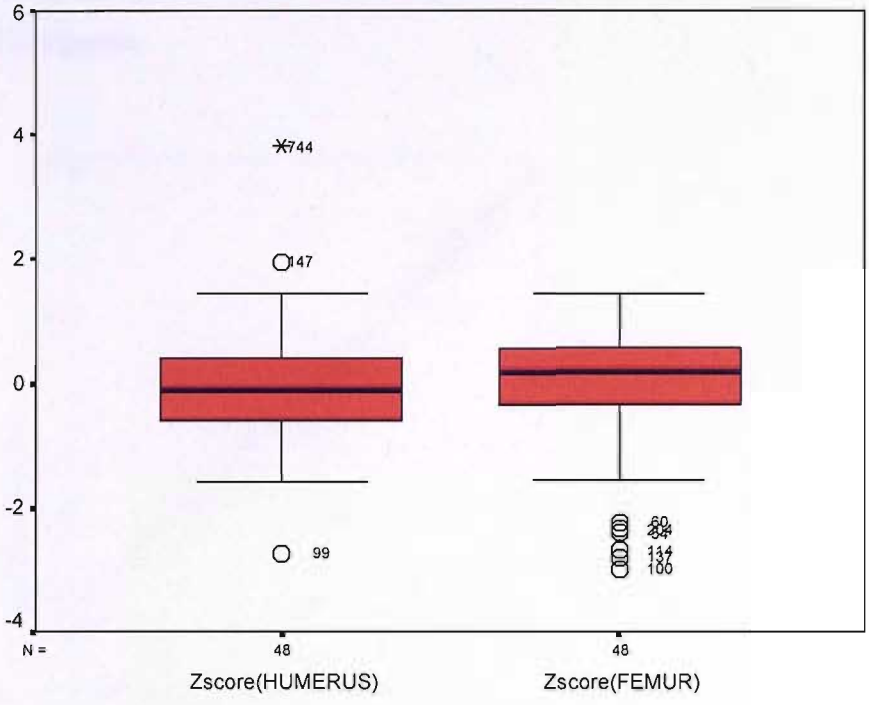

Figure 7.11 Humerus and femur length as Z-scores for the combined adult population

The median and distribution for each element suggest homogeneity in the sample, which supports the lack of significant difference between the two populations. Nevertheless, the outliers indicate greater variation. The two individuals with a large humerus are from Chelsea, whereas the negatively scored individuals are all members of the Redcross population. Using Table 7.1, a score of less than –2 is a sign of moderate to severe stunting, and it seems that this was at least a partial problem for the poorer group.

Fluctuating asymmetries

Asymmetries in the height and width of the orbits and the width of mandibular M1 will correspond to a deficient environment in the same way that stature does. The second prediction stated that the poor population would have a wider scatter on a regression of left orbit width against right, since there would be greater variation in the bilateral measurements as a result of developmental instability; while the third maintained that molar width would not differ appreciably between populations.

Orbit width appears to show little difference between the two populations, as Figure 7.12 suggests:

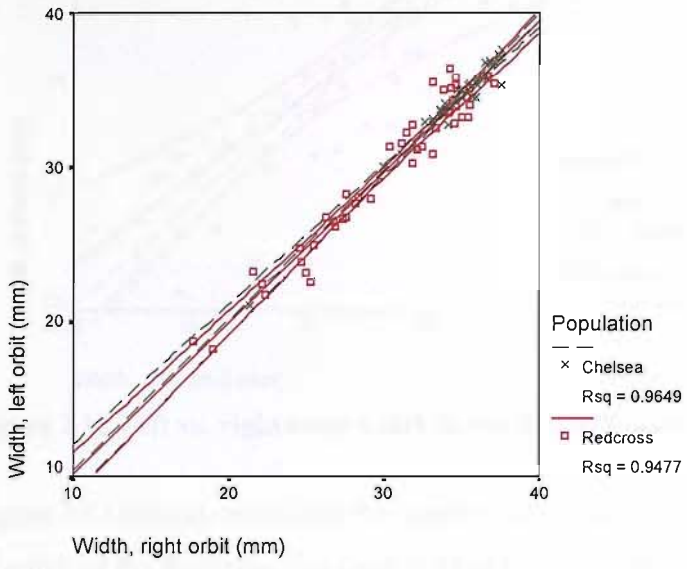

Figure 7.12 Left vs. right orbit width in the Redcross and Chelsea populations

There is an excellent correlation between the two orbits, implying a high degree of symmetry and thus little developmental instability. However, when the juvenile results were removed from the regression, the disjunction between the two groups becomes more apparent. Despite the inequality in the proportion of juveniles in each population, their removal produced an almost balanced number of individuals in each group: 27 in Redcross, and 31 in Chelsea.

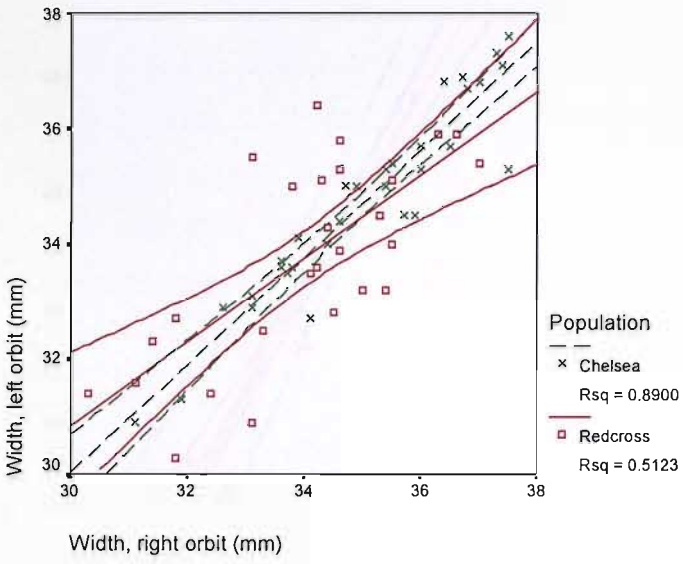

Figure 7.13 Left vs. right orbit width in the Redcross and Chelsea adult populations

Figure 7.13 demonstrates that the removal of the juvenile measurements reduces the R^2 value of the Redcross line from 0.95 to 0.51, and the scatter of points is wide. Notably, when the juvenile measurements are regressed on their own they generate an R^2 of 0.92, n = 20, as Figure 7.14 illustrates. Thus, much of the Redcross correlation appears to be due to a relative lack of variation in the juveniles. To confirm this, the regression statistics show that the slopes of the lines produced in Figure 7.14 below are almost 1: in the Redcross group the value of the slope is 0.905 ($p < 0.001$) while for the Chelsea group it reaches 1.03 ($p = 0.016$).

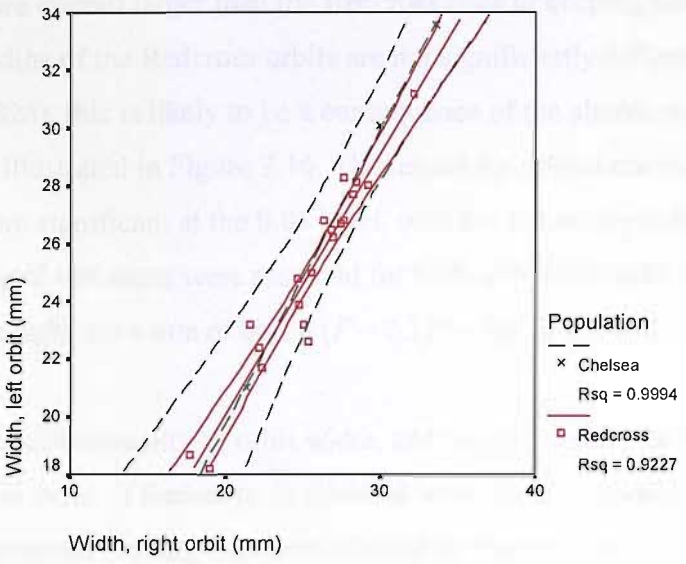

Figure 7.14 Left vs. right orbit width in the Redcross and Chelsea juvenile populations

Moreover, the narrower confidence bands surrounding the Chelsea adult regression point to less developmental instability, as predicted earlier. The adult trend for the Redcross sample displays wider bands, and the increased presence of such instability in the adult population indicates that they may have experienced harsher conditions than the next generation at the same developmental stage. This is reflected in Table 7.5 below, which reveals tighter confidence intervals for the Chelsea adult population compared to the equivalent Redcross group (the patterned is reversed, however, for the juvenile groups, but may be due to the small Chelsea sample size):

Table 7.5 95% confidence intervals for left-right orbit width linear regression

Population	Age	R-squared	Lower limit	Upper limit
Redcross	Adult	0.512	0.433	1.015
Redcross	Juvenile	0.923	0.775	1.035
Chelsea	Adult	0.89	0.809	1.058
Chelsea	Juvenile	0.99	0.702	1.359

To test these results further, a *t*-test established the significance of the variation between the two populations. A preliminary examination of the data revealed that the right orbit was predominantly larger than the left, and that the Chelsea orbits

were overall larger than the Redcross ones in keeping with this pattern. Although the widths of the Redcross orbits are not significantly different from each other (p = 0.326), this is likely to be a consequence of the almost equal fluctuating asymmetry, as illustrated in Figure 7.16. The results for orbital comparison between populations were significant at the 0.05 level, with the left orbit producing a p-value of 0.036 (equal variances were assumed for both; F = 0.085 with 56 d.f. and t = -2.151) and the right a p-value of 0.026 (F = 0.210 with 56 d.f. and t = -2.28).

The directionality of orbit width, and the increase in the size of the Chelsea orbits over those of Redcross, is clarified when the $R_i - L_i$ values were plotted as a histogram (having first been divided by the mean to control for size), since fluctuating asymmetry is characterised by a normal distribution about a mean of zero (Kellner and Alford 2003: 931). Figure 7.15, comprising every individual in the study, displays fluctuating asymmetry, albeit with a slight tendency for the right to be larger. This graph also demonstrates a normal distribution for orbit widths, a prerequisite for any t-test, thus supporting the findings above:

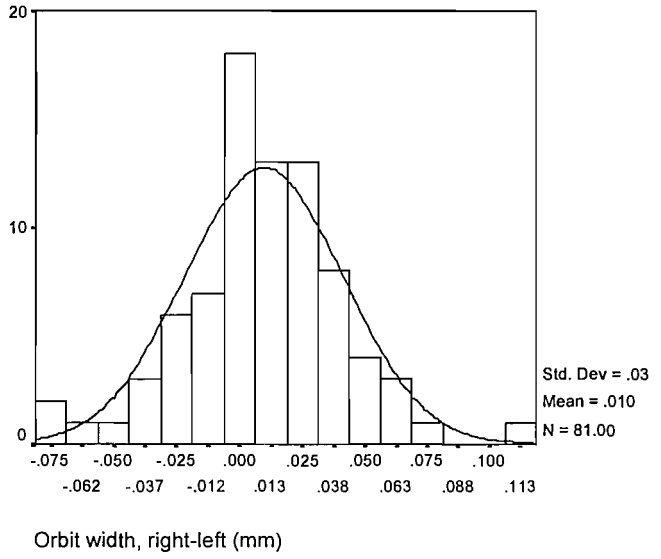

Figure 7.15 Distribution of $R - L$ orbit width for the whole dataset

The differences between the two populations become more apparent when they are examined separately. Figure 7.16 shows a wide distribution of orbit width variation

in the Redcross population, with the largest peak occurring towards the right of the graph, consistent with the overall findings above, and a smaller peak on the left to suggest fluctuating rather than directional asymmetry (although without a normal distribution):

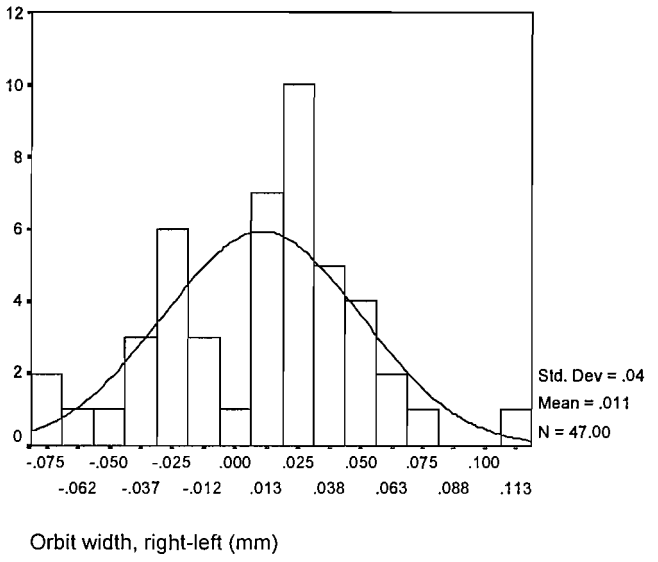

Figure 7.16 Distribution of $R - L$ orbit width for the Redcross population

In contrast, the distribution for the Chelsea population (Figure 7.17) exhibits less asymmetry in orbit width, in accordance with previous predictions. Here, the largest peak occurs at zero, indicating that the majority of individuals in this population were symmetrical in orbit width. Again, there is a tail towards the right, in keeping with the general trend, but to a far lesser extent than that seen in Redcross.

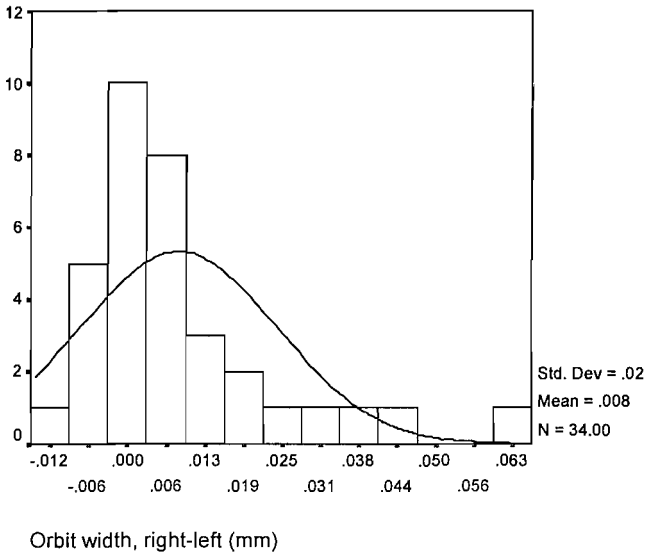

Figure 7.17 Distribution of $R - L$ orbit width for the Chelsea population

Orbit width appears to be more subject to fluctuating instability than orbit height, presumably because of the constraints of the size of the eye itself. Fewer individuals retained enough of an intact facial structure to permit the measurement of this variable (12 in Redcross, 18 in Chelsea), but the result is convincing. The left and the right orbits registered a mean height of around 35mm for both populations. The standard deviation value was higher than that seen for orbit width, and the results of the *t*-test recorded a *p*-value of 0.502 for the height of the left orbits (equal variances assumed and 28 d.f. for both; $F = 0.1$ and $t = 0.681$), and 0.908 for the right ($F = 0.8$ and $t = 0.117$). The little variation there is between populations is not significant.

Molar width produced a similar pattern. As predicted above, the mean width of the left molar for each population was within 0.2mm of the mean width of the right molar. Surprisingly, and contrary to prediction 3 above, a paired-samples *t*-test signified that the mean widths of the left and right M_1 were significantly different in Chelsea ($p = 0.035$; $t = -2.53$ with 8 d.f.), but not in Redcross ($p = 0.943$; $t = 0.073$ with 15 d.f.). Figure 7.18 helps to explain this, demonstrating that the wide asymmetry in the Redcross population creates too much variation for a significant result to be derived.

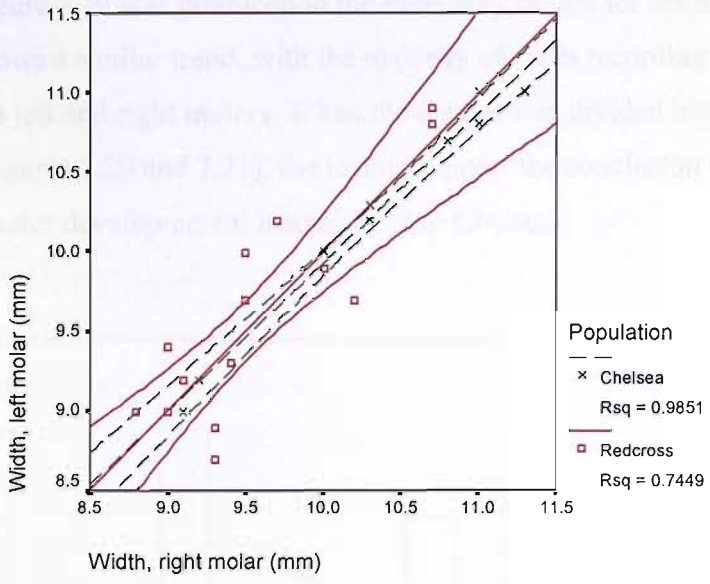

Figure 7.18 Left vs. right M_1 width in the Redcross and Chelsea adult populations

Furthermore, like the orbits, the mean widths of the Chelsea molars were greater than those of the Redcross sample, in this case by 0.7mm. This difference was significant, with a *p*-value of 0.023 for the left molar (equal variances assumed and 23 d.f. for both; $F = 0.013$ and $t = -2.429$), and 0.008 for the right ($F = 0.986$ and $t = -2.9$).

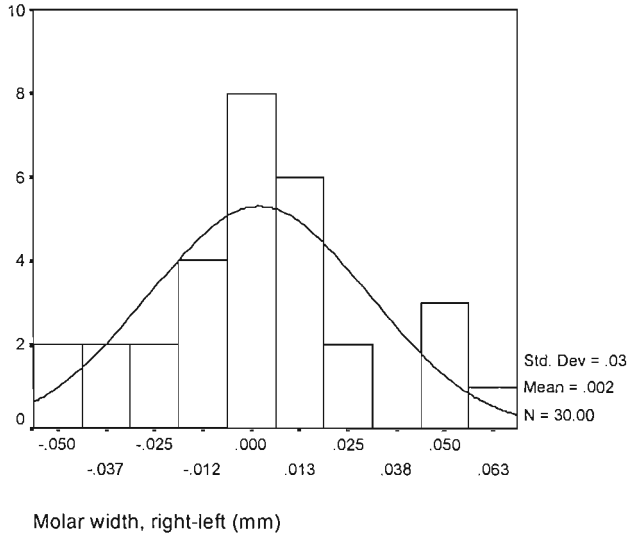

Figure 5.19 Distribution of $R - L$ molar width for the whole dataset

Figure 7.19 was produced in the same way as that for orbit width in Figure 7.15, and shows a similar trend, with the majority of cases recording no differences between the left and right molars. When the dataset was divided into the two populations (Figures 7.20 and 7.21), the results support the conclusion that Redcross experienced greater developmental instability than Chelsea.

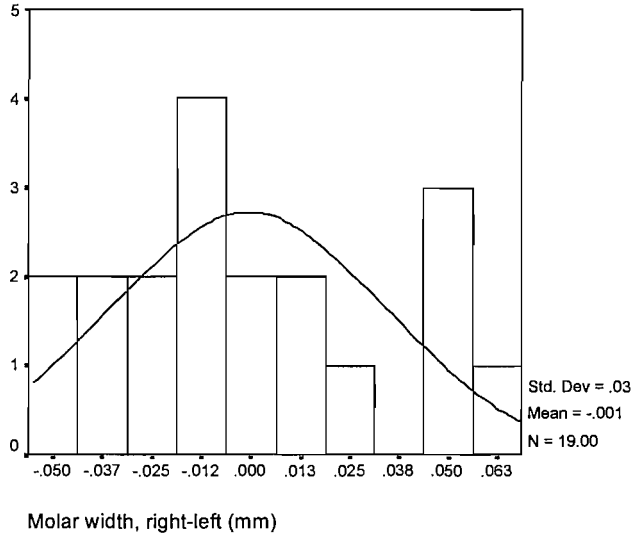

Figure 7.20 Distribution of $R - L$ molar width for the Redcross population

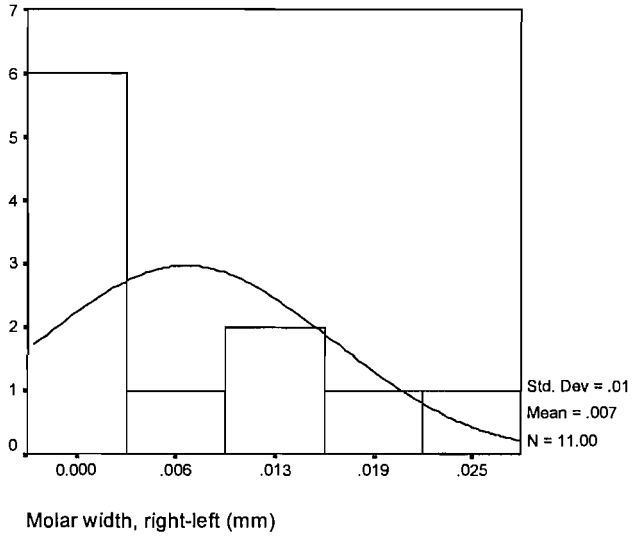

Figure 7.21 Distribution of $R - L$ molar width for the Chelsea population

A total of 16 individuals from the Redcross sample had sufficient material for inclusion in the molar analysis, compared to only nine from the Chelsea group. The latter is on the boundary of a viable sample size, which might have affected the outcome. Even so, the Chelsea regression records a higher R^2 value and much narrower confidence bands than the Redcross sample, suggesting that this reflects a true demographic trend. Not only were the teeth of the Chelsea inhabitants larger than those of Redcross, they also showed far less bilateral variation. The combination of evidence from orbital width and molar width indicates that Redcross was a stressed population. Molar width was originally included as a relatively stable control for bilateral measurements, but instead the analysis showed that, such was the developmental instability of this population, strong asymmetries were detected.

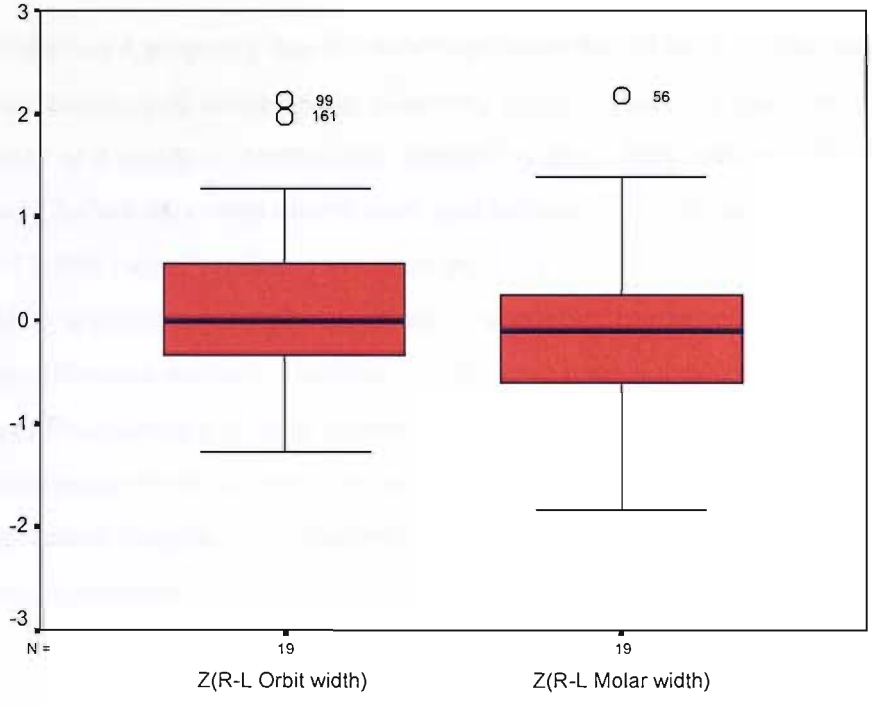

Figure 7.22 Asymmetry in orbit width and in molar width as Z-scores for the combined adult population

Figure 7.22 shows the distribution of Z-scores, with those for molar width in particular approaching a value of –2. Since the three labelled outliers belong to the

Redcross population, it is likely that the developmental instability identified in this group is also responsible for the marked deviation from the median.

Platybasia

The analyses carried out thus far have indicated a strong tendency towards developmental instability in the 'poor' population, conforming to predictions of growth in stressful environments. If variation in the skull is subject to environmental influence in the same way as stature, it may therefore be a biological principle that can be seen in *H. erectus*. This would not necessarily suggest that *H. erectus* was living and growing in stressful conditions; it could show alternative growth trajectories in different environments. Correlation with the environment will be of principal use in determining which of the two applies.

Prediction 4 proposed that the poor population would have a flatter cranium than their advantaged counterparts, following Angel (1982). He used the skull base height index as a means of comparison: (cranial height x 100)/cranial width. The Redcross and Chelsea data were transformed into this new variable and assessed: a *t*-test gave $p = 0.008$ (equal variances assumed and 50 d.f. for both; $F = 0.009$ and $t = 2.761$). While a significant result was expected according to prediction 4, the direction of the difference was not: Chelsea was shown to have a smaller skull base height index than Redcross (91.576mm against 95.087mm), indicating a smaller height for width. To investigate this further, the two relevant measurements, basion-bregma and auriculare-bregma, were regressed against each other for the adult members of the two populations:

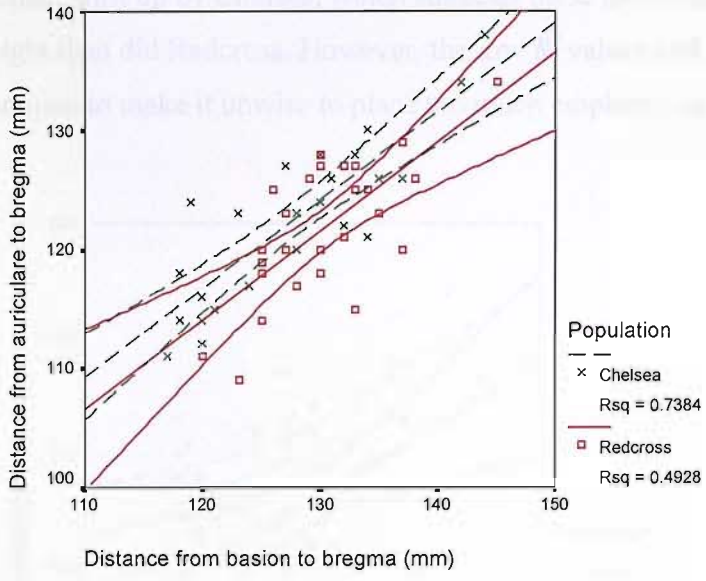

Figure 7.23 Assessment of adult cranial base height in the Redcross and Chelsea populations

There is a distinct shift upwards by the Chelsea population in Figure 7.23, showing a greater distance of auriculare-bregma (width) for basion-bregma (height), and thus indicating, contrary to expectation, a comparatively flatter cranial base in this population rather than in Redcross. However, the R^2 value for Redcross (0.493) is not convincing, and the wide confidence intervals make it impossible to judge whether this apparent shift is a demographic reality. Neither measurement supplied a significant result in a *t*-test between the populations, with $p = 0.119$ for basion-bregma (equal variances are not assumed; $F = 5.313$ and $t = 1.589$ with 42.648 d.f.), and $p = 0.966$ for auriculare-bregma (equal variance are assumed; $F = 0.667$ and $t = -0.043$ with 51 d.f.). These results do not fit with the clear indications of developmental instability in the orbits and the molars, and could be affected in part by the skew to the right in Chelsea, as seen in Appendix III.

The dimension auriculare-bregma is a chordal measurement of skull width, rather than a measurement of height. It makes sense then to compare this with the regression of bi-temporal width against basion-bregma height, as an additional measure of width, and thus to give another opportunity to integrate these findings with Angel's (1982) hypothesis. Figure 7.24 indicates that, as before, there is a

distinct shift up by Chelsea, which suggests these individuals had a greater width for height than did Redcross. However, the low R^2 values and the relatively wide scatter continue to make it unwise to place too much emphasis on these findings.

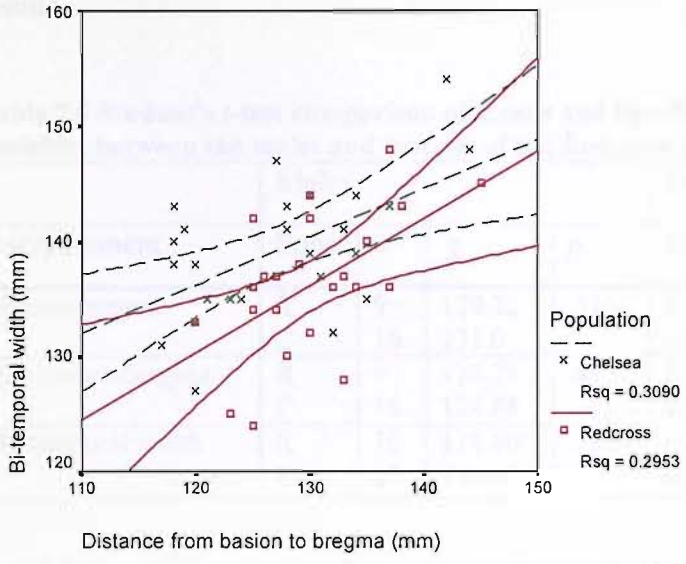

Figure 7.24 Relationship between cranial width and cranial height in the Redcross and Chelsea adult populations

It is important to establish how these results were obtained, since they are contrary to previous predictions. Accordingly, *t*-tests were performed on the three dimensions in question, controlled for sex (Table 7.6) (equal variances are assumed for all). At this point in the analysis, it is useful to introduce the Bonferroni correction. When using a large number of *t*-tests, as this study does, the alpha value needs to be adjusted to avoid false positive results. For example, with $p = 0.05$, there is a 64.15% chance of finding one or more significant differences in 20 tests, whether or not this difference exists in reality. Sidak's correction[2] recommends lowering p to 0.00256. This value will be adopted as the boundary of significance for all the following *t*-tests.

Although variation in sample size may adversely affect the strength of the results, the pattern that emerges is that the females show greater variability between

[2] See http://home.clara.net/sisa/bonfer.htm (24.2.05)

populations than the males, and that for both significant results in Table 7.6 (although only the basion-bregma finding is accepted) Redcross has a higher mean value. Differences in sample size failed to have the same effect on the male groups, so it may be concluded that this is not (at least wholly) responsible for the significant results.

Table 7.6 Student's *t*-test comparison of means and significance (*p*) of three cranial variables between the males and females of the Redcross and Chelsea populations

	Males				Females			
Measurement	Popn	*n*	$\bar{x}$	*p*	Popn	*n*	$\bar{x}$	*p*
Basion-bregma	R C	9 16	129.22 131.0	.519	R C	17 9	130.94 120.78	.000
Auriculare-bregma	R C	9 16	122.78 124.88	.444	R C	18 10	121.50 117.40	.053
Bi-temporal width	R C	10 17	138.80 140.35	.531	R C	18 14	136.67 137.00	.874

Angel believed that platybasia was a symptom of environmental stress, caused by a weakening of the skull base in relation to the weight of the brain and head. He appeared to demonstrate this convincingly, but it has not been possible to replicate his results with these two populations. On the contrary, Figure 7.24 suggests that the opposite is true; Chelsea appears to have a flatter cranial base. This may be explained through environmental sensitivity, with asymmetry a more refined measure of developmental stress than platybasia.

Alternatively, the problem may be with Angel's technique. As mentioned above, although Angel controlled for width, he did not do so for circumference, and therefore gross overall cranial size. A *t*-test on circumference between the two populations in this study was not significant ($p = 0.056$), although the mean circumference of the Redcross sample was 517mm, while that of the Chelsea group reached 526mm. To integrate this disparity, basion-bregma height and bi-temporal width were each regressed against circumference, and the residuals from each regression saved and plotted as a scatter (Figure 7.25).

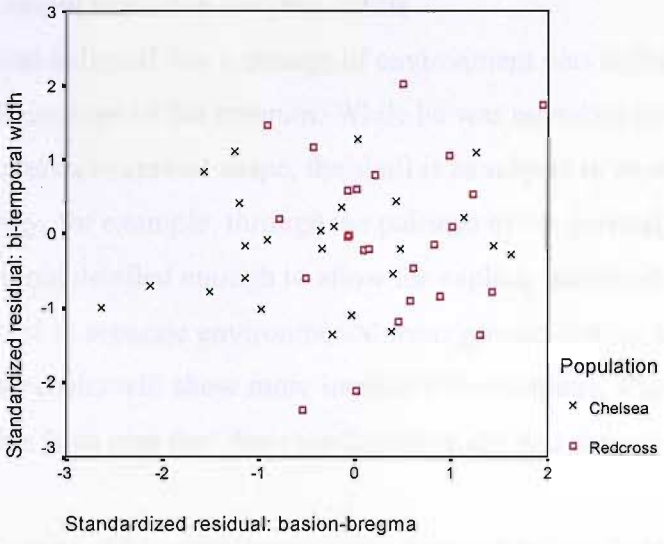

Figure 7.25 Relationship between cranial width and cranial height in the Redcross and Chelsea adult populations, controlled for circumference

Although these results are too widely distributed to be suitable for the fitting of a regression line or calculation of R^2 values ($R^2 = >0.1$ for both populations), nevertheless there are two distinct clusters. Redcross appears towards the right of the graph while Chelsea, although more diffuse, is grouped further over to the left. This suggests that circumference has a strong enough impact through its relationship with cranial height and width to separate the two populations. This conclusion is further supported by a *t*-test between the populations on a new variable of cranial height divided by circumference, which shows a solidly significant difference ($p = 0.002$. Equal variances assumed; $F = 3.176$ and $t = 3.353$ with 45 d.f.).

These findings have implications for the acceptability of Angel's theory of platybasia. Figures 7.23 and 7.24 show that Chelsea, and not Redcross as Angel would have predicted, had the flattest skulls, although the difference between them was not significant. However, when height was controlled for circumference a significant result was generated, suggesting that Chelsea skulls were larger than those of Redcross in this latter dimension, to a degree great enough to overrule the apparently flatter skulls. Angel's results have not been replicated here, and the question of platybasia remains unresolved, at least in these populations, as it is the more advantaged group that demonstrates an overall tendency towards flatter crania.

Cranial variation and the orbits

Boas believed that a change of environment was sufficient to alter the relative dimensions of the cranium. While he was mistaken in underestimating the role of genetics in cranial shape, the skull is as subject to asymmetry as any other part of the body, for example, through the pairings of the parietal bones. The data that follow are not detailed enough to allow for explicit statistical analysis of this question in order to separate environmental from genetic factors, but it is possible that instead the results will show more implicit non-allometric fluctuations in growth patterns. This is an area that deserves further study, and can only be touched on here.

A series of bivariate correlations were carried out between the five cranial dimensions and the width of the left orbit, for each population individually. Throughout this analysis all correlations are calculated as Pearson's statistic, which requires random sampling rather than a normal distribution. The *p*-value for significance is set at 0.002, in accordance with the Bonferroni correction. The full results from the correlation analyses, beginning with Chelsea, are given in Table 7.7:

Table 7.7 Correlation coefficients (*r*) and significance (*p*) for the five cranial dimensions and orbit width in the Chelsea adult population (n >20)

	Length		Bi-temp		Basion-bregma		Auric-bregma		Circ		Orbit width	
	r	*p*	*r*	*p*	*r*	*p*	*r*	*p*	*r*	*p*	*r*	*p*
Cranial length	/	/	.574	.001	.535	.006	.624	.001	.884	.000	.566	.003
Bi-temporal width	.574	**.001**	/	/	.556	.004	.723	.000	.858	.000	.121	.564
Basion-bregma	.535	.006	.556	.004	/	/	.859	.000	.590	.002	.415	.069
Auriculare-bregma	.624	**.001**	.723	**.000**	.859	**.000**	/	/	.731	.000	.391	.080
Circumference	.884	**.000**	.858	**.000**	.590	**.002**	.731	**.000**	/	/	.411	.052
Orbit width (left)	.566	.003	.121	.564	.415	.069	.391	.080	.411	.052	/	/

With the exception of cranial height, the cranial dimensions for the Chelsea individuals are all correlated with each other. This suggests that the proportions of cranial morphology are all highly constrained with respect to each other, probably

due to the size and shape of the brain and the limited variation that may occur. The width of the left orbit was not significantly correlated with any skull measurement. The pattern was a little different in Redcross. In this second population, fewer cranial dimensions correlated significantly with each other (Table 7.8).

Table 7.8 Correlation coefficients (*r*) and significance (*p*) for the five cranial dimensions and orbit width in the Redcross adult population (n >20)

	Length		Bi-temp		Basion-bregma		Auric-bregma		Circ		Orbit width	
	r	*p*	*r*	*p*	*r*	*p*	*r*	*p*	*r*	*p*	*r*	*p*
Cranial length	/	/	.315	.102	.426	.038	.550	.004	.706	.000	.490	.021
Bi-temporal width	.315	.102	/	/	.543	.006	.779	.000	.713	.000	.241	.280
Basion-bregma	.426	.038	.543	.006	/	/	.702	.000	.507	.014	.037	.877
Auriculare-bregma	.550	.004	.779	**.000**	.702	**.000**	/	/	.737	.000	.263	.249
Circumference	.706	**.000**	.713	**.000**	.507	.014	.737	**.000**	/	/	.204	.363
Orbit width (left)	.490	.021	.241	.280	.037	.877	.263	.249	.204	.363	/	/

Cranial variation and stature

Cranial length, cranial height and circumference were correlated with femur length (for stature), in order to examine the relationship between stature and the skull and thereby find a link to environmental stress. However, the Redcross group did not demonstrate the expected significant correlation between stature and cranial length, although Chelsea did (Figure 7.9). It is possible that this is a consequence of small sample sizes, but may simply be an indication of the range of human variability.

Table 7.9 Correlation coefficients (*r*) and significance (*p*) for three cranial dimensions and stature in the Redcross and Chelsea adult populations

	Length		Height		Circ.	
Femur length	*r*	*p*	*r*	*p*	*r*	*p*
Redcross	.478	.061	-.003	.993	.283	.288
Chelsea	.641	**.002**	.562	.029	.605	.008

The populations were then broken down by sex (Table 7.10), but almost certainly due to small sample sizes (n = 6-17) the significant result is no longer seen. These two study populations cannot therefore validate a connection between the cranium, stature and, indirectly, the environment.

Table 7.10 Correlation coefficients (r) and significance (p) for three cranial dimensions and stature in the Redcross and Chelsea adult populations, divided by sex

	Length		Height		Circ.	
Femur length	*r*	*p*	*r*	*p*	*r*	*p*
Redcross males	.470	.287	-.090	.866	.427	.339
Redcross females	.438	.238	.137	.747	.049	.901
Chelsea males	.546	.102	.289	.451	.531	.141
Chelsea females	.269	.424	.251	.631	.444	.231

Variation in cranial shape

Variation in cranial form has previously been well documented. Although it has not proved possible to differentiate the modern American white population on a geographical basis (Sparks et al 2002: 145), such findings have been reported, to varying extents, for the peoples of the Marquesas Islands in Polynesia (Stefan and Chapman 2003) and for ancient and modern Amerindians (Pucciarelli et al 2003). However, in each case this is hypothesised to be principally the result of migration and isolation, with a small amount due to (environmental) adaptation (Pucciarelli et al 2003). In this context, any evidence in this study for a difference in general head shape between Redcross and Chelsea, may be more to do with the relative isolation of social class and economic status, rather than the effects of that status itself. A series of t-tests were performed on length, bi-temporal width and circumference to highlight any separation between the populations.

Circumference is increased in Chelsea, as noted above, but determining the origin of this increase is less straightforward. For bi-temporal width and maximum length, n =

28 for Redcross and n = 31 for Chelsea, and the mean difference between populations for these measurements is only 1-2mm. Consequently, for length p = 0.375 (equal variances are assumed; F = 0.76 and t = -0.895 with 57 d.f.) and p = 0.211 for bi-temporal width (equal variances are not assumed; F = 5.75 and t = -1.266 with 52.398 d.f.). A linear regression between these dimensions did not yield a discernable relationship; Chelsea produced an R^2 value of 0.33 in the adult population, while Redcross showed an even weaker trend with R^2 = 0.1.

A regression of circumference against width created a clearer separation between the two adult populations. The advantaged population produced a stronger relationship with R^2 = 0.78, compared to R^2 = 0.50 in Redcross. Figure 7.26 illustrates the discrepancy between the two samples, and indicates that for Chelsea, circumference is more heavily influenced by an increase in cranial length than it is for the Redcross group:

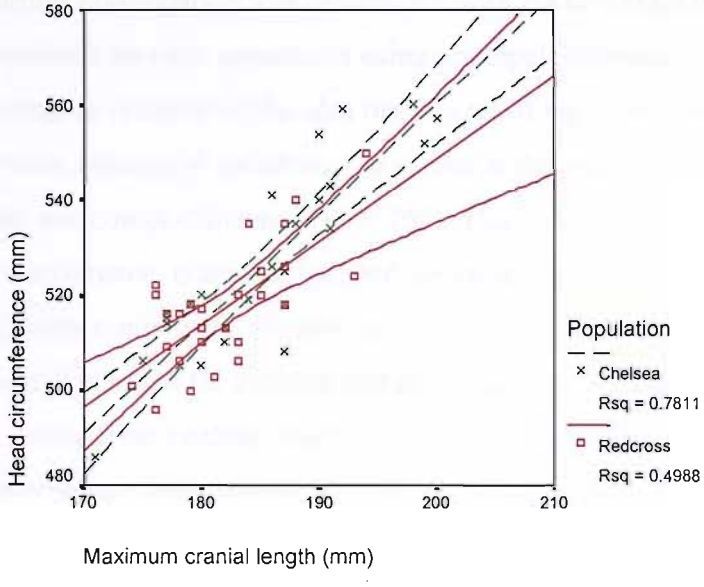

Figure 7.26 The relationship between circumference and maximum cranial length in the Redcross and Chelsea adult populations

A similar pattern is produced when bi-temporal width is regressed against circumference, and at 0.74 and 0.51 the R^2 results almost match those of Figure 7.26

above. With a much stronger trend in evidence for Chelsea, width seems to be a better predictor of circumference for the rich group than for the poor.

Cranial height was regressed against cranial length and then bi-temporal width to show a distinct shift upwards by Chelsea, implying that both length and width were greater for height in this population than in Redcross. However, in each case the R^2 value denoted a very weak relationship (0.29 in Chelsea and 0.18 in Redcross for height against length, and 0.31 in Chelsea and 0.30 in Redcross for height against width), similar to that seen in the platybasia investigations. The significance of these results lies in the inference that head shape is slightly different in the richer population. This difference is expressed most strongly through cranial circumference, although there is no increase in any one dimension that is solely responsible for this. Instead, there is a mosaic of changes, linking length, breadth and height. Unfortunately, this is not reflected in cephalic index, which did not differ significantly between the two populations ($p = 0.921$ with 57 degrees of freedom). Further investigation was carried out, with the covariation between variables measured for each population using principal components analysis (PCA). This technique is based on the idea that if a set of variables can be summarised by a smaller number of variables, the values of the original variables must be correlated with each other (Shennan 1997: 269). Thus, bi-temporal width, cranial length, circumference, cranial height and auriculare-bregma height were reduced to one principal component. Despite only extracting only a single component, the results are still of value for comparative purposes. Cephalic index and cranial capacity were excluded from analysis since they are a product of length, breadth and height and therefore not independent (Table 7.11).

Table 7.11 Principal Components matrix results for Redcross

	Component 1	
	All	Adults
Bi-temporal width	.783	.823
Glabella-inion	.711	.736
Circumference	**.909**	**.915**
Basion-bregma	.729	.710
Auriculare-bregma	.884	.898

Circumference contributed the most to variance within Redcross when adults and juveniles were considered together, accounting for 65.16% of variance. The measurement of auriculare-bregma also had a high Eigenvalue (0.884) and was responsible for 17.61% of variance. In adults alone, the principal component was again circumference (67.34%) followed by auriculare-bregma, contributing 14.85%. This pattern was repeated within the Chelsea population (Table 7.12).

Table 7.12 Principal Components matrix results for Chelsea

	Component 1	
	All	Adults
Bi-temporal width	.895	.891
Glabella-inion	.825	.844
Circumference	**.923**	**.932**
Basion-bregma	.808	.816
Auriculare-bregma	.900	.900

For the whole Chelsea population, component 1 was derived from circumference, contributing 75.92% of variance, with auriculare-bregma accounting for 13.93%. For the adults, this trend was repeated, with similar levels of variance (77.00% and 13.46% respectively). The range of the Eigenvalues can separate the populations, as those for Chelsea do not fall below .800, whereas Redcross shows greater variation. If indeed the symmetry of skull development can be linked to environmental stress, this may explain why there is a higher degree of correlation between the selected data for Chelsea compared to Redcross. However, this theory is unsupported at present.

Variation in cranial capacity

The final variable to be tested is cranial capacity. A *t*-test was performed on this variable between the populations but the result was not significant, $p = 0.365$ (equal variances are assumed; $F = 1.731$ and $t = -0.914$ with 47 d.f.). Sample sizes may not be great enough for a more refined result (from 24 individuals Redcross had a standard deviation of 101.56, while Chelsea, with 25 individuals, produced a

standard deviation of 140.29). However, it could be that brain size poses too much of a constraint, more so than environmental influence can overcome, and thus it has a relatively narrow reaction norm.

To examine this variable in more detail, the populations were tested according to sex. There was no significant difference between the males of Redcross and Chelsea, $p = 0.131$ (equal variances are assumed; $F = 0.001$ and $t = -1.567$ with 22 d.f.). Although the result for the females was also insignificant ($p = 0.05$. Equal variances are assumed; $F = 0.672$ and $t = 2.065$ with 23 d.f.), there was nevertheless an unexpectedly larger mean female cranial capacity in the Redcross population (a gain of 82.4cc, or 7.2%). It is not clear from where this increase is derived, since Chelsea adult females have a larger circumference by 0.7mm than the Redcross cohort, a larger mean bi-temporal width by 0.3mm, and a smaller mean cranial length by 1.9mm (a 1.06% increase by Redcross); it is possible these increases were substantial enough to account for such a marked increase in cranial capacity. All dimensions for both population subsets satisfied a prior screening for a normal distribution.

Perhaps less surprisingly, when all males were compared to all females across both populations, a significant difference in cranial capacity was found between the two groups, with males averaging 1331.9cc and females 1200cc ($p < 0.001$. Equal variances are assumed; $F = 0.01$ and $t = 4.431$ with 47 d.f.). Twenty-four males were included in the analysis and 25 females, eliminating the problem of unequal sample sizes. This sexual dimorphism is also reflected in stature, with a similar result.

Finally, a discriminant function analysis was applied to both populations, by sex, to see if the difference in female cranial capacity was reflected in overall cranial relationships (Figure 7.27). This technique is applied in order to assess the likelihood of a specimen belonging to one particular group or another by creating a new variable, Z, based on existing variables. The cranial variables included were length, breadth, circumference, capacity, and the indices cephalic index and cranial

ratio. These latter three are not independent, since they are derived from length, breadth and height, but do indicate the relationships between those variables.

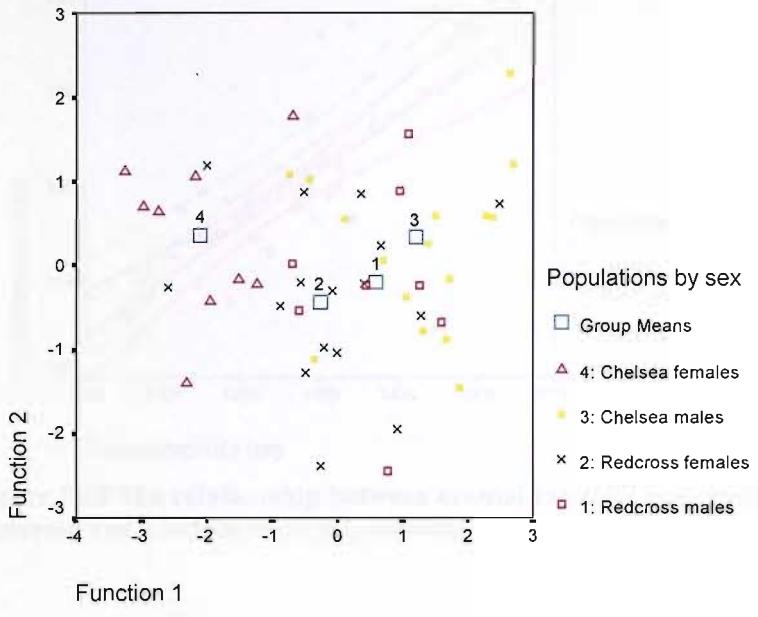

Figure 7.27 Discriminant function analysis for the cranial dimensions of the Redcross and Chelsea adult populations, by sex

As expected, Figure 7.27 shows the two female groups more to the left of the scatter, while the males tend to be clustered on the right, although there is some overlap. However, following the *t*-test results mentioned above, the green crosses of the Redcross females strongly overlap with the Chelsea males and, to a slightly lesser extent, the Redcross males. This suggests a similarity in the cranial morphology of these subgroups that is not shared by the Chelsea females.

Circumference appears to have a notable effect when regressed against other variables, and this reinforces the conclusion that it is the measurement most responsible for separating the two populations. This is seen below in Figure 7.28, with cranial capacity (the only dimension from which cranial capacity is not derived), and in both populations a bivariate correlation between the two gives a *p*-value of <0.001 (with a correlation coefficient of 0.812 in Redcross, and 0.844 in Chelsea).

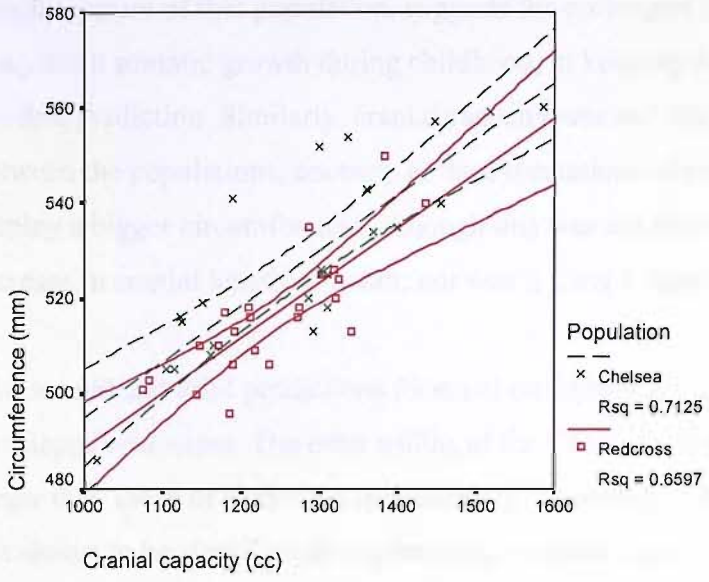

Figure 7.28 The relationship between cranial capacity and circumference in the Redcross and Chelsea adult populations

Discussion

Through the analysis of two modern human populations it has been possible to demonstrate the presence of developmental instability in an economically deprived group, signifying that there was a mismatch between the Redcross population and its environment; or more accurately, that the environment did not fit the needs of its inhabitants. This lack of correlation between need and supply is seen through the directional and fluctuating asymmetry of the orbits, and through the relationship of various cranial measurements to each other. There is no systematic pattern of overall morphology for either population, so it can be accepted that there is no genetic basis to these asymmetries, and that they occur as a result of environmental stressors. The presence of developmental instability has further repercussions for juvenile survival, since environmental stress implies differential allocation of energy to growth.

Five predictions were made regarding developmental variation between the rich and poor populations. The difference in mean stature between Redcross and Chelsea was

not significant, but the greater range of heights in Redcross, and the generally smaller stature of that population, suggests the prolonged diversion of resources away from somatic growth during childhood, in keeping with the growth-faltering of the first prediction. Similarly, cranial capacity was not significantly different between the populations, contrary to the expectations of prediction 5. Chelsea did display a bigger circumference, although this was not derived from a significant increase in cranial length or width; nor was it itself a significant increase.

The second and third predictions focussed on asymmetry as a measure of developmental stress. The orbit widths of the Chelsea population were significantly larger than those of Redcross, and although the widths of the Redcross orbits were not shown to be significantly asymmetric, a scatter regression revealed a wide distribution of points, indicating greater irregularity. A similar result was gained for the investigation into molar width, contradicting expectations of stability. Chelsea molars were significantly larger than those of Redcross, and although significant differences in width could not be proved, wider confidence intervals for the poor population suggested greater variability between left and right.

The fourth prediction was not borne out by the data. It could not be shown that Redcross had a flatter cranial base than the richer population of Chelsea, contrary to previous socio-economic studies, but platybasia may require more extreme conditions for visibility than those experienced by these populations. Alternatively, it may be that Angel's hypothesis (1982) is flawed, since fluctuating asymmetry clearly shows that Redcross was under stress. Rather than acting as a sign that Chelsea was nutritionally deprived, it may be a symptom of a general change in cranial form.

A number of potential problems must be taken into account. Cranial capacity was derived from three measurements and so is more subject to error and inference than any of the three taken alone. Investigation of sex-related differences also means that sample size is smaller, making any apparent changes less reliable than they first

appear. For example, only nine females from Chelsea had a known cranial capacity, compared to 16 from Redcross, and it is likely this had an effect. Similarly, only nine females were intact enough to provide measurement of basion-bregma for Chelsea (mean = 120.8mm), while 17 Redcross females qualified for inclusion (mean = 130.9). Despite the considerable disparity between the two means, it is not safe to draw conclusions regarding, for example, platybasia, due to the discrepancy in sample sizes. To complicate analyses based on sex differentiation, the true sex of the individuals was in the vast majority of cases unknown, and has only been assessed. It is therefore possible that there is an inadvertent overlap between the groups.

Similarly, small sample size may have been responsible for the lack of correlation between cranial length and stature, a known relationship that had the potential to link cranial shape (through the cephalic index) to environmental status (although small sample size did not prevent significant results for orbital and molar asymmetry). In this respect, cranial morphology is not under enough environmental control to allow for the statistical separation of two populations of contrasting economic and nutritional background. Like Sparks and Jantz (2002), it is concluded here that the genetic component of cranial development is paramount, due to the constraints of the brain, and head shape does not adjust according to environment. When populations have been distinct and relatively isolated groups, there may be population-specific traits that are independent of environmental influence. Related to this is the possibility of a 'founding effect', although there is no evidence in this study for a population-level genetic background to the changes seen above. However, these genetic patterns may potentially be identified in a species with a wide temporal and spatial distribution. The cranial morphology of the *H. erectus* p-demes is explored in the following and final chapter.

CHAPTER EIGHT

Regional variation in *Homo erectus*

This chapter is divided into two parts. The first section will address the cranial variation in *H. erectus* that was demonstrated in Chapter Five's encephalisation study, using the same techniques as in Chapter Seven, in order to test hypotheses three and four regarding regional variation by latitude. The previous chapter concluded that genetic differences in cranial morphology might be more readily identified in widely distributed populations, such as the *H. erectus* p-demes. The wide geographical range of *H. erectus* places populations in different regions at different geological times with varying juvenile mortality, which could suggest variation in stress by latitude. However, this presupposes that *H. erectus* would have lived in marginal environments, or would not have been well adapted to its surroundings. In life history terms, possible responses to environmental variation are expressed through the competing hypotheses five and six. These are further tested here, since the study of Chapter Seven was not able to distinguish the two populations adequately to account for genetic influence.

Cranial variation must be placed into a life historical context. Chapter Three explored the relationships between encephalisation and traits such as altriciality and mortality patterns, and these will now be related to *H. erectus*. This species inhabited diverse environments, and it is proposed that these can be divided into a core area of optimum adaptation, with species typical traits (such as delayed reproduction, a long period of growth and juvenile dependence, and a decrease in juvenile mortality), and a periphery of the range, which reached the extremes of tolerance and reaction norms. Habitation of the periphery would be expected to result in an alternative pattern of development, since growth rates vary under different life history regimes. It would also present greater problems of survival, with subsequent reduced selection for encephalisation and a higher risk of juvenile mortality. Attendant changes, such as the lowering of the age at first reproduction and a decreased birth interval, have their own problems from the infant's

perspective, since weaning at an earlier age, and at a lower weight, is a known risk in long-term survival. A lengthening of the lifespan could be a less risky strategy, although evidence is limited to the relative prevalence of 'elderly' specimens.

In Chapter Four, the age-specific mortality profiles showed higher juvenile mortality in Europe and China, thus addressing hypotheses three and four, although, with a larger sample size, the Zhoukoudian population provides the most reliable data of the two regions. The model proposes that China and Europe are periphery p-demes. Brain size in these populations is unlikely to have been large enough to provoke the modern human condition of secondary altriciality, and so postcranial growth would have been more rapid than that of *H. sapiens*, but still constrained by the larger brain size compared to earlier specimens of *H. erectus*. In those regions characterised by a smaller brain size and lower juvenile mortality, an increase in both postcranial and cranial growth rate would have allowed earlier reproductive maturity. The ecological context of this is discussed and explored in further detail below.

Instability of development was demonstrated in a deprived modern human population in the previous chapter, although cranial length did not vary as expected. There are problems involved in a direct comparison with *H. erectus* because of the divergence in morphology and life history profile, the discrepancy between industrial and Palaeolithic environments, and the timescale involved. To account for this, the second section of this chapter will assess the Zhoukoudian population in the context of the remains from Sima de los Huesos ('Pit of Bones') at Atapuerca, northern Spain. This narrows the species and time span, as both are Palaeolithic populations. The analysis is also carried out using the methods from Chapter Seven.

The use of fossil populations has its own particular problems. The prime ones for this study are determining whether the individuals represented in the record belonged to a single biological population, and whether the derived mortality profile is typical of the age structure of the living population. The taphonomy of sheltered cave sites was explored in Chapter Four, using various South African populations of

baboons and australopithecines, and with reference to the demography of living baboon troops. In this chapter, the comparison between the Zhoukoudian and Atapuerca cave sites might further assist in taphonomic interpretations of the *H. erectus* sample. Taphonomic bias can affect understanding of life history and environmental susceptibility, and its impact is likely to have been greatest on the open-air sites in Africa, making this area difficult to interpret.

1. The impact of the environment

The life history strategy of *H. erectus* first evolved in the heat and aridity of Africa, rather than the temperate climates of China and Europe. These regions are exposed to greater fluctuations in temperature and rainfall than the more equatorial *erectine* sites in Africa and Indonesia. If these factors varied enough to exceed the tolerance limits of the species, then life history strategy would have had to alter accordingly in order to ensure the survival of juveniles to reproductive maturity. Variation in the juvenile mortality rate is difficult to calculate as it depends heavily on the discovery and identification of immature individuals, whilst controlling for taphonomic biases, but in conjunction with other indicators such as encephalisation, it provides a window onto life history. It is possible that this interpretation of climate is too simplistic, or that regions are affected more by a continental rather than a temperate climate. Nevertheless, it remains the case that regional differences are important for determining life history variation in *H. erectus*.

Method

The *H. erectus* dataset for this analysis was restricted to those specimens with both cranial length and breadth measurements (Table 8.1). The same definition of length was used as in Chapter Seven (Table 7.2), but in this chapter cranial width was taken as maximum bi-parietal breadth rather than bi-temporal breadth, since this alternative measurement was more frequently reported in the literature. The variable preservation of the fossils limited measurement of cranial height (basion to bregma) to only seven specimens, making it unsuitable for statistical analysis on a regional basis. Cranial index could not therefore be calculated, but cephalic index is used for

inter-group comparison (the formula is given in Chapter Seven). Cranial length and bi-parietal width as raw measurements are informative of individual variation only; the proportional measure of cephalic index is much more useful in this regard.

Table 8.1 Latitudes of *H. erectus* sites and corresponding juvenile mortality[1]

Latitude/Site	**Specimens used in this chapter (* = juvenile)**	**Environment**	**Juvenile mortality[2]**
Zhoukoudian **39° 41' N**	PA 830 (Hexian), PA 16*, PA 98, PA 99, PA 100	Temperate **China**	38.88 %
Dmanisi **42° N**	D2700*, D2280, D2282*, Ceprano	Temperate **Europe**	28.57 %
Kenya, Tanzania **1° - 6° S**	WT 15000*, ER 3733, ER 3883, OH 9, BOU-VP-2/66, UA 31	Tropical **Africa**	9.38 %
Indonesia **3° - 10° S**	Sm 1, Sm 3, Trinil, Sangiran 2, 17, Ngandong 1, 6, 7, 9, 11, 12	Tropical **Indonesia**	11.54 %

In this chapter, where juvenile mortality is concerned, the specimens are largely self-selecting, since only intact skulls are admissible and these generally are the more robust adult individuals. However, age at death analyses in Chapter Four agree with the figures in Table 8.1, which indicate that juvenile mortality is highest in the designated temperate zones and much lower in the tropical regions. Latitude is acceptable as an estimate of climate since it influences the seasonal range in solar intensity and the degree of precipitation, given that evaporation is temperature dependent. Sample sizes for this study are small, but may be enough to detect trends of environmental influence. The validity of these climatic distinctions will also be tested using geographical proximity, with east (China and Indonesia) and west (Europe and Africa) as a predictor of morphology. With the exception of Zhoukoudian, all the other specimens in this sample are from open sites and so problems of taphonomic bias must be considered.

[1] With the exception of Dmanisi (Dennell 2003: 428), all latitude and longitude references are derived from http://www.bcca.org/misc/qiblih/latlong_oc.html (12.11.03), a database of the positions of major cities around the world. The cities closest to the sites in question are used as reference points.
[2] Calculated according to the ages at death and method described in Chapter Four (see Table 4.6) for the regions overall.

Statistical analysis

The procedures applied to this data overlap with those in Chapter Seven, with some additions: Pearson's statistic for bivariate correlation, Student's 2-tailed *t*-test for independent samples, analysis of variance (ANOVA) with Tukey's post hoc tests, and discriminant function analysis. All analysis was carried out using SPSS for Windows, Release 11.5.0. As with Chapter Seven, the *p*-value for significance is set at 0.002 to take into account the large number of *t*-tests performed.

2. The impact of time span

A Palaeolithic context will be created for *H. erectus* by comparing the Zhoukoudian population, chosen for the greater temporal unity of the sample, to a different species from an equivalent time frame. As such, I examine the evidence from the Middle Pleistocene cave site of Sima de los Huesos in the Sierra de Atapuerca, near Burgos, in north-central Spain. First discovered in 1976, the fossils are dated by ESR and uranium series from a minimum of 320ka to a likely 400-500ka (Bermúdez de Castro et al 2003: 1422; Bermúdez de Castro et al 2004: 26-27), making them contemporaneous with the Zhoukoudian population. These fossils are thought to be representative of an archaic *H. sapiens* but are also described as *H. heidelbergensis* (Bermúdez de Castro et al 2004), perhaps on the evolutionary line giving rise to *H. neanderthalensis* and modern humans (Arsuaga et al 1997b; Arsuaga et al 2001; see also Chapter Two). Therefore, this population is used to provide a link to the modern populations investigated in Chapter Seven due to their species, and *H. erectus* due to their age.

Table 8.2 The Zhoukoudian and Atapuerca comparative populations

Specimen	Age at death	Cranial capacity (cc)	Cranial length (mm)	Cranial breadth (mm)
Zhoukoudian III	16	915	187.6	133.0
Zhoukoudian X	Adult	1225	199.0	137.0
Zhoukoudian XI	Adult	1015	192.0	136.0
Zhoukoudian XII	Adult	1030	195.0	140.0
Atapuerca IV	Adult	1390	201.0	164.0
Atapuerca V	Adult	1125	185.0	146.0
Atapuerca VI	Elderly	1247.9	186.0	136.0

Sample

Reconstruction of past populations is made problematic by the inadvertent pooling together of individuals who may in life have been spatially and temporally separated. Thus, the mortality profile would be affected by the conflation of several generations that did not overlap in life, even if the site was in constant occupation over this period. It is claimed (Bermúdez de Castro and Nicolás 1997: 334) that the Sima de los Huesos individuals belong to the same biological population, and as such the mortality and age at death distribution is explored in greater detail below.

Illustrated below in Figure 8.1, the demographic profile is indicative of a population experiencing high juvenile mortality, similar to that seen in China. Despite there being 28 individuals in the Sima de los Huesos cohort, only three adult crania (skulls IV, V and VI; skull V belongs to an elderly adult) are complete enough to allow for the measurement of length, breadth, height and capacity (derived from these three dimensions following the formula set out in Chapter Seven). This sample size is too small to permit meaningful statistical analysis, so the results are only considered as a guide to cranial relationships.

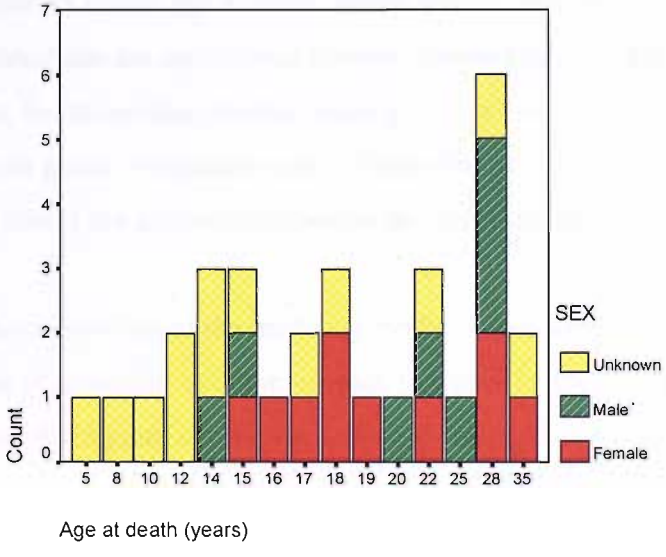

Figure 8.1: Age at death distribution of the Sima de los Huesos population, by sex

From a total of 32 individuals, 59% (19) are juveniles, defined as being aged up to but excluding 21 years old using M_3 eruption, as for *H. erectus* (see Chapter Four). Although the biological difference between a 20 year old and a 21 year old is not significant enough to justify their separation into different demographic groups, for many of these older adolescents their ages were given as 16-20 years (i.e. just prior to or at the time of eruption of the third molar) (Bermúdez de Castro and Nicolás 1997), averaged to 18 years for statistical analysis. On these grounds, the boundary between juvenile and adult was set at the upper limit of this age range. Alternatively, if adulthood is taken to begin at 16 years, the proportion of juveniles in the profile is reduced to 37.5%. However, since it is impossible to age adolescents this precisely, they will be classified into broad age ranges.

The account of high juvenile mortality in the Atapuerca population, during this period of the Palaeolithic, contrasts heavily against similar mortality profiles for *H. erectus* and modern humans, as seen in Chapters Four and Seven respectively. Mortality is high during the mid-teenage years, with eight individuals aged between 11-15, and the same number aged between 16-20. Each of these two age groups (young adolescents and older adolescents) accounts for more deaths than the apparent modal age at death, which occurs around 10 years later. Only two individuals are considered to have survived into old age (as denoted by the 35 years bar, for those described as 'elderly' in the literature). These figures vary a little from those given in a recent review (Bermúdez de Castro et al 2004), but not sufficiently to distort the picture of mortality presented above.

The conversion of the mortality profile into a survivorship curve indicates a constant risk of mortality over the lifespan (a Type II pattern; see Figure 3.2), but with a steep drop during late adolescence, thus reflecting the greater risk of death at this age.

Figure 8.2: Probability of surviving to successive age classes for the Sima de los Huesos population (assuming an attritional mortality profile)

However, this curve only applies if the population remains are indicative of a natural process of mortality; in the case of catastrophic accumulation it represents a cross-section of the population. As this cannot be satisfactorily determined (for opposing views, see for example Arsuaga et al 1997a; Bermúdez de Castro and Nicolás 1997; Bocquet-Appel and Arsuaga 2000; Carbonell et al 2003), the level of juvenile mortality of Atapuerca will not be considered any further, with the focus resting on cranial morphology.

Predictions

The previous chapter found that the majority of variation in cranial form is due to genetic control, with population-specific traits independent of environmental influence. Although it was not possible to separate the morphology of two modern human populations, the demic nature of *H. erectus* could lead to regional variation in cranial morphology, due to isolation and genetic drift:

1. The four regional groups described in Table 8.1 will each exhibit a distinct pattern of cranial morphology.
2. One of more of these groups will form the core, the remainder the periphery. The core group will show an overall greater cranial size, both in terms of capacity and circumference, and will cluster further up the line in a regression of length against breadth.

3. This core group will be one or both of the tropical regions, since this environment generally has more constant and predictable temperature and rainfall, which may in turn promote greater juvenile survival.
4. Due to similarities in latitude and geologic age, Atapuerca and Zhoukoudian will share a similar cranial morphology.

Results: Environmental influence

Cranial variation

Due to the more fragmentary nature of the fossil evidence for *H. erectus*, cranial length, breadth and capacity, as well as cephalic index, were the principle measurements available for analysis and were regressed against each other in turn. In this case, cranial capacity has not been calculated from the three linear dimensions, and so the problems of circularity encountered in the previous chapter will not be repeated. Instead, values for this dimension have been gained from the literature, and have generally been obtained through direct measurement using small-grained seed such as millet.

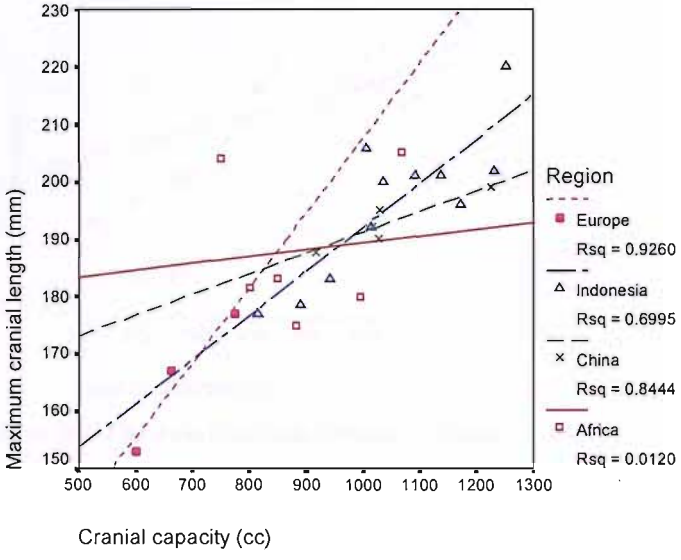

Figure 8.3 The relationship between cranial length and cranial capacity in *H. erectus*

While three of the regions express a strong regression (Figure 8.3), Africa has a very low R^2 value due to the wide spread of data points. Despite comprising only three

fossils, Europe also shows a strong trend. Indonesia has the largest sample size and so there can be the greatest confidence in the result for that region, which is all the more striking considering that it includes specimens a million years apart in age. These results are reflected in the *p*-values for the regressions, two of which (China and Indonesia) are significant at the 0.05 level (Table 8.3).

Table 8.3 Significance values for the regression between cranial capacity and maximum cranial length

	p
Africa	0.837
China	0.027
Indonesia	0.001
Europe	0.175

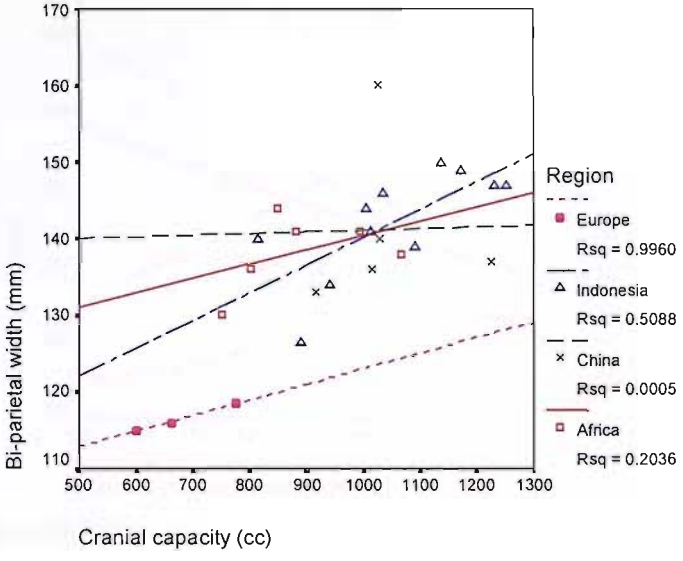

Figure 8.4 The relationship between cranial width and cranial capacity in *H. erectus*

Europe showed the strongest relationship between cranial width and cranial capacity (Figure 8.4), with $R^2 > 0.99$, although Indonesia produced the lowest *p*-value in the regression (Table 8.4). Africa retained a weak correlation between the two, but the scatter for China was too wide to allow the detection of any relationship at all. For

this latter region, Hexian (PA830) was an outlier, with a bi-parietal width of 160mm. It was removed, since the Zhoukoudian specimens show a tendency to cluster together. This action raised the R^2 value to 0.2043. In Figure 8.3, Hexian was not an outlier, having a comparable length to the Zhoukoudian skulls.

Table 8.4 Significance values for the regression between cranial capacity and bi-parietal width

	p
Africa	0.102
China	0.972
Indonesia	0.006
Europe	0.04

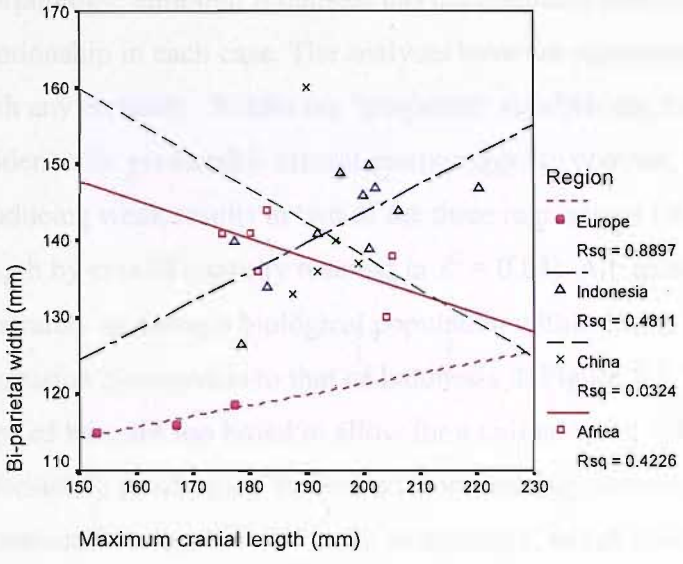

Figure 8.5 The relationship between cranial length and cranial width in *H. erectus*

A regression of cranial width and cranial length (Figure 8.5) produced two negative (China and Africa) and two positive (Europe and Indonesia) associations. However, although Europe again has the highest R^2 value, Table 8.5 shows that only Indonesia has a significant relationship between these two variables. The groupings in the graph do not appear to be related to either geography or latitude. China exhibits too

extensive a scatter to give an R^2 greater than 0.04. When the outlier Hexian was removed, the R^2 value increased to 0.4973. Although this remains low, it is suggestive of a common morphology in the remaining Zhoukoudian fossils.

Table 8.5 Significance values for the regression between maximum cranial length and bi-parietal width

	p
Africa	0.969
China	0.772
Indonesia	0.013
Europe	0.215

Thus far it has been difficult to detect any consistent regional patterns in cranial morphology, although Indonesia has maintained a reasonably strong and significant relationship in each case. The analyses have not supported a climatic dichotomy with any certainty. Within the 'temperate' subdivision, Europe has produced evidence for predictable cranial morphology. In contrast, China followed Africa by producing weak results in two of the three regressions (in the third case, cranial length by cranial capacity resulted in $R^2 = 0.84$). Alternatively, treating Zhoukoudian separately as a single biological population within China creates a stronger regression comparable to that of Indonesia in Figure 8.5. The climatic subdivisions applied here are too broad to allow for a unified trend within them, and more informative results may be derived from treating each region separately. This compounds the problem of small sample size, which could have influenced these results. Nevertheless, there is a tendency to cluster, particularly in the European and Chinese fossils, which bears closer investigation.

Cephalic index, itself a measure of the relationship between two cranial variables, failed to produce any recognisable trend when regressed against cranial capacity, with a wide scatter and extremely low R^2 result. This signifies that there is neither a constant nor a predictable relationship between the ratio of skull length and breadth,

and cranial capacity; thus any increase in cranial capacity is not due solely to the interplay between these two variables. However, exceptions to this finding occurred when the Chinese outlier was removed to leave the Zhoukoudian cluster. The deletion of Hexian from the regression produced a rise in the R^2 value to 0.6151, a vast improvement. The results of this action suggest that the closer biological population remaining at Zhoukoudian has a much tighter cranial morphology compared to other individuals from elsewhere in the region. Whether this is due to genetic isolation or a common response to the environment cannot yet be determined. It is also possible that this group (and Dmanisi, a similarly clustered sample) may not fully represent the wider population from which it came.

The *x-y* scatters have revealed little evidence for any regional trend in cranial morphology in *H. erectus*. However, this might only be an indication that there is too much variation in the few fossil crania available, rather than an absence of a regional pattern. These specimens are arrayed across a long period of evolutionary time, and it is inevitable that there would be change in morphology, particularly as it was demonstrated in Chapter Five that the cranial capacity of this species has not remained static over time. It also stands to reason that there has not been stasis in any of the other cranial variables under investigation here.

As in Chapter Seven, a series of correlations were carried out within each region in order to examine these variables in greater detail. This was a better method for comparing the regions than the R^2 values generated by the regressions, in order to uncover trends relating two or more regions to each other. Once more, the high number of significance tests carried out make it necessary to apply the Bonferroni correction, in order to reduce the number of false positives that might otherwise be obtained. The lower *p*-value of 0.002, also adopted in Chapter Seven, is assumed here for these correlations. The four dimensions were correlated against one other for each of the four regions individually, and geologic age was added to provide a context. Multiple regression would ordinarily be used to answer this type of question, but the small sample sizes were too much of a constraint.

Considering Africa first (Table 8.3), only cephalic index and cranial length were significantly correlated with each other. The African sample comprises more than one p-deme, but all six specimens are aged to approximately 1-1.5 million years old. However, the result is interdependent as cephalic index is derived from both cranial length and cranial breadth.

Table 8.6 Correlation coefficients (*r*) and significance (*p*) for the four cranial dimensions and geologic age in African *H. erectus* (n = 6)

	Length		Bi-parietal		Cephalic index		Cranial capacity		Geologic age	
	r	*p*	*R*	*p*	*r*	*P*	*r*	*p*	*r*	*p*
Cranial length	/	/	-.650	.162	-.959	**.002**	.110	.836	-.554	.254
Bi-parietal width	-.650	.162	/	/	.837	.038	.451	.369	.573	.238
Cephalic index	-.959	**.002**	.837	.038	/	/	.089	.867	.606	.202
Cranial capacity	.110	.836	.451	.369	.089	.867	/	/	-.172	.745
Geologic age	-.554	.254	.573	.238	.606	.202	-.172	.745	/	/

The Chinese population showed more variability in cranial morphology, with no significant intracranial correlations evident at the low *p*-value required by the Bonferroni correction. It is possible that this is due to the influence of the Hexian cranium, which is shown in Figure 8.4 to have a much larger bi-parietal width for cranial capacity, and is also 200ka younger than the Zhoukoudian crania (although it is considered to belong to the Zhoukoudian p-deme; see Chapter Two).

Table 8.7 Correlation coefficients (*r*) and significance (*p*) for the four cranial dimensions and geologic age in Chinese *H. erectus* (n = 5)

	Length		Bi-parietal		Cephalic index		Cranial capacity		Geologic age	
	r	*p*	*r*	*p*	*r*	*P*	*r*	*p*	*r*	*p*
Cranial length	/	/	-.180	.772	-.428	.472	.919	.027	-.195	.753
Bi-parietal width	-.180	.772	/	/	.966	.008	.022	.972	.881	.048
Cephalic index	-.428	.472	.966	.008	/	/	-.219	.723	-.758	.138
Cranial capacity	.919	.027	.022	.972	-.219	.723	/	/	-.348	.566
Geologic age	-.195	.753	.881	.048	-.758	.138	-.348	.566	/	/

Table 8.8 Correlation coefficients (*r*) and significance (*p*) for the four cranial dimensions and geologic age in European *H. erectus* (n = 3)

	Length		Bi-parietal		Cephalic index		Cranial capacity		Geologic age	
	r	*p*	*r*	*p*	*r*	*p*	*r*	*p*	*R*	*p*
Cranial length	/	/	.943	.215	-.992	.079	.962	.175	-.910	.272
Bi-parietal width	.943	.215	/	/	.895	.295	.998	.040	-.721	.488
Cephalic index	-.992	.079	-.895	.295	/	/	-.921	.255	.954	.193
Cranial capacity	.962	.175	.998	.040	-.921	.255	/	/	-.763	.448
Geologic age	-.910	.272	-.721	.488	.954	.193	.954	.448	/	/

Comprising only three skulls, Europe (Table 8.5) was the smallest group in the analysis. Despite coming from the same site within a restricted time period (1.7-1.75Ma), there is no significant relationship between any of these cranial variables. The Indonesian group had the largest sample size, yet only produced one significant correlation, between cranial length and cranial capacity (Table 8.6). Chapter Five had previously identified Indonesia as being a population likely to have undergone encephalisation over the course of its evolutionary history, and the relationship seen here between cranial capacity and cranial length suggests that the latter dimension also increased over time. Following Holloway (2002), this may be an indirect signal

of the fitness of the Indonesian environment to the growth and development of the *H. erectus* p-demes found there.

Table 8.9 Correlation coefficients (*r*) and significance (*p*) for the four cranial dimensions and geologic age in Indonesian *H. erectus* (n = 11)

	Length		Bi-parietal		Cephalic index		Cranial capacity		Geologic age	
	r	*P*	*r*	*p*	*r*	*p*	*R*	*p*	*r*	*p*
Cranial length	/	/	.694	.018	-.640	.034	.836	**.001**	-.341	.305
Bi-parietal width	.694	.018	/	/	.107	.754	.713	.014	-.207	.541
Cephalic index	-.640	.034	.107	.754	/	/	-.410	.210	.286	.394
Cranial capacity	.836	**.001**	.713	.014	-.410	.210	/	/	-.615	.044
Geologic age	-.341	.305	-.207	.541	.286	.394	-.615	.044	/	/

The study undertaken in Chapter Seven was aided by having specimens from the same restricted time period. Unfortunately, it is not possible to identify a dichotomy as clear as this in the fossil populations, as the regressions above show very few significant results. However, while these results rule out any within-group patterns of morphology that might identify a fossil as belonging to a particular population, it is possible that cranial shape varies sufficiently between regions to separate these four main groups. Thus, the cranial measurements between regional groups are tested for significance. Ordinarily, a number of *t*-tests would be carried out between regions for cranial capacity, cranial length and breadth and cephalic index. However, in order for *t*-tests to be reliable, they require group sizes bigger than those available here. They also carry with them the problems of Type I (the rejection of a true null hypothesis) and Type II (the acceptance of a false null hypothesis) errors, made all the more likely by small sample sizes (Sokal and Rohlf 1995: 158-9). Although the Bonferroni correction has been used to negate this as far as possible, analysis of variance (ANOVA) with Tukey's post hoc tests is applied instead (with the proviso that cephalic index, as noted above, is not independent). An ANOVA can be used to

test differences among two or more sample means and its generality is therefore more useful in this case.

The Chinese group has an outlier (Hexian) that may affect measures of difference, so each test including this region will be repeated with the outlier removed. Beginning with the full complement of fossils, it was apparent that cephalic index does not vary significantly between the regions (Table 8.7). While this might imply that the proportions of cranial length and width have remained stable in the species no matter the region, cranial width and cranial capacity nevertheless exhibit significant differences. It is also noted that the sum of squares and mean squares values indicate far more variation in cephalic index within the groups, than between groups.

Table 8.10 One-way ANOVA results for the cranial dimensions of the four *H. erectus* regions

		Sum of squares	df	F	Sig.
Glabella-inion	Between groups Within groups Total	2240.353 2859.325 5099.678	3 21 24	5.485	.006
Bi-parietal width	Between groups Within groups Total	1626.781 1095.679 2722.460	3 21 24	10.393	.000
Cranial capacity	Between groups Within groups Total	393489.5 332912.3 726401.8	3 21 24	8.274	.001
Cephalic index	Between groups Within groups Total	24.863 539.557 564.420	3 21 24	.323	.809

The post hoc tests indicate that Europe is ultimately responsible for the significant results: $p = 0.001$ for cranial capacity when compared to Indonesia; for bi-parietal width, the Dmanisi crania were significantly different from those of Africa, China and Indonesia ($p = 0.002$, 0.001 and <0.000 respectively). These figures must be treated with some caution, since a test of homogeneity (an assumption of ANOVA) suggested that unequal group sizes increases the risk of Type I errors. In effect, this

makes it unwise to reject the null hypothesis that there are no significant differences between the regions, although the Bonferroni-lowered *p*-value helps ensure the validity of the results.

When Hexian was removed from the cohort (Figure 8.8), significant differences were seen in three of the four cranial variables. The post-hoc results show that these have been generated by strong intra-group similarities in the Zhoukoudian fossils and Indonesia compared to the Dmanisi crania, which must also be morphologically like one another (as Table 8.11 also indicates). The same was not true for Africa, which contains too much variation to produce an equivalent result, although this region did differ significantly from Europe in bi-parietal width.

Table 8.11 One-way ANOVA results for the cranial dimensions of *H. erectus*, excluding Hexian

		Sum of squares	df	F	Sig.
Glabella-inion	Between groups Within groups Total	2249.573 2850.077 5099.650	3 20 23	5.262	0.008
Bi-parietal breadth	Between groups Within groups Total	1562.580 653.879 2216.458	3 20 23	15.931	0.000
Cranial capacity	Between groups Within groups Total	390268.8 332551.1 722819.8	3 20 23	7.824	0.001
Cephalic index	Between groups Within groups Total	38.056 391.221 429.278	3 20 23	0.649	0.593

These analyses suggest limited but strong regional morphology for selected fossils that may be linked to genetic isolation. Kidder and Durband (2004) focussed on the uniqueness of the Zhoukoudian fossils' morphology, specifically skulls III, V, X, XI and XII, compared to a *H. erectus* sample (consisting of Hexian, ER 3733, ER 3883, OH 9, Ngandong 1, 6, 7, 11 and 12, Sangiran 2 and 17, Sambungmacan 1, 3 and 4, and a new *Pithecanthropus* skull from Sangiran, Tjg-1993.05). Similar to my own study, Kidder and Durband distinguished Hexian from the Zhoukoudian skulls,

instead relating it to the examples from Africa and Indonesia (Kidder and Durband 2004: 13).

The selected Chinese skulls have a large biauricular breadth but relatively smaller frontal and biasterionic breadths (Kidder and Durband 2004: 13). While this study agrees that the Zhoukoudian specimens are a p-deme of *H. erectus* and have a similar cranial shape (cranial length varies by 7mm, bi-parietal breadth by 4mm; cephalic index and cranial ratio are similarly close in value), the tests carried out thus far have not established the separation of this group of fossils to the exclusion of the rest of the sample. Figures 8.4 and 8.5 show Hexian as distinct from the Zhoukoudian sample through variation in cranial morphology, although the group as a whole remains firmly within the *erectine* trend.

Kidder and Durband's sample size was roughly equivalent to that of this study, so a larger number of variables might be beneficial. To account for this, and to test the strength of Kidder and Durband's results, two further measurements were selected for the current analysis, based on those most available for a wide range of specimens: minimum frontal breadth and biasterionic breadth. Asterion is located on the side of the skull where the lambdoid, paretomastoid and occipitomastoid sutures meet, making biasterionic breadth a measure of the width of the back of the head. In total 22 specimens were collated, including three examples of *A. boisei* from Koobi Fora (ER 406, 407 and 732) as a comparison, since these would be expected to separate from the *H. erectus* sample. The remaining fossils used were ER 3733 and 3883; OH 9; Sangiran 2, 4, 10, 12 and 17; Trinil; Sambungmacan 1 and 3; D2700, D2280 and D2282; and Zhoukoudian X, XI and XII (Wood 1991; Ascenzi et al 2000; Marquez et al 2001; Vekua et al 2002). The two new measurements are regressed in Figure 8.6.

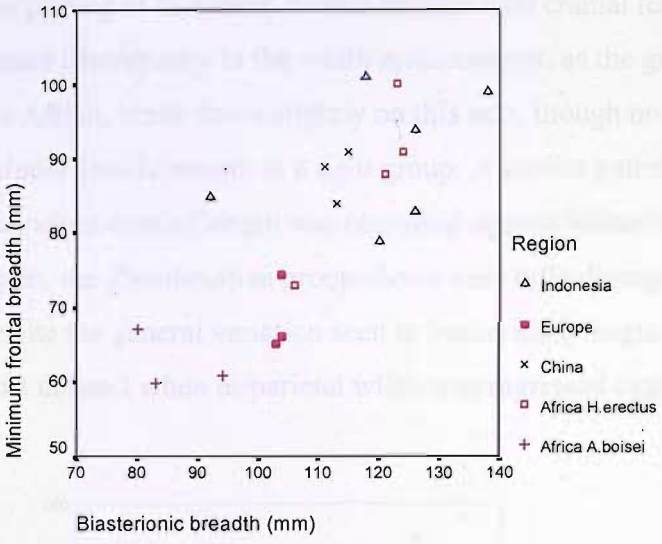

Figure 8.6 The relationship between biasterionic breadth and minimum frontal breadth in a sample of *A. boisei* and *H. erectus*

While this regression does not repeat Kidder and Durband's morphological isolation of China (2004), this region, as well as Europe and, to some extent Africa, form clearly defined groupings. Indonesia presents a wide spread of points when compared to these much tighter scatters. As expected, the *A. boisei* specimens are also differentiated, forming a distinct group.

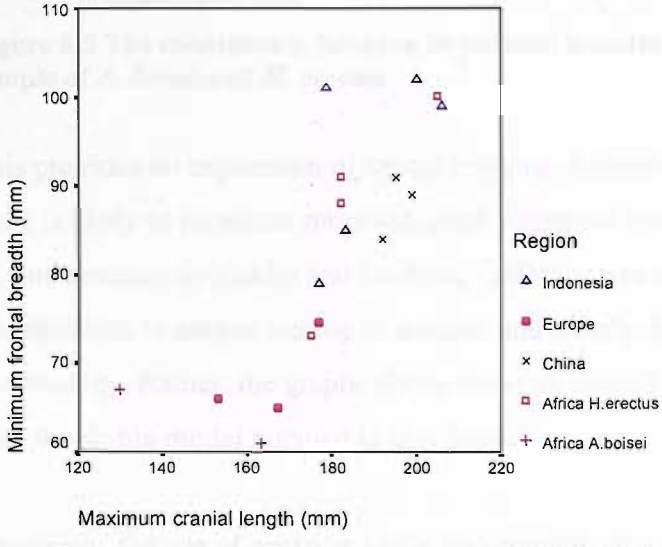

Figure 8.7 The relationship between cranial length and minimum frontal breadth in a sample of *A. boisei* and *H. erectus*

The pairing of minimum frontal breadth with cranial length in Figure 8.7 suggests greater discrepancy in the width measurement, as the groups, most notably Indonesia and Africa, break down slightly on this axis, though not along the *x* axis. The Chinese fossils remain in a tight group. A similar pattern to that in Figure 8.7 was seen when cranial length was regressed against biasterionic length (Figure 8.8). Again, the Zhoukoudian group shows very little divergence in either measurement, despite the general variation seen in biasterionic length. Regional groupings were most defined when bi-parietal width was regressed against biasterionic width.

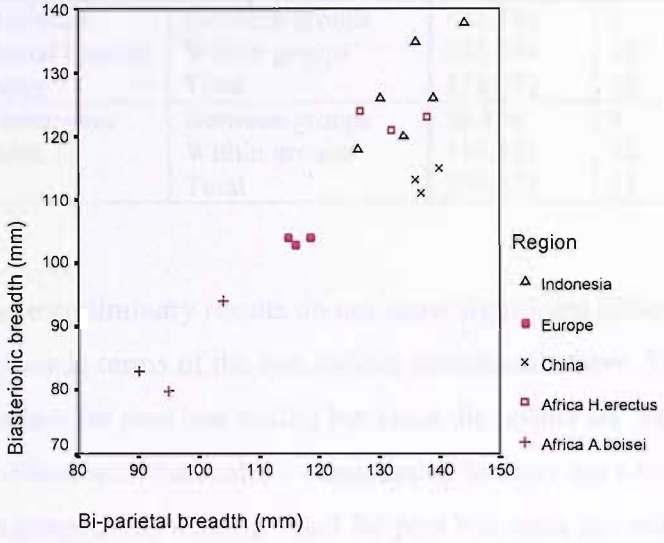

Figure 8.8 The relationship between bi-parietal breadth and biasterionic breadth in a sample of *A. boisei* and *H. erectus*

This provides an expression of strong regional differentiation in *H. erectus*, although there is likely to be robust morphological constraint between the two variables. Even so, and contrary to Kidder and Durband (2004), it has not been demonstrated that Zhoukoudian is unique among *H. erectus* and clearly discriminated by its cranial morphology. Rather, the graphs above show an overall regional variability, in line with the demic model pursued in this thesis.

Previously, the use of cephalic index was considered to be a useful method for comparison, since it is proportional rather than absolute. A gross increase in size does not inform the nature of the increase. For this reason, two indices were created

relating the additional width measurements of minimum frontal breadth and biasterionic breadth, in the same way that cephalic index is derived, in order to allow an analysis of variance between the regions in the relationships of these dimensions.

[minimum frontal breadth x 100] / glabella-inion length

[biasterionic breadth x 100] / glabella-inion length

Table 8.12 One-way ANOVA results for two new cranial indices in *H. erectus*

		Sum of squares	Df	F	Sig.
Minimum frontal breadth index	Between groups	132.884	4	1.642	.228
	Within groups	242.794	12		
	Total	375.679	16		
Biasterionic index	Between groups	78.806	4	.678	.621
	Within groups	319.631	11		
	Total	398.437	15		

These preliminary results do not show significant differences between the four regions in terms of the two indices introduced above. The sample size is too reduced to allow for post hoc testing but since the results are insignificant this is not a problem, and also make it unnecessary to carry out *t*-tests between paired regions (if the sample size was too small for post hoc tests, the reliability of *t*-tests would be prohibitively low).

A proportional comparison of the measurements of minimum frontal breadth and biasterionic breadth has shown that, while the argument for regional variation is not undermined, these data do not support the idea that China is morphologically isolated to the extent proposed by Kidder and Durband (2004). Although China did display some distance from Africa and Europe, it is not known for certain whether this is due to geographical isolation and genetic drift, although this seems likely. The pattern of significance was not repeated for cephalic index, derived from bi-parietal width, and so any change in morphology is necessarily limited in its scope.

The question of regional separation can be further addressed through discriminant function analysis, whereby a new variable, *Z*, is a linear function of two or more existing variables (such as cranial dimensions) and is defined in such a way that members of one population will have high values for *Z* and members of the other will have low values (Sokal and Rohlf 1995: 678-9). By using the variables of cranial length, cranial width, cephalic index and cranial capacity, and calculating *Z*, it should be possible to differentiate between regions. This section of the analysis involves all the specimens originally selected for study, and listed in Table 8.1 above (NB independents were entered together, rather than stepwise).

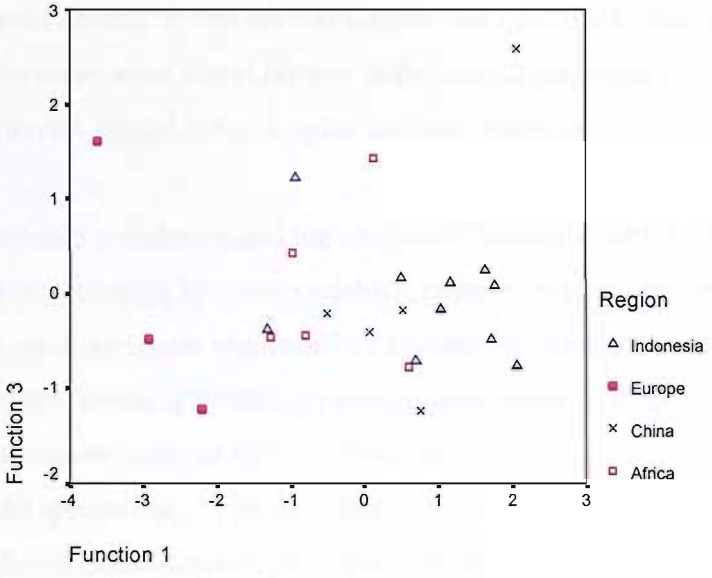

Figure 8.9 Discriminant function analysis of the four regions of *H. erectus*, using four cranial variables

In Figure 8.9, function 1, which accounts for 89.4% of variance, is controlled mainly by cranial length (with a coefficient of 0.919). Although function 2 accounted for 10.3% of variance, it too was weakly controlled by cranial length (0.135). Function 3 was therefore used for the regression instead, since cephalic index produced a correlation coefficient of 0.793. This variable is calculated from two others, but it nonetheless illustrates the proportional relationship between them. China and Indonesia are seen to cluster into regional groups and are also close to each other, but it is still possible to discern some distance between the regions. The three

Dmanisi crania do not, on this occasion, display morphological unity and show an even greater scatter than Africa, but Asian *H. erectus* seems to group together well. This might be an indication of a geographically isolated gene pool that developed independently from the western hemisphere, or perhaps Africa alone, which has displayed great variation in the dimensions of the crania in many of the tests above.

Cranial variation and latitude

The final part of this investigation set out to determine significant differences in cranial morphology between the 'temperate' zone crania and the 'tropical' ones. The above results indicate that no such differences would be found, and this supposition proved correct. When the full sample was compared using ANOVA, no significant differences were found for any of the cranial variables, including cephalic index, minimum frontal breadth index and biasterionic index.

Pearson's correlation and the analysis of variance, which both assess the strength of the relationships between variables, failed to uncover any patterns in *H. erectus* morphology across regions or by climate. An alternative strategy, introduced in Chapter Seven, is to look at covariation between variables using principal components analysis (PCA). Since circumference is not widely available for the fossil specimens, the proportional measure of cephalic index is used to compare the different populations of *H. erectus*. Additional variables used were cranial length, cranial width and cranial capacity. These four variables were tested according to each region individually, and then subdivided as 'tropical' and 'temperate', and 'east' and 'west.' The results of the first section of the test are displayed below in Table 8.13.

Table 8.13 Results of the Principal Components analysis by region

	Component	Variable	% Variance	Eigenvalue
Africa	1	Cephalic index	56.841	0.887
	2	Cranial length	37.953	0.859
China	1	Cephalic index	59.196	0.863
	2	Cranial capacity	39.321	0.717
Indonesia	1	Cranial length	67.412	0.969
	2	Cephalic index	28.343	0.902
Europe	1	Cranial length	96.402	0.992
	2	N/A	N/A	N/A

The relationship between cranial length and breadth has not remained constant in the African line; the high degree of variance accounted for by cranial length may explain this. A similar pattern is evident in China, when variation in cephalic index is seen in association with variation in cranial capacity. Indonesia shows the opposite pattern, with variation in cranial length creating some unpredictability in cranial form. For Europe, only one component was produced, for cranial length, as sample size was too small to allow for the extraction of a second component.

The regions were next condensed into two pairs, based on climate (latitude) and hemisphere. Table 8.14 looks first at the climate dichotomy, comparing tropical Indonesia and Africa against temperate Europe and China. The results suggest a split between the subsets based on size and shape, with high variance in capacity for the tropical group and variation in width for the temperate sample. It seems that the high variation in cephalic index for the Chinese population has affected the temperate zone's outcome.

Table 8.14 Results of Principal Components analysis by climate

	Component	Variable	% Variance	Eigenvalue
Tropical	1	Cranial capacity	59.919	0.934
	2	Cephalic index	36.089	0.998
Temperate	1	Cranial width	60.966	0.936
	2	Cephalic index	33.475	0.955

For the hemispheric division of east and west (China and Indonesia, and Africa and Europe respectively), the Indonesian sample had a powerful influence over the extraction, showing equivalent results (Table 8.15) to those for this region alone. The variation in bi-parietal width has had an impact on both the temperate and the western extraction but it is not known whether this is due to the variance in cephalic index seen in China and Africa.

Table 8.15 Results of Principal Components analysis by hemisphere

	Component	Variable	% Variance	Eigenvalue
East	1	Cranial length	55.862	0.939
	2	Cephalic index	38.668	0.980
West	1	Cranial width	63.407	0.917
	2	Cephalic index	33.061	0.972

Although there is much variation in cranial shape, the wide time span and disparate nature of the fossils make it difficult to draw definite conclusions. The solution here is to base the comparisons on geologic age, rather than region, using the Zhoukoudian *erectus* sample and *Homo* from Spain, both of a similar Middle Pleistocene age. If there are no distinct differences in cranial morphology between the two populations (noting that the Chinese crania, with the exception of Hexian, have tended to cluster on the scatter plots), it will imply localised short-term variation in response to the environment. Significant separation between Chinese *H. erectus* and post–*erectus* European *Homo* will point alternatively to genetic drift over evolutionary time. The problem of small sample sizes remains, so once more ANOVA is the method of analysis.

Atapuerca and the time scale of variation

Pearson's correlations were applied to the four cranial dimensions of length, breadth, height and capacity for the three crania combined, as well as the additional indices used previously: cranial index [length/height] and cephalic index [(breadth x 100)/length]. None of these variables correlated significantly with each other for the three Spanish fossils, indicating that the Atapuerca crania differ greatly from each other. With the inclusion of the Zhoukoudian crania, additional significant correlations would indicate either a merging in the morphology of the two sets of crania, or overwhelming uniformity in the Chinese fossils.

Zhoukoudian was first tested alone but did not present any significant correlations. Fewer variables were available for analysis in the Chinese group compared to Atapuerca (cranial height, and thus the cranial index, were unavailable), but otherwise there are no major differences between the regions. Similarly, the merging of the two groups did not change the pattern of results (Table 8.16).

Table 8.16 Correlation coefficients (*r*) and significance (*p*) for five cranial dimensions in Zhoukoudian *H. erectus* and Atapuerca *Homo* (n = 7)

	Cranial length		Bi-parietal width		Cranial capacity		Cephalic index	
	r	*p*	*r*	*p*	*r*	*p*	*r*	*p*
Cranial length	/	/	.504	.249	.477	.279	.059	.900
Bi-parietal width	.504	.249	/	/	.705	.077	.891	.007
Cranial capacity	.477	.279	.705	.077	/	/	.568	.184
Cephalic index	.659	.900	.891	.007	.568	.184	/	/

However, a separation between Atapuerca and China is apparent when cranial length and width are regressed against each other. There is a distinct gap between the two groups (Figure 8.10), since the Chinese skulls are long and narrow, whereas the Atapuerca population show a reduced length but greater width. There is also a difference in the pattern of distribution, with the Spanish skulls showing a wide scatter compared to the relatively tight cluster of the Chinese fossils.

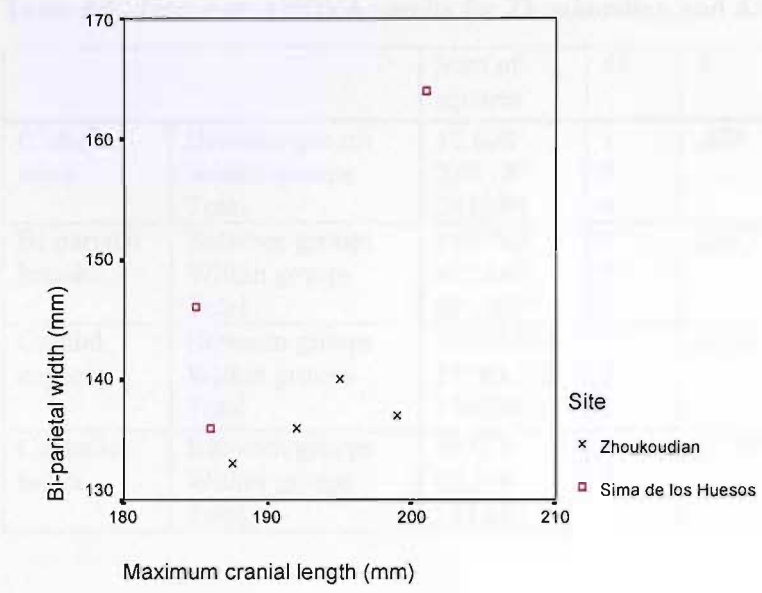

Figure 8.10: The relationship between cranial length and width in a sample of Chinese and Spanish hominins

On the evidence available here, only the Zhoukoudian results suggest an isolated biological population with relatively restricted gene flow. However, there are only three Atapuerca crania available and so it cannot be determined whether these fossils represented a population with greater access to and movement between other populations, or whether this particular lineage simply expressed greater phylogenetic variation than the *H. erectus* p-demes.

Using one-way ANOVA, further comparisons in cranial morphology were made between the Sima de los Huesos sample and Zhoukoudian (Table 8.17). The use of just two groups meant that it was not possible to conduct additional post-hoc tests. However, despite the variation in cranial morphology between the Chinese and Spanish groups, it is not enough to generate significant differences between them, due to excessive variation within each population, and so the post-hoc tests were not necessary. As with the four original regions studies in this chapter, sample sizes are too small to permit sufficient analysis on the relationship between region and morphology.

Table 8.17 One-way ANOVA results for Zhoukoudian and Atapuerca

		Sum of squares	df	F	Sig.
Glabella-inion	Between groups Within groups Total	12.808 230.187 242.994	1 5 6	.278	.620
Bi-parietal breadth	Between groups Within groups Total	253.762 427.667 681.429	1 5 6	2.967	.146
Cranial capacity	Between groups Within groups Total	74190.630 85593.332 159784.0	1 5 6	4.334	.092
Cephalic index	Between groups Within groups Total	91.015 42.189 133.203	1 5 6	10.787	.022

Discussion

In Chapter One, it was hypothesised that variation in cranial morphology may have an environmental basis (Hypothesis 5), but it is likely that the influence of genetic drift and demic isolation is greater (Hypothesis 6). Following this second hypothesis, it was thus expected that the four regions of Africa, China, Indonesia and Europe would exhibit distinct cranial morphologies to a greater degree than that possible in the modern human populations of Redcross and Chelsea in Chapter Seven. The proportional measure of the cephalic index was used to look for a significant difference in cranial length, a correlate of stature, which in turn can be a relative marker of nutritional (and thus environmental) status. Any difference was predicted to have a life historical context, in that favourable environmental conditions would have lower juvenile mortality and select for encephalisation.

Chapter One anticipated this by dividing the *H. erectus* p-demes into a core and a periphery, whereby lower risk of juvenile mortality and selection for encephalisation is expected in the core. In contrast, the periphery is recognised by higher juvenile mortality and stasis in cranial capacity due to being at the extremes of tolerance of the species. This was explored using latitude as a proxy for environment, on the

basis that the fluctuations in temperature, solar radiation and rainfall in temperate climates create an unpredictable and potentially unstable habitat.

Several statistical tests were carried out on the cranial variables in *H. erectus* in order to differentiate the core and the periphery. Regressions indicated strong trends within regions, notably Indonesia and Europe, and also China when Hexian was removed from the group (for example Figures 8.3 and 8.4), and it could be that morphological variation is relatively constrained in these regions, perhaps as a result of geographic isolation. This does not seem to be true for Africa, which displays too much diversity in morphology for the specimens of this continent to be considered a discrete genetic group. The collection of fossils from Atapuerca represented a population closer in age to the Zhoukoudian group, and with a similar degree of juvenile mortality. However, unlike the Chinese sample, there was no equivalence in cranial morphology within the group (whilst clearly showing an overall change in size and length:breadth ratio), although sample sizes were too small for this to be concluded for certain.

The cranial data from *H. erectus* will now be placed into a context of evolutionary ecology, linking the traits of juvenile mortality and encephalisation, examined in previous chapters, with variation in the environment. Hypothesis five, that *H. erectus* was a well-adapted species, might not be accepted for all four regions, since survivorship and the rate of increase of brain size varies. In spite of this, *H. erectus* appears to have maintained a long-term presence even under these circumstances, and so it must be concluded that the species was adaptable to a range of environmental conditions; an adaptation achieved through variation in the rate of encephalisation.

Having proposed in Chapter One the correlating characteristics that account for the variation in *H. erectus* morphology, on the basis of latitude, it was expected that Europe and China would follow the pattern of the periphery, while Africa and Indonesia would display the traits expected of the core. However, the results of this

chapter show that such a straightforward division is not possible. Indonesia and China both show a strong relationship between cranial length and cranial capacity (Figure 8.3), which suggests a commonality in morphology separate from that in Africa and Europe. Further regressions indicate that biological populations (notably Dmanisi and Zhoukoudian) form clusters, more so than on a regional level. This might be a sign of genetic isolation rather than climatic influence, supporting hypothesis six. The discriminant function and principal components analyses also failed to highlight morphological separation either between tropical and temperate or between east and west. In a comparison between Zhoukoudian and Atapuerca, sites of similar age, the populations did appear to be separated, with the Chinese group clustering much more tightly, but differences in the relationship between length and breadth suggest that this likely to be a result of long-term evolutionary changes in morphology.

An understanding of regional variation in cranial morphology has thus far relied upon a climatic division between the core and periphery p-demes of *H. erectus*, but these results have failed to support such a division. The *H. erectus* demes are generally regionally defined in their cranial morphology, but this alone cannot differentiate them on the basis of environmental fitness. It is clear from the work of earlier chapters that life history varied in the species on a regional basis, and this seems likely to be due to variation in adaptation through genetic isolation. The movement of *H. erectus* through time and space gave rise to the cladistic splitting of the lineage into regional demes, each of which adapted its life history strategy to that particular environment.

The core-periphery model requires that one of more of these demes is less well adapted, and thus could not 'afford' to select for encephalisation, for example, which does not necessarily have to be the case. The centre-edge model holds that fitness and behaviour varies according to spatial position in a group, with the centre experiencing higher fitness due to lower energy costs of territory defence, which can then be invested in growth and reproduction (Meadows 2001; although evidence for

centre abundance is sparse [Sagarin and Gaines 2002: 144]). It is tempting to apply this to the smaller brained Dmanisi crania, or to the wide variation in African cranial capacity. However, the territorial distribution of *H. erectus* is too great to allow one area to be the 'centre' and the remainder the 'edge'. In a more narrow focus on the regions themselves, the impetus for the initial dispersal of *H. erectus* out of Africa is thought to have been generated by an increase in home range size, body size, and improved dietary quality (Antón et al 2002). The first of these factors in particular may have created the potential for a centre-edge fitness structure within each region, but the fossil record at present is not fine-grained enough to discern this.

The biogeographic model that frames this research thus posits a number of adaptive dichotomies to explain spatially-determined life history variation in a species. This approach has proved to be a useful tool in mapping the behavioural and ecological flexibility of the *H. erectus* p-demes, as a way of accessing the life history strategy of this species. Although it has not been possible to convincingly and consistently demonstrate that the cranial morphology of *H. erectus* varied according to climate, the regions do show the potential for wide disparity in life history strategy, and a degree of genetic isolation, supporting hypotheses four and six. It is clear that the species was flexible in its approach, and was able to survive in a range of habitats through the modification of life history.

CHAPTER NINE

Conclusion

In this thesis, I have examined the evolutionary ecology of *Homo erectus* within a demic framework. My research was designed to contextualise the life history strategy of *H. erectus* through its relationship to environmental variation by investigating each trait as a separate study, but linking them through their common ecological context and impact upon each other. Overall, I found that there was not stasis in *H. erectus*, but rather that it was a divergent lineage, regionally divided into subspecific demes that have resulted in an inherently adaptable species, able to cope with a range of environments through the modification of life history strategy (as evidenced by the variation in encephalisation rate and differences in juvenile mortality). This is shown in the regional variations of the species, which are most likely to be the result of genetic drift and isolation. However, I have proposed that this is also a product, in part, of differential adaptation to varying environments, demonstrating the flexibility of *H. erectus* life history strategy, particularly with regards to encephalisation and its relationship to juvenile mortality and reproduction. The debate over the differences between classically defined *H. erectus* and *H. ergaster* is, therefore, answered by looking at the separate demes as the products of regional genetic isolation or localised adaptation, resulting in morphological changes.

Chapters Two and Three provided the theoretical basis for the investigation, establishing the principle of paleo-demes and regional specialisation (defined and summarised in Table 2.1). This was complemented by an analysis of the relationships between life history traits, which are generally expressed in terms of the *r-K* dichotomy (MacArthur and Wilson 1967), set up as polarities encompassing patterns of survivorship, body size and reproductive schedules, and by Charnov's trade-offs between birth, growth and death (Charnov 1991, 1997, 2001). In addition, I introduced the concept of reaction norms as a way of identifying instability in growth and development. I hypothesised (in Chapter One's hypothesis three) that *H.*

erectus would display variation in patterns of brain size and juvenile mortality in each of the species' p-demes across a broad dichotomy of core and periphery, influenced overall by environment (measured as latitude).

The following two chapters, dealing with age-specific mortality and encephalisation respectively, contributed to this aim by relating these complementary factors to regional ecology. Chapter Four concluded that *H. erectus* generally experienced a low mortality rate during the juvenile period compared to earlier hominin species, despite a potential infant mortality rate of 50% (by reference to modern hunter-gatherer populations). Due to the restrictions of sample size, these results are applied to the species as a whole, rather than to individual regions.

A more focused understanding of regional (or demic) variation is gained when the patterns of survivorship for the species (for example, Table 8.1 suggests a disparity between Indonesia and Africa, and China and Europe) are related to encephalisation, as an increase in brain size also impacts upon somatic growth rates and the scheduling of energetic resources, which vary at different stages of life. Looking at all available specimens of *H. erectus*, the evidence favoured a trend in increasing cranial capacity over evolutionary time, with a regression producing an R^2 value of 0.51. Dividing the dataset into regional sub-groups brought problems of decreased sample size, which made interpretation of the regressions difficult. Nevertheless, it was possible to identify a tendency to cluster in certain regions, particularly Europe and China, and even more so when the four regions are broken down into their constituent demes. These results are important in showing that brain size and the rate of encephalisation may not necessarily have been an over-arching evolutionary trend, but instead may be more a product of local adaptation and variation in life history strategy.

Reproductive strategy would also vary by region if, as I propose, the rate of brain size increase was not uniform. This is closely related to resource distribution, which although cannot be considered a variable, is certainly a driver for adaptation. As

such, the energetic costs of encephalisation were considered in Chapter Six. A comparison of the relative brain and body size for three estimated African *H. erectus* individuals placed these examples within the confidence intervals for a series of primate trends, and so it is unlikely that this region required a move to secondary altriciality, as seen in modern humans to cope with the energetic demands of an enlarged brain. However, since I noted in Chapter Five that encephalisation might have been selected for in the Indonesian p-demes, life history strategy would have been modified to account for a population with a brain bigger than expected for body size. In this way, it is possible that both encephalisation and the timing of growth varied on a regional basis, thus reinforcing the idea of the adaptability of *H. erectus* according to the environment.

The effect of the environment is a vital factor in human evolution, since I have shown that the rate of brain increase was not uniform in *H. erectus*, implying that connected traits were not uniform either. However, the sample size available for *H. erectus* was far too small and incomplete to allow for a conclusive examination of this question. Instead, I decided to assess the role of the environment in two modern human populations, where sample size and conditions of growth could be controlled with more certainty; the findings of this study, and its comparison to the fossil material, provide the final elements of the thesis.

Chapter Seven examined the relationship between cranial morphology and the environment. Developmental instability was shown in the deprived population of Redcross through asymmetries in the widths of the orbits and the first mandibular molar, separating the members of this population from the more advantaged group of Chelsea. This population also had a (non-significantly) larger mean cranial size than the poorer group, although it could not be shown whether cranial shape also varied at a population level. I suggested that the predominance of genetics obscured the influence of the environment in two very closely related populations. Thus, a link between shape and the environment was not supported by these data, but the

study did open up the possibility that greater genetic distance in the *H. erectus* p-demes would allow for the recognition of ecologically defined traits.

The lack of an established correlation between morphology and environment hampered an equivalent study in *H. erectus*, and so Chapter Eight concentrated on the identification of population-specific traits that might inform the encephalisation study in Chapter Five, and provide a morphological dimension to life history variation. This idea of a regional morphology was corroborated by a series of regressions that revealed distinct clusters of specimens, most notably those from purported biological populations (Zhoukoudian and Dmanisi). In contrast, the African representatives bore little resemblance to each other in cranial morphology, possibly because these fossils did not form a single population or come from the same area, or because they were not the only hominin species on the continent at that time (although this is by no means a certain proposition and remains hypothetical).

These results link back to Chapter One, where I hypothesised that the environmental adaptations of *H. erectus* would divide the species into a core and a periphery (hypothesis three). A genetic component can be added to the life history characteristics listed in Table 1.1, in that the core should have greater genetic variation as a result of constancy and within-population diversity. This is contrasted with the periphery, which, in addition to its adverse effects on encephalisation, juvenile mortality and growth, would also (I hypothesise) experience local population extinction, genetic isolation and founder effects, creating greater between-population diversity.

This model is applied to Indonesia, the evidence for which suggests that this region was a core environment for the species. There was selection for encephalisation in this population, and an apparent low juvenile mortality, indicating a successful change in life history profile to secondarily altricial, slow-growing offspring. The increase in brain size alone reflects the long-term stability of the group, and taking

the time scale of habitation into account it is concluded that the Indonesian populations comprise the core of the species.

Africa was the second tropical region, hypothesised to form the second half of the *H. erectus* core, although it has not been shown to behave like a core region. The evidence in favour of this designation was compromised by the small cranial capacities of the individuals of this region. Moreover, the wide diversity of cranial morphology could either have been due to genetic variation as part of the core model, or a symptom of a number of local, isolated populations. This also makes it difficult to accept the apparent low juvenile mortality as evidence in support of the core hypothesis. Africa is a good example in demonstrating the weaknesses of the model, in that it relies on clear demic division in order to identify the life history strategy of a population, rather than the life history possibilities of the species as a whole.

The Zhoukoudian and Dmanisi populations share a tendency to cluster on regression lines, indicating close similarities in cranial morphology that might be evidence for the genetic isolation of these periphery groups. Both exhibited comparatively higher juvenile mortality than Indonesia and Africa, and there was no evidence for a trend of increasing brain size over time. These traits mark out China and Dmanisi as periphery regions, following a life history strategy of stasis and faster growth as a way of countering higher juvenile mortality in an unpredictable, temperate environment. However, the analyses of this thesis emphasise that these are isolated populations close in space and time, and so it is not clear whether these results are due to regional adaptation or to genetic drift.

This work has allowed for the development of a new model to explain variation in *H. erectus* according to time and space. Figure 9.1 presents the model findings of the thesis by relating morphological and life historical variation to regional groupings. This diagram incorporates the main aspects of life history that have been examined in this thesis, and places each deme along a spectrum of latitude and growth

conditions. It is proposed that the p-demes in the centre of the diagram, at the tropical Equator, will experience the optimum conditions for growth, following a *K*-selected reproductive type and with encephalisation selected for. This thesis most clearly identifies Indonesia as belonging to this area of the model. Moving away from the Equator and towards the outer latitudes, the environment becomes less predictable and more suited to a beg-hedging strategy of reproduction. Under these conditions encephalisation is not selected for. These peripheral p-demes thus adapt their life history strategy to a more unstable environment, and are exemplified in this thesis by the genetically isolated Dmanisi and Zhoukoudian populations. This work has show the core-periphery model to be a useful way to divide up space and consider aspects of biogeography in relation to life history, without necessarily assuming that one p-deme will be less well adapted than another.

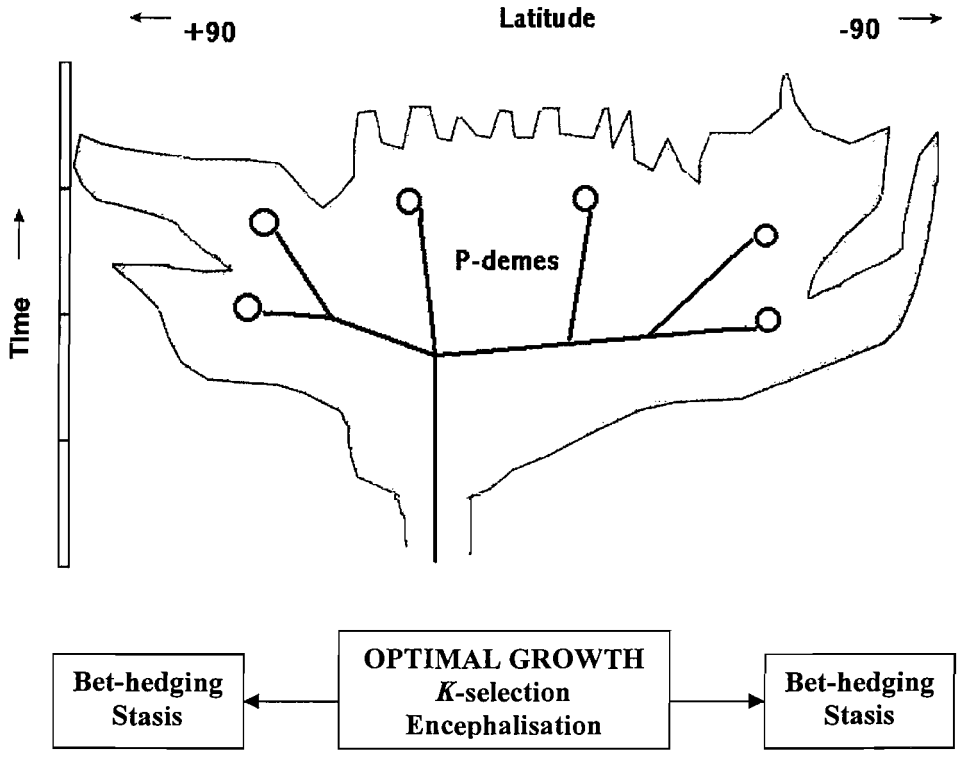

Figure 9.1 Biogeographic model for life history variation in the *H. erectus* p-demes (adapted from Foley 1999, with additions)

While my approach to the evolutionary ecology of *H. erectus* has gone some way towards reconstructing the variation in life history strategy in this species, my research into the effect of latitude and environment richness on cranial morphology indicates that there is much more to be said. If fluctuating asymmetry does represent a deviation from allometry, then pairings in the skull, such as the parietal bones, might also generate a form of asymmetry. This might be further pursued in order to compensate for the lack of intact orbits and paired molars in *H. erectus* and other hominin species, as a route to assess the developmental stability of a population. Moreover, this could be applied to modern human populations at different degrees of latitude, in order to provide a greater understanding of the impact of the environment on growth and mortality throughout life, in archaeological as well as living populations.

The integrated approach to the study of life history evolution pursued in this thesis offers a more developed understanding of the relationship between an organism and its environment, and has wide potential for application. The core-periphery model for life history variation developed here should be tested against other species with wide regional distribution, examining their maturation rates, mortality profile and the level of environmental stress encountered. Moreover, these do not have to be the only categories of data included. Hopwood (2003) relates variation in environment and regional isolation to lithic style and production, as he demonstrates a higher degree and rate of behavioural change, combined with closer group networking, in Africa. In comparison, similar changes in China are never as drastic, positioning these two regions during the early to mid-Pleistocene within a core-periphery setting. Hopwood argues that the more intensive resource competition in Africa, due to the presence of large predators and the co-existence of up to three hominin species in the region, was responsible for forcing *H. erectus* to find more efficient ways of exploiting resources. The integration of this behavioural aspect into the biogeography of a species can only strengthen the model overall.

This study has, therefore, contributed to existing work on the life history and evolutionary ecology of *H. erectus* in a number of ways. These results, and their placement in the context of the model, indicate that evolutionary change in the species was driven by genetic factors and shaped by the environment. *H. erectus* exhibited a long-term trend of an increasing cranial capacity, but this was not uniform across the species and had varying success, with subsequent energetic stress in the young resulting in high juvenile mortality in some areas. Although this could be less to do with the environment of habitation than the relative isolation of the population groups, the results of this investigation suggest that propagation of the species was most successful in conditions of stability, but nevertheless *H. erectus* was able to adapt to unstable conditions in order to survive. In conclusion, it is clear that *H. erectus* was an adaptable and flexible species that had a number of strategies available to maximise survival in a range of environmental conditions.

APPENDIX I

Catalogue of *H. erectus* finds and dates used

CHINA

Site	Cat. Number	Sex, age	Cc *	Geologic age (kyr)	Testing method	Dating reference
Hexian	PA 830	M, ad.	1025	240-280	OIS 8 (fauna)	Day 1986
Gongwangling	PA 1051-6	F, 30-40 yrs	780	1150	O_2 isotope	An et al 1990
Zhoukoudian	PA 21,78	M, ad.	-	292 ± 26 299 ± 55	TL Fission track	Pei (1985) Guo et al (1991)
	PA 17	Ad.	1030	578	ESR deer teeth	Huang et al (1991)
	PA 16	M, juv 16	915	578	ESR deer teeth	Huang et al (1991)
	PA 23	M, juv 16	-	370-400	Palaeomagnetism	Qian et al (1985)
	PA 74, 86, 109	M, ad. (old)	1140	282	ESR	Huang et al (1991)
	PA 90-93	F, ad.	850	>400 418	Uranium series ESR deer teeth	Xia 1982 Huang et al (1991)
	PA 326	M, juv 7	-	418	ESR deer teeth	Huang et al (1991)
	PA 95	?F, inf<3	-	418	ESR deer teeth	Huang et al (1991)
	PA 315	M, juv 6	-	418	ESR deer teeth	Huang et al (1991)
	PA 98	M, ad.	1225	418	ESR deer teeth	Huang et al (1991)
	PA 99	F, ad.	1015	418	ESR deer teeth	Huang et al (1991)
	PA 100	M, ad.	1030	418	ESR deer teeth	Huang et al (1991)

INDONESIA

Site	Cat. Number	Sex, age	Cc	Geologic age (kyr)	Testing method	Dating reference
Ngandong	1	Ad.	1172	40	ESR	Swisher et al (1996)
	2	Juv. 9	-	40	ESR	Swisher et al (1996)
	3	Ad.	-	40	ESR	Swisher et al (1996)
	5	Ad.	-	40	ESR	Swisher et al (1996)
	6	Ad.	1251	40	ESR	Swisher et al (1996)
	8	Juv. 16	-	40	ESR	Swisher et al (1996)
	9	Ad.	1135	40	ESR	Swisher et al (1996)
	11	Ad.	1231	40	ESR	Swisher et al (1996)
	12	Ad.	1090	40	ESR	Swisher et al (1996)
Sambungmachan	1	Ad.	1035	~40	ESR	Swisher et al (1996)
	3	F, ad.	890	~40	ESR	Swisher et al (1996)
Sangiran	2	Ad.	813	1100	$^{40}Ar/^{39}Ar$	Larick et al (2001)
	4	Ad.	908	1500	$^{40}Ar/^{39}Ar$	Larick et al (2001)
	10	Ad.	855	1100	$^{40}Ar/^{39}Ar$	Larick et al (2001)
	12	Ad.	1059	1100	$^{40}Ar/^{39}Ar$	Larick et al (2001)
	17	Ad.	1004	1100	$^{40}Ar/^{39}Ar$	Larick et al (2001)
Trinil	Trinil 2	Ad.	940	830	O2 isotope	Anton (2002)
Modjokerto	N/A	Juv ~5	673	1810	$^{40}Ar/^{39}Ar$	Swisher et al (1994)

AFRICA

Site	Cat. Number	Age, sex	Cc	Geologic age (kyr)	Testing method	Dating reference
Bouri	BOU-VP-2/66	Ad.	995	1042	$^{40}Ar/^{39}Ar$	Asfaw et al (2002)
Danakil	UA 31	Ad.	750	1000	Palaeomagnetic	Abbate et al
Olduvai Gorge	OH 9	Ad.	1067	1250	Palaeomagnetic	Rightmire (1990)
	OH 12	Ad.	727	700	Palaeomagnetic	Rightmire (1990)
Turkana	ER 3733	Ad.	848	1600	Palaeomagnetic	Wood (1991)
	ER 3883	Ad.	800	1500	Palaeomagnetic	Wood (1991)
	WT15000	M, juv 16	880	1530	$^{40}Ar/^{39}Ar$	Brown & McDougall (1993)
Salè	Salè	Ad.	945	400	Marine deposits	Rightmire (1990)

EUROPE

Site	Cat. Number	Age, sex	Cc	Geologic age (kyr)	Testing method	Dating reference
Dmanisi	D2700	Juv 14	600	1750	Palaeomagnetic	Vekua et al (2002)
	D2280	Ad.	775	1700	Palaeomagnetic	Gabunia et al (2000)
	D2282	Juv 16	650	1700	Palaeomagnetic	Gabunia et al (2000)

- Cc = cranial capacity (cm^3)

The question of Ceprano

The Ceprano cranium has been dated to approximately 750ka, if not older, on the basis of overlying volcaniclasts (Manzi et al 2001: 10011). By virtue of its cranial morphology it has been likened in turn to Sangiran 17, Petralona, the Zhoukoudian specimens and ER 3733 (Manzi et al 2001: 10012), although it was acknowledged that it did not fit comfortably into either an *erectine* grouping or with *H. heidelbergensis* (Manzi et al 2001: 10016). Recently it was proposed (Mallegni et al 2003) that this cranium is the representative of a new species, dubbed *H. cepranensis sp. nov.*, characterised by those elements of morphology that, it was felt, prevented it from being classed as fully *H. erectus* or fully *H. heidelbergensis*. These include a low, short and broad vault, and a cranial capacity of around 1180-1220cc (Mallegni et al 2003: 154-155).

APPENDIX II

Brain and basal metabolic rates for selected anthropoid species

Species[1]	Body weight (g)	Brain weight (g)	BMR (kcal/ day)	Brain MR (kcal/ day)	Log body weight	Log brain weight	Log BMR	Log brain MR
Alouatta palliata	6400	51	293.7	15.6	8.76	3.93	5.68	2.75
Saimiri sciureus	680	22	58.2	7.5	6.52	3.09	4.06	2.01
Aotus trivirgatus	850	16	45.7	5.7	6.75	2.77	3.82	1.74
Macaca mulatta	8000	110	312.3	28.3	8.99	4.70	5.74	3.34
M. fuscata	5900	84	309.6	24.1	8.68	4.43	5.74	3.18
M. fascicularis	5500	74	331.0	21.6	8.61	4.30	5.80	3.07
Papio papio	18000	190	658.8	49.2	9.80	5.25	6.49	3.90
P. anubis	26000	205	729.6	52.6	10.17	5.32	6.59	3.96
P. cynacephalus	19000	195	827.8	50.4	9.85	5.27	6.72	3.92
P. ursinus	18000	190	625.6	49.2	9.80	5.25	6.44	3.90
Cercocebus spp.	7900	104	326.9	29.1	8.97	4.64	5.79	3.37
Cercopithecus mitis	6500	76	333.4	22.1	8.78	4.33	5.81	3.10
Colubus guereza	7000	73	265.0	21.3	8.85	4.29	5.58	3.06
Erythrocebus patas	8000	118	390.0	32.5	8.99	4.77	5.97	3.48
Hylobates lar	6000	102	292.3	28.6	8.7	4.62	5.68	3.35
Pongo pygmaeus	55000	370	1423.4	88.2	10.92	5.91	7.26	4.48
Pan troglodytes	46000	420	1161.7	98.5	10.74	6.04	7.06	4.59
Homo sapiens	53500	1295	1428.4	315.2	10.89	7.17	7.26	5.75
Homo erectus 1	68000	909	N/A	N/A	11.13	6.81	7.47	5.65
Homo erectus 2	63000	800	N/A	N/A	11.05	6.68	7.41	5.54
Homo erectus 3	52300	848	N/A	N/A	10.86	6.74	7.26	5.59

Species	% brain weight[1]	% brain cost[2]	Species	% brain weight	% brain cost
Alouatta palliata	0.797	5.3	*P. ursinus*	1.056	7.9
Saimiri sciureus	3.235	12.8	*Cercocebus spp.*	1.316	8.9
Aotus trivirgatus	1.882	12.4	*Cercopithecus*	1.169	6.6
Macaca mulatta	1.375	9.1	*mitis*	1.043	8.0
M. fuscata	1.424	7.8	*Colubus guereza*	1.475	8.3
M. fascicularis	1.345	6.5	*Erythrocebus*	1.700	9.8
Papio papio	1.056	7.5	*patas*	0.673	6.2
P. anubis	0.788	7.2	*Hylobates lar*	0.913	8.5
P. cynacephalus	1.026	6.1	*Pongo pygmaeus*	2.421	22.1
			Pan troglodytes		
			Homo sapiens		

[1] Primate and human data taken from Leonard and Robertson (1992)
[2] Brain weight/body weight x 100%
[3] Brain metabolic rate/basal metabolic rate x 100%

APPENDIX III

Skeletal data from the Redcross and Chelsea populations

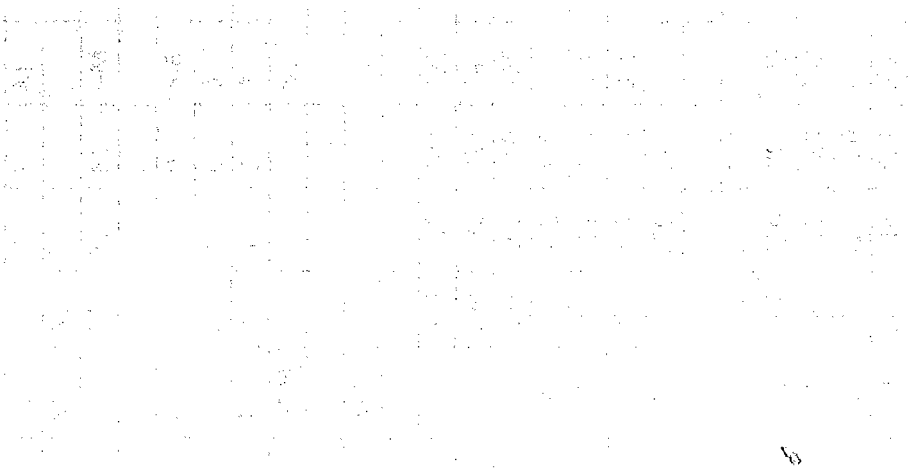

KEY

NB – newborn
UE – unerupted
UF – unfused
C – Clavicle unfused
H – proximal humerus unfused
S – S1 unfused
M2 – tooth unerupted
M3 – tooth unerupted
Pubic symphysis and auricular surface assigned to phases as set out in Buikstra and Ubelaker (1994)

	REW	SPECIMEN														
		72	**85**	**86**	**96**	**161**	**56**	**99**	**165**	**155**	**118**	**157**	**44**	**89**	**124**	**62**
SEX	Ventral arc	-							F	M		F				F
	Subpubic concavity	-							F	M		F		F		F
	Greater sciatic notch	F				M	F	F	F	M	F	F	~M	F		F
	Nuchal crest	M			F	M	M	F			F	~M	M	F		F
	Mastoid process	~M			F	M	M	M	M	~M	F	F	F			F
AGE	Pubic symphysis	-				-	-	-	9	5-6	3	5				8
Adult	Auricular surface	7				2	2	4	6	3	1	8	5	2		4
	Cranial sutures	2			1	2	3	3	2	2	1	2-3	3	1	0	3
Juvenile	Epiphyseal fusion	-	UF			SCH				S	S					
	Longbone length	-														
	Dentition	-	UE	6-7		M2									6	
STATURE	Humerus	299	106	-	-	-	332	245	304	333	309	277	301	291	-	-
	Radius	213	78	-	-	-	234	182	223	249	-	193	221	215	-	-
	Ulna	228	86	-	-	-	252	202	250	265	235	-	241	-	-	236
	Femur	-	131	190	-	482	451	352	435	-	439	-	430	400	-	-
	Tibia with spine	251	-	-	-	391	382	281	354	378	344	318	351	327	-	-
	Tibia without spine	241	108	157	-	382	372	271	349	369	-	309	342	317	-	-
	Fibula	-	-	149	-	371	-	270	347	-	342	314	342	315	-	-
CRANIAL	Basion-bregma	-	-	-	125	130	130	132	138	-	137	130	126	120	126	130
	Bi-temporal width	140	-	111	136	144	142	136	143	145	136	132	137	133	138	132
	Glabella-inion	176	-	159	178	194	184	177	180	183	185	180	177	174	165	182
	Auriculare-bregma	-	-	-	119	127	128	121	126	-	120	118	125	111	120	120
	Circumference	522	-	146	506	550	535	516	513	520	525	517	509	501	492	513

		72	85	86	96	161	56	99	165	155	118	157	44	89	124	62
F.A.	M1 width, L	-	-	-	9.0	9.0	8.7	9.4	-	9.7	10.0	-	-	8.9	9.5	-
	M1 width, R	-	-	-	9.0	8.8	9.3	9.0	-	9.5	9.5	-	-	9.3	9.8	-
	Orbit width, L	31.4	26.8	27.7	35.9	33.2	35.4	30.9	35.1	-	35.3	32.8	33.6	32.7	28.0	35.8
	Orbit width, R	32.4	27.6	28.2	36.3	35.4	37.0	33.1	35.5	-	34.6	34.5	34.2	31.8	29.1	34.6
	Orbit height, L	-	-	30.2	-	-	-	35.0	36.6	-	35.6	-	-	-	-	32.3
	Orbit height, R	-	-	31.0	-	-	-	33.0	37.6	-	36.0	-	-	-	-	30.9

	REW	SPECIMEN														
		159	46	136	91	119	153	135	150	60	52	01	02	116	164	101
SEX	Ventral arc		M													
	Subpubic concavity		M													
	Greater sciatic notch	F	~M	F	F	M			F	F				F		F
	Nuchal crest	F	F	F		M			F		~M		M			M
	Mastoid process	~M	~M	~M		M			F		~M					M
AGE	Pubic symphysis	9	1	9		2-3										
Adult	Auricular surface	6	1	6	5	7			8	5		8		2		3
	Cranial sutures	2	1	3	3				2-3		3			1		1
Juvenile	Epiphyseal fusion		<20				<13									
	Longbone length															
	Dentition		M3				12	18m							<1.5	
STATURE	Humerus	-	-	300	316	301	241	-	312	320	-	313	-	-	-	306
	Radius	-	-	213	226	220	-	-	218	232	-	249	-	215	-	224
	Ulna	222	-	227	247	338	-	-	-	249	-	263	-	-	-	240
	Femur	-	-	435	-	416	-	-	-	437	-	466	-	407	-	-
	Tibia with spine	341	342	353	356	337	-	-	352	362	-	388	397	342	-	349
	Tibia without spine	330	331	347	346	329	-	-	344	355	-	380	392	334	-	338
	Fibula	322	-	345	-	-	-	-	347	-	-	378	-	335	-	-
CRANIAL	Basion-bregma	125	133	125	135	137	-	-	133	-	134	-	-	-	-	145
	Bi-temporal width	142	137	124	140	148	-	-	128	-	136	144	-	150	-	145
	Glabella-inion	179	178	181	185	188	-	-	183	-	187	176	-	187	-	187
	Auriculare-bregma	120	125	118	123	129	-	-	115	-	125	-	-	125	-	134
	Circumference	518	516	503	520	540	-	-	506	-	526	520	-	535	-	-

		159	**46**	**136**	**91**	**119**	**153**	**135**	**150**	**60**	**52**	**01**	**02**	**116**	**164**	**101**
F.A.	M1 width, L	-	10.9	10.8	-	9.2	9.5	-	-	-	-	-	10.9	-	-	-
	M1 width, R	-	10.7	10.7	-	9.1	9.2	-	-	-	-	-	10.6	-	-	-
	Orbit width, L	35.0	34.0	32.5	-	33.9	-	28.3	33.2	35.5	-	31.4	-	35.9	26.5	-
	Orbit width, R	33.8	35.5	33.3	-	34.6	-	27.6	35.0	33.1	-	30.3	-	36.6	26.8	-
	Orbit height, L	-	35.6	34.4	-	37.1	-	-	-	-	-	-	-	35.9	-	-
	Orbit height, R	-	34.9	34.0	-	36.7	-	-	-	-	-	-	-	35.0	-	-

	REW	SPECIMEN														
		167	**75**	**78**	**67**	**71**	**70**	**79**	**69**	**48**	**100**	**114**	**6**	**24**	**32**	**204**
SEX	Ventral arc	M														
	Subpubic concavity	M														
	Greater sciatic notch	M								M	F		M	F		F
	Nuchal crest	M									F	M	M	F	F	
	Mastoid process	M									F	M	M	F	F	
AGE	Pubic symphysis	6									6					1
Adult	Auricular surface	4								5	3		2	6	3	2
	Cranial sutures	3			0							2	2	2	1-2	1
Juvenile	Epiphyseal fusion															
	Longbone length															
	Dentition		~6m	18m	5	4	NB	<3m	<3m							
STATURE	Humerus	312	-	-	165	-	-	-	-	-	285	299	324	299	312	315
	Radius	214	-	-	123	-	-	-	-	-	-	-	241	218	-	-
	Ulna	227	-	-	136	-	-	-	-	236	-	233	267	241	226	-
	Femur	441	-	-	224	-	-	-	-	-	404	423	-	425	444	443
	Tibia with spine	357	-	-	-	-	-	-	-	-	319	-	359	337	360	385
	Tibia without spine	348	-	-	185	-	-	-	-	-	313	-	352	330	355	374
	Fibula	344	-	-	179	-	-	-	-	-	-	-	350	-	351	-
CRANIAL	Basion-bregma	123	-	-	122	-	-	-	-	-	-	-	129	127	128	-
	Bi-temporal width	125	-	-	143	-	-	-	-	-	-	-	138	134	130	-
	Glabella-inion	183	-	-	179	-	-	-	-	-	-	-	193	180	179	-
	Auriculare-bregma	109	-	-	-	-	-	-	-	-	-	-	126	120	117	-
	Circumference	510	-	-	517	-	-	-	-	-	-	-	524	510	500	-

		167	**75**	**78**	**67**	**71**	**70**	**79**	**69**	**48**	**100**	**114**	**6**	**24**	**32**	**204**
F.A.	M1 width, L	9.0	-	-	-	-	-	-	-	-	-	-	-	10.2	-	9.7
	M1 width, R	9.0	-	-	-	-	-	-	-	-	-	-	-	9.7	-	10.2
	Orbit width, L	-	-	24.8	31.2	-	-	-	-	-	33.5	30.3	36.4	34.5	32.3	-
	Orbit width, R	-	-	24.6	32.1	-	-	-	-	-	34.1	31.8	34.2	35.3	31.4	-
	Orbit height, L	-	-	-	-	-	-	-	-	-	-	-	31.9	40.4	-	-
	Orbit height, R	-	-	-	-	-	-	-	-	-	-	-	32.8	38.5	-	-

	REW	SPECIMEN														
		200	28	140	54	11	137	138	130	132	134	139	143	113a	147a	144
SEX	Ventral arc				M											
	Subpubic concavity				M		F									
	Greater sciatic notch			F	F		F									
	Nuchal crest		M	M	M	M										
	Mastoid process		M	F	M	M										
AGE	Pubic symphysis			6	4	6	8									
Adult	Auricular surface		2	3	2	3	5									
	Cranial sutures	2-3	3	1	1	1										
Juvenile	Epiphyseal fusion							<6m	<6m							
	Longbone length												2			
	Dentition								6m	3	5	2		<6m	1	<3m
STATURE	Humerus	326	295	268	312	-	294	-	69.8	155	162	102	100	59.8	-	68.0
	Radius	-	222	-	236	244	210	-	56.2	109	113	-	73	47.9	-	-
	Ulna	-	-	199	250	262	226	-	62.6	119	125	79	80	54.5	-	61.8
	Femur	-	410	-	427	486	415	-	-	211	200	134	128	69.0	125	77.0
	Tibia with spine	-	324	302	353	389	333	-	-	-	-	-	-	-	-	-
	Tibia without spine	-	316	295	344	380	324	67.8	69.0	161	168	105	103	60.3	102	67.5
	Fibula	-	309	296	344	-	327	-	65.0	156	170	-	99	57.9	98	63.7
CRANIAL	Basion-bregma	132	125	133	-	127	-	-	-	-	-	-	-	-	-	-
	Bi-temporal width	-	134	-	-	137	-	-	-	-	-	-	-	-	-	-
	Glabella-inion	-	176	-	-	187	-	-	-	-	-	-	-	-	-	-
	Auriculare-bregma	127	114	127	-	123	-	-	-	-	-	-	-	-	-	-
	Circumference	-	496	-	-	518	-	-	-	-	-	-	-	-	-	-

		200	28	140	54	11	137	138	130	132	134	139	143	113a	147a	144
F.A.	M1 width, L	-	-	9.3	9.9	-	-	-	-	8.1	-	-	-	-	-	-
	M1 width, R	-	-	9.4	10.0	-	-	-	-	8.0	-	-	-	-	-	-
	Orbit width, L	-	-	31.6	34.3	35.1	-	25.0	-	28.1	-	26.8	-	18.2	22.6	23.2
	Orbit width, R	-	-	31.1	34.4	34.3	-	25.5	-	28.4	-	26.3	-	19.0	25.3	21.5
	Orbit height, L	-	-	-	36.5	36.3	-	-	-	-	-	-	-	-	-	-
	Orbit height, R	-	-	-	35.5	37.0	-	-	-	-	-	-	-	-	-	-

	REW	SPECIMEN													
		148	**149**	**106a**	**102**	**107**	**38**	**36**	**50a**	**58**	**40**	**15**	**50b**	**42a**	**42b**
SEX	Ventral arc														
	Subpubic concavity														
	Greater sciatic notch														
	Nuchal crest														
	Mastoid process														
AGE	Pubic symphysis														
Adult	Auricular surface														
	Cranial sutures														
Juvenile	Epiphyseal fusion														
	Longbone length				5	2-3									
	Dentition	<3m	<3m	5			3	<3m	18m	<3m	18m	9m	6m	NB	<3m
STATURE	Humerus	61.2	64.8	107	144	-	132	-	101	64.3	101	73.3	81.5	51.4	57.1
	Radius	48.4	52.4	-	-	96	98	-	71	49.4	78.6	57.9	64.3	42.6	46.4
	Ulna	57.0	59.7	-	117	105	106	-	-	57.5	84.2	64.3	78.3	-	53.1
	Femur	71.7	74.5	125	196	166	170	-	-	75.1	123	82.1	102	56.4	-
	Tibia with spine	-	-	-	-	-	-	-	-	-	-	-	-	-	-
	Tibia without spine	61.3	66.3	-	152	133	137	-	-	63.8	-	-	84.2	48.9	59.6
	Fibula	57.4	62.5	-	149	-	-	-	79	60.8	-	-	-	45.1	55.9
CRANIAL	Basion-bregma	-	-	-	-	-	-	-	-	-	-	-	-	-	-
	Bi-temporal width	-	-	-	-	-	-	-	-	-	-	-	-	-	-
	Glabella-inion	-	-	-	-	-	-	-	-	-	-	-	-	-	-
	Auriculare-bregma	-	-	-	-	-	-	-	-	-	-	-	-	-	-
	Circumference	-	-	-	-	-	-	-	-	-	-	-	-	-	-

		148	149	106a	102	107	38	36	50a	58	40	15	50b	42a	42b
F.A.	M1 width, L	-	-	-	-	-	-	-	-	-	-	-	-	-	-
	M1 width, R	-	-	-	-	-	-	-	-	-	-	-	-	-	-
	Orbit width, L	22.4	23.2	-	-	26.7	-	-	26.2	23.9	-	-	-	18.7	21.7
	Orbit width, R	22.1	25.0	-	-	27.4	-	-	26.9	24.7	-	-	-	17.7	22.3
	Orbit height, L	-	-	-	-	-	-	-	-	-	-	-	-	-	-
	Orbit height, R	-	-	-	-	-	-	-	-	-	-	-	-	-	-

	OCU	SPECIMEN														
		841	**810**	**1023**	**1112**	**802**	**918**	**1068**	**600**	**608**	**759**	**716**	**453**	**1021**	**635**	**948**
SEX	Ventral arc	F					F		F		M	M				M
	Subpubic concavity	F					F		F		M	M				M
	Greater sciatic notch	F	M		F	F	F		F		M	M		M	M	M
	Nuchal crest	F		F						~M						M
	Mastoid process	F		F						~M						M
AGE	Pubic symphysis	8					8	5	6		9	10				9
Adult	Auricular surface	5	3		4	5	7	3	3		6	7		8	4	7
	Cranial sutures			3			2-3			3			2-3			2
Juvenile	Epiphyseal fusion															
	Longbone length															
	Dentition															
STATURE	Humerus	-	-	-	272	-	295	-	310	295	315	316	311	342	-	331
	Radius	229	-	-	192	217	232	225	220	-	-	219	-	256	-	250
	Ulna	241	255	-	211	226	250	244	237	-	256	-	-	272	-	262
	Femur	404	444	405	400	431	406	398	438	-	457	457	457	483	480	477
	Tibia with spine	380	349	-	317	-	367	341	-	-	380	369	376	397	405	387
	Tibia without spine	372	342	-	309	-	359	331	-	-	369	359	370	390	398	375
	Fibula	-	-	-	308	-	-	329	-	-	-	-	361	386	390	369
CRANIAL	Basion-bregma	-	-	124	-	-	-	-	-	132	-	-	128	-	-	137
	Bi-temporal width	131	-	135	-	-	135	-	-	132	-	-	143	-	-	143
	Glabella-inion	175	-	182	-	-	179	-	-	189	-	-	180	-	-	188
	Auriculare-bregma	-	-	117	-	-	117	-	-	122	-	-	123	-	-	126
	Circumference	506	-	510	-	-	518	-	-	-	-	-	520	-	-	535

		841	**810**	**1023**	**1112**	**802**	**918**	**1068**	**600**	**608**	**759**	**716**	**453**	**1021**	**635**	**948**
F.A.	M1 width, L	-	-	-	-	9.0	-	-	-	-	-	-	10.2	-	-	-
	M1 width, R	-	-	-	-	9.1	-	-	-	-	-	-	10.3	-	-	-
	Orbit width, L	35.3	34.1	-	-	-	35.3	-	-	-	-	-	35.0	-	-	33.7
	Orbit width, R	36.0	33.9	-	-	-	37.5	-	-	-	-	-	34.7	-	-	33.6
	Orbit height, L	32.1	34.3	-	-	-	38.8	-	-	-	-	-	35.0	-	-	38.5
	Orbit height, R	32.4	34.9	-	-	-	38.4	-	-	-	-	-	35.9	-	-	38.1

	OCU	SPECIMEN														
		856	**885**	**675**	**511**	**152**	**154**	**1126**	**1133**	**583**	**812**	**713**	**980**	**990**	**509**	**805**
SEX	Ventral arc	M						F			F					
	Subpubic concavity	M						F			F		M			
	Greater sciatic notch	M	F			F	M	F	M	M	F		~M	F	F	
	Nuchal crest	M		M	M					M	F	M	F	F		F
	Mastoid process	M		M	M						F		F	F		F
AGE	Pubic symphysis	3									7		8			
Adult	Auricular surface	1	2			7	8	6	5		4		5	2	3	
	Cranial sutures	1-2		1-2	1				3	2	1-2	3	2-3			2-3
Juvenile	Epiphyseal fusion															
	Longbone length															
	Dentition															
STATURE	Humerus	295	-	-	-	306	-	-	-	-	-	318	292	-	285	-
	Radius	223	-	-	-	204	202	-	-	-	221	238	209	-	200	-
	Ulna	242	-	-	-	228	-	-	-	-	236	260	225	-	217	-
	Femur	411	-	-	-	447	-	400	416	-	422	-	436	420	-	-
	Tibia with spine	344	-	-	-	368	-	331	-	-	342	357	344	341	-	-
	Tibia without spine	333	-	-	-	361	-	322	330	-	335	350	337	332	-	-
	Fibula	328	-	-	-	-	341	323	323	-	323	340	-	-	-	-
CRANIAL	Basion-bregma	135	-	130	-	-	-	-	-	123	118	144	131	-	-	-
	Bi-temporal width	135	-	144	-	-	-	-	137	135	138	148	137	-	-	-
	Glabella-inion	182	-	190	-	-	-	-	174	187	178	192	187	-	-	-
	Auriculare-bregma	126	-	124	-	-	-	-	-	123	118	138	126	-	-	-
	Circumference	513	-	540	-	-	-	-	-	525	505	559	525	-	-	-

		856	**885**	**675**	**511**	**152**	**154**	**1126**	**1133**	**583**	**812**	**713**	**980**	**990**	**509**	**805**
F.A.	M1 width, L	-	-	11.0	9.2	-	-	-	-	10.3	-	-	10.8	-	-	-
	M1 width, R	-	-	11.3	9.1	-	-	-	-	10.3	-	-	11.0	-	-	-
	Orbit width, L	35.0	-	35.7	37.3	-	-	-	-	37.6	33.5	-	37.1	-	-	32.9
	Orbit width, R	35.4	-	36.5	37.3	-	-	-	-	37.5	33.7	-	37.4	-	-	33.1
	Orbit height, L	34.6	-	33.2	-	-	-	-	-	35.6	-	-	34.4	-	-	-
	Orbit height, R	33.8	-	32.1	-	-	-	-	-	36.0	-	-	34.6	-	-	-

	OCU	SPECIMEN														
		171	**697**	**730**	**754**	**790**	**970**	**972**	**744**	**490**	**587**	**1059**	**1055**	**654**	**509**	**527**
SEX	Ventral arc								M							
	Subpubic concavity								M							
	Greater sciatic notch			F	F	F			M		F	M	F	M		F
	Nuchal crest		F								M	M	F		F	F
	Mastoid process		F								M				F	F
AGE	Pubic symphysis					2			7		7			10		
Adult	Auricular surface			3	2	2			4			2	3	7		3
	Cranial sutures		3										3		1	2-3
Juvenile	Epiphyseal fusion															
	Longbone length															
	Dentition	<3m					1	18m		7						
STATURE	Humerus	-	-	286	-	335	-	-	397	-	306	-	-	305	-	326
	Radius	-	-	204	-	233	-	-	-	-	215	-	-	230	-	227
	Ulna	-	-	-	-	253	-	-	-	-	-	-	-	251	-	-
	Femur	-	-	400	450	464	-	-	422	-	423	446	-	421	-	444
	Tibia with spine	-	-	328	-	382	-	-	355	-	381	344	-	346	-	-
	Tibia without spine	-	-	320	-	373	-	-	349	-	375	337	365	338	-	-
	Fibula	-	-	-	-	368	-	-	-	-	-	336	360	333	-	-
CRANIAL	Basion-bregma	-	121	-	-	-	-	-	134	127	-	-	-	-	120	127
	Bi-temporal width	-	135	-	-	-	-	-	139	133	137	-	-	-	138	147
	Glabella-inion	-	184	-	-	-	-	-	191	171	177	-	-	-	177	190
	Auriculare-bregma	-	115	-	-	-	-	-	121	120	-	-	-	-	116	127
	Circumference	-	519	-	-	-	-	-	543	523	-	-	-	-	515	554

		171	697	730	754	790	970	972	744	490	587	1059	1055	654	509	527
F.A.	M1 width, L	-	-	-	-	11.0	-	-	-	8.8	-	-	-	-	-	-
	M1 width, R	-	-	-	-	11.0	-	-	-	8.8	-	-	-	-	-	-
	Orbit width, L	21.0	35.7	-	-	-	-	-	36.8	30.1	35.3	-	-	-	32.9	36.9
	Orbit width, R	21.3	36.0	-	-	-	-	-	36.4	29.9	35.4	-	-	-	32.6	36.7
	Orbit height, L	-	35.2	-	-	-	-	-	-	31.8	-	-	-	-		38.0
	Orbit height, R	-	35.5	-	-	-	-	-	-	31.5	-	-	-	-		37.3

	OCU	SPECIMEN														
		1164	1063	147	35	206	496	544	143	238	119	43	494	460	516	239
SEX	Ventral arc			M									M	~M	M	
	Subpubic concavity			M									M	~M	M	
	Greater sciatic notch		F	M				M		~F	~F	M	M	M	M	
	Nuchal crest			M	M	F	M	M	M							
	Mastoid process			M	M	F	M	M								
AGE	Pubic symphysis				9								7	1	7	
Adult	Auricular surface		5	7	7			2		1		7	4	1	5	
	Cranial sutures			2-3	2	1	2-3	1	3	1						
Juvenile	Epiphyseal fusion									H	12					
	Longbone length															
	Dentition	2														6m
STATURE	Humerus	-	-	354	333	313	-	326	-	277	258	-	-	-	333	123
	Radius	-	-	256	-	214	235	221	-	-	194	225	229	-	247	-
	Ulna	-	-	-	-	227	-	240	-	-	209	-	256	-	265	95
	Femur	137	417	490	449	-	-	-	-	-	-	441	475	463	477	-
	Tibia with spine	-	338	409	-	-	-	-	-	-	-	373	391	-	380	-
	Tibia without spine	107	330	403	-	-	-	-	-	-	298	366	381	-	373	-
	Fibula	108	-	401	-	-	-	-	-	-	-	354	-	-	-	-
CRANIAL	Basion-bregma	-	-	142	128	120	130	117	-	-	-	-	-	-	-	-
	Bi-temporal width	-	-	154	141	133	139	131	-	-	-	-	-	-	-	-
	Glabella-inion	-	-	198	186	180	187	187	-	-	-	-	-	-	-	-
	Auriculare-bregma	-	-	134	120	112	128	111	-	-	-	-	-	-	-	-
	Circumference	-	-	560	526	505	518	508	-	-	-	-	-	-	-	-

		1164	1063	147	35	206	496	544	143	238	119	43	494	460	516	239
F.A.	M1 width, L	-	-	-	-	-	-	-	-	10.0	-	-	-	-	-	-
	M1 width, R	-	-	-	-	-	-	-	-	10.0	-	-	-	-	-	-
	Orbit width, L	-	-	36.7	34.5	33.1	35.4	34.5	35.0	33.6	-	-	-	34.0	-	-
	Orbit width, R	-	-	36.8	35.9	33.1	35.5	35.7	34.9	33.6	-	-	-	34.4	-	-
	Orbit height, L	-	-	32.2	34.9	-	35.9	35.2	-	-	-	-	-	-	-	-
	Orbit height, R	-	-	32.3	34.9	-	35.6	34.9	-	-	-	-	-	-	-	-

	OCU										
		436	**534**	**1018**	**507**	**112**	**31**	**274**	**258**	**485**	**722**
SEX	Ventral arc		F				F	F			F
	Subpubic concavity	F	F	M			F	F			F
	Greater sciatic notch	F	F	~M	M		F	F	F	M	F
	Nuchal crest	F		M		F		F	F	M	F
	Mastoid process	F		M		M		F	F	M	F
AGE	Pubic symphysis	7	1	6	3		7	8	3	7	
Adult	Auricular surface	4		3	2		4	5	2	4	4
	Cranial sutures					1		2-3		2	
Juvenile	Epiphyseal fusion										
	Longbone length										
	Dentition										
STATURE	Humerus	301	284	332	309	355	285	291	304	330	290
	Radius	219	205	246	240	-	212	217	218	244	217
	Ulna	-	225	255	262	292	-	228	235	262	231
	Femur	436	404	448	459	-	421	414	410	464	427
	Tibia with spine	344	335	368	367	-	339	343	320	386	341
	Tibia without spine	338	327	364	364	-	332	335	311	377	335
	Fibula	299	-	-	-	-	330	-	-	-	335
CRANIAL	Basion-bregma	118	-	118	-	134	-	120	119	133	-
	Bi-temporal width	140	-	143	-	144	-	127	141	141	141
	Glabella-inion	177	-	199	-	200	-	171	186	191	177
	Auriculare-bregma	114	-	118	-	130	-	114	124	128	-
	Circumference	516	-	552	-	557	-	486	541	534	514

		436	534	1018	507	112	31	274	25-8	485	722
F.A.	M1 width, L	-	-	10.7	-	-	-	-	-	-	-
	M1 width, R	-	-	10.8	-	-	-	-	-	-	-
	Orbit width, L	33.6	-	36.8	-	-	-	34.4	31.3	35.0	30.9
	Orbit width, R	33.8	-	37.0	-	-	-	34.6	31.9	35.3	31.1
	Orbit height, L	-	-	-	-	-	-	35.8	34.8	36.5	-
	Orbit height, R	-	-	-	-	-	-	35.8	34.7	36.9	-

APPENDIX IV

Data screening

Redcross adults

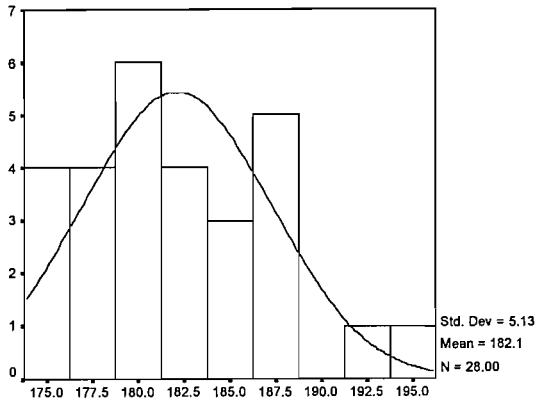

Glabella-inion length (mm)

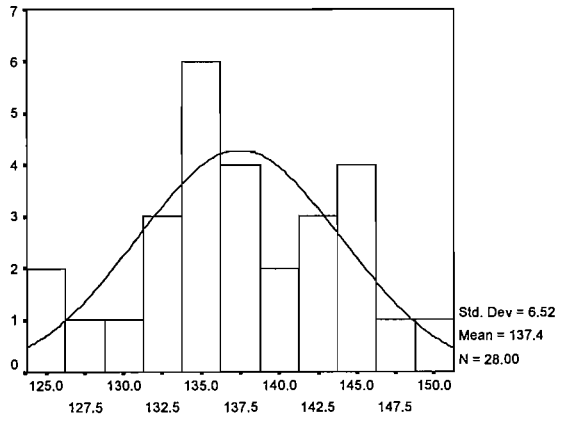

Bi-temporal width (mm)

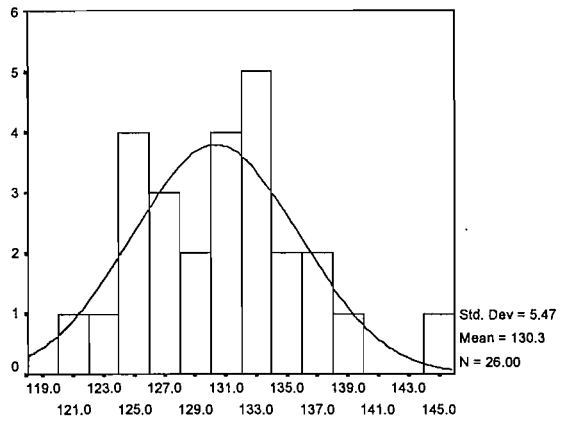

Basion-bregma height (mm)

Chelsea adults

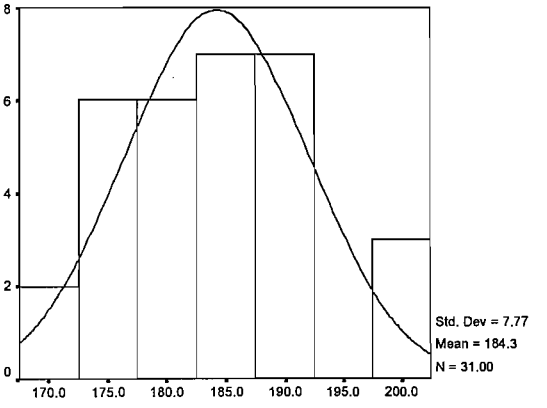

Glabella-inion length (mm)

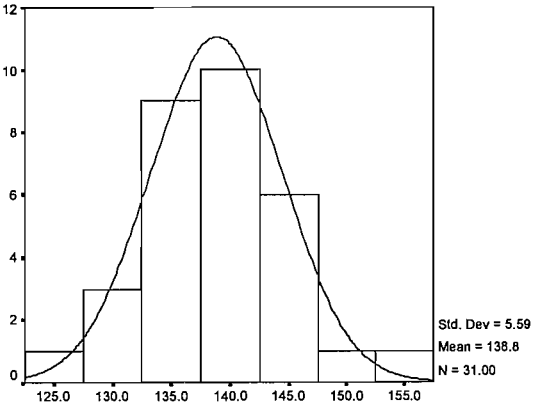

Bi-temporal width (mm)

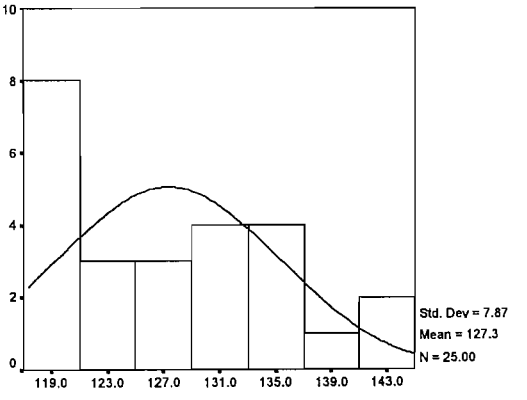

Basion-bregma height (mm)

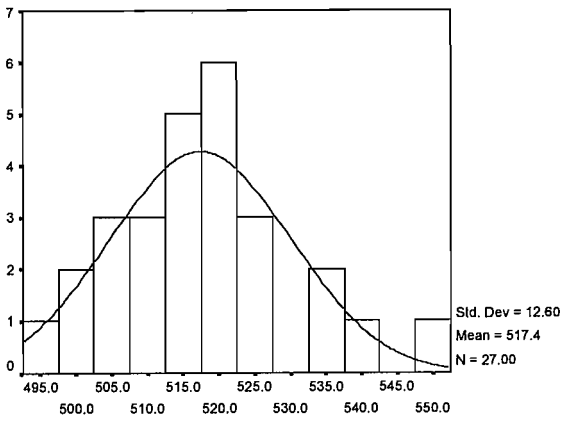

Circumference (mm)

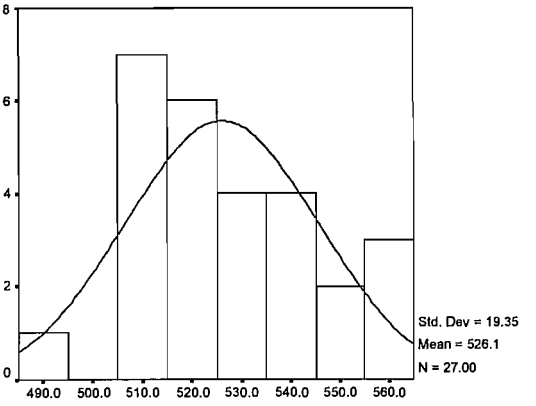

Circumference (mm)

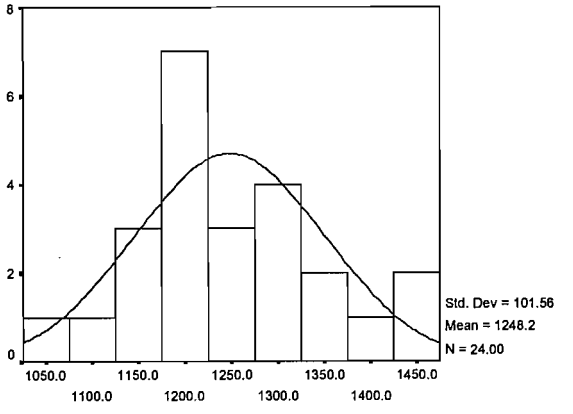

Cranial capacity (cc)

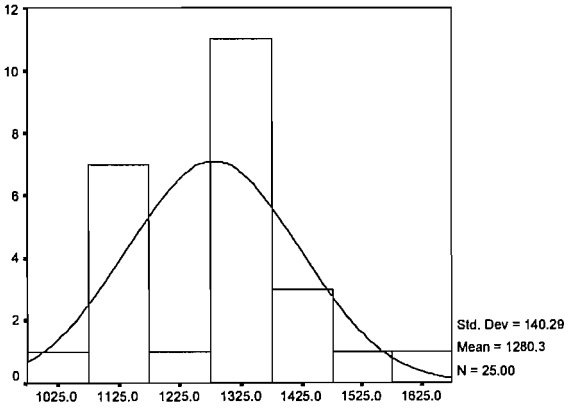

Cranial capacity (cc)

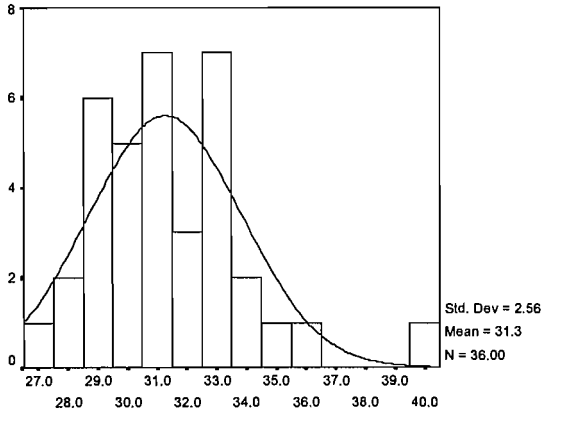

Humerus length (mm)

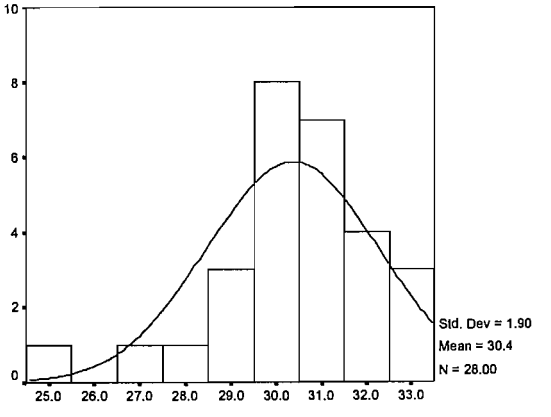

Humerus length (mm)

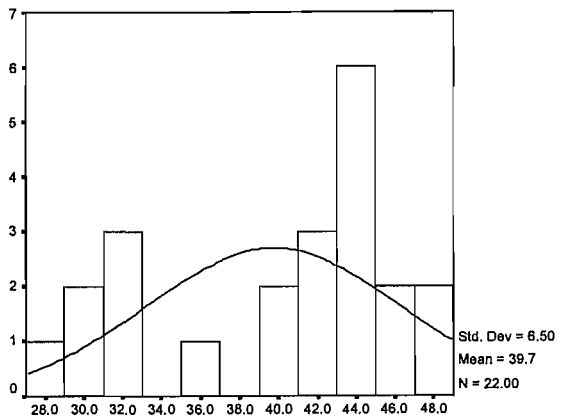

Femur length (mm)

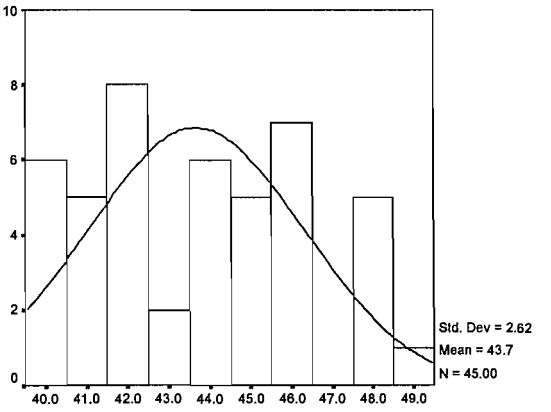

Femur length (mm)

REFERENCES

Abbate, E., A. Albianelli, et al. (1998). A one-million-year-old *Homo* cranium from the Danakil (Afar) Depression of Eritrea. *Nature* 393: 458-460.

Acsádi, G. and J. Nemeskéri (1970). *History of human life span and mortality.* Budapest: Akademiai Kiado.

Aiello, L. C. and R. I. M. Dunbar (1993). Neocortex size, group size, and the evolution of language. *Current Anthropology* 34: 184-193.

Aiello, L. C. and C. Key (2002). Energetic consequences of being a *Homo erectus* female. *American Journal of Human Biology* 14: 551-565.

Albert, A. M. and D. L. Greene (1999). Bilateral asymmetry in skeletal growth and maturation as an indicator of environmental stress. *American Journal of Physical Anthropology* 110: 341-349.

Alvarez, H. P. (2000). Grandmother hypothesis and primate life histories. *American Journal of Physical Anthropology* 113: 435-450.

Andrews, P. (1984). An alternative interpretation of the characters used to define *Homo erectus. Courier Forschungsinstitut Senckenberg* 69: 167-175.

Angel, J. L. (1982). A new measure of growth efficiency: Skull base height. *American Journal of Physical Anthropology* 59: 297-305.

Angel, J. L. and L. M. Olney (1981). Skull base height and pelvic inlet depth from prehistoric to modern times. *American Journal of Physical Anthropology* 54: 197.

Angilletta Jr, M. J., R. S. Wilson, et al. (2003). Tradeoffs and the evolution of thermal reaction norms. *Trends in Ecology and Evolution* 18: 234-240.

Antón, S. C. (1997). Developmental age and taxonomic affinity of the Mojokerto child, Java, Indonesia. *American Journal of Physical Anthropology* 102: 497-514.

Antón, S. C. (1999). Cranial growth in *Homo erectus*: How credible are the Ngandong juveniles? *American Journal of Physical Anthropology* 108: 223-236.

Antón, S. C. (2002). Evolutionary significance of cranial variation in Asian *Homo erectus. American Journal of Physical Anthropology* 118: 301-323.

Antón, S. C. (2003). Natural history of *Homo erectus. Yearbook of Physical Anthropology* 46: 126-170.

Antón, S. C. and S. R. Leigh (2003). Growth and life history in *Homo erectus.* J. L. Thompson, G. E. Krovitz and A. J. Nelson (Eds.) *Patterns of growth and development in the genus Homo.* Cambridge: Cambridge University Press.

Antón, S. C., W. R. Leonard, et al. (2002). An ecomorphological model of the initial hominid dispersal from Africa. *Journal of Human Evolution* 43: 773-785.

Arnold, S. J. and C. R. Peterson (2002). A model for optimal reaction norms: The case of the pregnant garter snake and her temperature-sensitive embryos. *The American Naturalist* 160: 306-316.

Arsuaga, J. L., I. Martínez, et al. (2001). Analyse phylogenetique des hominides de la Sierra de Atapuerca (Sima de los Huesos et Gran Dolina TD-6): l'evidence cranienne. *L'Anthropologie* 105: 161-178.

Arsuaga, J. L., I. Martínez, et al. (1997a). Sima de los Huesos (Sierra de Atapuerca, Spain). The site. *Journal of Human Evolution* 33: 109-127.

Arsuaga, J. L., I. Martínez, et al. (1997b). The Sima de los Huesos crania (Sierra de Atapuerca, Spain). A comparative study. *Journal of Human Evolution* 33: 219-281.

Ascenzi, A., I. Biddittu, et al. (1996). A calvarium of late *Homo erectus* from Ceprano, Italy. *Journal of Human Evolution* 31: 409-423.

Ascenzi, A., F. Mallegni, et al. (2000). A re-appraisal of Ceprano calvaria affinities with *Homo erectus*, after the new reconstruction. *Journal of Human Evolution* 39: 443-450.

Aschoff, J., B. Gunther, et al. (1971). *Energiehaushalt und Temperaturregulation.* Munchen: Urban & Schwarzenberg.

Asfaw, B., W. H. Gilbert, et al. (2002). Remains of *Homo erectus* from Bouri, Middle Awash, Ethiopia. *Nature* 416(6878): 317-320.

Barclay, H. J. and P. T. Gregory (1981). An experimental test of models predicting life-history characteristics. *American Naturalist* 117: 944-961.

Barton, R. A. and R. I. M. Dunbar (1997). Evolution of the social brain. A. Whiten and R. Byrne (Eds.) *Machiavellian intelligence II.* Cambridge: Cambridge University Press, 240-263.

Bartstra, G. J., S. Soegondho, et al. (1988). Ngandong man: age and artifacts. *Journal of Human Evolution* 17: 325-337.

Bateson, P. (2001). Fetal experience and good adult design. *International Journal of Epidemiology* 30: 928-934.

Begun, D. and A. Walker (1993). The endocast. A. Walker and R. Leakey (Eds.) *The Nariokotome Homo erectus skeleton.* Cambridge, MA: Harvard University Press, 326-358.

Bell, G. (1986). A reply to Reznick et al. *Evolution* 40: 1344-1346.

Bermúdez de Castro, J. M., M. Martinón-Torres, et al. (2004). The Atapuerca sites and their contribution to the knowledge of human evolution in Europe. *Evolutionary Anthropology* 13: 25-41.

Bermúdez de Castro, J. M., M. Martinón-Torres, et al. (2003). Gran Dolina-TD6 versus Sima de los Huesos dental samples from Atapuerca: evidence of discontinuity in the European Pleistocene population? *Journal of Archaeological Science* 30: 1421-1428.

Bermúdez de Castro, J. M. and M. E. Nicolás (1997). Palaeodemography of the Atapuerca-SH Middle Pleistocene hominid sample. *Journal of Human Evolution* 33: 333-355.

Black-Samuelsson, S. and S. Andersson (2003). The effect of nutrient stress on developmental instability in leaves of *Acer platanoides* (Aceraceae) and *Betula pendula* (Betulaceae). *American Journal of Botany* 90: 1107-1112.

Blurton Jones, N. G., L. C. Smith, et al. (1992). Demography of the Hadza, an increasing and high density population of savanna foragers. *American Journal of Physical Anthropology* 89: 159-181.

Boas, F. (1912a). *Changes in bodily form of descendants of immigrants*. New York: Columbia University Press.

Boas, F. (1912b). Changes in the body form of descendants of immigrants. *American Anthropologist* 14: 530-562.

Bocquet-Appel, J.-P. and J. L. Arsuaga (2000). Probable catastrophic mortality of the Atapuerca (SH) and Krapina hominid samples. P. V. Tobias, M. A. Raath, J. Moggi-Cecchi and G. A. Doyle (Eds.) *Humanity from African naissance to coming millennia*. Florence: University of Florence Press, 149-157.

Bogin, B. (1999). *Patterns of human growth*. Cambridge: Cambridge University Press.

Brain, C. K. (1981). *The hunters or the hunted? An introduction to African cave taphonomy*. Chicago: University of Chicago Press.

Brain, C. K. (1993). A taphonomic overview of the Swartkrans fossil assemblages. C. K. Brain (Ed.) *Swartkrans: A cave's chronicle of early man*. Pretoria: Transvaal Museum, 257-264.

Brain, C. K. and V. Watson (1992). A guide to the Swartkrans early hominid cave site. *Annals of the Transvaal Museum* 35: 343-365.

Bräuer, G. (1994). How different are Asian and African *Homo erectus*? *Courier Forschungsinstitut Senckenberg* 171: 301-318.

Brickley, M. (1999). *The cross bones burial ground*. London: The Museum of London Archaeology Service.

Buikstra, J. E. and D. H. Ubelaker (1994). *Standards for data collection from human skeletal remains: Proceedings of a seminar at the Field Museum of Natural History*. Fayetteville: Arkansas Archeological Survey.

Buretic-Tomljanovic, A., S. Ristic, et al. (2004). Secular change in body height and cephalic index of Croatian medical students (University of Rijeka). *American Journal of Physical Anthropology* 123: 91-96.

Butte, N., L. Barbosa, et al. (1997). Total energy expenditure and physical activity level of lactating Mesoamerindians. *Journal of Nutrition* 127: 299-305.

Butte, N., J. M. Hopkinson, et al. (1999). Adjustments in energy expenditure and substrate utilization during late pregnancy and lactation. *American Journal of Clinical Nutrition* 69: 299-307.

Butte, N., W. W. Wong, et al. (2001). Energy requirements of lactating women derived from doubly labeled water and milk energy output. *Journal of Nutrition* 131: 53-58.

Cachel, S. and J. W. K. Harris (1998). The lifeways of *Homo erectus* inferred from archaeology and evolutionary ecology: A perspective from East Africa. M. D. Petraglia and R. Korisettar (Eds.) *Early human behaviour in global context: The rise and diversity of the Lower Palaeolithic record*. London: Routledge, 108-131.

Carbonell, E., M. Mosquera, et al. (2003). Les premiers comportements funéraires auraient-ils pris place a Atapuerca, il y a 350 000 ans? *L'Anthropologie* 107: 1-14.

Caspari, R. and S.-H. Lee (2004). Older age becomes common late in human evolution. *Proceedings of the National Academy of Sciences* 101: 10895-10900.
Caughley, G. (1966). Mortality patterns in mammals. *Ecology* 47: 906-918.
Charnov, E. L. (1991). Evolution of life history variation among female mammals. *Proceedings of the National Academy of Sciences* 88: 1134-1137.
Charnov, E. L. (1997). Trade-off-invariant rules for evolutionarily stable life histories. *Nature* 387: 393-394.
Charnov, E. L. (2001a). Evolution of mammal life histories. *Evolutionary Ecology Research* 3: 521-535.
Charnov, E. L. (2001b). Reproductive efficiencies in the evolution of life histories. *Evolutionary Ecology Research* 3: 873-876.
Charnov, E. L. (2002). Reproductive effort, offspring size and benefit-cost ratios in the classification of life histories. *Evolutionary Ecology Research* 4: 749-758.
Charnov, E. L. (2004). The optimal balance between growth rate and survival in mammals. *Evolutionary Ecology Research* 6: 307-313.
Clegg, M. and L. C. Aiello (1999). A comparison of the Nariokotome *Homo erectus* with juveniles from a modern human population. *American Journal of Physical Anthropology* 110: 81-93.
Conroy, G. C. (1997). *Reconstructing human origins: A modern synthesis*. New York: W.W. Norton & Company.
Cowie, R. (2000). *2-4 Old Church Street, Chelsea, London SW3: Progress Report (Unpublished)*. London: Museum of London.
Daan, S. and J. M. Tinbergen (1997). Adaptation of life histories. J. R. Krebs and N. B. Davies (Eds.) *Behavioural ecology: an evolutionary approach*. Oxford: Blackwell Science, 311-333.
Day, M. H. (1986). *Guide to fossil man*. London: Cassell.
Day, M. H., R. E. F. Leakey, et al. (1976). New hominids from East Turkana, Kenya. *American Journal of Physical Anthropology* 45: 369-436.
de Onis, M., C. Monteiro, et al. (1993). The worldwide magnitude of protein-energy malnutrition: an overview from the WHO Global Database on Child Growth. *Bulletin of the World Health Organisation* 71: 703-712.
Deevey, E. S. (1947). Life tables for natural populations of animals. *The Quarterly Review of Biology* 22: 283=314.
Delson, E., K. Harvati, et al. (2001). The Sambungmacan 3 *Homo erectus* calvaria: A comparative morphometric and morphological analysis. *The Anatomical Record* 262: 380-397.
Dennell, R. (2003). Dispersal and colonisation, long and short chronologies: how continuous is the Early Pleistocene record for hominids outside East Africa? *Journal of Human Evolution* 45: 421-440.
DeVito, J. L., J. Graham, et al. (1986). Morphometry of the developing brain in *Macaca nemestrina*. J. G. Else and P. C. Lee (Eds.) *Primate ontogeny, cognition and social behaviour*. Cambridge: Cambridge University Press, 131-139.

Dewey, K. G. (1997). Energy and protein requirements during lactation. *Annual Review of Nutrition* 17: 19-36.
Dienske, H. (1986). A comparative approach to the question of why human infants develop so slowly. J. G. Else and P. C. Lee (Eds.) *Primate ontogeny, cognition and social behaviour*. Cambridge: Cambridge University Press, 147-154.
Dunbar, R. I. M. (1980). Demographic and life history variables of a population of gelada baboons (*Theropithecus gelada*). *Journal of Animal Ecology* 49: 485-506.
Dunbar, R. I. M. (1992). Neocortex size and group size in primates: A test of the hypothesis. *Journal of Human Evolution* 22: 297-297.
Dunbar, R. I. M. (1993). Co-evolution of neocortical size, group size and language in humans. *Behavioral and Brain Sciences* 16: 681-694.
Dunbar, R. I. M. (1996). On the evolution of language and kinship. J. Steele and S. Shennan (Eds.) *The archaeology of human ancestry: Power, sex and tradition*. London: Routledge, 380-396.
Elberse, I. A. M., J. M. M. Van Damme, et al. (2003). Plasticity of growth characteristics in wild barley (*Hordeum spontaneum*) in response to nutrient limitation. *Journal of Ecology* 91: 371-382.
Elia, M. (2001). Fuels of the tissues. J. S. Garrow, W. P. T. James and A. Ralph (Eds.) *Nutrition and dietetics*. London: Churchill Livingstone.
Elton, S., L. C. Bishop, et al. (2001). Comparative context of Plio-Pleistocene hominin brain evolution. *Journal of Human Evolution* 41: 1-27.
Eveleth, P. B. and J. M. Tanner (1976). *Worldwide variation in human growth. 2nd edition*. Cambridge: Cambridge University Press.
Expert Group, I. C. M. R. (1990). *Nutrient requirements and recommended dietary allowances for Indians*. New Delhi: Indian Council of Medical Research.
Ferguson, S. H. (2002). The effects of productivity and seasonality on life history: Comparing age at maturity among moose (*Alces alces*) populations. *Global Ecology and Biogeography* 11: 303-312.
Ferguson, S. H. and P. D. McLoughlin (2000). Effect of energy availability, seasonality, and geographic range on brown bear life history. *Ecography* 23: 193-200.
Foley, R. A. (1987). *Another unique species: Patterns in human evolutionary ecology*. London: Longman.
Foley, R. A. (1992). Evolutionary ecology of fossil hominids. E. A. Smith and B. Winterhalder (Eds.) *Evolutionary ecology and human behaviour*. New York: Aldine de Gruyter, 131-164.
Foley, R. A. (1994). Speciation, extinction and climatic change in hominid evolution. *Journal of Human Evolution* 26: 275-289.
Foley, R. A. (1995). Evolution and adaptive significance of hominid maternal behaviour. C. R. Pryce, R. D. Martin and D. Skuse (Eds.) *Motherhood in human and nonhuman primates*. Basel: Karger, 27-36.
Foley, R. A. (1999). Evolutionary geography of Pliocene African hominids. T. G. Bromage and F. Schrenk (Eds.) *African biogeography, climate change, and human evolution*. New York: Oxford University Press, 328-348.

Foley, R. A. (2002). Adaptive radiations and dispersals in hominin evolutionary ecology. *Evolutionary Anthropology* Suppl. 1: 32-37.
Foley, R. A. and M. M. Lahr (2003). On stony ground: Lithic technology, human evolution, and the emergence of culture. *Evolutionary Anthropology* 12: 109-122.
Foley, R. A. and P. Lee (1991). Ecology and energetics of encephalization in hominid evolution. *Philosophical Transactions of the Royal Society of London, B* 334: 223-232.
Gabounia, L., M.-A. de Lumley, et al. (2002). Découverte d'un nouvel hominidé à Dmanissi (Transcaucasie, Géorgie). *Comptes Rendus Palevol* 1: 243-253.
Gabunia, L., A. Vekua, et al. (2000). Earliest Pleistocene hominid cranial remains from Dmanisi, Republic of Georgia: Taxonomy, geological setting, and age. *Science* 288: 1019-1025.
Garza, C. and K. M. Rasmussen (2001). Pregnancy and lactation. J. S. Garrow, W. P. T. James and A. Ralph (Eds.) *Nutrition and dietetics*. London: Churchill Livingstone, 437-448.
Gavan, J. A. (1971). Longitudinal, postnatal growth in chimpanzee. G. H. Bourne (Ed.) *The Chimpanzee, vol.4*. Baltimore: University Park Press. **4,** 46-102.
Golden, B. E. (2001). Infancy, childhood and adolescence. J. S. Garrow, W. P. T. James and A. Ralph (Eds.) *Nutrition and dietetics*. London: Churchill Livingstone, 449-464.
Golden, M. H. N. and B. E. Golden (2001). Severe malnutrition. J. S. Garrow, W. P. T. James and A. Ralph (Eds.) *Human nutrition and dietetics*. London: Churchill Livingstone, 515-526.
Gravlee, C. C., H. R. Bernard, et al. (2003). Heredity, environment, and cranial form: A reanalysis of Boas's immigrant data. *American Anthropologist* 105: 125-138.
Gray, P. B. and F. Marlowe (2002). Fluctuating asymmetry of a foraging population: the Hadza of Tanzania. *Annals of Human Biology* 29: 495-501.
Groves, C. and V. Mazak (1975). An approach to the taxon of Hominidae: Gracile Villafranchian hominids of Africa. *Casopsis SPro Mineralogii a Geologii* 20: 225-246.
Grün, R. and A. Thorne (1997). Dating the Ngandong humans. *Science* 276: 1575.
Hasson, O. and Y. Rossler (2002). Character-specific homeostasis dominates fluctuating asymmetries in the medfly (Diptera: Tephritidae). *Florida Entomologist* 85: 73-82.
Hawkes, K. (2003). Grandmothers and the evolution of human longevity. *American Journal of Human Biology* 15: 380-400.
Henneberg, M. and C. de Miguel (2004). Hominins are a single lineage: brain and body size variability does not reflect postulated taxonomic diversity of hominins. *HOMO - Journal of Comparative Human Biology* 55: 21-37.
Hill, K. and A. M. Hurtado (1996). *Ache life history: The ecology and demography of a foraging people*. New York: Aldine de Gruyter.
Hochachka, P. W., B. Emmett, et al. (1988). Limits and constraints in the scaling of oxidative and glycolytic enzymes in homeotherms. *Canadian Journal of Zoology* 66: 1128-1138.

Holliday, M. A. (1978). Body composition and energy needs during growth. F. Falkner and J. M. Tanner (Eds.) *Human growth, vol. 2: postnatal growth.* New York: Plenum Press, 117-139.

Holloway, R. L. (2002). Head to head with Boas: Did he err on the plasticity of head form? *Proceedings of the National Academy of Sciences* 99: 14622-14623.

Hopwood, D. E. (2003). Behavioural differences in the early to mid-Pleistocene: Were African and Chinese *Homo erectus* really that different? *American Journal of Physical Anthropology* 120(Suppl. 36): 117-118.

Howell, F. C. (1999). Paleo-demes, species clades, and extinctions in the Pleistocene hominin record. *Journal of Anthropological Research* 55: 191-243.

Jacob, T. (1975). Morphology and paleoecology of early man in Java. R. Tuttle (Ed.) *Paleoanthropology, morphology and paleoecology.* The Hague: Mouton, 311-325.

Johnson, S. E. (2003). Life history and the competitive environment: Trajectories of growth, maturation, and reproductive output among Chacma baboons. *American Journal of Physical Anthropology* 120: 83-98.

Jones, S., R. D. Martin, et al. (Eds.) (1992). *The Cambridge encyclopedia of human evolution.* Cambridge: Cambridge University Press.

Jordan, M. A. and H. L. Snell (2002). Life history trade-offs and phenotypic plasticity in the reproduction of Galapagos lava lizards (*Microlophus delanonis*). *Oecologia* 130: 44-52.

Kaplan, H. and K. Hill (1992). The evolutionary ecology of food acquisition. E. A. Smith and B. Winterhalder (Eds.) *Evolutionary ecology and human behavior.* New York: Aldine de Gruyter, 167-201.

Kaplan, H., K. Hill, et al. (2000). A theory of human life history evolution: Diet, intelligence, and longevity. *Evolutionary Anthropology* 9: 156-185.

Kappelman, J. (1996). The evolution of body mass and relative brain size in fossil hominids. *Journal of Human Evolution* 30: 243-276.

Kellner, J. R. and R. A. Alford (2003). The ontogeny of fluctuating asymmetry. *The American Naturalist* 161: 931-947.

Kennedy, G. E. (2005). From the ape's dilemma to the weanling's dilemma: early weaning and its evolutionary context. *Journal of Human Evolution* 48: 123-145.

Kidder, J. H. and A. C. Durband (2004). A re-evaluation of the metric diversity within *Homo erectus*. *Journal of Human Evolution* In press.

Korenchevsky, V. (1961). *Physiological and pathological ageing.* Basel: Karger.

Lampl, M. and F. E. Johnston (1996). Problems in the aging of skeletal juveniles: Perspectives from maturation assessments of living children. *American Journal of Physical Anthropology* 101: 345-355.

Langbroek, M. and W. Roebroeks (2000). Extraterrestrial evidence on the age of the hominids from Java. *Journal of Human Evolution* 38: 595-600.

Larick, R., R. Ciochon, et al. (2001). Early Pleistocene $^{40}Ar/^{39}Ar$ ages for Bapang Formation hominins, Central Jawa, Indonesia. *Proceedings of the National Academy of Sciences* 98(9): 4866-4871.

Lasker, G. W. (1995). The study of migrants as a strategy for understanding human biological plasticity. C. G. N. Mascie-Taylor and B. Bogin (Eds.) *Human variability and plasticity*. Cambridge: Cambridge University Press, 110-114.
Leakey, L. S. B. (1959). A new fossil skull from Olduvai. *Nature* 184: 491-493.
Lee, P. C., P. Majluf, et al. (1991). Growth, weaning and maternal investment from a comparative perspective. *Journal of Zoology* 225: 99-114.
Lee, S. and M. H. Wolpoff (2002). *Evolutionary patterns in Pleistocene human brain size*. Seventy-first annual meeting of the American Association of Physical Anthropologists, Buffalo, New York.
LeGros Clark, W. E. (1978). *The fossil evidence for human evolution: an introduction to the study of paleoanthropology*. Chicago: The University of Chicago Press.
Leigh, S. R. (1992). Cranial capacity evolution in *Homo erectus* and early *Homo sapiens*. *American Journal of Physical Anthropology* 87: 1-13.
Leonard, W. R. and M. L. Robertson (1992). Nutritional requirements and human evolution: A bioenergetics model. *American Journal of Human Biology* 4: 179-195.
Leutenegger, W. (1982). Encephalisation and obstetrics in primates with particular reference to human evolution. E. Armstrong and D. Falk (Eds.) *Primate brain evolution: Methods and concepts*. New York: Plenum Press, 85-21.
Levinton, J. S. (1982). Estimating stasis: Can a null hypothesis be too null? *Paleobiology* 8: 307.
Lewontin, R. C. (1965). Selection for colonizing ability. H. G. Baker and G. L. Stebbins (Eds.) *The genetics of colonizing species*. New York: Academic Press, 77-94.
Lockwood, C. A. and P. V. Tobias (1999). A large male hominin cranium from Sterkfontein, South Africa, and the status of *Australopithecus africanus*. *Journal of Human Evolution* 36: 637-685.
MacArthur, R. H. and E. O. Wilson (1967). *The theory of island biogeography*. Princeton: Princeton University Press.
Manjunath, K. Y. (2002). Estimation of cranial volume in dissecting room cadavers. *Journal of The Anatomical Society of India* 51: 168-172.
Marquez, S., K. Mowbray, et al. (2001). New fossil hominid calvaria from Indonesia - Sambungmacan 3. *The Anatomical Record* 262: 344-368.
Martin, R. D. (1995). Phylogenetic aspects of primate reproduction: the context of advanced maternal care. C. R. Pryce, R. D. Martin and D. Skuse (Eds.) *Motherhood in human and nonhuman primates*. Basel: Karger, 16-26.
Martin, R. D. (1996). Scaling of the mammalian brain: The maternal energy hypothesis. *News in Physiological Sciences* 11: 149-156.
Mayr, E. (1944). On the concepts and terminology of vertical subspecies and species. *National Research Council Committee on Common Problems of Genetics, Paleontology and Systematics* Bulletin No. 2: 11-16.
McHenry, H. M. (1994). Behavioral ecological implications of early hominid body size. *Journal of Human Evolution* 27: 77-87.

Meadows, D. W. (2001). Centre-edge differences in behaviour, territory size and fitness in clusters of territorial damselfish: Patterns, causes, and consequences. *Behaviour* 138: 1085-1116.
Mink, J. W., R. J. Blumenschine, et al. (1981). Ratio of central nervous system to body metabolism in vertebrates: its constancy and functional basis. *American Journal of Physiology* 241: R203-R212.
Møller, A. P. and J. Manning (2003). Growth and developmental instability. *The Veterinary Journal* 166: 19-27.
Møller, A. P. and J. P. Swaddle (1997). *Asymmetry, developmental stability, and evolution*. Oxford: Oxford University Press.
Molleson, T. I. and M. Cox (1993). *The Spitalfields Project volume 2: The anthropology. The middling sort. CBA Research Report 86*. York: Council for British Archaeology.
Murphy, G. I. (1968). Pattern in life history and the environment. *American Naturalist* 102: 391-403.
Nehlig, A. (1996). Metabolism of the central nervous system. S. Mraovitch and R. Sercombe (Eds.) *Neurophysiological basis of cerebral blood flow control: An introduction*. London: John Libbey, 177-196.
Niewiarowski, P. H. (2001). Energy budgets, growth rates, and thermal constraints: toward an integrative approach to the study of life-history variation. *The American Naturalist* 157: 421-433.
Oakley, K. P., B. G. Campbell, et al. (1975). *Catalogue of fossil hominids Part three: Americas, Asia, Australasia*. London: Trustees of The British Museum (Natural History).
Opie, K. (2004). *Testing the Grandmothering Hypothesis: The provisioning of Homo erectus infants and juveniles*. London: University College London. Unpublished M.Sc manuscript.
Partridge, T. C., D. E. Granger, et al. (2003). Lower Pleistocene hominid remains from Sterkfontein. *Science* 300: 607-612.
Passingham, R. E. (1982). *The human primate*. Oxford: W.H. Freeman and Company.
Paus, T., D. L. Collins, et al. (2001). Maturation of white matter in the human brain: A review of magnetic resonance studies. *Brain Research Bulletin* 54: 255-266.
Pennington, R. (2001). Hunter-gatherer demography. C. Panter-Brick, R. H. Layton and P. Rowley-Conwy (Eds.) *Hunter-gatherers: An interdisciplinary perspective*. Cambridge: Cambridge University Press, 170-204.
Philippi, T. and J. Seger (1989). Hedging one's evolutionary bets, revisited. *Trends in Ecology and Evolution* 4: 41-44.
Pianka, E. R. (1970). On r- and K-selection. *The American Naturalist* 104: 592-597.
Pianka, E. R. (1972). r and K selection or b and d selection? *The American Naturalist* 106: 581-589.
Pianka, E. R. (1994). *Evolutionary ecology*. New York: Harper Collins.
Pochron, S. T., W. T. Tucker, et al. (2004). Demography, life history, and social structure in *Propithecus diadema edwardsi* from 1986-2000 in Ranomafana

National Park, Madagascar. *American Journal of Physical Anthropology* 125: 61-72.
Potts, R. (1998). Variability selection in hominid evolution. *Evolutionary Anthropology* 7: 81-96.
Potts, R., B. K. Behrensmeyer, et al. (2004). Small mid-Pleistocene hominin associated with east African Acheulean technology. *Science* 305: 75-78.
Price, T. D., A. Qvarnström, et al. (2003). The role of phenotypic plasticity in driving genetic evolution. *Proceedings of the Royal Society of London, B* 270: 1433-1440.
Pritchard, D. J. (1995). Plasticity in early development. C. G. N. Mascie-Taylor and B. Bogin (Eds.) *Human variability and plasticity*. Cambridge: Cambridge University Press, 18-45.
Pucciarelli, H. M., M. L. Sardi, et al. (2003). Early peopling and evolutionary diversification in America. *Quaternary International* 109-110: 123-132.
Ranta, E., V. Kaitala, et al. (2000). Nonlinear dynamics and the evolution of semelparous and iteroparous reproductive strategies. *The American Naturalist* 155: 294-300.
Reed, K. E., J. W. Kitching, et al. (1993). Proximal femur of *Australopithecus africanus* from Member 4, Makapansgat, South Africa. *American Journal of Physical Anthropology* 82: 1-15.
Relyea, R. A. (2002). Costs of phenotypic plasticity. *The American Naturalist* 159: 272-282.
Reznick, D. N., E. Perry, et al. (1986). Measuring the cost of reproduction: a comment on papers by Bell. *Evolution* 40: 1338-1344.
Richard, A. F. (1985). *Primates in nature*. New York: W.H.Freeman and Company.
Rightmire, G. P. (1981). Patterns in the evolution of *Homo erectus*. *Paleobiology* 7: 241-246.
Rightmire, G. P. (1982). Reply to Levinton. *Paleobiology* 8: 307-308.
Rightmire, G. P. (1986). Stasis in *Homo erectus* defended. *Paleobiology* 12: 324-325.
Rightmire, G. P. (1990). *The evolution of Homo erectus: Comparative anatomical studies of an extinct human species*. Cambridge: Cambridge University Press.
Rightmire, G. P. (1998). Evidence from facial morphology for similarity of Asian and African representatives of *Homo erectus*. *American Journal of Physical Anthropology* 106: 61-85.
Roberts, D. F. (1995). The pervasiveness of plasticity. C. G. N. Mascie-Taylor and B. Bogin (Eds.) *Human variability and plasticity*. Cambridge: Cambridge University Press, 1-17.
Ross, C. (1998). Primate life histories. *Evolutionary Anthropology* 6: 54-63.
Rossi, M., E. Ribeiro, et al. (2003). Craniofacial asymmetry in development: An anatomical study. *Angle Orthodontist* 73: 381-385.
Ruff, C. B., E. Trinkhaus, et al. (1997). Body mass and encephalization in Pleistocene *Homo*. *Nature* 387: 173-176.

Ruff, C. B. and A. Walker (1993). Body size and body shape. A. Walker and R. Leakey (Eds.) *The Nariokotome Homo erectus skeleton.* Cambridge, MA: Harvard University Press, 234-265.

Sagarin, R. D. and S. D. Gaines (2002). The 'abundant centre' distribution: To what extent is it a biogeographical rule? *Ecology Letters* 5: 137-147.

Sasaki, A. and G. de Jong (1999). Density dependence and unpredictable selection in a heterogeneous environment: compromise and polymorphism in the ESS reaction norm. *Evolution* 53: 1329-1342.

Savage, V. M., J. F. Gillooly, et al. (2004). Effects of body size and temperature on population growth. *The American Naturalist* 163: 429-441.

Schell, L. M. (1995). Human biological adaptability with special emphasis on plasticity: History, development and problems for future research. C. G. N. Mascie-Taylor and B. Bogin (Eds.) *Human variability and plasticity.* Cambridge: Cambridge University Press, 213-237.

Sharma, D. N. and K. C. Lal (1986). Age-related growth patterns of colony-born rhesus monkeys. J. G. Else and P. C. Lee (Eds.) *Primate ontogeny, cognition and social behaviour.* Cambridge: Cambridge University Press, 141-146.

Shennan, S. (1997). *Quantifying Archaeology.* Edinburgh: Edinburgh University Press.

Sibly, R. M., L. Linton, et al. (1991). Testing life-cycle theory by computer-simulation. 2: Bet-hedging revisited. *Computers in Biology and Medicine* 21: 357-367.

Smith, B. H. (1991). Standards of human tooth formation and dental age assessment. M. A. Kelley and C. S. Larsen (Eds.) *Advances in Dental Anthropology.* New York: Wiley-Liss, 143-168.

Smith, B. H. (1993). The physiological age of KNM-WT 15000. A. Walker and R. Leakey (Eds.) *The Nariokotome Homo erectus skeleton.* Cambridge, MA: Harvard University Press, 195-220.

Smith, B. H. and R. L. Tompkins (1995). Toward a life history of the Hominidae. *Annual Review of Anthropology* 24: 257-279.

Sokal, R. R. and F. J. Rohlf (1995). *Biometry: The principles and practice of statistics in biological research. 3rd edition.* New York: W.H. Freeman and Company.

Sokoloff, L. (1972). Circulation and energy metabolism of the brain. R. W. Albers, G. J. Siegel, R. Katzman and B. W. Agranoff (Eds.) *Basic neurochemistry.* Boston: Little, Brown and Company.

Sonakia (1985). Skull cap of an early man from the Narmada Valley alluvium (Pleistocene) of central India. *American Anthropologist* 87: 612-616.

Sparks, C. S. and R. L. Jantz (2002). A reassessment of human cranial plasticity: Boas revisited. *Proceedings of the National Academy of Sciences* 99: 14636-14639.

Sparks, C. S. and R. L. Jantz (2003). Changing times, changing faces: Franz Boas's immigrant study in modern perspective. *American Anthropologist* 105: 333-337.

Sparks, C. S., K. Spradley, et al. (2002). Cranial variation in the American white population: a temporal and geographic perspective. *American Journal of Physical Anthropology* Supplement 34: 145.
Stearns, S. C. (1976). Life-history tactics: A review of the ideas. *The Quarterly Review of Biology* 51: 3-47.
Stearns, S. C. (1977). The evolution of life history traits: A critique of the theory and a review of the data. *Annual Review of Ecology and Systematics* 8: 145-71.
Stearns, S. C. (1989). Trade-offs in life-history evolution. *Functional Ecology* 3: 259-268.
Stearns, S. C. (1992). *The evolution of life histories*. Oxford: Oxford University Press.
Steele, J. and S. Mays (1995). Handedness and directional asymmetry in the long bones of the human upper limb. *International Journal of Osteoarchaeology*(5): 39-49.
Stefan, V. H. and P. M. Chapman (2003). Cranial variation in the Marquesas Islands. *American Journal of Physical Anthropology* 121: 319-331.
Stringer, C. and H. Ullrich (1990). *British Isles and Eastern Germany*. Brussels: Universite Libre de Bruxelles.
Suwa, G., B. Asfaw, et al. (1997). The first skull of Australopithecus boisei. *Nature* 389: 489-492.
Swisher, C. C., G. H. Curtis, et al. (1994). Age of the earliest known hominids in Java, Indonesia. *Science* 263: 1118-1121.
Swisher, C. C., W. J. Rink, et al. (1996). Latest *Homo erectus* of Java: Potential contemporaneity with *Homo sapiens* in Southeast Asia. *Science* 274: 1870-1874.
Taylor, C. E. and C. Condra (1980). *r*- and *K*-selection in *Drosophila pseudoobscura*. *Evolution* 34: 1183-1193.
Taylor Parker, S. (2000). *Homo erectus* infancy and childhood. S. Taylor Parker, J. Langer and M. L. McKinney (Eds.) *Biology, brains and behavior: The evolution of human development*. Santa Fe: School of American Research Press, 279-318.
Tobias, P. V. (1999). Biological equipment, environment and survival in the Australopithecine world. H. Ullrich (Ed.) *Hominid evolution: Lifestyles and survival strategies*. Gelsenkirchen: Edition Archaea, 55-71.
Toussaint, M., G. A. Macho, et al. (2003). The third partial skeleton of a late Pliocene hominin (Stw 431) from Sterkfontein, South Africa. *South African Journal of Science* 99: 215-223.
Trotter, M. (1970). Estimation of stature from intact limb bones. T. D. Stewart (Ed.) *Personal identification in mass disasters*. Washington, DC: Smithsonian Institution, 71-83.
Ulijaszek, S. J. (1995). Plasticity, growth and energy balance. C. G. N. Mascie-Taylor and B. Bogin (Eds.) *Human variability and plasticity*. Cambridge: Cambridge University Press, 91-109.
Vander, A., J. Sherman, et al. (2001). *Human physiology: The mechanisms of body function*. Boston: McGraw-Hill.

Vekua, A., D. Lordkipanidze, et al. (2002). A new skull of early *Homo* from Dmanisi, Georgia. *Science* 297: 85-89.
Vrba, E. S. (1999). Habitat theory in relation to the evolution in African Neogene biota and hominids. T. G. Bromage and F. Schrenk (Eds.) *African biogeography, climate change, and human evolution.* New York: Oxford University Press, 19-34.
Waldron, T. (1994). *Counting the dead: The epidemiology of skeletal populations.* Chichester: John Wiley & Sons.
West-Eberhard, M. J. (2003). *Developmental plasticity and evolution.* Oxford: Oxford University Press.
WHO (2000). *Nutrition for health and development: A global agenda for combating malnutrition.* Geneva: World Health Organisation.
Wich, S. A., S. S. Utami-Atmoko, et al. (2004). Life history of wild Sumatran orangutans (*Pongo abelii*). *Journal of Human Evolution* 47: 385-398.
Winterhalder, B. and E. A. Smith (1992). Evolutionary ecology and the social sciences. E. A. Smith and B. Winterhalder (Eds.) *Evolutionary ecology and human behaviour.* New York: Aldine de Gruyter, 3-23.
Wolpoff, M. H. (1984). Evolution in *Homo erectus*: The question of stasis. *Paleobiology* 10: 389-406.
Wolpoff, M. H. (1986). Stasis in the interpretation of evolution in *Homo erectus*: A reply to Rightmire. *Paleobiology* 12: 324-328.
Wolpoff, M. H. (1996). *Human evolution.* New York: McGraw-Hill.
Wood, B. (1984). The origin of *Homo erectus*. *Courier Forschungsinstitut Senckenberg* 69: 99-111.
Wood, B. (1991). *Koobi Fora research project volume 4: Hominid cranial remains.* Oxford: Clarendon Press.
Wood, B. and M. Collard (1999). The changing face of genus *Homo*. *Evolutionary Anthropology* 8: 195-207.
Wood, B. and B. G. Richmond (2000). Human evolution: taxonomy and paleobiology. *Journal of Anatomy* 196: 19-60.
Wood, B. and D. S. Strait (2004). Patterns of resource use in early *Homo* and *Paranthropus*. *Journal of Human Evolution* 46(119-162).
Wu, L., Z. Yinyun, et al. (2005). Middle Pleistocene human cranium from Tangshan (Nanjing), southeast China: A new reconstruction and comparisons with *Homo erectus* from Eurasia and Africa. *American Journal of Physical Anthropology* 127: 253-262.
Wu, X. and F. E. Poirier (1995). *Human evolution in China: A metric description of the fossils and a review of the sites.* New York: Oxford University Press.
Zuckerman, S. (1928). Age-changes in the chimpanzee, with special reference to growth of brain, eruption of teeth, and estimation of age; with a note on the Taungs ape. *Proceedings of the Zoological Society* 1: 1-42.